

# **ANNUAL REPORT**

**East Texas and Western Louisiana Coastal Erosion Study**

**Year 2**

**Robert A. Morton, James C. Gibeaut, William A. White, and Roberto Gutierrez  
Assisted by Joan M. Drinkwin, Cynthia A. Jennings, and Lisa Remington**

**Prepared for the U.S. Department of Interior  
U.S. Geological Survey**

**Cooperative Agreement No. 14-08-0001-A0912**

**Bureau of Economic Geology  
W. L. Fisher, Director  
The University of Texas at Austin  
Austin, Texas 78713**

**July 1993**

## CONTENTS

Work Element 1: Coastal Erosion Analysis .....	2
Work Element 2: Regional Geologic Framework .....	4
Work Element 3: Coastal Processes .....	5
Work Element 4: Prediction of Future Coastal Response .....	7
Work Element 5: Sand Resources Investigations .....	8
Work Element 6: Technology Transfer .....	8
Addendum 1: Shoreline Movement Along Developed Beaches Of The Texas Gulf Coast: A Users Guide To Analyzing And Predicting Shoreline Changes .....	1-1
Addendum 2: Submergence And Erosion Of Wetlands, Galveston-Trinity Bay And Sabine Lake Estuarine Systems .....	2-1
Addendum 3: Geologic Framework Of Incised Coastal Plain Rivers .....	3-1
Addendum 4: Releveling Profile Across The Trinity River Valley .....	4-1
Addendum 5: Beach And Dune Sedimentation On Galveston And Follets Island: Hurricane Alicia And Beyond .....	5-1
Addendum 6: Large-Scale Transfer Of Sand During Storms: Implications For Modeling And Prediction Of Shoreline Movement .....	6-1
Addendum 7: Beach Morphology And Volumetric Changes Determined With GPS Kinematic Surveys .....	7-1
Addendum 8: Shoreline Shape And Prediction Program (SSAP): A Computer Program For The Statistical Analysis Of Shoreline Change And Morphology .....	8-1

## Report Organization

The following report summarizes the major accomplishments achieved by the Bureau of Economic Geology during the second year of study of coastal erosion and wetlands loss along the southeastern Texas coast. The report covers activities between July 1, 1992 and June 30, 1993 and includes the activities for the eighth quarter of the project. Major accomplishments are reported for each work element and task identified in the cooperative agreement. Documents summarizing the major accomplishments and containing the important scientific conclusions are included as Addendums 1-8.

### Work Element 1: Coastal Erosion Analysis

This work element is intended to (1) establish a computerized database of historical shoreline positions (1882-1982), (2) update the database using the most recent shoreline information (1990), (3) analyze historical trends of shoreline movement in the context of the regional geologic framework and human modifications, (4) synthesize the physical and habitat characteristics of different shoreline types, (5) establish a network of field monitoring sites for surveying coastal changes, and eventually (6) prepare a document of shoreline changes suitable for coastal planning and resource management.

**Task 1: Shoreline Mapping.** Black and white aerial photographs at a scale of 1:24,000 taken in 1990 by the Texas Department of Transportation were used to map the most recent shoreline position from High Island to Sargent Beach. This most recent shoreline was optically transferred (Zoom Transfer Scope) to the most recent USGS topographic maps (1:24,000 scale), digitized, and then entered into ARC-INFO, the Bureau's GIS used for the coastal erosion study. Shoreline positions in 1974 and 1990 were then compared using the GIS. Distances and rates of shoreline change from 1974 to 1990 were calculated at 100 transects spaced 5,000 ft apart between High Island and Sargent Beach. These distances and rates of change were combined with the same measurements for earlier time periods and the results were compiled in an open file report (**Addendum 1**).

We also spent several months testing the Digital Shoreline Mapping System (DSMS) developed by Bill Danforth and Rob Theiler of the USGS. This recently released computer software is configured so that shorelines can be digitized directly from uncontrolled aerial photographs. Results of our first tests, which determined the error associated with digitizing directly from the photographs, indicated that directly digitized shoreline positions are comparable to optically transferred positions when there is sufficient cultural control and photographic overlap to minimize

the locational errors. We encountered some software problems with DSMS and with GIANT, which is a subroutine used in the iterative process. Most of these software problems were resolved; however, digitization of the 1990 shoreline directly from the aerial photographs resulted in large shoreline discontinuities and spatial errors that were not resolved. Several discussions with Rob Theiler suggested that more geomorphic-based passing points are needed in areas lacking cultural control. The results of this unsuccessful test were not incorporated into the shoreline change analysis because of the large errors. The results of our DSMS tests also reconfirm our recommendation to retain the intermediate step of optically transferring shorelines to a stable base before digitization. Direct digitization of shorelines from aerial photographs is not recommended for accurate analysis of shoreline movement.

Task 2: Geomorphic Characterization. During year 2 we conducted field investigations between Rollover Pass and Follets Island. Beach profile sites were reoccupied and observations made that allowed an initial classification of shoreline characteristics including physical characteristics of the beach (morphology, composition, slope, width, dune development, substrates, stabilization projects) as well as shoreline stability determined from the preceding erosion analysis. We also began synthesizing results of several Bureau of Economic Geology studies that examined wetland changes in the study area. This work focused on wetland losses within the entrenched valleys, around the bay margins, and along the barrier islands.

SIGNIFICANT RESULTS. To provide current information about shoreline movement to local governments and to State agencies in Texas, we prepared a users guide that combines text with tables and graphical displays of historical shoreline movement for specific shoreline segments. The text introduces users to the concepts necessary to interpret the shoreline movement data and to apply the results for purposes of planning and regulating coastal development activities. The open-file report (**Addendum 1**), including the shoreline movement data for the southeastern Texas coast, have been incorporated into the States Coastal Zone Management plan that is administered by the Texas General Land Office. State regulations that deal with coastal erosion recognize the Bureau of Economic Geology as the official source of shoreline movement data in Texas.

We also prepared a brief report that summarizes and illustrates significant wetland losses within the Galveston-Trinity Bay system and the Sabine Lake estuarine system (**Addendum 2**). The report concludes that most of these losses are caused by land-surface subsidence, reductions in fluvial sediment supply to the flood basins and river deltas, and wave erosion around the open shores of the major bays and Gulf of Mexico.

## **Work Element 2: Regional Geologic Framework**

This work element focused on the geologic origin and evolution of the principal subenvironments that are present along the southeastern Texas coast. This is being accomplished by establishing a chronostratigraphic framework for the coastal systems and reconstructing the evolution of coastal environments during the post-glacial rising phase and highstand in sea level. This work element will also provide data on the physical characteristics and natural habitats of the various shoreline types in the context of shoreline stability.

Task 1: Stratigraphic Analysis. The study area encompasses a diverse assemblage of depositional environments ranging from non-marine fluvial systems and transitional coastal systems to the marine continental shelf. During year two, we used vibracores, faunal assemblages, isotopic dates, and seismic surveys to investigate the late Quaternary and Holocene stratigraphy of several of these environments. These data were used to construct cross sections illustrating the various coastal and non-marine facies. Eventually we plan to construct a detailed sea-level curve for the late Holocene and Modern time periods. Results of these investigations will provide a basis for predicting future magnitudes and rates of land loss.

Subtask 1: Data Inventory and Compilation. During the second year of study, we continued to gather maps, cross sections, and reports as well as basic data such as isotopic dates, foundation borings, and core descriptions for the Sabine-Neches fluvial system, Trinity-San Jacinto fluvial system, Sabine Lake, Galveston Bay, the chenier plain of southeastern Texas, and Sabine Bank, which is offshore in the Gulf of Mexico. The surficial and shallow subsurface data are being used to construct subregional cross sections showing the distribution of sedimentary facies, sequence boundaries, and age relationships. These shallow subsurface data (foundation borings, cross sections, and seismic profiles) of the southeastern Texas Coast were compiled from available industry and government sources.

Subtask 2: Field Studies. During year 2, we prepared a plan for obtaining precise elevations across the Trinity River valley. We also collected several moderately deep subsurface cores in the entrenched valley fill of the Neches River, the chenier plain of southeastern Texas, and the coastal wetland interfluvium between the Sabine and Trinity River systems.

SIGNIFICANT RESULTS. Lithologic logs of selected foundation borings were constructed and stratigraphic cross sections were prepared that illustrate the composite entrenched valleys of the Sabine, Neches, Trinity, and San Jacinto fluvial systems. Both cross-valley and longitudinal

sections were constructed to illustrate the sedimentary characteristics of the Holocene valley fill. Preliminary versions of selected cross sections and a brief discussion of the sedimentary facies and the geological significance of the stacking patterns of sedimentary facies are presented in **Addendum 3**.

### **Work Element 3: Coastal Processes**

Understanding coastal processes is the key to understanding coastal erosion and predicting future coastal changes. Therefore, this work element involves numerous tasks that attempt to quantify basin energy, sediment motion, and the forcing functions that drive the coastal system. Objectives of this work element are to evaluate the magnitudes and rates of the relative rise in sea level during geological and historical time, to provide a basis for assessing wave and current energy as well as sediment transport, to assess climatic and meteorological influences on coastal processes, to evaluate the impacts of storms on shoreline stability and instantaneous erosion potential, and to begin quantifying the coastal sediment budget.

Task 1: Relative Sea-Level Rise and Subsidence. Sea level is perhaps the single most important factor that influences coastal erosion and planning for future development of the coast. The analysis of relative sea level through time involves acquiring from NOAA (1) tidal data at selected gauges with long-term records and (2) releveling surveys. This task focuses on the major factors causing the relative rise in sea level within the study area and the recent acceleration in the rate of sea-level rise. During year two, we obtained from NOS hourly records from the tide gauge at Galveston Pier 21, which is the longest continuous record of tides in Texas and extends back to the early 1900s.

Task 2: Sediment Transport. This task will examine seasonal beach and nearshore profiles as a first approximation of time-averaged sediment transport. The data for this phase of the investigation are taken from post-Alicia beach profiles on Galveston and Follets Islands. During the second year of study, preliminary field experiments were being designed to measure the frequency and duration of sediment movement, as well as the response of sandy and muddy substrates to similar levels of wave and current energy.

Task 3: Sediment Budget. This task will evaluate the primary sediment sources (updrift erosion and fluvial sediment supply) and the principal sinks (beach accretion, onshore washover, dune construction, and offshore deposition). Some additional sediment losses occur at tidal inlets and some unknown quantity is trapped in the deep-draft navigation channels. Material periodically

dredged from the ship channels deserves further evaluation as a potential source of beach nourishment material. During the second year of study, we examined the available erosion analyses, bathymetric surveys, beach profiles, sediment transport analyses, stream discharge records, and vibracore descriptions for the area of interest and combined this information with the geomorphic analysis of shoreline types (Work element 1). At year end, we were beginning to identify the major components of the sediment budget for each coastal compartment. The boundaries of each coastal compartment are now defined by the long, impermeable jetties that border the deep-draft navigation channels at each of the harbor entrances (Sabine Pass, Bolivar Roads, Freeport Harbor). The only natural boundary of a littoral cell is at San Luis Pass, which separates Galveston Island from Follets Island.

Task 4: Storm Impacts. This task involves evaluating storm impacts and developing process-response models to predict the response of each shoreline type to storms having variable characteristics. During the second year of study, we repeated a field experiment to test the concept of using GPS techniques to monitor nearshore changes in elevation and sediment volume. As in year 1, the test site was at Galveston Island State Park. State-of-the-art GPS equipment (2 multichannel receivers, tripods, mounting brackets) was provided by the University of Texas Department of Geological Sciences and the Center for Space Research.

SIGNIFICANT RESULTS. Releveling surveys along Interstate 10 that cross the Trinity River valley were obtained from NOAA. The surveys were compared and rates of vertical movement were calculated for the period between 1973 and 1978. Results of this comparison are presented as **Addendum 4**.

The Interactive Survey Reduction Program (ISRP) was obtained and installed to help quantify sediment transport and sediment budgets along the southeastern Texas coast. ISRP is a beach profile management and analysis computer program developed by the U.S. Army Corps of Engineers Waterways Experiment Station (WES). This program provides an efficient means to manage and to check for errors in beach profile data. In addition, its data storage format is compatible with companion programs developed by WES that analyze and model beach profile variation. The computer program "VOLUME" was also installed. VOLUME works with ISRP and provides batch processing of volumetric and elevation data for sets of beach profiles.

Beach profile data for 10 stations between Sabine Pass and Follets Island dating from 1983 to 1993 have been entered into ISRP and checked for errors. The geological results of the beach profile measurements on Galveston Island and Follets Island are included as **Addendum 5**. These profiles are being used to track the recovery and later adjustment of the beaches after Hurricane Alicia in 1983. Results of this task will be presented at the Symposium on Large-Scale

Coastal Behavior, which will be held in St. Petersburg in November, 1993. The abstract of these results is included as **Addendum 6**.

The National Geodetic Survey's OMNI software was obtained and installed to assist in post-processing kinematic GPS data. The OMNI software processes field data from either static or kinematic GPS surveys and provides accurate estimates of three-dimensional positions. Data from the 1993 kinematic GPS surveys was processed with OMNI.

Differential GPS surveying techniques were used to conduct three kinematic surveys in the vicinity of Galveston Island State Park. The first experiment repeated the November, 1991 driving pattern and sampling rate so that comparison of results in April, 1993 with the November, 1991 GPS survey results would be the best estimate of true beach changes for the past 17 months. The second set of experiments tested different driving patterns (single pass zig-zag pattern and double-pass out-of-phase zig-zag pattern) to optimize position density and efficiency of beach surveying. Preliminary results indicate that rapid accelerations and decelerations of the antenna associated with the zig-zag patterns contribute to lower signal-to-noise ratios and more frequent cycle slips. A third experiment was conducted to determine if longer segments of the beach (16 km) could be surveyed using the same short baseline that was used for the initial GPS beach surveys. This experiment tested how far away from the baseline we could drive down the beach and still get accurate results. A summary of results from the previous two experiments and recommendations for future GPS surveys are included as **Addendum 7**. Relatively large operational errors are still being reported for shoreline changes determined from topographic maps and aerial photographs. GPS land-based surveys have the potential for eliminating the large errors associated with one-dimensional shoreline change analyses while at the same time providing information about the two-dimensional beach surface including elevations, and allowing accurate measurements of volumetric changes with repeat surveys.

#### **Work Element 4: Prediction of Future Coastal Response**

Many of the graphical displays of shoreline movement (**Addendum 1**) demonstrate that simple time-averaged linear regressions are inappropriate for most future predictions of shoreline position. Objectives of this work element are to improve estimating rates of shoreline movement, to develop conceptual models that synthesize coastal changes during geological and historical time, and to develop quantitative models that improve our predictions of shoreline changes and coastal inundation.

Task 1: Mathematical Analysis of Rates of Change. During year two we continued to design and modify a procedure within ARC/INFO that generates shore-normal transects at user specified



intervals, determines distances between consecutive shorelines at those transects, calculates rates of change, and transfers the data to an ASCII file. This subroutine is used to generate data sets that will be statistically analyzed in order to develop better predictive models of shoreline movement.

**SIGNIFICANT RESULTS.** A Fortran program was written that takes the shoreline movement measurements at each shore-normal transect and performs various statistical analyses of the data. The program is designed on the basis of work published by Mike Fenster and Bob Dolan at the University of Virginia. The computer program is capable of determining the best curve fit of the data (least squares analysis), identifying whether the best fit is a straight line linear regression or a higher order polynomial curve, identifying the critical points, or turning points, of the curve where the trends or rates of change are significantly different for different time periods, and calculating the rates of change for the linear regression of all the data or for the most recent time period that satisfies the Fenster-Dolan criteria. A brief discussion of the program and its results is presented in **Addendum 8.**

#### **Work Element 5: Sand Resources Investigations**

During year 2 we interpreted the seismic surveys obtained in the vicinity of Sabine Bank, collected 8 vibracores (3 to 6 m deep) from Sabine Bank, and completed descriptions and textural analyses of the vibracores. The vibracores were obtained in cooperation with the Minerals Management Service (MMS) Sand Assessment project.

**SIGNIFICANT RESULTS.** A report summarizing the quality and quantity of sand in Sabine Bank was prepared for the MMS and a copy of the report was sent to Jack Kindinger (USGS) for inclusion in the geologic framework studies.

#### **Work Element 6: Technology Transfer**

The technology transfer work element provides for the timely reporting of project results and makes the interpretations and conclusions available to users as needed. It also establishes a repository to preserve raw data and materials that would be a significant source of information for future studies.

**SIGNIFICANT RESULTS.** In year 2, we continued to expand the coastal GIS for Texas by adding maps of (1) the digitized 1990 Gulf shoreline between High Island and Sargent Beach, (2)

the locations of rotary cores, vibracores, and over 500 foundation borings in the Gulf of Mexico, (3) the locations of production platforms and oil and gas pipelines in the vicinity of Sabine and Heald Banks, and (4) shot point locations of offshore seismic data in the vicinity of Sabine and Heald Banks.

**ADDENDUM 1**

**SHORELINE MOVEMENT ALONG DEVELOPED BEACHES OF THE TEXAS GULF COAST:  
A USERS GUIDE TO ANALYZING AND PREDICTING SHORELINE CHANGES**

**HIGH ISLAND TO SARGENT BEACH**  
(Jefferson, Chambers, Galveston, Brazoria, and Matagorda Counties)

**MUSTANG AND NORTH PADRE ISLANDS  
PORT ARANSAS TO PADRE BALLI PARK**  
(Nueces County)

**SOUTH PADRE ISLAND  
MANSFIELD CHANNEL TO BRAZO SANTIAGO PASS**  
(Willacy and Cameron Counties)

**Robert A. Morton assisted by Cynthia Jennings and Lisa Remington**

**Open File Report 93-1  
Bureau of Economic Geology  
The University of Texas at Austin**

**August 1993**

## CONTENTS

INTRODUCTION.....	1
UNDERSTANDING SHORELINE MOVEMENT.....	2
Water-Level Oscillations.....	3
Sediment Volume.....	4
SHORELINE SOURCES AND THEIR LIMITATIONS.....	4
Topographic Maps.....	5
Aerial Photographs.....	6
Beach Profiles.....	7
GPS Surveys.....	10
QUANTIFYING SHORELINE MOVEMENT.....	12
Comparing Shoreline Positions.....	12
Presenting Shoreline Changes.....	13
Interpreting Graphical Displays.....	15
Calculating Rates of Change and Predicting Future Positions.....	19
COASTAL EROSION AND SUBMERGENCE MODELS.....	20
Statistical Models.....	22
Geometric Models.....	23
Combined Statistical and Geometric Models.....	25
Numerical (Deterministic) Models.....	25
SUMMARIES OF SHORELINE MOVEMENT, TEXAS GULF COAST.....	27
Methods.....	27
High Island to Bolivar Peninsula.....	29
Galveston Island.....	29
San Luis Pass to Sargent Beach.....	30
Mustang and North Padre Islands (Port Aransas to Padre Balli Park).....	30

South Padre Island (Mansfield Channel to Brazos Santiago Pass).....	31
ACKNOWLEDGMENTS.....	31
REFERENCES.....	32
APPENDIX A: Shoreline Movement—High Island to Sargent Beach	
APPENDIX B: Shoreline Movement—Mustang and North Padre Islands	
APPENDIX C: Shoreline Movement—South Padre Island	

### Figures

1. Shoreline movement related to changes in water levels and sediment volumes.....	2
2. Scales of shoreline movement for historical and geological time periods.....	3
3. Surveyed beach profiles showing rapid erosion at Sargent Beach, Texas.....	8
4. Map showing historical shoreline positions and rapid erosion at Sargent Beach.....	14
5. Generalized graph of shoreline position through time illustrating fields of beach stability.....	15
6. Graph of shoreline position through time showing rapid erosion at Sargent Beach.....	16
7. Anomalous shoreline movement related to droughts and storms.....	18
8. Graph of shoreline position through time showing reversals in the long-term trend of shoreline movement.....	18
9. Illustration of the Bruun Rule that relates shoreline retreat to a rise in sea level.....	19

### Tables

1. Principal errors associated with measurement and prediction of shoreline movement.....	5
2. Important decisions to make before establishing a beach and dune monitoring program.....	8
3. The common forms of expressing shoreline movement and their utility.....	13
4. An example of historical shoreline changes and rates of change.....	14
5. Comparison of assumptions, advantages, and disadvantages for the different types of shoreline movement models.....	21

## INTRODUCTION

Coasts worldwide are eroding, and in many areas, including Texas, the rates of shoreline retreat are accelerating. The causes of shoreline erosion at a particular site are not always known, but this lack of explanation should not be a reason to ignore the past changes in shoreline position. Indeed, it is imperative that future coastal plans and management strategies include the best available data regarding historical shoreline changes.

Most coastal states are in the process of developing comprehensive data bases of shoreline movement, but in Texas detailed shoreline mapping has been underway since 1971. In 1973 the State Legislature recognized the need for coastwide information on beach stability, and special funds were appropriated during the 1973–75 biennium for the Bureau of Economic Geology to investigate movement along the Texas Gulf shore. The results of that investigation were published as a series of reports (Morton, 1974; 1975; Morton and Pieper, 1975a, 1975b, 1976, 1977; Morton and others, 1976). Each report summarizes shoreline movement for a particular segment of the Texas coast and offers reasons for the changes in beach stability. In 1989, the Bureau of Economic Geology published an addendum to the original shoreline reports (Paine and Morton, 1989). The addendum examined shoreline movement between 1974 and 1982 and updated the rates of coastal erosion. In 1991, the Bureau of Economic Geology entered into a cooperative agreement with the U.S. Geological Survey to conduct coastal studies along the southeastern Texas coast. The purpose of the cooperative agreement was to provide updated information on coastal erosion and land loss between Sabine Pass and Sargent Beach. Through this joint effort the shoreline erosion data are being revised to include the 1990 shoreline positions. Also in 1991, the Texas Legislature (SB 1053) directed the Bureau of Economic Geology to cooperate with the Texas General Land Office and local governments to quantify erosion rates of Texas beaches. Rules adopted by the Texas General Land Office and published in the Texas Register (February 2, 1993; p. 661–707) confirm that the Bureau of Economic Geology is the official source of coastal erosion data in Texas.

The following report is a response to the legislative directive that recognizes the need to make shoreline movement data more accessible to potential users and also easier to use. This users' guide is intended to assist those who have a need to determine beach stability at a particular coastal site but who are not necessarily trained in coastal geology. The guide summarizes the sources of shoreline information and explains how the shorelines are compared, how shoreline movement data are analyzed, and how they can be used to estimate where the shoreline will be in the future. The guide also illustrates the history of shoreline movement at selected sites, explains anomalous data at some sites, and reports the most recent rate of change that is appropriate for predicting future shoreline positions.

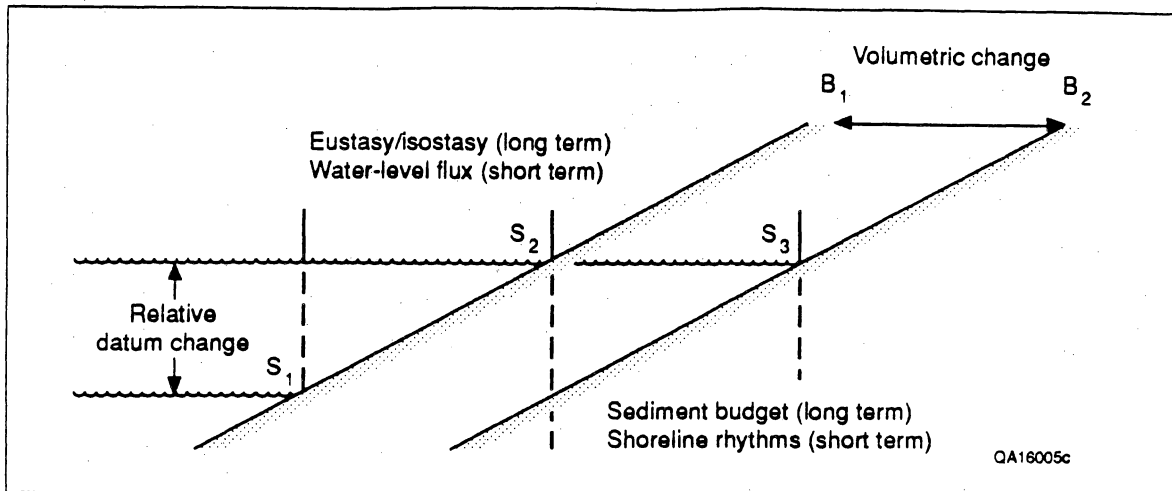


Figure 1. Shoreline movement related to changes in water levels and sediment volumes. From Morton (1991).

## UNDERSTANDING SHORELINE MOVEMENT

Predicting future shoreline positions requires an understanding of the factors that cause fluctuations in water levels and sediment volumes near the coast. The shores of oceanic coasts are constantly changing in response to a hierarchy of processes that occur as a result of daily tides, weather events, storms, and changes in climate. The distances and rates of shoreline movement caused by these processes are highly variable. Furthermore, some of the shoreline changes are temporary, whereas others are permanent. Coastal scientists and engineers currently face the dilemma of distinguishing between long-term shoreline movement and short-term shoreline oscillations, which may not be the same as the long-term trend of movement. Distinguishing between temporary beach fluctuations and permanent movement is made even more difficult because in some areas human activities have either accelerated beach erosion or caused reversals from beach accretion to beach erosion.

When reduced to its simplest terms, shoreline movement is a function of two independent variables: water level and beach volume (fig. 1). These variables are interactive, and they operate on different scales of time and space. Water levels change at time scales ranging from seconds to more than 100,000 years, and they produce shoreline changes that range from a few feet to more than 100 mi (fig. 2). Shorelines can also build seaward or retreat landward several miles as a result of changes in sediment supply even when sea level is more or less constant. The shoreline forms where the land and water meet, so any changes in the vertical relationship between these two masses will cause a shift in the shoreline.

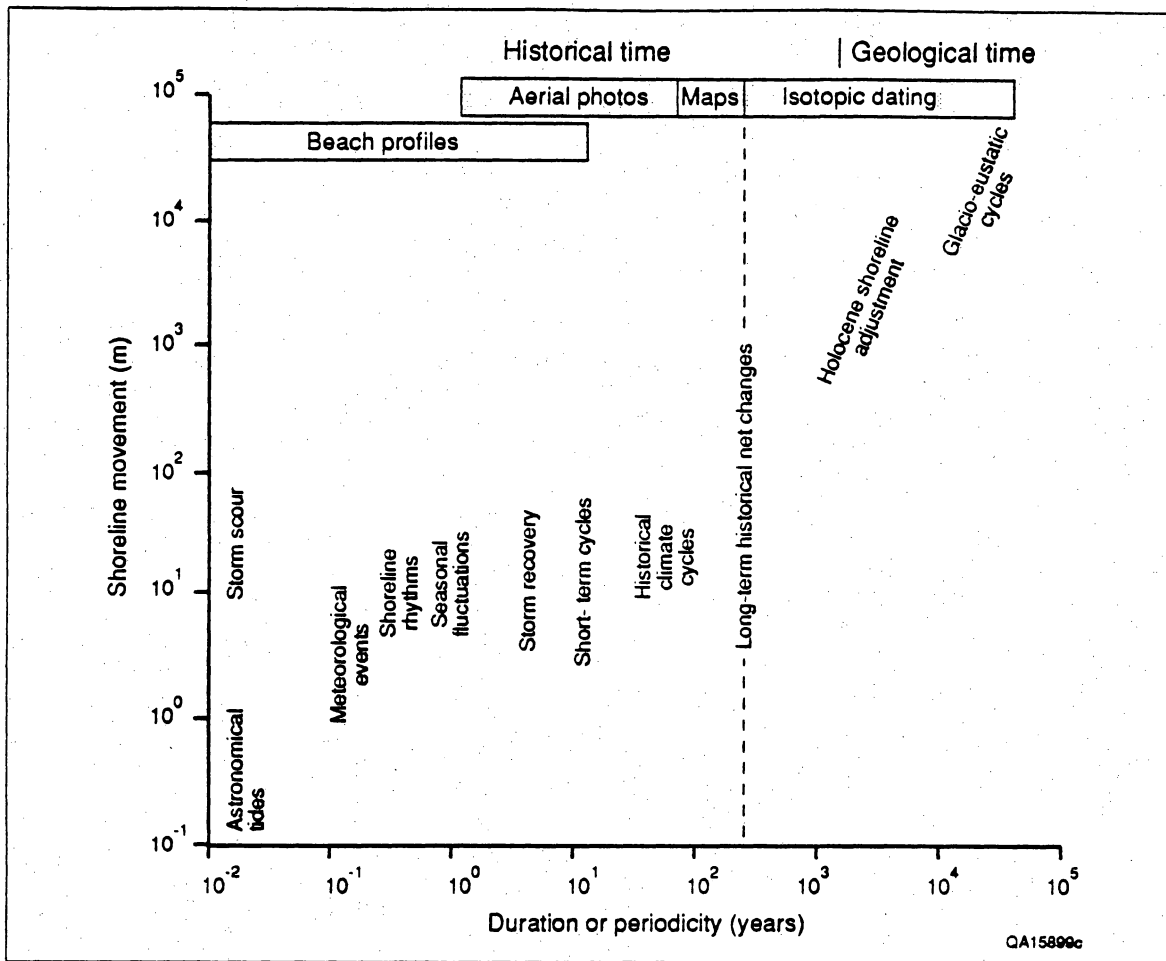


Figure 2. Scales of shoreline movement for historical and geological time periods. From Morton (1991).

### Water-Level Oscillations

At geological and intermediate time scales, changes in water level are controlled mainly by climate and movements in the Earth's crust (fig. 2). Over time spans of several thousand or hundreds of thousands of years, fluctuations in sea level are capable of shifting the shoreline more than 100 mi regardless of the volume of sediment supplied to the coast (fig. 2). Sea-level fluctuations at progressively shorter recurrence intervals are related to climatic effects (Little Ice Ages, droughts, and floods), seasonal cycles between summer and winter, and daily tides.

Water-level fluctuations cause both actual and apparent shoreline changes depending on whether or not they are also accompanied by changes in sediment volume. Temporary shoreline changes caused solely by water-level fluctuations are most pronounced along low-gradient coasts. These anomalous shoreline changes can occur as a result of high water levels (abundant rainfall, floods, storms) or low



water levels (droughts) at the time of photography. Hourly readings at selected tide gauges are used to determine differences in water levels between consecutive sets of aerial photographs to prevent misinterpreting water-level changes as true beach changes.

### Sediment Volume

Beach erosion and accretion are responses to changes in sediment volume (fig. 1 between  $S_2$  and  $S_3$ ). Deficits and surpluses in the sediment budget account for long-term beach erosion and accretion, whereas short-term shoreline fluctuations may involve only temporary removal or addition of beach sediment. Alongshore migration of sand bars is an example of short-term shoreline fluctuations caused by temporary changes in sediment volume. Where the bars are attached to the shore, the beach will be as much as 25 ft wider than where the bars are absent. This type of fluctuation in sediment volume needs to be taken into account when shoreline movement is analyzed.

Fluctuations in sediment volume are much more irregular and difficult to predict than water-level oscillations. Also, the length of shoreline affected by fluctuations in sediment volume is usually restricted, whereas water-level oscillations typically involve the entire shore surrounding a body of water.

### SHORELINE SOURCES AND THEIR LIMITATIONS

Coastal planners and property managers need to understand past coastal changes in order to anticipate where the shoreline will be in the future and to predict what the rates of shoreline movement might be. These objectives are best accomplished by using shoreline maps, which provide a basis for understanding the dynamics of the coast. Former shoreline positions can come from several sources, but the most common sources are topographic maps, aerial photographs, and ground surveys. The most common errors encountered when using maps and aerial photographs are summarized in table 1.

All shoreline change analyses involve plotting several shorelines at the same site, comparing the shoreline positions through time, and calculating rates of shoreline movement for several time periods (Stafford, 1971; Leatherman, 1983; Morton, 1991). If coastal managers or property owners are making decisions based on predicted shoreline stability, they should carefully examine the sources of shoreline positions and understand how the shoreline-change analysis was conducted. Also, the decision-makers should evaluate the methods used to determine the rate of shoreline movement or to project the future shoreline position.

Table 1. Principal errors associated with measurement and prediction of shoreline movement.

Sources of Error	Ways of Minimizing the Error
<b>Maps</b>	
Old topographic surveys	Use triangulation stations for geographic control
Datum changes	Use published or annotated corrections
<b>Photos</b>	
Radial distortion, tilt	Spatial resection transformations
High water line interpretation	Experience and familiarity with coast
High water line representation	Use large-scale format and fine-point pen
<b>GIS</b>	
Digitizing table and cursor	Use large-scale maps and double-precision digitization
Boundary tracing	Operator experience, perform repeatability tests
Biased geographic control	Use closely spaced features near the shoreline
Nonuniform beach movement	Extend the period of record to improve prediction
Nonlinear beach movement	Use the most recent reliable period for prediction

### Topographic Maps

The oldest reliable shorelines in Texas are preserved on coastal topographic maps commonly referred to as T-sheets (Shalowitz, 1964). Most of these maps were surveyed during the mid to late 1800's. The old topographic maps can be compared with more recent surveys or topographic maps using the geographic coordinates (latitude and longitude) drawn on the original maps. Many of these old maps also accurately portray stable land features, such as interior ponds and tidal creeks, which can be compared with the same features on more recent land surveys or aerial photographs. In this case, the land features provide horizontal control for map comparison that does not depend on knowledge of precise latitude and longitude.

The 1800's topographic maps contain a potential source of error that is not present when aerial photographs are used to detect shoreline changes. This is because the positions of the 1800's shoreline have undergone two corrections, known as the North American Datums of 1927 and 1983 (NAD-27 and NAD-83). These datum corrections have moved the position of the shoreline relative to latitude

and longitude coordinates as much as 120 ft (Wade, 1986). The latitude and longitude corrections are not always marked on the maps, and the unsuspecting user might think that the coordinates shown on the map are correctly located when they are not. If you are presented with beach stability data that are partly based on shoreline positions before 1930, make sure that the proper datum and map projections were used to compare with the more recent shorelines.

There are both advantages and disadvantages associated with using the old topographic maps for shoreline-change analyses. The principal advantage is that the period of record is extended as far back as possible without sacrificing shoreline accuracy. A minor disadvantage is that the documented shoreline changes may be difficult to interpret because information for that period regarding storms and other events affecting the coast is generally lacking. Most coastal scientists think that the longest reliable record of shoreline change will provide the most reliable basis for predicting future changes. This normally means that the oldest reliable shoreline should be used in the shoreline-change analysis.

### Aerial Photographs

Vertical aerial photographs are the most common source of shoreline positions because air photos are much cheaper and faster to obtain than ground surveys. Both stable geomorphic features and cultural features (buildings and roads) observed on the air photos can be used to compare them with other air photos or with topographic maps. The positions of some ground features observed on air photos may be slightly inaccurate because of minor scale differences and distortions that occur across the photograph. These minor errors are caused by movement of the plane that prevents the camera from being exactly perpendicular to the surface of the earth. Slight up-and-down movement of the plane causes minor changes in scale from one photograph to another, whereas slight tilting of the wings or nose of the plane causes distortions across the photograph. The distortion errors are small near the center of the photograph, so, if possible, the center of the photograph should be used for mapping the shoreline. The minor errors caused by movement of the plane are inconvenient, but there are several optical and digital techniques that can be used to correct for the distortions and scale differences. Anders and Byrnes (1991) and Crowell and others (1991) reviewed the types of errors typically associated with the original topographic maps and aerial photographs and estimated how large the errors might be if they depend on the scale of the original material.

The shoreline proxy most commonly mapped on aerial photographs is the high water line that separates the wet beach from the dry beach (Stafford, 1971; Morton, 1979; Dolan and Hayden, 1983). The wet beach-dry beach line is not a tidal datum, such as the mean high water line, and it represents the highest water levels occurring immediately before the photographs were taken. Because wave runup is large on low-gradient sandy beaches, the high water line on those beaches is sensitive to changes in

water level caused by strong winds or unusual tides. As a result, shoreline movement mapped for some sandy beaches may be caused by differences in water levels rather than by actual changes in sediment volume (fig. 1). Theoretically, shorelines mapped on aerial photographs could be reconstructed to a specific tidal datum using local correction factors for beach slope and water levels (Stafford, 1971), but in reality, the dynamics of sandy beach profiles preclude making these corrections with much confidence. The potential for mislocating the shoreline on air photos due to water-level fluctuations is not a problem on steep beaches or steep rocky shores.

The stability of beaches can also be inferred from aerial photographs by monitoring other shoreline proxies, such as the vegetation line and dune line. These boundaries are secondary indicators of shoreline movement that can provide supplementary information about local beach dynamics or can serve as additional ground control for mapping the high water line. Where bluffs are the predominant shoreline type, the bluff top and bluff toe are the most reliable indicators of shoreline stability. These shoreline indicators are more stable than the wet beach-dry beach line since they are not influenced by changes in water level.

Perhaps the most tenuous assumption made regarding aerial photographs is that the photographed shoreline is of an equilibrium beach representing typical or average conditions. This assumption can be verified only indirectly by examining tide gauge records, meteorological reports, and other historical documents that indicate either abnormal conditions or the lack of unusual events preceding the photographic mission.

### Beach Profiles

Shoreline movement can also be documented by profiling the beach (fig. 3). Beach profiling is a standard field method that involves making repeated measurements at ground-control stations along the beach. These measurements may consist of a single observation, such as dry beach width, or they may involve surveying the entire beach surface. Beach profiles require establishing a reference mark from which distances and elevations along a traverse are measured. The reference mark can be a surveyor's benchmark or some other stable feature such as the corner of a seawall or sign post.

There are a number of decisions that must be made before a beach is surveyed (table 2). The results expected from the survey will determine where and how frequently the survey will be conducted and the type of equipment that will be used. Beach surveys that rely on a tidal datum (mean high water or mean low water) or property boundaries must be conducted by a registered surveyor with expensive equipment. On the other hand, accretion and erosion of the beach can be measured with portable inexpensive equipment as long as the same profile location is reoccupied.

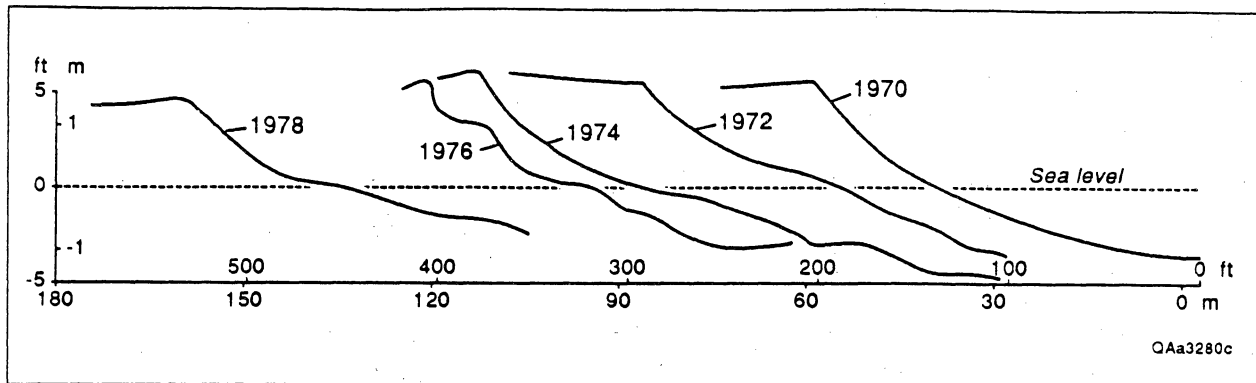


Figure 3. Surveyed beach profiles showing rapid erosion at Sargent Beach, Texas.

Table 2. Important decisions to make before establishing a beach and dune monitoring program.

The options are ranked depending on the objectives and expected results of the monitoring program. The ranking progresses from a simple comparison of beach width to complete surveys of the beach surface suitable for three-dimensional estimates of volumetric changes.

- A. Type of reference markers or baseline control—Existing uncontrolled features such as seawalls and signposts, or controlled features such as surveyed stations and geodetic benchmarks.
- B. Type of beach monitoring equipment—Compass and tape measure, graduated rods and chain, theodolite, electronic total station, Global Positioning System (GPS).
- C. Type of beach survey—Dry beach width, beach profiles, tidal datum (mean high water line), or entire beach surface including subaqueous as well as subaerial profiles.
- D. Frequency of beach surveys—Annual, semiannual, or monthly depending on inferred beach stability and anticipated information requirements.
- E. Training of personnel who are responsible for collecting field data.
- F. Training of personnel who are responsible for analyzing and storing beach survey data (comparative profiles or surfaces), preparing shoreline change maps, tables, graphs, calculating volumetric changes, and determining sediment budgets.
- G. Frequency of reporting the status of beaches and dunes—Annual or biannual reports on beaches (seasonal variability and storm response) and dunes (stability and extent of vegetation).

Beach profiles oriented perpendicular to the shoreline (fig. 3) can be obtained with various types of equipment ranging from simple graduated rods and chains (Emery, 1961), to standard stadia rod and level, to a more accurate autotracking geodimeter with a reflecting prism (Birkemier and others, 1991). The more sophisticated techniques offer greater measuring precision, but they also require more field support and data processing equipment, such as computers and specialized software.

The Emery method (Emery, 1961) is a simple but accurate profiling technique that can be quickly learned by anyone. The pieces of equipment needed to conduct this type of beach survey are two rods of equal length that are marked with uniformly spaced lines (inches, tenths of feet, centimeters), a long cloth or steel tape, and a form or field book for recording measurements and observations. Vertical changes in beach elevation and the horizontal distance between those changes are the data recorded in the field. At each point of the survey, notes are made regarding the features being measured (dune toe, dune crest, berm crest, erosional escarpment, high water line) and other information such as sediment grain size and presence or absence of shells. Also noted are the day and time of the profile, name of the profile station, tide stage, direction of littoral drift, and weather conditions. The high water line, used to approximate the shoreline on aerial photographs, is identified in the field and on the profile as the drift line of the most recent high tide (fig. 3).

The beach profile is obtained by adding the horizontal distances and corresponding changes in beach elevations and plotting those values on graph paper or entering the data into a computer that has graphics capabilities. Changes in the beach are detected by repeating the surveys at the same site every few months or years and comparing the profiles. Either the sea-level datum or the berm crest can be used to indicate beach movement between consecutive surveys. In the example from Sargent Beach, Texas (fig. 3), the beach retreated about 300 ft between 1970 and 1978 at an average rate of 37.5 ft/yr.

A typical shore-normal beach survey yields a one-dimensional profile that represents the relative height of the beach from a fixed reference marker. The profile also displays the position of particular beach features, such as high water line, berm crest, dunes, vegetation line, or a datum intercept such as the National Geodetic Vertical Datum (NGVD). Comparison of subsequent beach surveys yields a two-dimensional cross-sectional area, which represents the amount of beach erosion and deposition that occurred between surveys. A three-dimensional volumetric change in the beach can be derived from the profiles by integrating between adjacent cross-sectional areas.

There are three sources of error associated with these approaches to estimating beach erosion or deposition. The first is that all of the measurements are made relative to a reference marker. If this marker is lost or damaged, accurate comparison of previous surveys with subsequent surveys would be extremely difficult. The second potential error occurs if subsequent surveys do not follow the same course (compass bearing) as the previous survey. The third potential error involves the calculation of volumetric changes from two-dimensional data. Volumetric changes interpolated from adjacent profiles

will be unreliable if the two-dimensional comparisons neglect subtle changes in the beach surface or if the adjacent profiles are widely spaced.

Beach profiles are somewhat limited because (1) they are site specific and they do not provide a continuous shoreline position along the coast, (2) it takes several days to conduct extensive surveys, and (3) the "permanent" reference markers are commonly buried by sand or destroyed where the beach is rapidly eroding. Also there can be large errors if volumetric changes are estimated from inadequate data. Estimates of volumetric beach changes can be significantly improved if the beach is surveyed by an intersecting grid of profiles oriented both perpendicular and parallel to the shoreline. By providing a more accurate representation of the actual beach surface, a grid of profiles can reduce the error that currently is introduced when unknown elevation changes between profiles are ignored or estimated by interpolation.

A primary advantage of beach profiles is that the uncertainties of the wet beach-dry beach line are eliminated and observations of shoreline movement are based on actual field measurements rather than interpreted from aerial photographs. Another advantage of beach profiles is that frequent comparisons yield information about two-dimensional beach changes that can be used to calculate the volume of sediment added to or removed from the beach. These volumetric estimates of sediment movement cannot be accurately derived from aerial photographs.

Profiling is a rapid and inexpensive field method best suited for documenting changes in beach shape and evaluating the magnitude of seasonal or short-term movement in shoreline position. Normally beach profiles are not used to establish long-term trends of shoreline movement because more than a decade of continuous data is needed before the long-term trend can be established with confidence (Eliot and Clarke, 1989).

The shoreline changes presented in this report are based on compilation of shorelines from maps and aerial photographs, but not from beach profiles. However, the Bureau of Economic Geology has surveyed beach profiles for the entire Texas coast and has been monitoring profiles along the upper coast between Sabine Pass and Follets Island for several years. Several profiles along Galveston Island have been monitored annually since 1983 (Morton and Paine, 1985).

### GPS Surveys

GPS (Global Positioning System) is an advanced satellite-based electronic surveying technology that is being adapted to measure shoreline movement. It will be the field method most widely used to survey beaches and bluffs in the future. Originally developed by the U.S. Department of Defense for military applications, GPS is now used extensively for civilian navigation and surveying (Leick, 1990). A constellation of satellites orbiting in space transmit radio signals that are received by GPS equipment on

the ground. Atomic clocks determine how long it takes for the radio signal from each observed satellite to reach the receiver, and this information is electronically converted to determine precise geographic positions including latitude, longitude, and elevation.

A potential disadvantage of GPS is the inaccuracy that is introduced by selective availability. This procedure, controlled by the Department of Defense, deliberately degrades the radio signal transmitted by some satellites to prevent unauthorized users from determining precise locations, especially during war. This means that positions obtained by a single GPS receiver will only be accurate within about 300 ft of its actual position. Because of selective availability, the locations provided by single GPS receivers are not accurate enough to map shoreline positions.

Differential GPS techniques were developed to eliminate the uncertainty introduced by selective availability. In the differential mode of operation, two receivers are used; one stays at a reference point and the other moves about conducting the survey. The reference point is at a location such as a surveying monument or benchmark where the latitude, longitude, and elevation are known.

Beaches are nearly ideal environments for conducting GPS surveys because the field of view with the satellites is largely unobstructed. However, some developed shores may impede or prevent GPS surveys because of interference with the satellite signals. Isolated structures near the beach such as tall buildings may cause some minor shading, whereas dense high-rise developments may entirely block the signal from satellites near the horizon or cause multipath reflections severe enough to invalidate the surveys.

Techniques have been developed to accurately survey beaches by mounting a GPS antenna on a vehicle. Horizontal distances and elevations are recorded as the vehicle drives up and down the beach. An advantage of vehicle-mounted GPS surveys is that they can provide rapid, relatively inexpensive and repeatable topographic information over long distances with minimal manpower and equipment (Morton and others, 1993).

The entire beach surface between the water line and the dune line can be surveyed using GPS techniques. Shoreline positions can be frequently updated and changes in sediment volume can be determined by comparing the surfaces recorded by repeated surveys of the same beach segment. GPS surveying techniques provide positions without the need for permanent reference marks. Therefore they are particularly well suited for monitoring beaches where the reference marks may be destroyed during a storm.

Although beach monitoring will likely utilize GPS in the future, these techniques are in the developmental stage and are not commonly used to monitor beaches. At present the Bureau of Economic Geology is using GPS equipment to map the beach surface on a short segment of Galveston Island. This experimental work is being conducted to improve the methods and to establish a protocol for coastwide application (Morton and others, 1993). None of the shoreline changes presented in this report are based on GPS surveys.



## QUANTIFYING SHORELINE MOVEMENT

### Comparing Shoreline Positions

To many people the words *accuracy* and *precision* have the same meaning and they are often used interchangeably. But to scientists and engineers the words have different meanings as they pertain to shoreline mapping and shoreline-change analyses. Accuracy involves correctly identifying the long-term trends of shoreline movement (erosion, stability, accretion), whereas precision involves exactness in quantifying both the rates of movement and the variability of those rates. With computers and expensive mapping equipment we can measure the shorelines very precisely and calculate the rates of change to many decimal places, but this high level of precision is meaningless if the shoreline comparisons are not accurate.

To maximize the accuracy of comparing shorelines, many workers plot shorelines from maps and aerial photographs onto large-scale topographic base maps. Enlarged base maps allow highly precise measurement of shoreline movement; such precision is not always appropriate, however, because it may greatly exceed the mapping accuracy of the original shoreline (the wet beach-dry beach line).

Measurements of shoreline movement can be made directly from the base maps or the compiled shorelines can be digitized and entered into a geographic information system (GIS) for further processing and storage. Shorelines can also be digitized directly from the original topographic maps and aerial photographs. The errors related to digitizing and analyzing shoreline movement are listed in table 1. The GIS methods of comparing shorelines employ "rubber sheeting" or statistical least-squares adjustments designed to correct for distortions as well as different projections and scales of the original materials (Leatherman, 1983).

Digital formats and geographic information systems facilitate the comparison and printing of shoreline information; however, computers do not improve the accuracy of the original shoreline positions. Computers can increase the precision of mapping and statistical analyses, but the degree of accuracy depends entirely on the position of the shoreline indicator and its location within the spectrum of shoreline fluctuations (fig. 2).

The shoreline positions presented in this report as tables and illustrations (appendices A and B) were optically transferred to topographic base maps from the original materials. The compiled shorelines were then digitized from the base maps and formatted in files using ARC/INFO, which is the GIS used by the Bureau of Economic Geology. ARC/INFO is a common GIS that also is used by many State and Federal agencies as well as companies. Quality control was performed on the digital shoreline data to ensure that they conformed to standards established for the shoreline compilations.

## Presenting Shoreline Changes

Historical changes in shoreline position are usually presented as maps, in tables, and on graphs. All three forms of data presentation have advantages and disadvantages compared to the other two (table 3). Maps of sequential shoreline positions (fig. 4) illustrate shoreline movement as a series of lines that can be compared to determine whether the beach is stable, accreting, or eroding. The example map from Sargent Beach, Texas (fig. 4), depicts a rapidly eroding beach where sediment supply is so low that each subsequent shoreline position is far landward of the previous position and the beach does not accrete at any time. The map view allows the user to see where the shoreline is relative to other features (buildings, streets, inlets) and where the shoreline has been and to infer where it might be in the future. The rapid retreat of this beach segment can also be expressed in a table that contains the shoreline dates as well as distances and rates of shoreline movement (table 4). These numerical data quantify what is illustrated on the map and reduce the shoreline movement to an average rate of change expressed in distance per unit time, such as feet/yr or meters/yr. Graphs depicting shoreline movement through time illustrate the long-term trends and short-term variability, which also can be used to predict future

Table 3. The common forms of expressing shoreline movement and their utility.

Maps	Tables	Graphs
<b>Advant</b>		
1. Represent original data	1. Easy to duplicate	1. Easy to duplicate
2. Provide continuous shoreline coverage	2. Distances and rates of change are provided	2. Illustrate the history of shoreline movement
3. Easy to determine locations	3. Calculations or interpretations not required	3. Provide an empirical (visual) basis for predicting future beach stability
<b>Disadvant</b>		
1. May be difficult or expensive to duplicate large maps	1. Shoreline coverage is discontinuous	1. Shoreline coverage is discontinuous
2. Distances and rates of change are not provided	2. Locations must be determined from a map	2. Locations must be determined from a map
3. Interpretation is required	3. Important changes in shoreline movement may not be obvious	3. Rates of change are not provided
4. May be difficult to predict future beach stability if several shorelines are mapped	4. May be difficult to predict future beach stability if several time periods are presented	4. Some interpretation of plots may be required

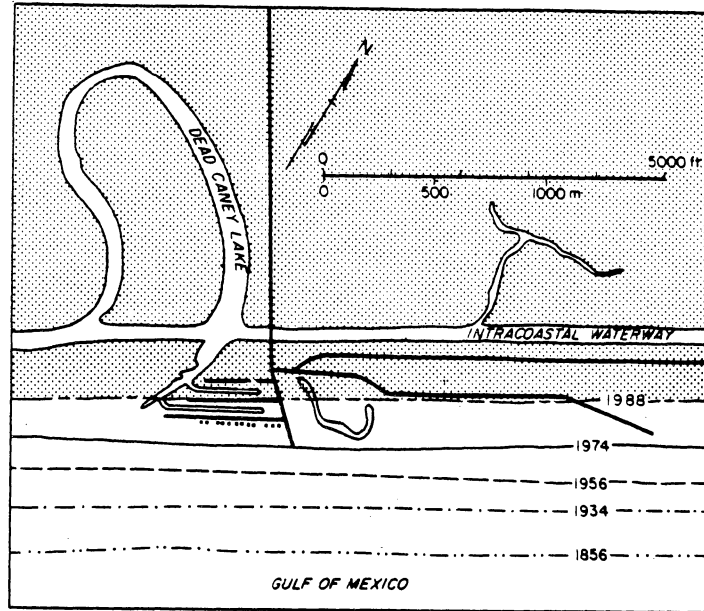


Figure 4. Map showing historical shoreline positions and rapid erosion at Sargent Beach, Texas.

Table 4. An example of historical shoreline changes and rates of change.

Period	1856–1934	1934–1956	1956–1974	1974–1988	1856–1988
Distance (ft)	-650	-600	-475	-440	-2165
Rate (ft/yr)	-8.4	-22.6	-23.6	-31.4	-16.5

shoreline positions. These plots contain three fields that represent stability, accretion, and erosion (fig. 5). Data that plot around the zero axis show that the shoreline position has fluctuated but that over the long-term period the beach position has remained nearly unchanged. In contrast, data that plot to the positive or negative side of the graph record long-term accretion or erosion (fig. 5).

The shape and slope of the line connecting a series of shoreline positions can also be used to interpret the relative rate of change and to predict future shoreline positions. In the example (fig. 6), the best linear statistical fit is not a straight line (fig. 6b) but a curved line that is flatter in recent time (fig. 6a). This shows that the rate of erosion has increased or accelerated in recent years. If the rate of erosion had decreased, then the curve would be steeper.

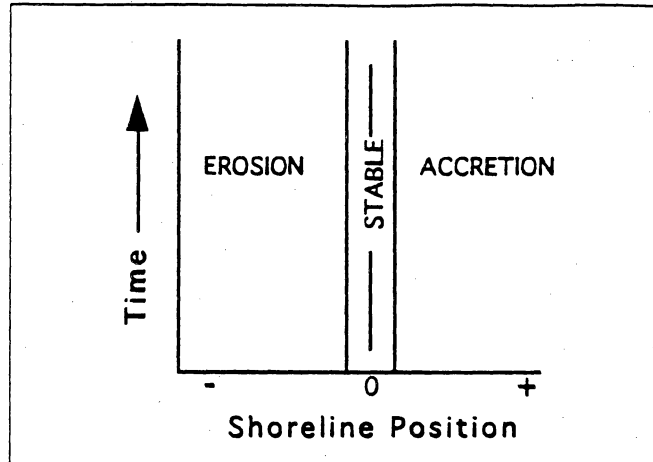


Figure 5. Generalized graph of shoreline position through time illustrating fields of beach stability.

#### Interpreting Graphical Displays

Most shorelines are dynamic and fluctuate within a predictable range of horizontal displacements regardless of their long-term stability. Furthermore, few shorelines are truly static during historical time periods, and static shorelines are profoundly different from stable shorelines. Few attempts are made to distinguish between stable and static shorelines, probably because both shoreline types exhibit no discernible net change in position. *Static shorelines*, which are invariant in their position, are products of unique conditions; they are unable to move because they are trapped against rocky cliffs, seawalls, or other immobile material with a steep slope. On the other hand, *stable shorelines* are also dynamic. They may exhibit relatively large, high-frequency fluctuations in position and still remain stable as long as their oscillations maintain an average position that does not change (fig. 5).

Shoreline positions derived from maps, aerial photographs, or ground surveys represent individual points in a continuum of shoreline movement. Most studies of shoreline changes are normally based on five to eight shoreline positions spanning as much as 150 yr (figs. 4 and 6). Studies of that duration typically employ two distinctly different data densities. The lowest data density is for the first 100 yr when shoreline movement is determined from two or three maps. In contrast, most of the shoreline movement data were collected during the past 50 yr and the highest data densities are available for the past 30 yr (figs. 6–8). The increased number of shoreline positions since 1960 provides a better measure of the short-term beach fluctuations and a way of distinguishing the long-term trend from the short-term fluctuations.

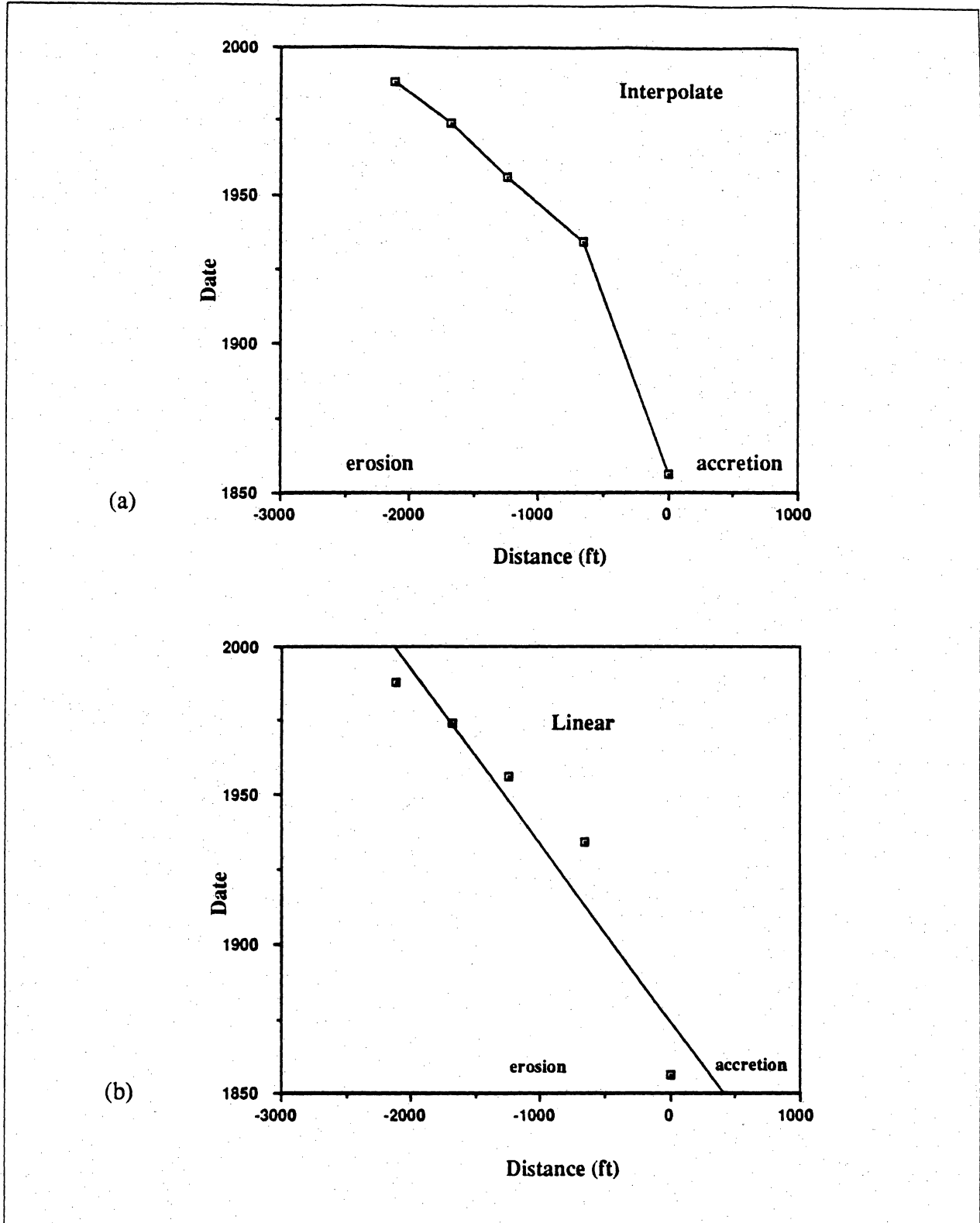


Figure 6. Graph of shoreline position through time showing rapid erosion at Sargent Beach, Texas.

Plots of cumulative shoreline movement at representative beach transects are shown in figures 6 through 8. These plots illustrate beach changes as if viewers were standing on the shore looking down the beach with the Gulf to their right and the land to their left. With this orientation and frame of reference, beach erosion is to the left and beach accretion is to the right.

The plots of cumulative shoreline movement commonly illustrate different rates of movement or reversals in shoreline movement (figs. 6–8). These plots also provide a basis for fitting statistically derived regression trends that can be used to predict future changes. The graphs of shoreline movement are useful for visualizing the long-term trends and for recognizing unusual departures from the trend (figs. 7 and 8). They also show how short-term shoreline positions oscillate around the average trend and how large excursions tend to cancel one another so that a relatively smooth shoreline form and orientation are maintained.

Distinguishing the actual trend of shoreline movement from “noisy” data is easy when the trend is uniform and the rate of change is so large that it cannot be confused by high-frequency beach cyclicity (fig. 6). On the other hand, this task of differentiation is extremely difficult for relatively stable beaches that experience large seasonal fluctuations. This is especially true of some dynamic sandy beaches that were stable or accreting on geological time scales but are beginning to erode as a result of both natural and human-induced decreases in sediment supply and a rise in relative sea level (Morton, 1979). For some of these transitional beaches, the short-term beach fluctuations exceed the long-term movement measured on consecutive aerial photographs (see fig. 7, 1937–1974).

Analytical problems associated with nonuniform and nonlinear shoreline changes are illustrated in figure 9, which shows two actual trend reversals near the mouth of the Brazos River that can be explained by examining historical documents and evaluating coastal processes. In figure 8, the rate of landward retreat of the shoreline between 1853 and 1930 is similar to the long-term erosion trend for this coastal compartment before navigation projects at Freeport Harbor altered the littoral system. The reversal in trend at 1930 is the result of river diversion and delta construction that caused rapid outbuilding of the shoreline at the mouth of the new Brazos River. A reduction in sediment supply after 1956 and focusing of wave energy on the delta caused renewed but more rapid erosion of the shoreline. In this example, the 1982 shoreline is still far seaward of the 1853 shoreline (net accretion), but the most recent trend is erosion and there was a decrease in the rate of erosion between 1956 and 1982. Calculated net rates of change would erroneously indicate long-term accretion when clearly the most recent trend and predicted future trend is erosion.

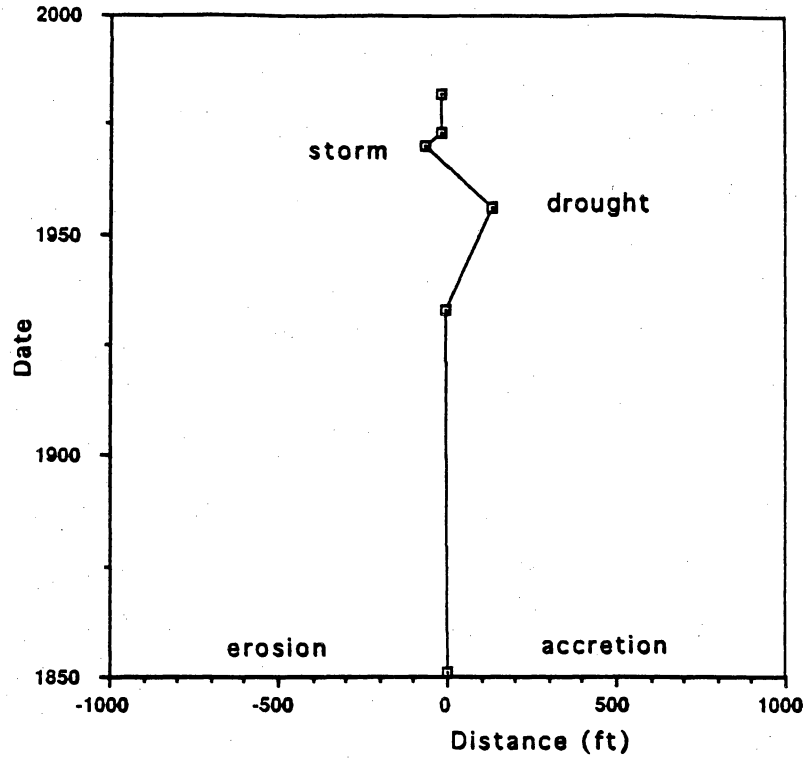


Figure 7. Anomalous shoreline movement related to droughts and storms.

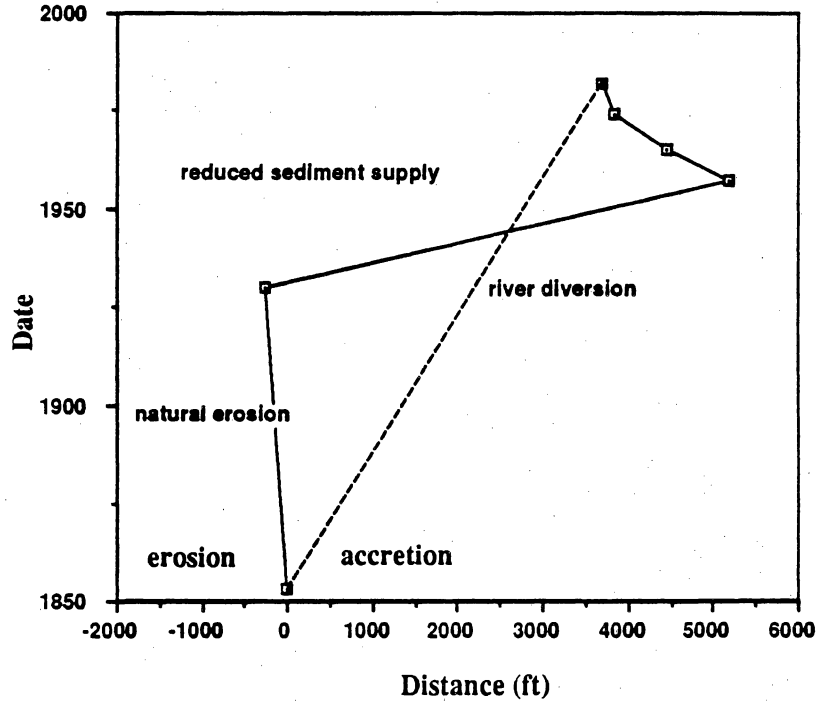


Figure 8. Graph of shoreline position through time showing reversals in the long-term trend of shoreline movement.

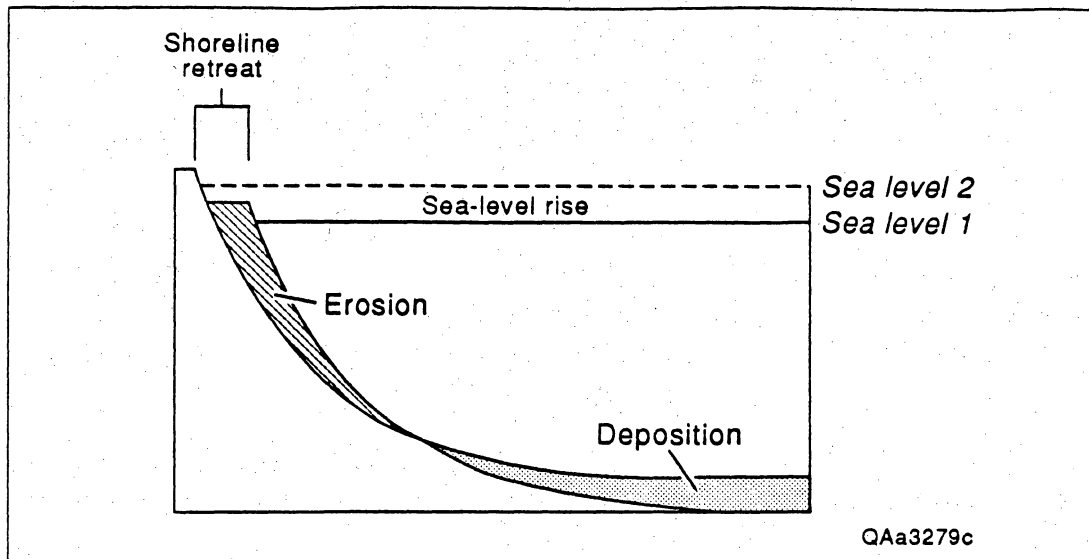


Figure 9. Illustration of the Bruun Rule that relates shoreline retreat to a rise in sea level. From Bruun (1962).

#### Calculating Rates of Change and Predicting Future Positions

Two assumptions are made when shoreline movement is analyzed, regardless of the sources of shoreline positions. First is the assumption that the state of shoreline stability does not change during each monitoring period. This assumption of uniformity requires continuous beach erosion, accretion, or stability throughout the entire monitoring period without any reversals in trend. If reversals in trend are detected in the data, then the length of record should include as much older reliable data as possible (table 1). Extending the period of record will provide the best indicator of why the trend reversals occurred and how they should be factored into the predictions of future shoreline positions. The second assumption is that the rates of change are also constant for the same period. This assumption rules out accelerations or decelerations in shoreline movement. If shoreline movement is nonuniform, then the most recent rates of change should be used to predict future shoreline positions (table 1). If either or both of these assumptions is incorrect, then the calculated rates of change probably underestimate the actual rates of change for the period of interest (Morton, 1978).

Coastal planners commonly want to know the optimum period for updating maps and tables of shoreline movement. Considering the diversity and dynamics of open coasts, it is impossible to determine the optimum monitoring period without some knowledge of local beach dynamics. Such decisions must be based on local factors including frequency of storms, overall rate of erosion, seasonal differences in beach shape, and economic considerations. Data obtained from long-term shoreline monitoring should be used to establish the beach stability for a particular shoreline segment. If the



beach shape or trend of shoreline movement has not changed over the entire period of record and if for geological reasons that trend can be expected to continue, then the monitoring interval is not extremely critical unless the area is being rapidly developed. If, however, long-term shoreline monitoring indicates numerous reversals in trend, then the frequency of reversals might suggest an appropriate interval for future beach monitoring.

Net rates of shoreline change, based on the entire monitoring period, are commonly calculated to summarize the overall direction and speed of shoreline movement. Net rates of change are useful for characterizing long-term trends and for establishing relative rates of change, but calculations based on net shoreline changes clearly are not the best predictor of future changes. This is because the net change is a straight-line average determined by the first and most recent shoreline positions (figs. 6–8). The net change analysis does not provide for irregular changes in beach position (fig. 8) that are reported for many coastal areas.

#### COASTAL EROSION AND SUBMERGENCE MODELS

Now that coastal erosion and land loss are identified as important social issues, questions are asked about how much land will be lost in the future, where the shoreline will be at some particular time, which communities will be threatened by land loss, and how much land will be flooded if sea level continues to rise. To answer these questions, several methods (models) have been developed that project shoreline positions based on assumptions regarding past shoreline changes and estimated rates of future sea level rise. It should be remembered that all the predictive models are limited because they are unable to anticipate significant changes in the factors that cause or control shoreline movement and therefore their forecasts may not be very accurate. Despite the uncertainties involved in the model results, some planners may want to use the model predictions because they provide at least some basis for deciding about future use and development of the coast.

Models that estimate future land loss can be either qualitative or quantitative. Qualitative predictions of coastal evolution and future shoreline positions are based on a general understanding of how nearshore environments respond to changing oceanic conditions. Studies of modern coasts show that a rapid rise in sea level will cause narrowing of some barrier islands and accelerate the migration of other barriers while saltwater marshes will replace fresh and brackish water marshes. Also during a rapid rise in sea level uplands are converted to wetlands, flood plains are enlarged, and the area that would be inundated by storms of historical record are increased. These nonquantitative predictions of coastal change are useful for dramatizing what will happen in the future, but they are of little use when it comes to knowing where and when the changes will occur.

Table 5. Comparison of assumptions, advantages, and disadvantages for the different types of shoreline movement models.

	Model Type Assumptions	Advantages	Disadvantages
Statistical	Conditions that caused land loss in the past will not change in the future.	Easy to understand and apply. Projections are derived from average rates of shoreline change or simple equations. Relies on observed shoreline changes.	Predictions will be inaccurate if physical conditions at the site change significantly. Difficult to accommodate large reversals in shoreline movement.
Geometric	Shoreline retreat and land loss are mainly caused by submergence. The beach and offshore profile are smooth and unchanging. Equilibrium conditions must be achieved before maximum recession is reached.	Easy to project shoreline positions using topographic maps and an estimate of relative sea-level rise.	May greatly underestimate shoreline retreat when land loss is caused by erosion as well as submergence.
Combinations	Shoreline retreat and land loss are mainly caused by submergence. Conditions that caused land loss in the past will not change in the future.	Improved prediction over static geometric models	Predictions will be inaccurate if physical conditions at the site change significantly. Difficult to accommodate large reversals in shoreline movement.
Numerical	Shoreline retreat and land loss are mainly caused by waves. Sea level is constant. The beach and offshore profile are smooth and unchanging. The equations in the model accurately simulate the physical conditions.	Mathematically sophisticated models that attempt to simulate the interactions of complex physical processes.	Requires site-specific data for parameters that generally are unavailable. Requires site-specific knowledge of coastal behavior. Difficult to know if results are valid.

Quantitative predictions of future coastal erosion and land loss rely on either *statistical* models, *geometric* models, or *numerical (deterministic)* models. Even though all of these models are used to predict future shoreline positions, they are based on completely different assumptions (table 5) and analytical methods. For example, statistical models do not attempt to understand the causes of shoreline change. Instead, they depend on actual observations that presumably include the important conditions that cause shoreline movement. Geometric models emphasize how shoreline movement is controlled by beach slopes and shapes responding to increased water levels. Numerical (deterministic) models

attempt to explain shoreline movement as a series of equations. The equations are written to represent observed physical conditions and coastal processes.

Both geometric and numerical models rely on the concept of a nearshore profile that is in equilibrium with the coastal processes. Coastal engineers have suggested that offshore profiles are smooth and have a concave shape that is controlled only by the size of sand grains and the dissipation of wave energy (Dean, 1991; Bodge, 1992). On the basis of these and other assumptions, the engineers have expressed the generalized shape of the offshore profile as a mathematical equation (Bruun, 1962; Dean, 1991) that relates the profile shape to sediment characteristics. Recent investigations of offshore profiles, however, show that a single mathematical expression does not adequately represent all offshore profiles (Bodge, 1992). Pilkey and others (1993) discussed the assumptions of the equilibrium profile and presented strong arguments that challenge the validity of the concept. Because an equilibrium profile does not exist at most coastal sites, they also questioned the validity of shoreline-change models that incorporate equilibrium profile conditions. Our incomplete understanding of complex coastal processes and the lack of an equilibrium profile are the main reasons why geometric and numerical models are unable to give reliable predictions of shoreline changes several decades into the future.

#### Statistical Models

Simple statistical models assume that shoreline movement in the future will be similar to movement in the past. Therefore, the historical record of observed changes is the best predictor of future changes. Simple statistical models also reduce the observed shoreline changes to a single value, which represents the average rate of movement. This rate of movement is then extrapolated to estimate future shoreline positions. Dolan and others (1991) summarized the most common linear analyses of shoreline movement and described the advantages and disadvantages of each technique. None of the linear time-averaging techniques used to calculate rates of change are appropriate if the historical record contains large reversals in the trend of shoreline movement (fig. 8). To accommodate irregular shoreline movement, Fenster and others (1993) developed a statistical method of analyzing historical shoreline changes and determining which data should be used to predict future changes.

Computer graphics programs can convert shoreline dates and positions to scatter diagrams (figs. 6–8), and they can generate regression curves and equations representing the best statistical fit. When used properly, the equations are particularly helpful because they can be used to estimate a future shoreline position when the date (such as 2050) or elapsed time (next 50 yr) is specified by the user.

Rates of shoreline change are generally reported as single values without the benefit of error bars indicating the uncertainty of projected shoreline positions. Furthermore, errors associated with the

predicted rates of change are magnified by at least 10 times and as much as 60 times when they are used to define projected erosion zones (National Research Council, 1990). Therefore, minimizing the uncertainty of these predictions should be a primary objective of coastal research.

The primary advantage of statistical models is that the historical data are easy to obtain and understand, but there are some disadvantages: (1) the data are empirical, site specific, and not broadly applicable, (2) the analyses assume uniform (linear) shoreline responses even though they may be irregular (nonlinear), (3) statistical analyses can be strongly biased by data clusters and single anomalous shoreline positions, and (4) physical processes summarized in historical shoreline change records may not adequately represent future conditions. The most severe limitation of historical projections is that they are incapable of accurately predicting future responses if some condition is greatly altered. Predictions of climatic changes (Hoffman and others, 1983; Titus, 1988) clearly indicate that the rate of sea-level rise will probably accelerate and other factors such as variable substrate composition, sediment influx, and storm activity could invalidate the extrapolation of even recent erosion rates.

#### Geometric Models

Geometric models are based on the premise that shoreline retreat is caused primarily by a relative rise in sea level (fig. 9, table 5). They also employ several simplistic assumptions such as a smooth, curved equilibrium profile (no offshore bars) that does not change shape as the beach retreats. Also these models only allow for onshore and offshore movement of sediment (no alongshore movement) and they presume a water depth on the profile beyond which no sediment is eroded or deposited. These generalized assumptions must be valid in order for the models to make accurate predictions of shoreline positions. However, none of the assumptions can be universally demonstrated with field data (Pilkey and others, 1993).

Simple submergence models, such as the one used by Daniels (1992), employ ground slopes, elevations, and projected sea levels to predict future shoreline positions. This static topographic technique, which does not account for coastal erosion or sediment transport, is used to estimate areas of inundation, potential losses of wetlands caused by flooding, or transformation of wetland types. Coastal flooding models that assume one-dimensional passive inundation may be adequate for predicting land loss around estuaries, but they are inappropriate for predicting shoreline changes along ocean beaches. This is because simple submergence models may greatly underestimate the landward retreat of shores that erode as a result of sea-level rise.

Bruun (1962, 1983, 1988) presented the first and most frequently applied geometric model that graphically relates shoreline recession to a relative rise in sea level (fig. 9). Most numerical models employ the Bruun Rule or a similar relationship to estimate the horizontal movement of the shoreline

for a particular sea-level rise scenario. The original mathematical expression of the Bruun Rule assumes (1) an equilibrium offshore profile, (2) material eroded onshore is directly deposited offshore with no gain or loss in sediment volume, (3) only cross-shore transport occurs, (4) the increase in offshore profile elevation is equal to the rise in water level so that water depth remains constant, (5) the profile shape remains unchanged as it is shifted landward and upward, and (6) a water depth on the profile beyond which there is no active sediment transfer. The stringent closed-system requirements of an equilibrium profile, fixed closure depth, negligible alongshore transport, and conservation of sediment volume across the same profile cannot be met at most coastal sites.

The fundamental issue involving predictive geometric models is the shape of beach and nearshore profiles, for it is this parameter that determines the horizontal displacement of the shoreline relative to an incremental rise in sea level (Bruun, 1962). Pilkey and Davis (1987) found little agreement between measured recession along the North Carolina coast and those predicted by several geometric shoreline response models including the Bruun Rule. It is clear from the analysis of Pilkey and Davis (1987) that steep slopes of the shoreface are only appropriate for prediction of short-term shoreline recession (decades) whereas gentle slopes of the coastal plain are the geometries that control shoreline recession over centuries and millennia. According to the Bruun Rule, shoreline recession is 50 to 100 times the rise in relative sea level (Komar and others, 1991); however evidence from the late Wisconsin/Holocene sea level history shows that shorelines actually retreated 1,500 to 2,500 times the rise in sea level over broad continental shelves.

Field tests have confirmed the general validity of the Bruun Rule (Hands, 1983) at least along coasts where profiles could rapidly equilibrate relative to the rise in sea level. However, the Bruun Rule commonly does a poor job of predicting changes at a specific site. Dean (1990) has argued that the Bruun Rule may be a better predictor of general or average shoreline response rather than being a good predictor at a particular location. If the Bruun Rule only approximates general erosion trends, then it may have little relevance to many site-specific applications. Komar and others (1991) recommended using large error bars with shoreline predictions derived from the Bruun Rule as a reminder of the large uncertainty associated with the method.

Geometric models only predict maximum potential shoreline recession, and therefore they are unable to accommodate such things as the time lag before equilibrium conditions are reached. Another major deficiency of most geometric models is that they fail to take into account sediment transport or its long-term equivalent, sediment budget.

## Combined Statistical and Geometric Models

Some methods of predicting shoreline movement combine long-term rates of change, determined by air photo methods (taken as background change), with shoreline retreat predicted by the Bruun Rule (Bruun, 1962). Future sea-level scenarios, such as those forecast by EPA (Titus, 1988), provide the input for estimating probable magnitudes of sea-level rise for the period of interest. An example of the hybrid method of predicting shoreline response was presented by Kana and others (1984) in their analysis of potential inundation at Charleston, South Carolina.

Although most land loss models focus on coastal erosion, one model has been specifically developed to investigate wetland changes and wetland losses as a result of predicted sea-level rise. Park and others (1989) developed the SLAMM model (Sea Level Affecting Marshes Model) to analyze what impacts a long-term (>100 yr) accelerated rise in sea-level would have on the composition and distribution of coastal wetlands. The model starts with initial conditions (wetland classes and elevation at a particular site) then predicts future conditions in time steps by combining geometric inundation (sea-level rise scenario) with coastal erosion (Bruun Rule). Although the model does not explicitly simulate salinity changes, it does accommodate sediment accumulation as well as inland wetland migration and conversion of biotic assemblages. Results of the study (Park and others, 1989) suggested that nearly half of the existing marshes and swamps in the contiguous U.S. would be destroyed if sea level rises 1 m during the next century. These models also predict a net loss of wetlands because old wetlands will be destroyed faster than new marshes can form.

## Numerical (Deterministic) Models

Numerical models, also known as deterministic models, presume that shoreline changes are mainly caused by wave energy (table 5). Like the geometric models, most of the deterministic models also assume a smooth, curved offshore profile that does not change shape as the beach retreats, only onshore and offshore movement of sediment, and a water depth on the profile beyond which no sediment is eroded or deposited (Bruun, 1962; Perlin and Dean, 1985). Most of these models also assume that sea level remains constant for the period of time that shoreline movement is being predicted. At many coastal sites these assumptions are either invalid or oversimplifications.

Most numerical models are designed to predict shoreline changes of short coastal segments and for brief periods (less than a decade). They are intended to evaluate the effects of coastal structures on shoreline evolution or to simulate specific conditions such as storm-induced beach erosion or bathymetric changes (LeMehaute and Soldate, 1980; Kriebel and Dean, 1985; Perlin and Dean, 1985).

Numerical models of shoreline movement require site-specific values for such parameters as wave climate, alongshore and cross-shore sediment transport, and sediment budget. The common lack of local oceanographic and geological data coupled with the fact that nearshore hydrodynamics are nonlinear and therefore nonadditive means that prediction confidence rapidly declines after the first few years of simulation. Subsequent simulations are further hampered by a poor understanding of nearshore physical relationships, especially the relationship of sediment transport to forcing events and profile recovery after storms that is necessary as a starting point for the next simulation. The result of this uncertainty is a probability distribution of shoreline positions with confidence bands that define an envelope of possible future shoreline positions. Verification of these models is also hampered by the need for detailed oceanographic data collected for the same time period as the observed shoreline changes. This generally means a short historical record when both shoreline movement and oceanographic data were available. Numerical models also rely heavily on intuition and extensive local experience of the user at the site being modeled. If the local data and engineering expertise are not available, then the model results will probably be erroneous.

LeMehaute and Soldate (1980) developed a mathematical model to predict the evolution of bluffs and shores near coastal structures on the Great Lakes. Their model, which does include sea level as a time-dependent variable, employs the concept of equilibrium offshore profiles and a depth of profile closure on the shoreface. Kriebel and Dean (1985) formulated a procedure for estimating cross-shore sediment transport resulting from the nearly instantaneous beach and dune erosion during a storm. Although this model is based on the equilibrium profile concept, it addresses the problem of maximum erosion potential not being achieved because of rapidly changing conditions during the storm. Instead it emphasizes nearshore profile adjustment that depends on the storm surge. This model employs a generalized beach/dune profile where the dunes form the onshore limit of sediment motion. Thus it is not applicable to overwash beaches where dunes are low or absent and surface elevations are below the storm surge elevations. The Kriebel and Dean model has some applications with regard to delineating erosion hazard zones and locating coastal structures, but it only addresses one phase of beach cyclicality and therefore it is inappropriate for predicting long-term shoreline changes.

GENESIS (Generalized Model for Simulating Shoreline Change) is a one-dimensional numerical model used to predict changes in shoreline position caused by coastal structures (Hanson and Kraus, 1989). In addition to the basic assumptions of numerical models (table 5) GENESIS assumes that all sediment transport is alongshore and it does not recognize onshore and offshore sediment movement. The model can handle a shoreline up to 100 km long but a prediction period of only 10 yr. Basic input parameters are starting shoreline position, wave statistics, beach profiles and bathymetry, boundary conditions, and the configurations of engineering structures. Although GENESIS is capable of simulating longer shorelines and greater durations than most other models, it is not

applicable to open-coast changes that are tidally dominated, storm induced, or caused by water-level fluctuations and its greatest utility is for predicting transitions from one beach stability state to another (Hanson and Kraus, 1989).

Advanced mathematical models that can accurately predict shoreline erosion and coastal land loss are still in the formative stages of development because the coastal processes being simulated are complex and existing equations do not adequately describe the physics of sediment transport across the beach and offshore profile (LeMehaute and Soldate, 1980; Komar and others, 1991). Furthermore, there is a general lack of field data (wave climate, wave-field transformation, sediment budget, offshore bathymetry) for calibrating the models. Although some of the numerical models incorporate future magnitudes of sea-level rise, a fully three-dimensional model has not been developed that will distinguish among different pathways of coastal evolution depending on variable rates of sediment supply and sea-level rise. For example, slow rates of sea-level rise typically allow eroding barrier islands to maintain a dune ridge that retards erosion. In contrast, rapid rates of rise cause dune breaching, washover, and eventually barrier migration. During highest rates of sea-level rise the barrier is drowned in place, overstepped, and partially preserved on the inner shelf. Furthermore, the models do not adequately provide for variable sediment textures. The existing models have been developed, tested, and verified for sandy beaches but not for muddy shores despite the fact that many eroding coasts are composed of thin sand beaches overlying muddy estuarine and marsh deposits.

Shoreline movement and wetland changes of many coastal regions were reasonably consistent and predictable before economic development because they were primarily controlled by unaltered processes and the geologic framework. However, post-development human activities have caused large-magnitude imbalances in the natural forces. As a consequence of this induced disequilibrium, future predictions of coastal change will be more difficult to make and will require better quantification of human alterations.

## SUMMARIES OF SHORELINE MOVEMENT, TEXAS GULF COAST

### Methods

Historical shoreline changes presented in this report were derived from shorelines compiled on topographic base maps. The shorelines were then digitized and entered into ARC/INFO, the geographic information system used by the Bureau of Economic Geology. To determine shoreline movement at specific sites, shore-normal transects were constructed on the topographic base maps at intervals equal to 5,000 ft along the coast. In appendices A, B, and C, the transects are identified by letters and numbers that indicate the shoreline segment and transect number within that segment. The letters are



abbreviations for common geographic features that are familiar to coastal residents and government officials. The geographic abbreviations are listed in the captions for each appendix.

In this report, tables and graphs are used to summarize shoreline movement along the developed Gulf beaches and barrier islands of Texas (appendices A, B, and C). These tables and graphs are keyed to transect numbers that appear in all previous reports of Gulf shoreline changes published by the Bureau of Economic Geology. The transect numbers also are illustrated on the beach stability maps on file with the Texas General Land Office. At each transect, distances between successive shorelines were measured and rates of change were calculated on the basis of the magnitude of change for a specific period. Typical time periods used to calculate rates of change are as follows: mid to late 1800's to early 1930's, early 1930's to mid 1950's, mid 1950' to 1965-1970, 1965-1970 to 1974-1975, 1974-1975 to 1982, and 1982-1990 (appendices A, B, and C).

The rates of change used to characterize shoreline stability at each transect were calculated from the long-term trends, as illustrated in appendices A, B, and C. The period over which the rate of change was averaged was determined by the shape of the shoreline movement curve at each transect and specific knowledge regarding coastal processes and human modifications to the littoral system. This procedure eliminated older periods when the rate or trend of movement was significantly different and focused on the most recent periods of shoreline movement that will probably continue into the foreseeable future unless there is a major change in sand supply to the beach. Most of the average rates of erosion incorporated at least 60 years of data and none are based on less than 20 years of data based on aerial photographs and beach profiles.

A few graphs depicting shoreline movement (appendices A, B, and C) contain brief notations that pertain to segments of the curve or inflection points where the curve shape changes abruptly. The notations briefly explain the changes in the trend of beach movement (erosion or accretion) or in the rate of movement (faster or slower) compared to earlier time periods. More detailed explanations of the changes in shoreline movement are commonly contained in the original reports (Morton, 1974, 1975; Morton and Pieper, 1975a, 1975b, 1976, 1977a, 1977b; Morton and others, 1976; Paine and Morton, 1989).

Beach stability data are not presented for remote and sparsely developed segments of the coast such as between Sabine Pass and High Island, east and west Matagorda Peninsula, Matagorda Island, San Jose Island, and Padre Island National Seashore (north and central Padre Island). Summaries of shoreline movement for these and other undeveloped coastal segments are available in the original Bureau reports (Morton and Pieper, 1975; Morton and others, 1976; Morton and Pieper, 1977; Paine and Morton, 1989).

## High Island to Bolivar Peninsula

Since the late 1800's, most of the Gulf shoreline between High Island and Bolivar Peninsula has undergone cycles of erosion and accretion or stability. The predominant trends have been erosion from the 1800's to the 1930's, accretion from the 1930's to the 1950's, erosion from the 1950's to 1974, and accretion or stability since 1974. Some of the beach accretion or stability since 1974 may be the result of low water levels in February 1990 when the aerial photographs were taken. However, beach profiles surveyed between 1984 and 1992 at High Island and at Caplen on Bolivar Peninsula confirm the accretion or beach stability that was documented by comparing the shoreline positions mapped on aerial photographs.

Although the long-term trend reversals occur approximately every 30 years, the cycles are impossible to predict accurately, therefore the entire time period (1800's to 1990) was used to calculate the average rate of change at most transects. According to the 1990 shoreline position, the beach has experienced net erosion at transects 32-50, whereas the beach has experienced net accretion at transects 51-62 (appendix A).

## Galveston Island

After the jetties were constructed at the east end of Galveston Island, East Beach began accreting rapidly because sand was trapped between the south jetty and the seawall. The accretion continued until the 1950's, when the shoreline position stabilized (appendix A). Since then, East Beach has undergone minor erosion, but the net change since the mid 1800's is still accretion. All the other beach segments of Galveston Island have experienced net erosion between the mid 1800's and 1990. The greatest net erosion and the largest fluctuations in shoreline position on Galveston Island have occurred at the southwestern end of the island near San Luis Pass.

At many transect sites on West Beach, erosion began or accelerated after 1956. Beach profiles surveyed by the Bureau of Economic Geology since Hurricane Alicia in 1983 show that the highest sustained erosion rates on Galveston Island are southwest of the seawall. Shoreline movement since 1983 recorded by the beach profiles confirm the trends of beach erosion determined from the aerial photographs.

Graphs illustrating shoreline movement at transects along the Galveston seawall are presented in appendix A, but recent rates of shoreline movement were not calculated for those transects because there is no sand beach at some sites and the limited sand beach at other sites is controlled by the seawall and rock groins. A preliminary analysis of beach erosion at the Galveston seawall showed that erosion increased as the seawall interacted with the waves and currents, but then erosion rates

decreased as the sand supply in front of the seawall was depleted (Morton, 1988). Beach profiles surveyed by the Galveston District Corps of Engineers are the best available data for an analysis of shoreline movement along the seawall before and during the period when the sand supply was being depleted.

#### San Luis Pass to Sargent Beach

Plots of shoreline movement along Follets Island (transects 1–12) show net erosion dominated by erosion between the mid 1800's and 1974. Since 1974 the beach has accreted, probably as a result of sand transferred down the island by Hurricane Alicia. Some of the beach accretion or stability since 1974 may be the result of low water levels in January 1990 when the aerial photographs were taken. However, beach profiles surveyed between 1984 and 1992 on Follets Island confirm the accretion or beach stability that was documented by comparing the shoreline positions mapped on aerial photographs.

The large and complicated changes in shoreline position recorded at transects 13–28 are related to changes in sediment supply associated with engineering projects. The projects included construction of the jetties at Freeport Harbor and diversion of the Brazos River mouth. More recent changes between transects 25 and 28 are related to the southwestward migration of the new Brazos delta caused by the longshore transport of sand. The beach has undergone net accretion from transect 13 to transect 26, but the most recent trend of shoreline movement has been erosion between transects 15 and 24. The change from accretion to erosion is related to the reduction in sediment supply and reworking of the beach sediments by waves. Morton and Pieper (1975b) presented the history of shoreline changes caused by human alterations of the Brazos River.

From transect 27 to transect 42 the beach has undergone net erosion. In fact the beach has eroded systematically at all transect sites except at 27–29 where the most recent trend is beach accretion. The trend reversal from erosion to accretion at these three sites is caused by the southwestward transport of sand from the new Brazos delta. At most of the other sites, beach erosion increased rapidly after the Brazos River was diverted. Beach profiles surveyed at Sargent Beach by the Galveston District Corps of Engineers confirm the beach erosion that was documented by comparing the shoreline positions mapped on aerial photographs.

#### Mustang and North Padre Islands (Port Aransas to Padre Balli Park)

The beaches of Mustang and North Padre Island generally have undergone net erosion since the late 1800's (appendix B). Even where net accretion has occurred, the most recent trend is erosion. A consistent pattern of shoreline movement between transects 9 and 19 is as follows: erosion from the

late 1800's to 1937, accretion from 1937 to the late 1950's, and erosion from the late 1950's to 1982. Recent erosion on North Padre Island near the seawall (transect 20) and at Padre Balli Park (transect 22) are confirmed by beach profiles surveyed by the Bureau of Economic Geology (Morton, 1988) and by the removal of the bathhouse at the park that was abandoned because of beach erosion.

The beach on Mustang Island has undergone net accretion at transects 1-4 (appendix B) related to southward migration of Aransas Pass in the late 1800's and impoundment of sand by the south jetty at Aransas Pass. The anomalous net accretion at point 21 on North Padre Island was caused by closing of Packery Channel and advancement of the shoreline until it reached a position that was in line with the beach on either side of the former inlet. The beach at transect 21 did not accrete beyond the normal trend of the shoreline. The beach at this site has been eroding since about 1970.

#### South Padre Island (Mansfield Channel to Brazos Santiago Pass)

The beaches of South Padre Island generally have eroded continuously since the late 1800's (appendix C). Highest sustained erosion has occurred between transects 10 and 13, where the shoreline orientation changes and wave energy is focused on the protrusion of land. At many of the transect sites, the average rate of erosion is greater than 10 ft/yr.

Exceptions to the trend of systematic erosion occur where the littoral drift system has been disrupted by jetties at deep-draft navigation channels. The shoreline change profile at transect 3 (appendix C) shows continuous erosion until 1960 and then accretion after 1960 when the jetty was built at Mansfield Channel. The beach at this site is accreting because sand transported northward by longshore currents is trapped on the south side of the jetty. Similarly, beaches on the southern end of South Padre Island (transects 19-21) have been either stable or accreting since 1935 as a result of sand trapped by the north jetty at Brazos Santiago Pass.

#### ACKNOWLEDGMENTS

This work was funded in part by the U.S. Geological Survey Coastal Geology Program under cooperative agreement 14-08-0001-A0912. Additional funding was provided by the Galveston District Corps of Engineers, Matagorda County Commissioners Court, the Texas General Land Office, and the Town of South Padre Island. We thank all these supporters who made it possible to conduct the study. The report was edited by Amanda Masterson and designed by Margaret Evans. Final manuscript processing was by Susan Lloyd.

## REFERENCES

- Anders, F. J., and Byrnes, M. R., 1991, Accuracy of shoreline change rates as determined from maps and aerial photographs: *Shore and Beach*, v. 59, p. 17-26.
- Birkemeier, W. A., Bichner, E. W., Scarborough, B. L., McConathy, M. A., and Eiser, W. C., 1991, Nearshore profile response caused by Hurricane Hugo, *in* Finkl, C. W., and Pilkey, O. H., eds., *Impacts of Hurricane Hugo, September 10-22, 1989: Journal of Coastal Research, Special Issue 8*, p. 113-127.
- Bodge, K. R., 1992, Representing equilibrium beach profiles with an exponential expression: *Journal of Coastal Research*, v. 8, p. 47-55.
- Bruun, P., 1962, Sea-level rise as a cause of erosion: *Journal of Waterways and Harbors Division, ASCE, WW1*, p. 117-133.
- \_\_\_\_\_, 1983, Review of conditions for uses of the Bruun Rule of erosion: *Coastal Engineering*, v. 7, p. 77-89.
- \_\_\_\_\_, 1988, The Bruun Rule of erosion by sea-level rise: a discussion of large-scale two- and three-dimensional usages: *Journal of Coastal Research*, v. 4, p. 627-648.
- Crowell, M., Leatherman, S. P., and Buckley, M. K., 1991, Historical shoreline change: error analysis and mapping accuracy: *Journal of Coastal Research*, v. 7, p. 839-852.
- Daniels, R. C., 1992, Sea-level rise on the South Carolina coast: two case studies for 2100: *Journal of Coastal Research*, v. 8, p. 56-70.
- Dean, R. G., 1990, Beach response to sea level change, *in* LeMehaute, B., and Hanes, D. M., eds., *Ocean Engineering Science: The Sea*: New York, John Wiley, Inc., v. 9.
- \_\_\_\_\_, 1991, Equilibrium beach profiles: characteristics and applications: *Journal of Coastal Research*, v. 7, p. 53-84.
- Dolan, R., Fenster, M. S., and Holme, S. J., 1991, Temporal analysis of shoreline recession and accretion: *Journal of Coastal Research*, v. 7, p. 723-744.
- Dolan, R., and Hayden, B., 1983, Patterns and prediction of shoreline change, *in* Komar, P. D., ed., *Handbook of coastal processes and erosion*: Boca Raton, Florida, CRC Press, Inc., p. 123-149.
- Eliot, I., and Clarke, D., 1989, Temporal and spatial bias in the estimation of shoreline rate-of-change statistics from beach survey information: *Coastal Management*, v. 17, p. 129-156.
- Emery, K. O., 1961, A simple method of measuring beach profiles: *Limnology and Oceanography*, v. 6, p. 90-93.
- Fenster, M. S., Dolan, R., and Elder, J. F., 1993, A new method for predicting shoreline positions from historical data: *Journal of Coastal Research*, v. 9, p. 147-171.

- Hands, E. B., 1983, The Great Lakes as a test model for profile responses to sea level changes, *in* Komar, P. D., ed., *Handbook of coastal processes and erosion*: Boca Raton, Florida, CRC Press, p. 167-189.
- Hanson, H., and Kraus, N. C., 1989, GENESIS: Generalized Model for Simulating Shoreline Change, Report 1: U.S. Army Corps of Engineers, Coastal Engineering Research Center, Technical Report CERC 89-19, 185 p.
- Hoffman, J. S., Keyes, D., and Titus, J. G., 1983, Predicting future sea level rise: methodology estimates to the year 2100: Washington, D.C., U.S. Environmental Protection Agency, 2nd edition, 121 p.
- Kana, T. W., Michel, J., Hayes, M. O., and Jensen, J. R., 1984, The physical impact of sea level rise in the area of Charleston, South Carolina, *in* Barth, M. C., and Titus, J. G., eds., *Greenhouse effect and sea level rise*: New York, Van Nostrand Reinhold Company, p. 105-150.
- Komar, P. D., Lanfredi, N., Baba, M., Dean, R. G., Dyer, K., Healy, T., Ibe, A. C., Terwindt, T. H. J., and Thom, B. G., 1991, The response of beaches to sea-level changes: a review of predictive models: *Journal of Coastal Research*, v. 7, p. 895-921.
- Kriebel, D. L., and Dean, R. G., 1985, Numerical simulation of time-dependent beach and dune erosion: *Coastal Engineering*, v. 9, p. 221-245.
- Leatherman, S. P., 1983, Historical and projected shoreline mapping: *American Society of Civil Engineers, Coastal Zone '83*, v. 3, p. 1902-1909.
- Leick, A., 1990, *GPS satellite surveying*: New York, John Wiley, Inc., 352 p.
- LeMehaute, B., and Soldate, M., 1980, Numerical modelling for predicting shoreline change: U.S. Army Corps of Engineers, Coastal Engineering Research Center, v. 80-6.
- Morton, R. A., 1974, Shoreline changes on Galveston Island (Bolivar Roads to San Luis Pass): The University of Texas at Austin, Bureau of Economic Geology Geological Circular 74-2, 34 p.
- \_\_\_\_\_ 1975, Shoreline changes between Sabine Pass and Bolivar Roads: The University of Texas at Austin, Bureau of Economic Geology Geological Circular 75-6, 43 p.
- \_\_\_\_\_ 1976, Shoreline changes on Matagorda Island and San Jose Island (Pass Cavallo to Aransas Pass): The University of Texas at Austin, Bureau of Economic Geology Geological Circular 76-4, 42 p.
- Morton, R. A., 1978, Analysis of sequential shoreline changes, *in* Tanner, W. F., *Standards for measuring shoreline changes*: Tallahassee, Florida State University, Department of Geology, p. 43-50.
- Morton, R. A., 1979, Temporal and spatial variations in shoreline changes, Texas Gulf Coast: *Journal of Sedimentary Petrology*, v. 49, p. 1101-1111.

- Morton, R. A., and Paine, J. G., 1985, Beach and vegetation-line changes at Galveston Island, Texas: erosion, deposition, and recovery from Hurricane Alicia: The University of Texas at Austin, Bureau of Economic Geology Geological Circular 85-5, 39 p.
- Morton, R. A., 1974, Shoreline changes on Galveston Island (Bolivar Roads to San Luis Pass): The Morton, R. A., 1988, Interactions of storms, seawalls, and beaches of the Texas Coast, *in* Kraus, N. C., and Pilkey, O. H., eds., The effects of seawalls on the beach: Journal of Coastal Research, Special Issue 4, p. 113-134.
- Morton, R. A., 1991, Accurate shoreline mapping-past, present and future: American Society of Civil Engineers, Coastal Sediments '91, v. 2, p. 997-1010.
- Morton, R. A., Leach, M. P., Paine, J. G., and Cardoza, M. A., 1993, Monitoring beach changes using GPS surveying techniques: Journal of Coastal Research, v. 9, p. 702-720.
- Morton, R. A., and Pieper, M. J., 1975a, Shoreline changes on Brazos Island and South Padre Island (Mansfield Channel to Mouth of the Rio Grande): The University of Texas at Austin, Bureau of Economic Geology Geological Circular 75-2, 39 p.
- \_\_\_\_\_ 1975b, Shoreline changes in the vicinity of the Brazos River delta (San Luis Pass to Brown Cedar Cut): The University of Texas at Austin, Bureau of Economic Geology Geological Circular 75-4, 47 p.
- \_\_\_\_\_ 1977a, Shoreline changes on Mustang Island and North Padre Island (Aransas Pass to Yarborough Pass): The University of Texas at Austin, Bureau of Economic Geology Geological Circular 77-1, 45 p.
- \_\_\_\_\_ 1977b, Shoreline changes on Central Padre Island (Yarborough Pass to Mansfield Channel): The University of Texas at Austin, Bureau of Economic Geology Geological Circular 77-2, 35 p.
- Morton, R. A., Pieper, M. J., and McGowen, J. H., 1976, Shoreline changes on Matagorda Peninsula (Brown Cedar Cut to Pass Cavallo): The University of Texas at Austin, Bureau of Economic Geology Geological Circular 76-6, 37 p.
- National Research Council, 1990, Managing coastal erosion: Committee on Coastal Erosion Zone Management, Marine Board, National Academy Press, Washington, D.C., 182 p.
- Paine, J. G., and Morton, R. A., 1989, Shoreline and vegetation-line movement, Texas Gulf Coast, 1974 to 1982: The University of Texas at Austin, Bureau of Economic Geology Geological Circular 89-1, 50 p.
- Park, R. A., Trehan, M. S., Mausel, P. W., and Howe, R. C., 1989, Coastal wetlands in the twenty-first century: profound alterations due to rising sea level, *in* Davis, F. E., ed., Wetlands: Concerns and Successes: Tampa, Florida, Proceedings, American Water Resources Association Annual Conference, p. 71-80.
- Perlin, M., and Dean, R. G., 1985, 3-D models of bathymetric response to structures: Journal of Waterways and Ports, Coastal Ocean Engineering, Agricultural Stabilization and Conservation Service, v. 111, p. 153-170.

- Pilkey, O. H., and Davis, T. W., 1987, An analysis of coastal recession models: North Carolina coast, in Nummedal, D., Pilkey, O. H., and Howard, J. D., eds., Sea-level fluctuation and coastal evolution: Society of Economic Paleontologists and Mineralogists Special Publication 41, p. 59-68.
- Pilkey, O. H., Young, R. S., Riggs, S. R., Smith, A. W., Wu, H., and Pilkey, W. D., 1993, The concept of shoreface profile of equilibrium: a critical review: Journal of Coastal Research, v. 9, p. 255-278.
- Shalowitz, A. L., 1964, Shore and sea boundaries: U.S. Department of Commerce Publication 10-1, v. 2, 749 p.
- Stafford, D. B., 1971, An aerial photographic technique for beach erosion surveys in North Carolina: U.S. Army Corps of Engineers, Coastal Engineering Research Center, Technical Memorandum 36.
- Titus, J. G., ed., 1988, Greenhouse effect, sea-level rise and coastal wetlands: Washington, D.C., U.S. Environmental Protection Agency, EPA-230-05-86-013, 152 p.
- Wade, E. B., 1986, Impact of North American Datum of 1983: Journal of Surveying Engineering, v. 112, p. 49-62.

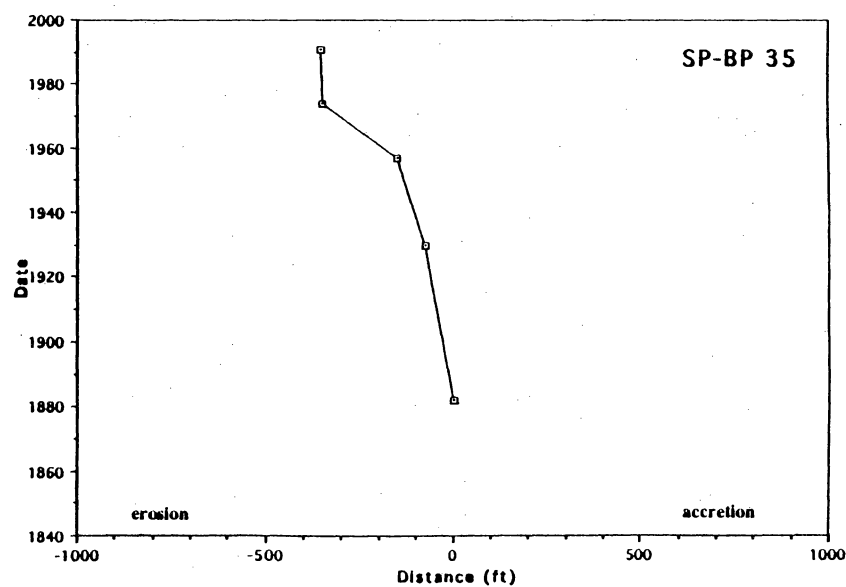
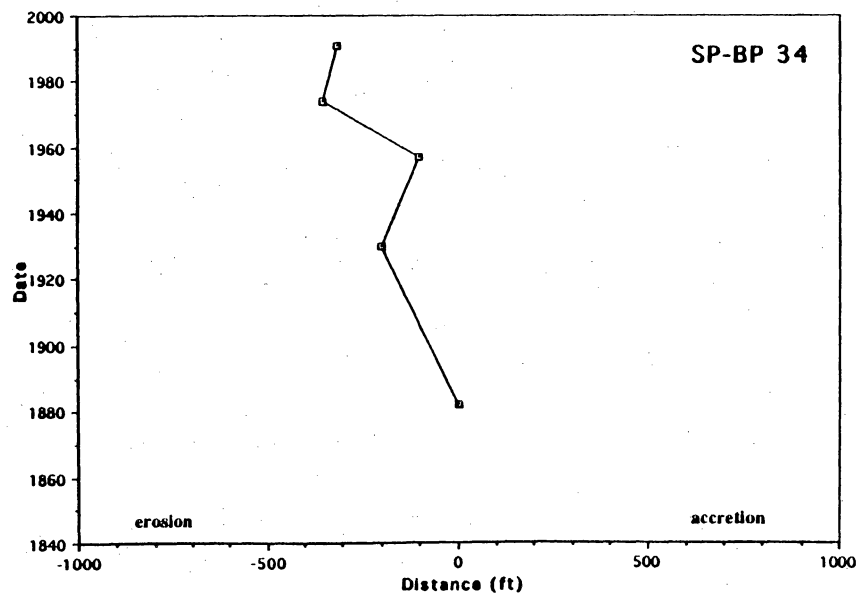
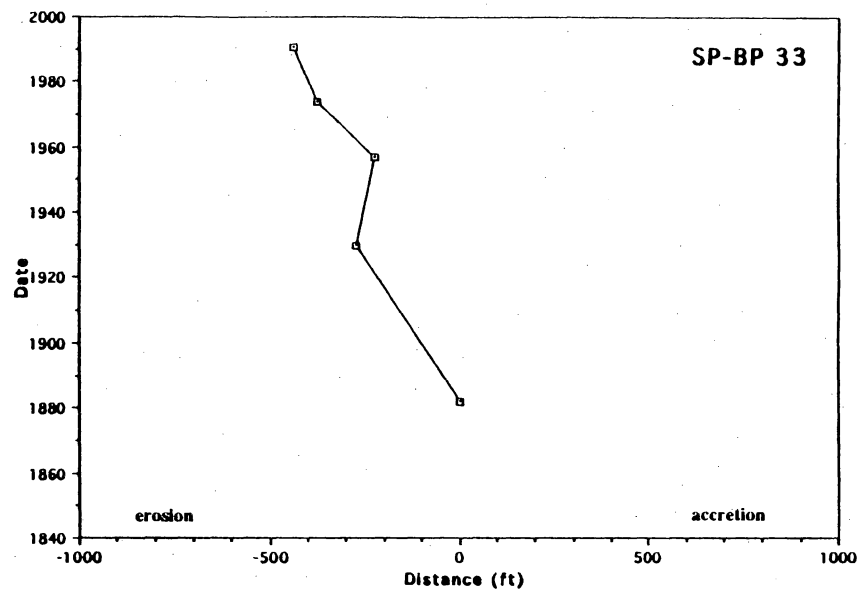
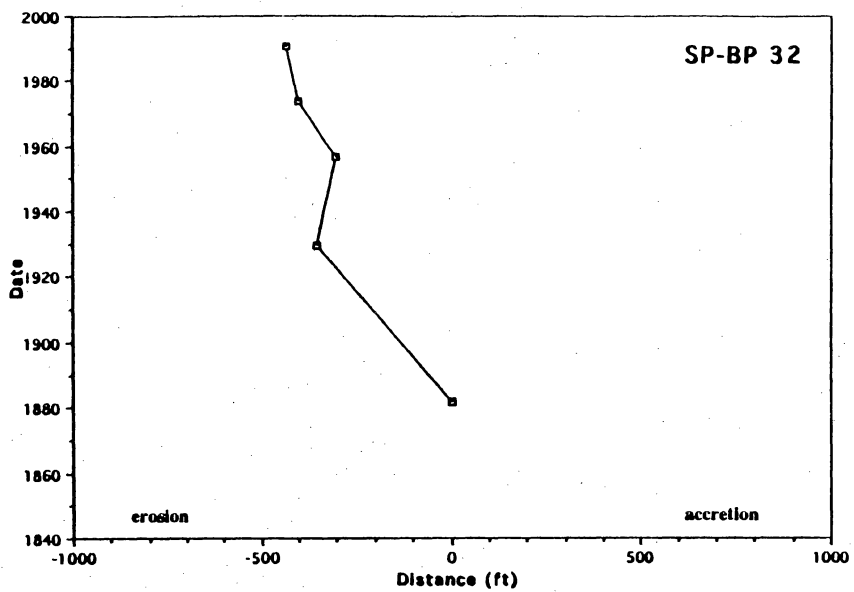


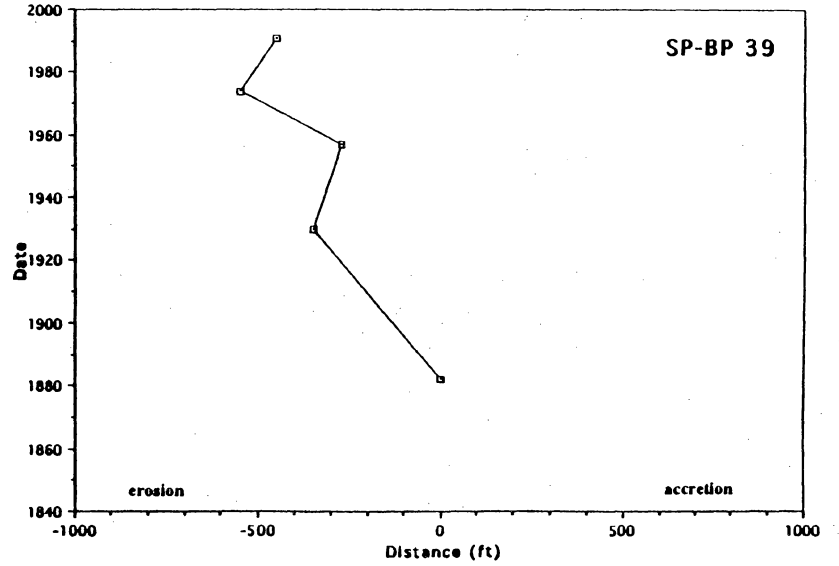
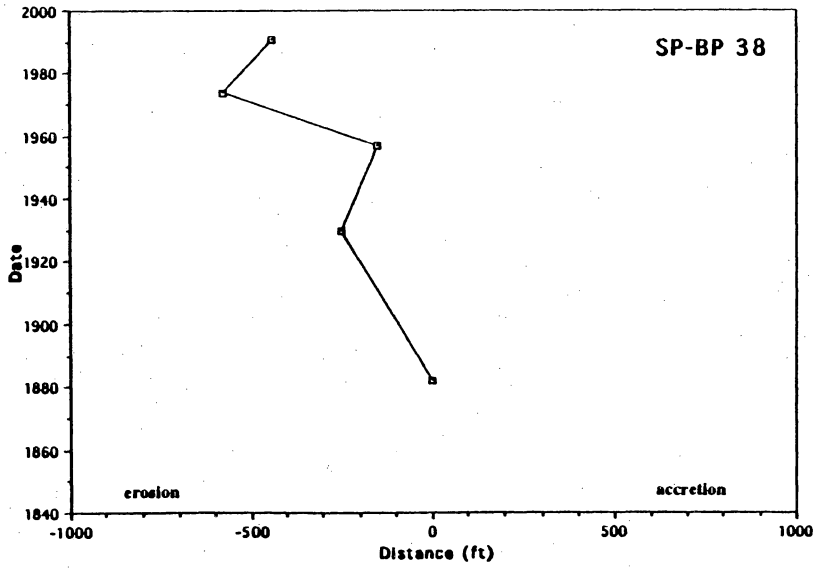
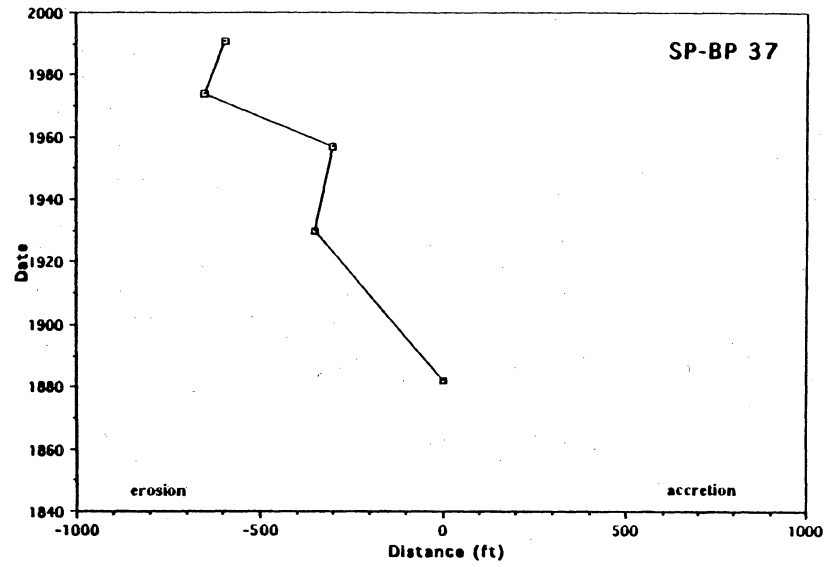
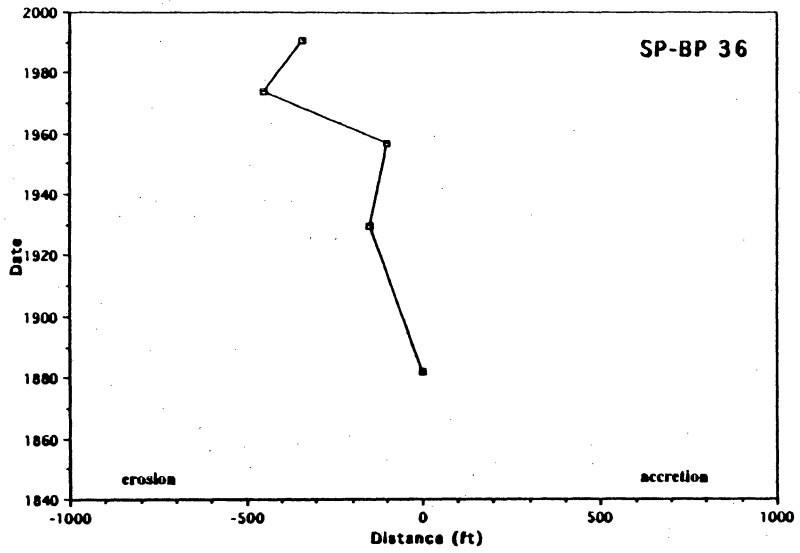
APPENDIX A. Tables and graphs of Shoreline Movement—High Island to Sargent Beach. Geographic abbreviations for graphs depicting movement of the Texas Gulf shoreline; Class Intervals: A = accretion, S = stability, 1 = -2 to -5 ft/yr, 2 = -5 to -10 ft/yr, 3 = >10 ft/yr.

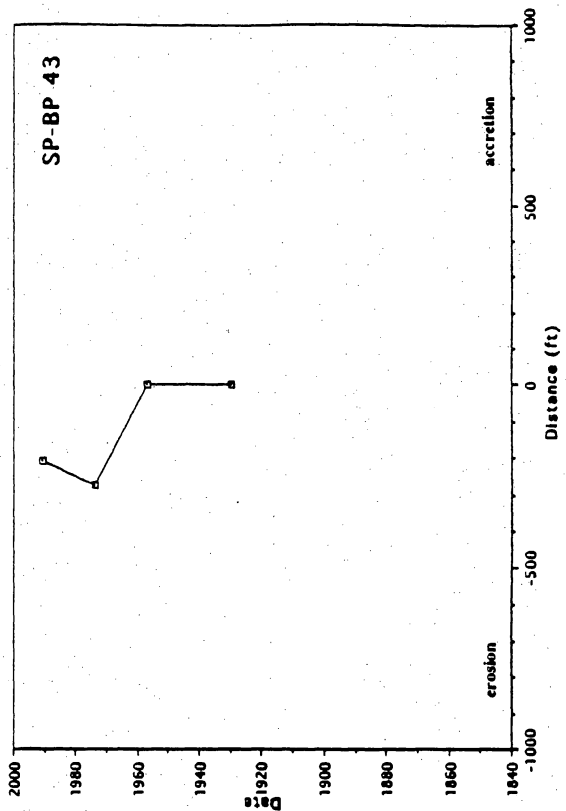
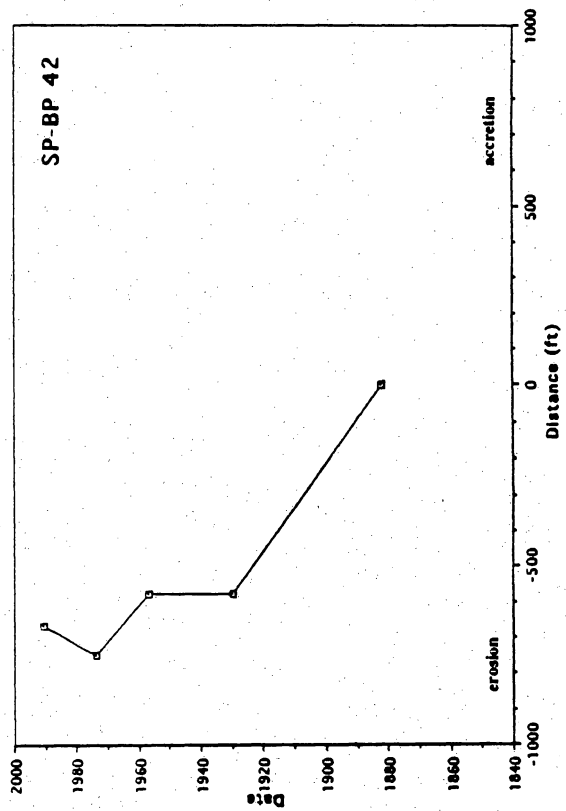
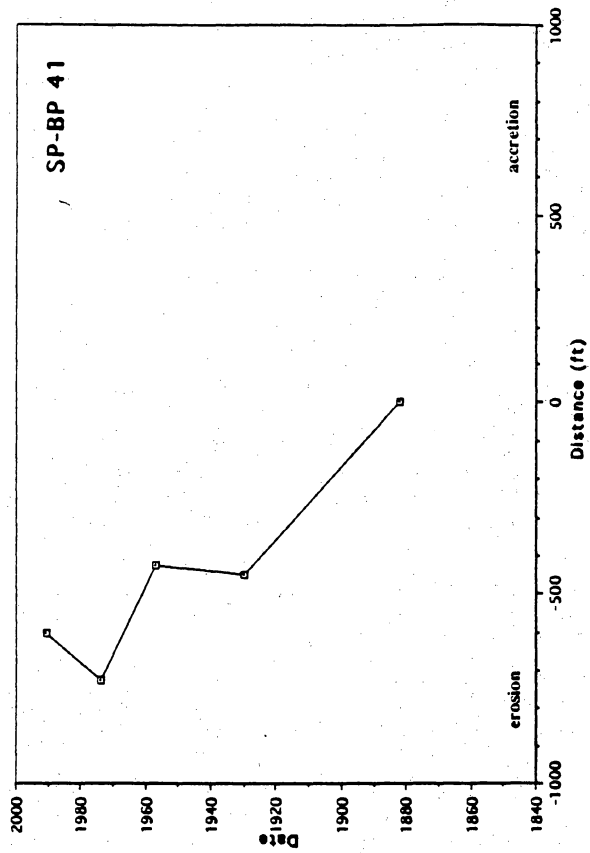
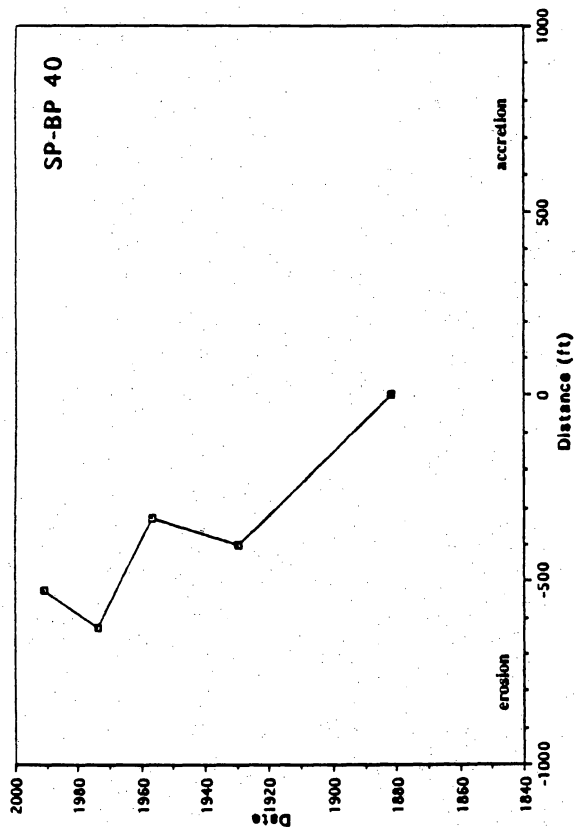
Shoreline Segment: Sabine Pass to Bolivar Roads

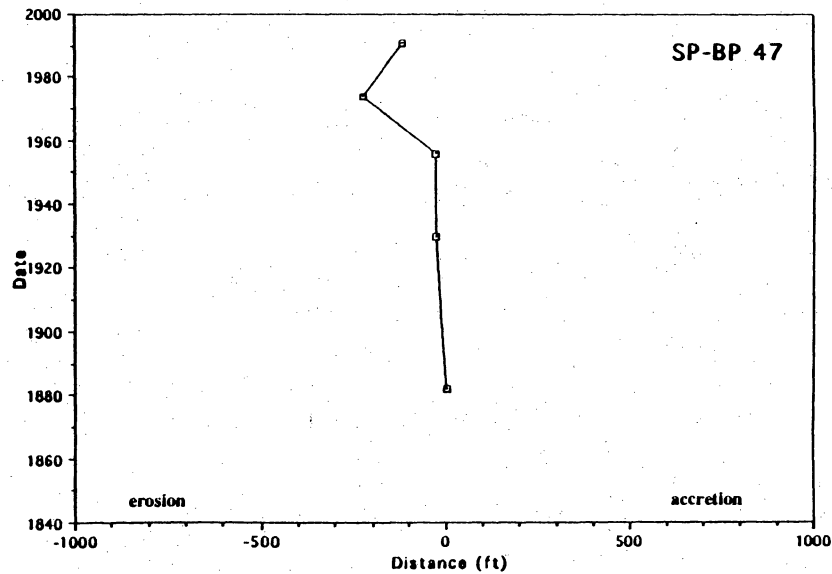
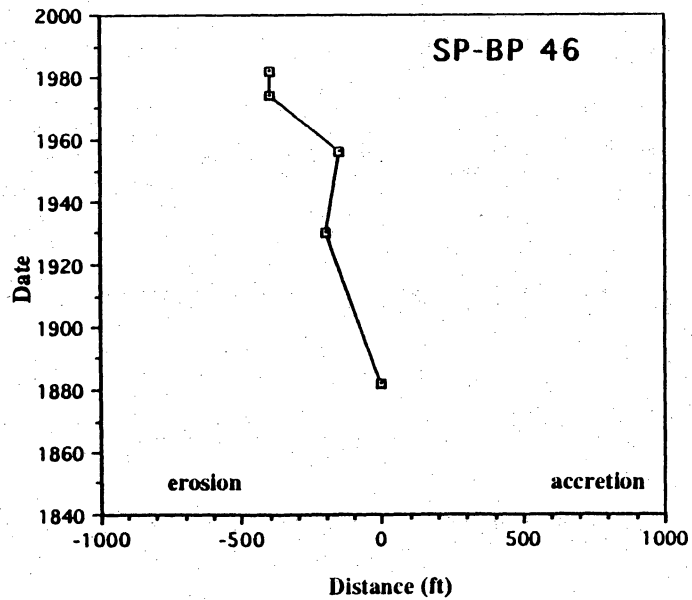
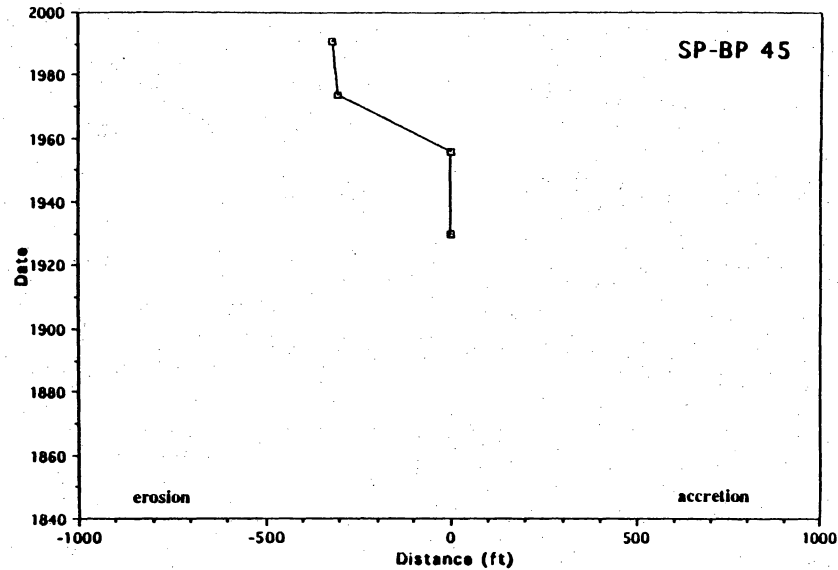
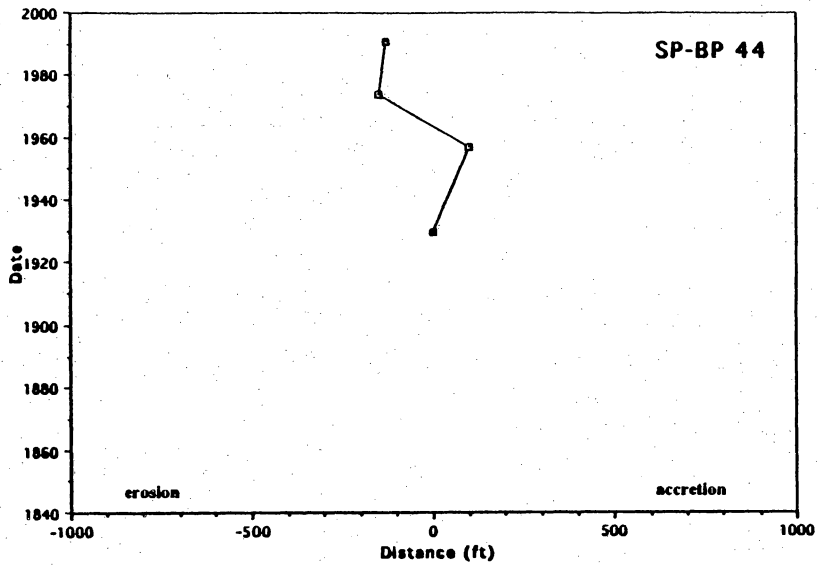
Transect	Period	Average rate (ft/yr)	Class interval
32	1930-1990	-4.0	1
33	1930-1990	-2.7	1
34	1882-1990	-2.9	1
35	1882-1990	-3.0	1
36	1882-1990	-3.1	1
37	1882-1990	-5.5	2
38	1882-1990	-4.1	1
39	1882-1990	-4.2	1
40	1882-1990	-4.9	1
41	1882-1990	-5.6	2
42	1882-1990	-6.2	2
43	1930-1990	-3.5	1
44	1930-1990	-2.2	1
45	1930-1990	-5.3	2
46	1882-1982	-4.0	1
47	1882-1990	-1.1	S
48	1882-1990	-1.3	S
49	1882-1982	-1.2	S
50	1882-1990	-0.9	S
51	1882-1990	+0.5	S
52	1882-1990	+1.3	S
53	1882-1990	+0.4	S
54	1882-1990	+0.2	S
55	1882-1990	+0.9	S
56	1882-1990	+1.0	S
57	1882-1990	+0.6	S
58	1882-1990	+0.9	S
59	1882-1990	+3.0	A
60	1882-1990	+6.8	A
61	1882-1990	+13.9	A
62	1882-1990	+27.2	A

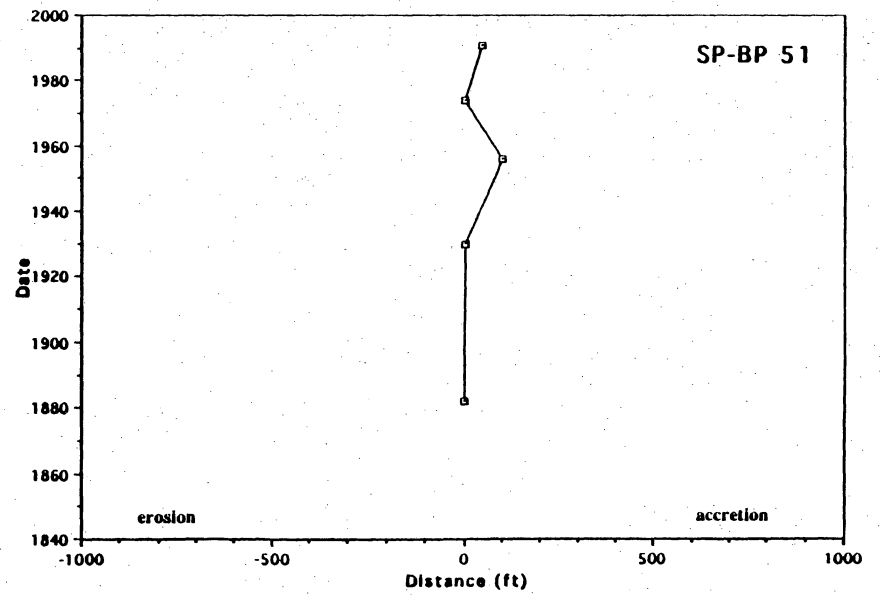
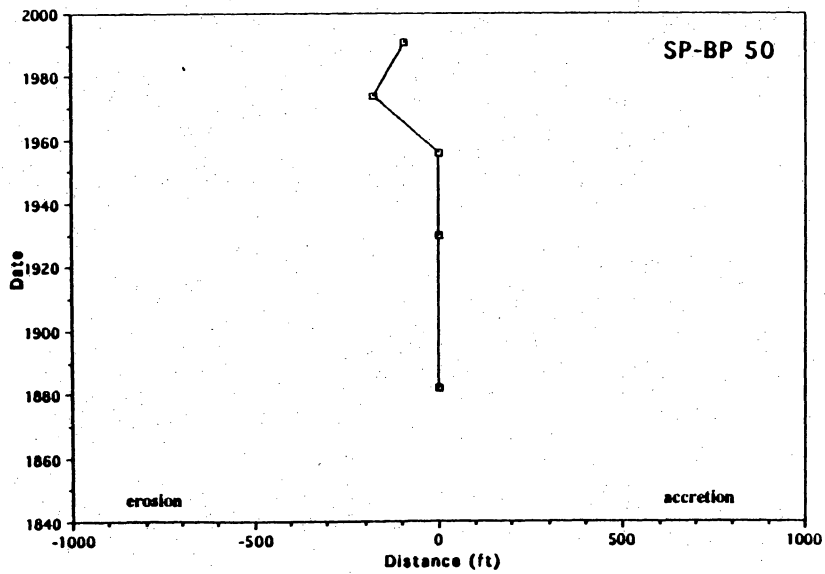
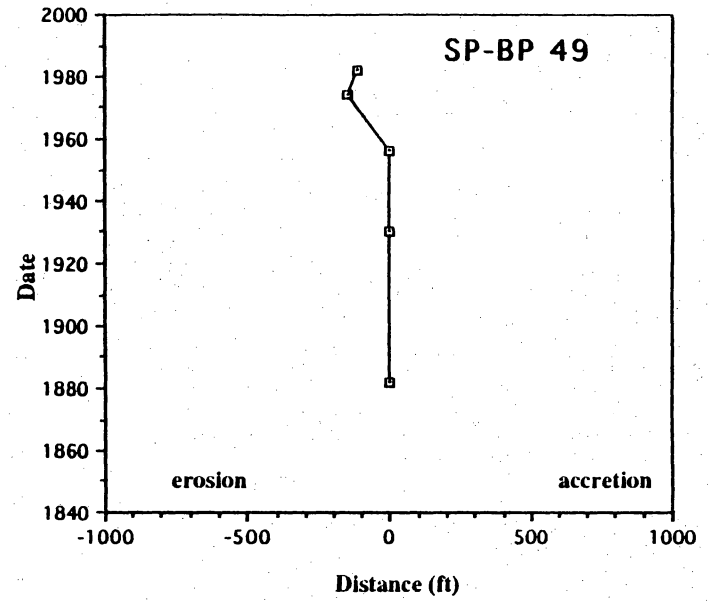
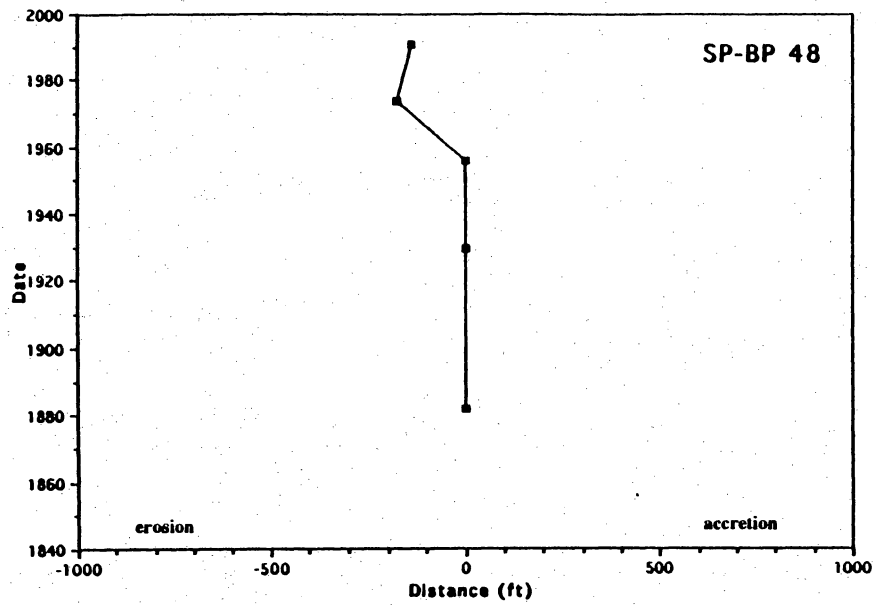
SP-BP = Sabine Pass to Bolivar Peninsula, GI = Galveston Island, SLP-BCC = San Luis Pass to Brown Cedar Cut.

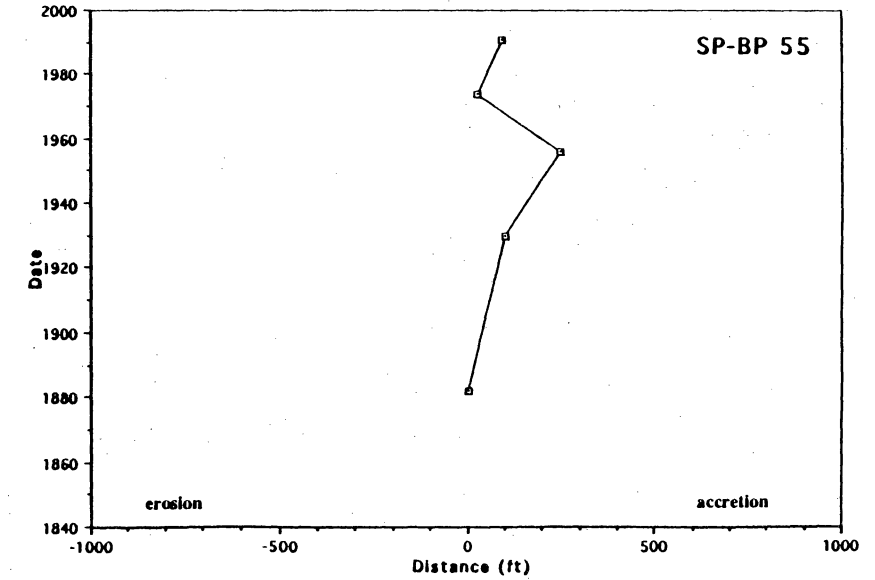
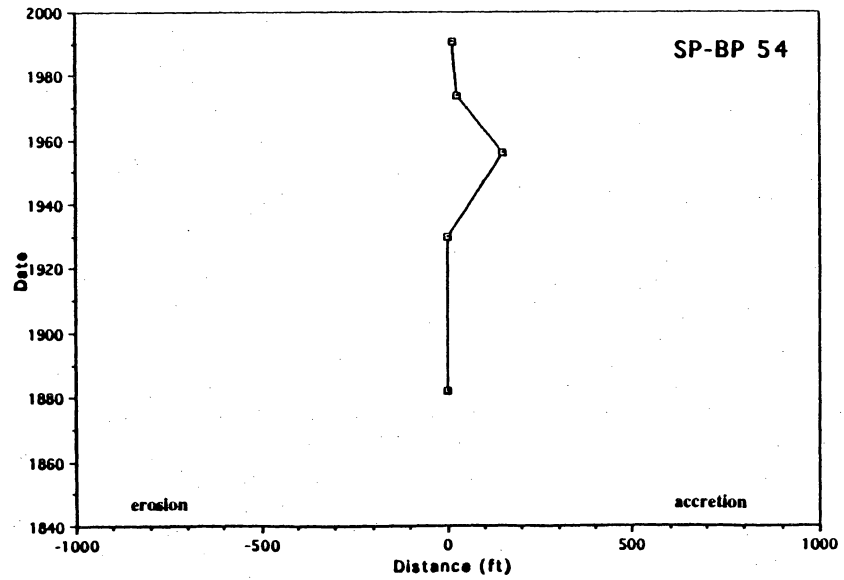
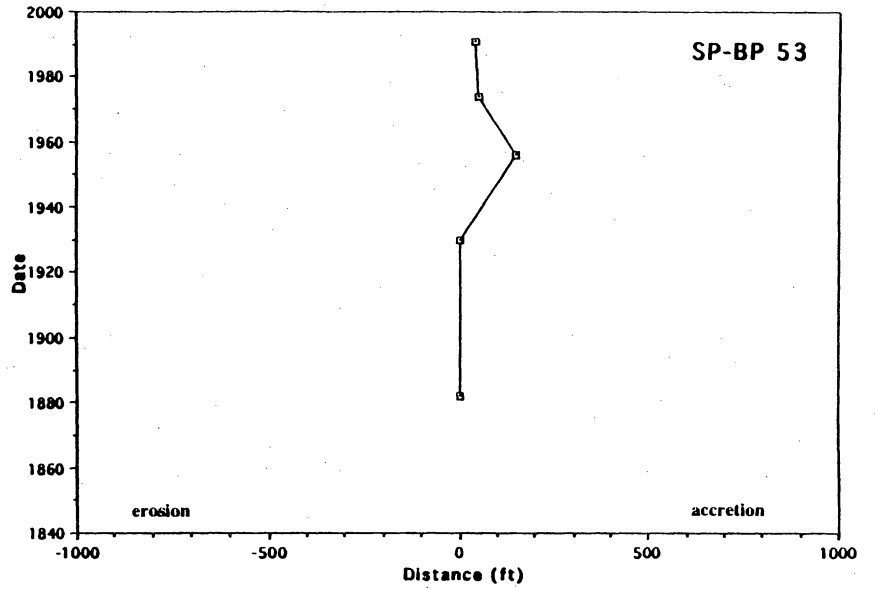
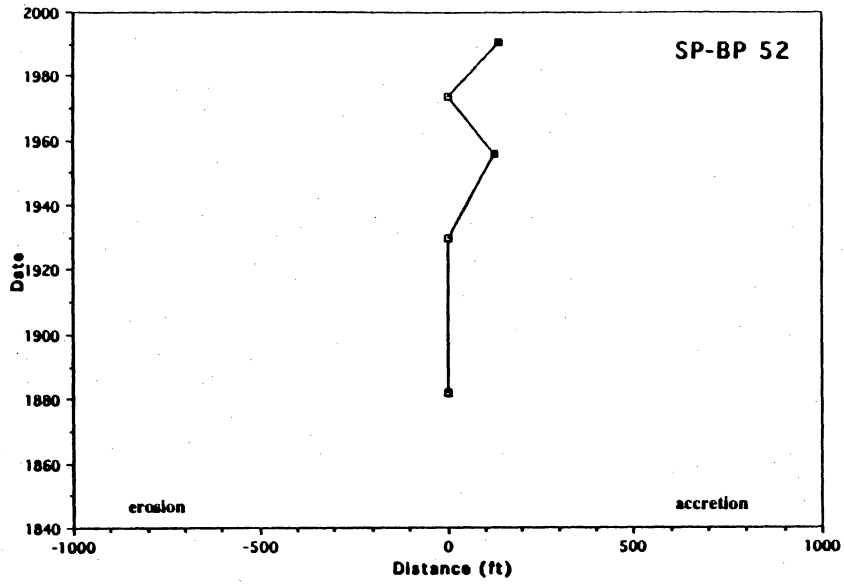


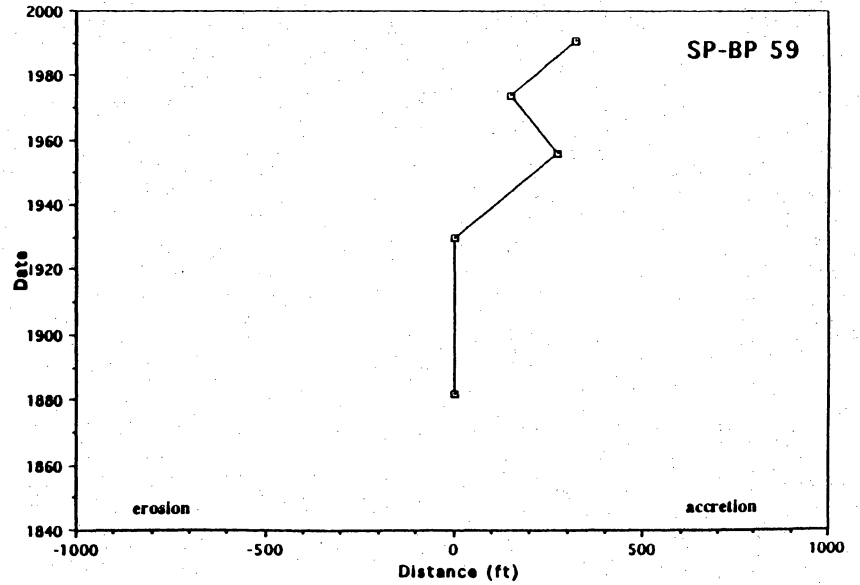
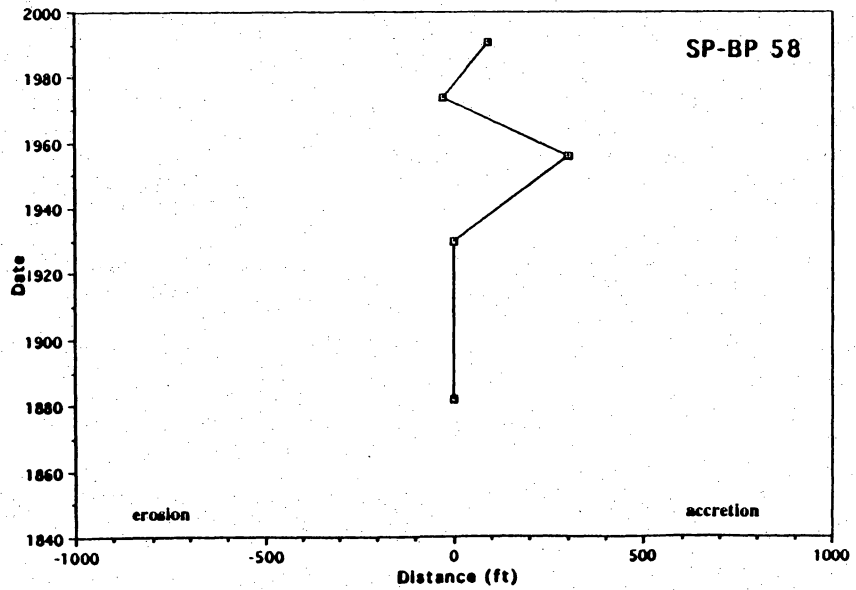
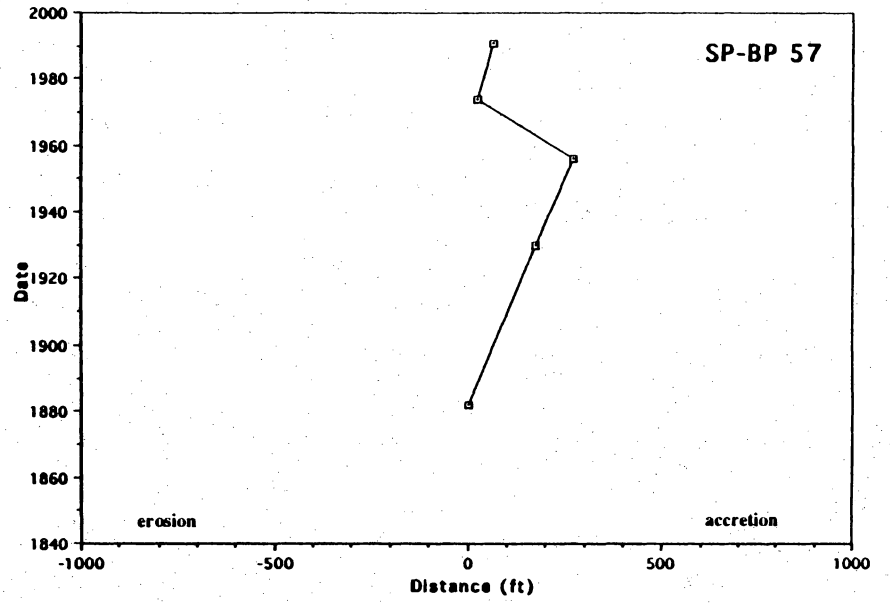
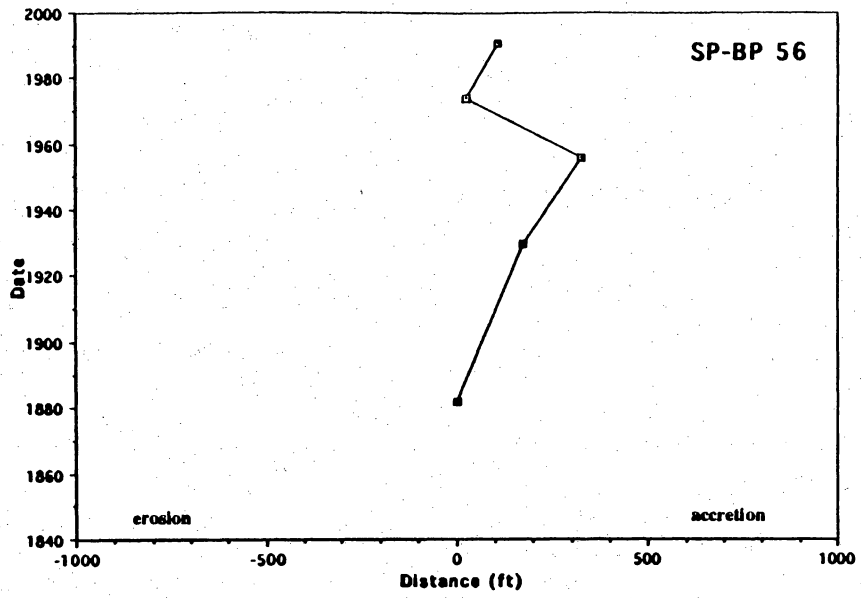




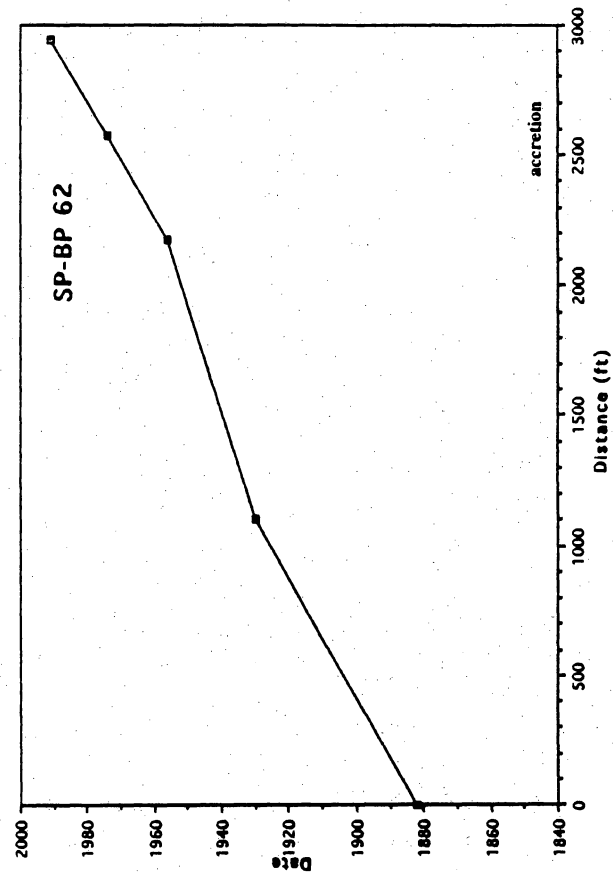
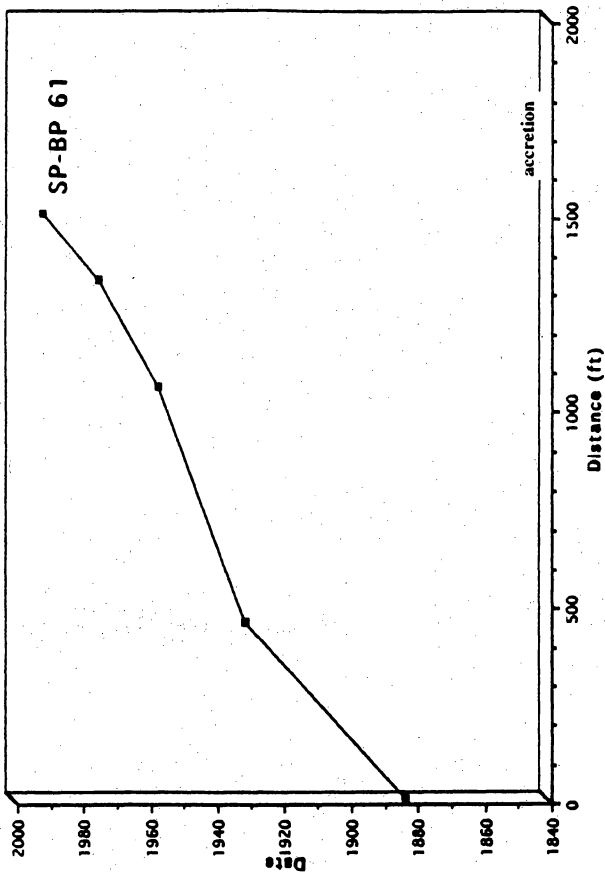
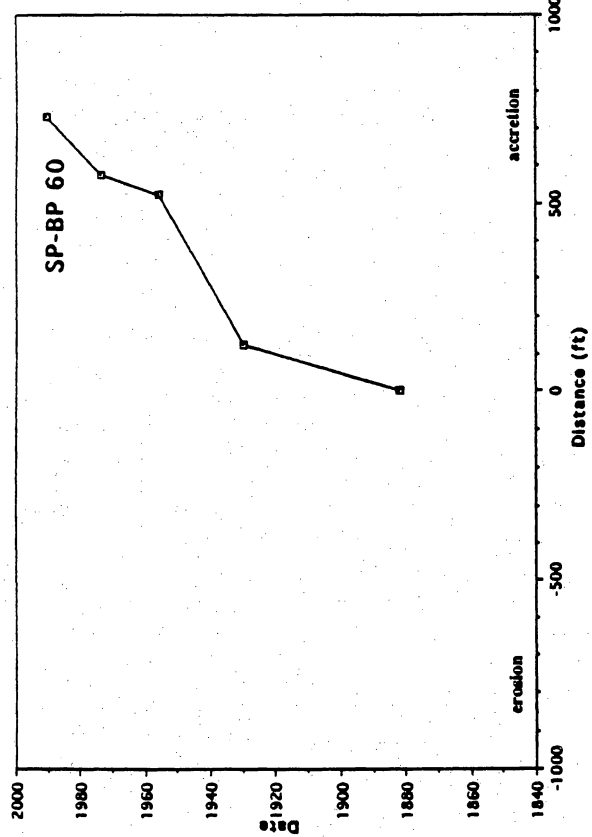






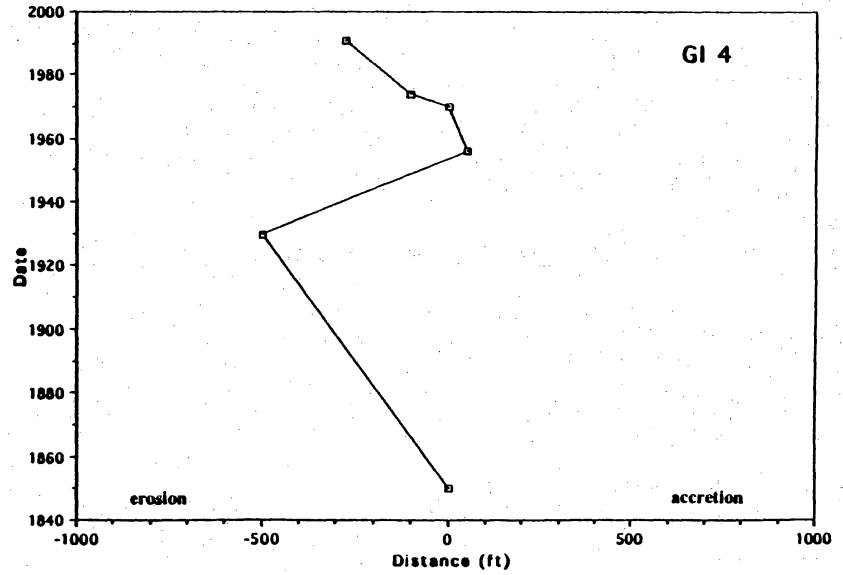
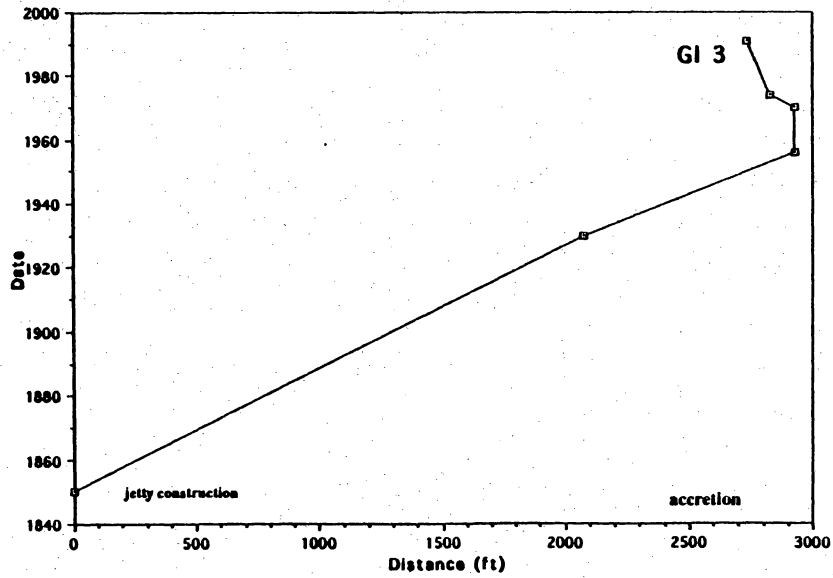
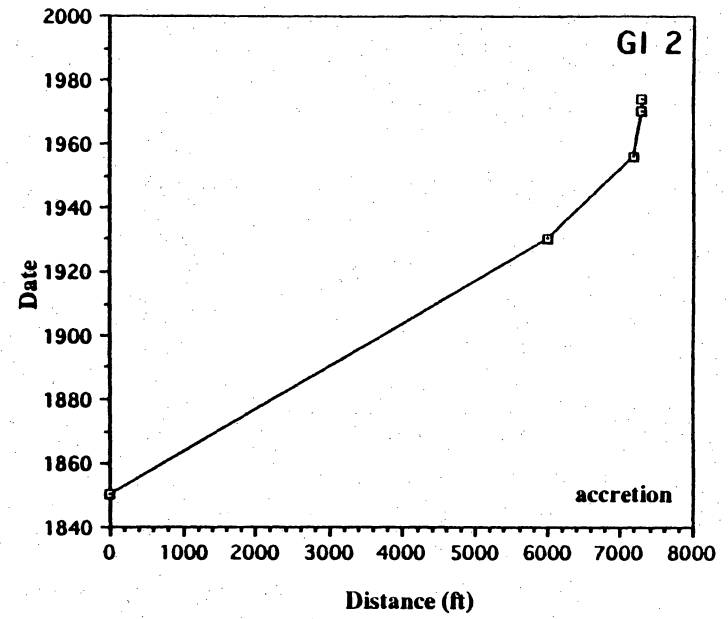
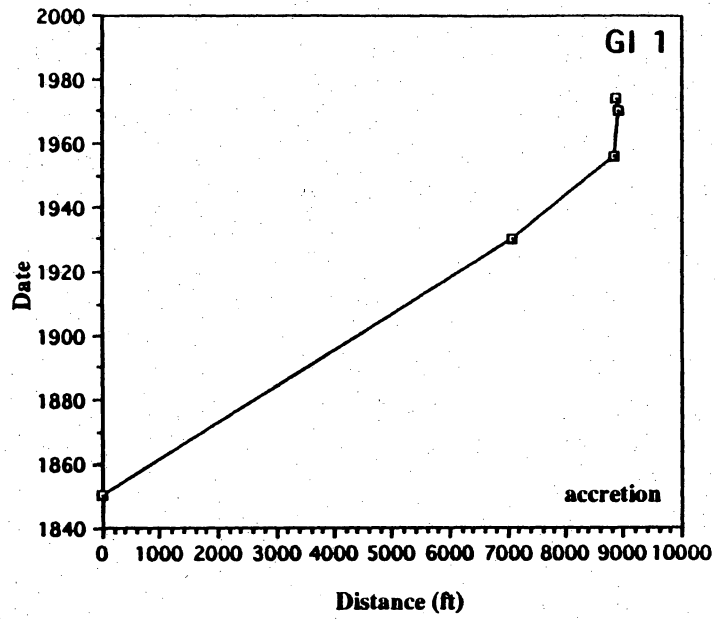


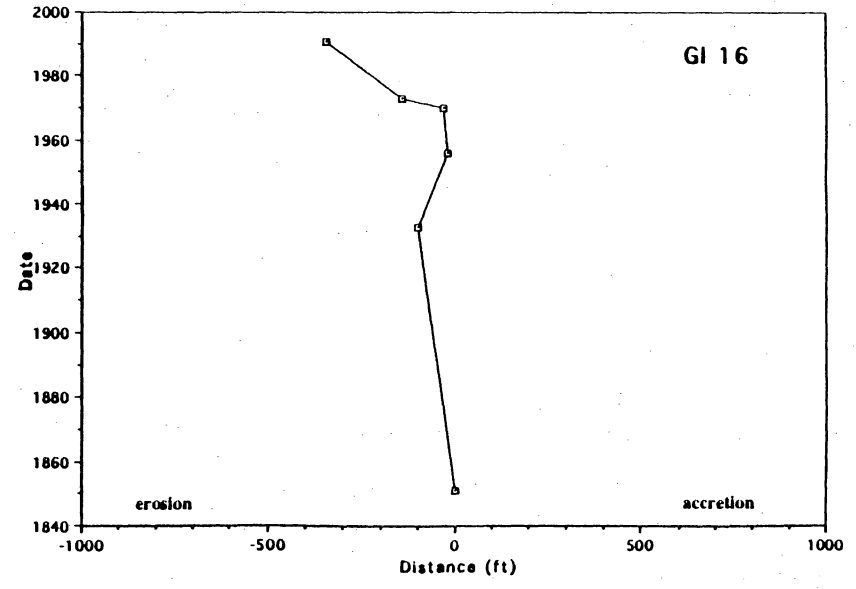
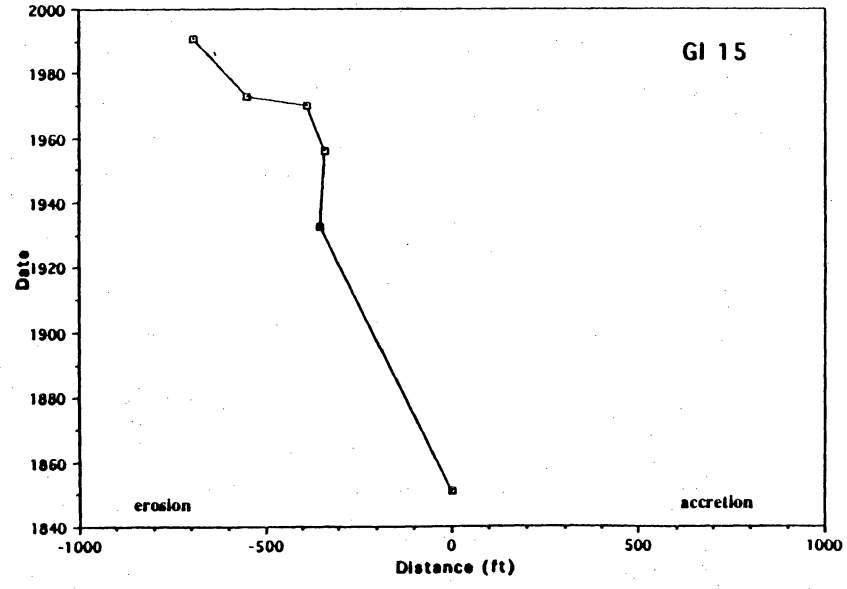
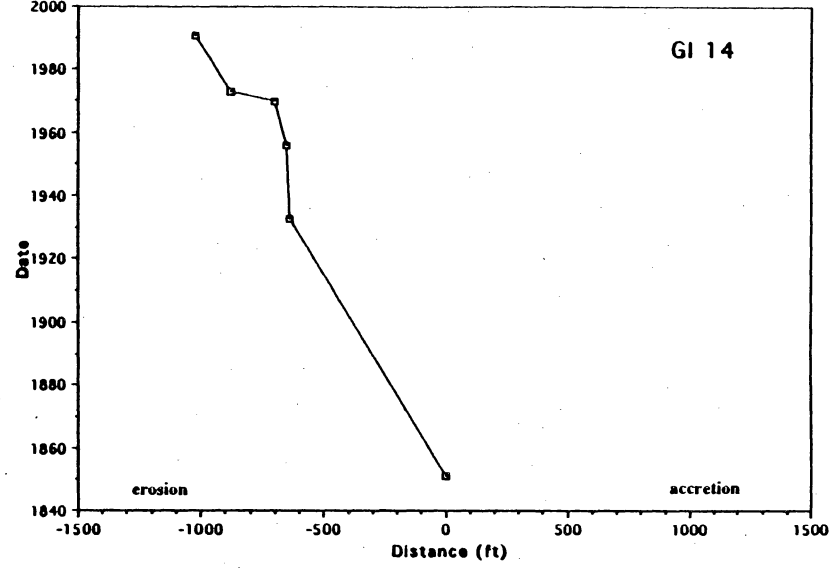
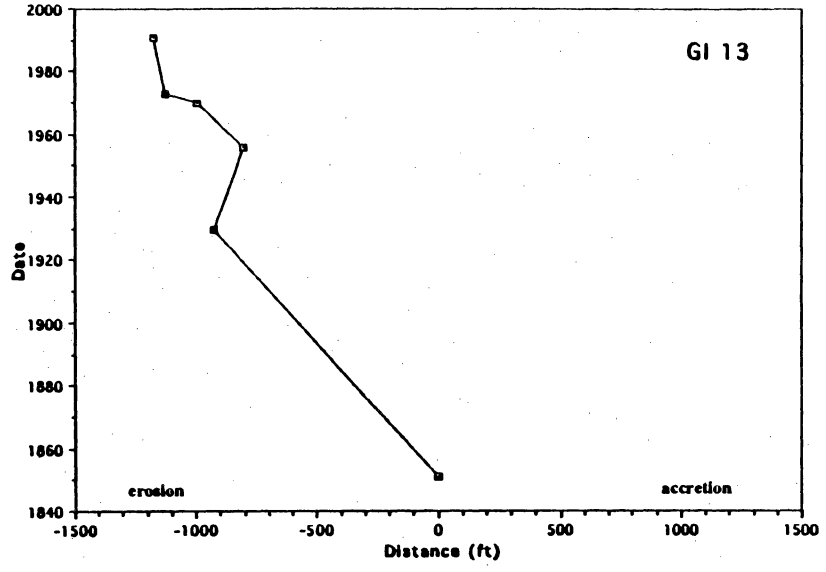


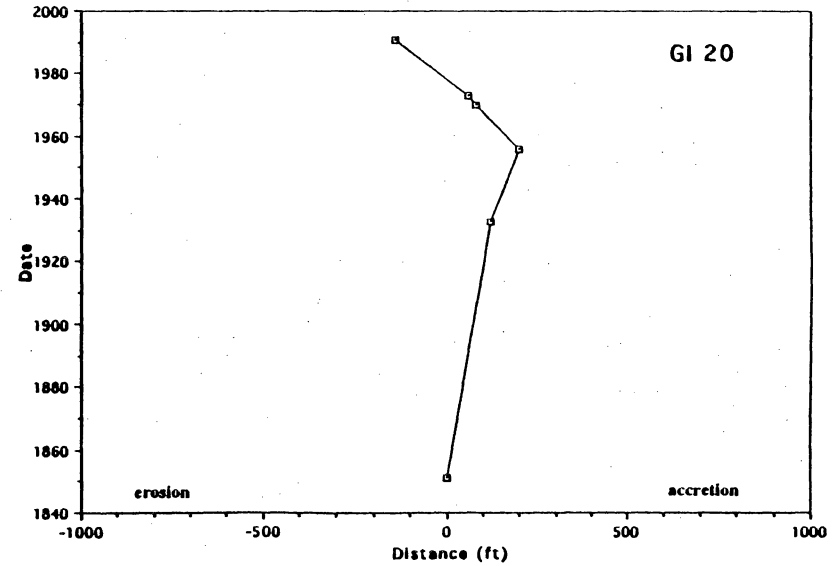
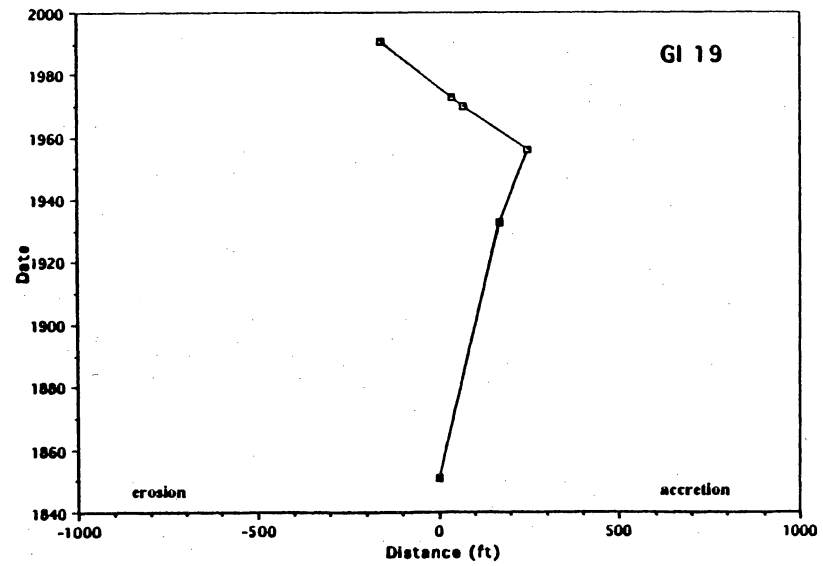
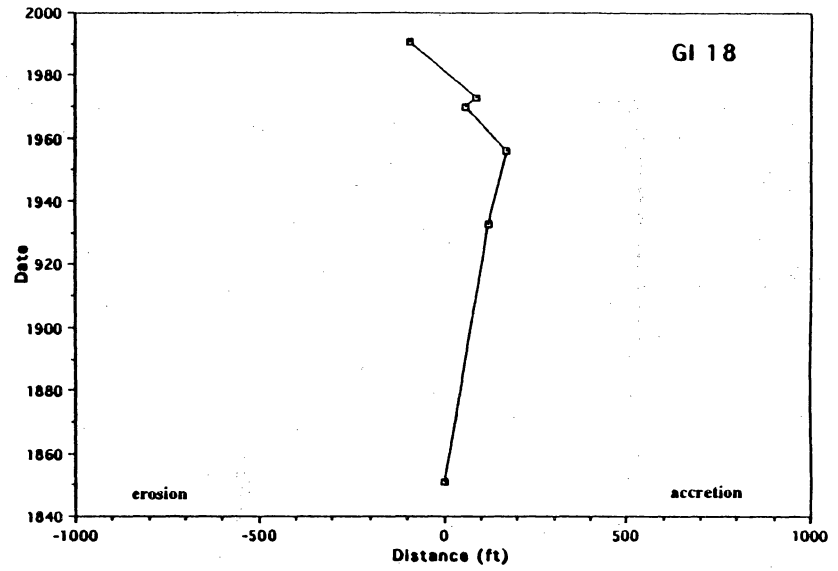
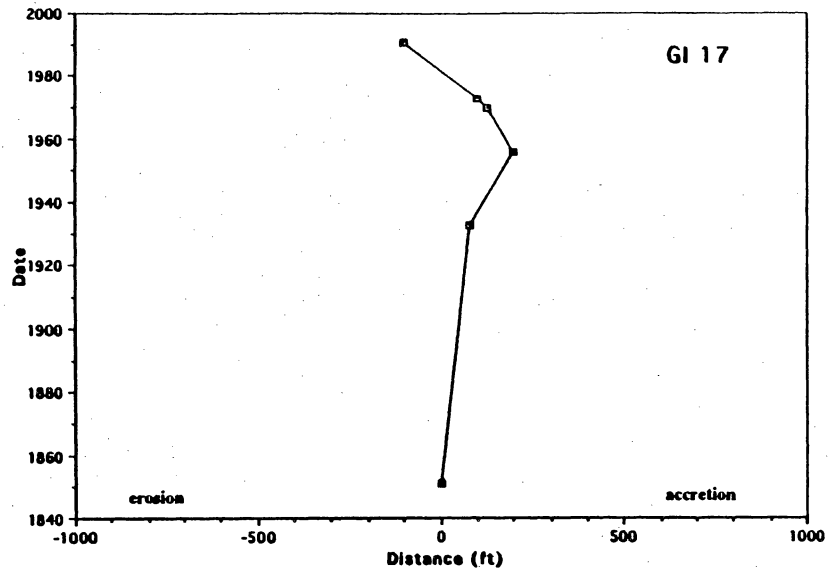


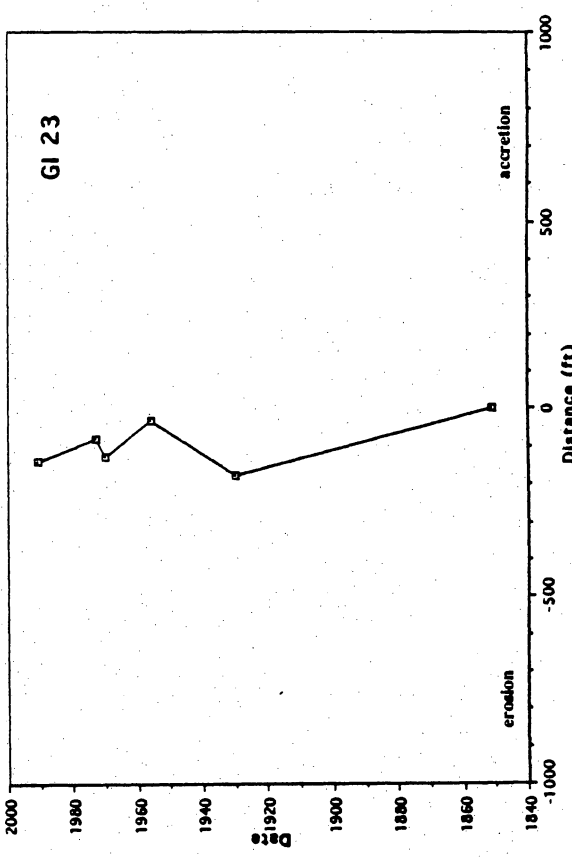
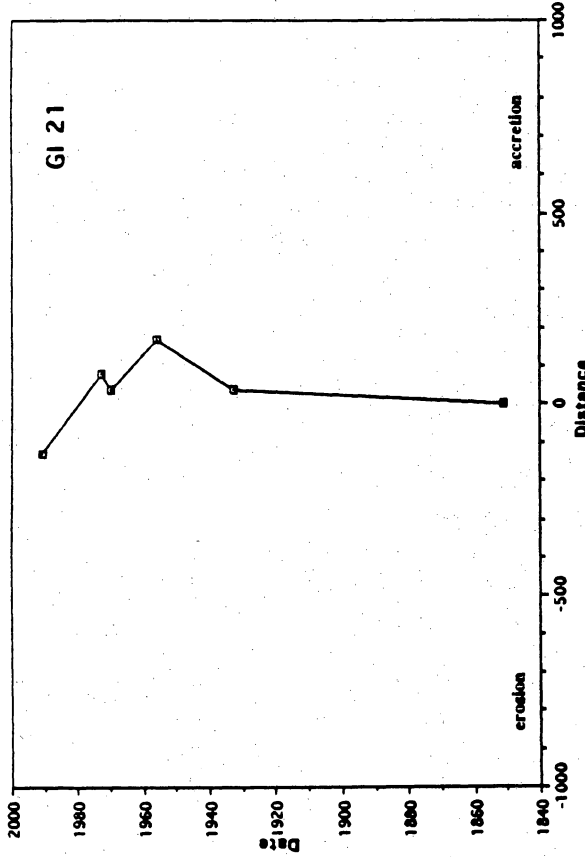
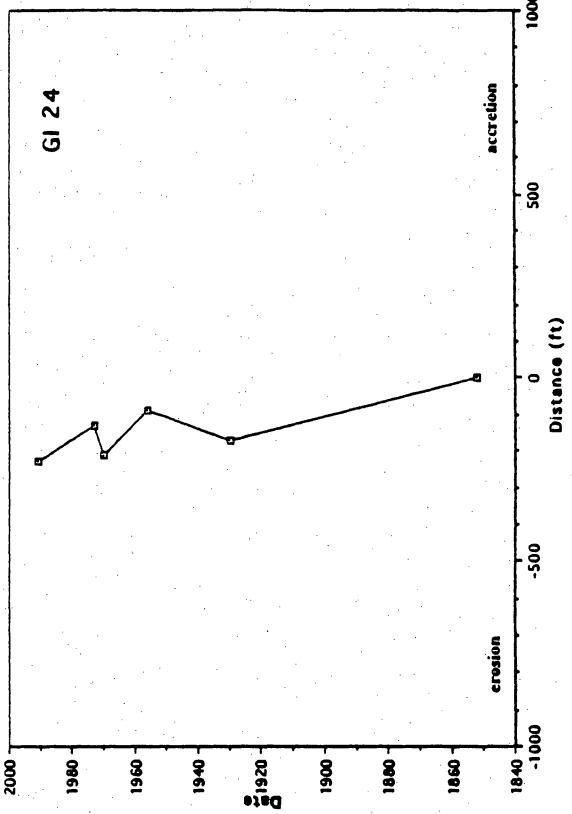
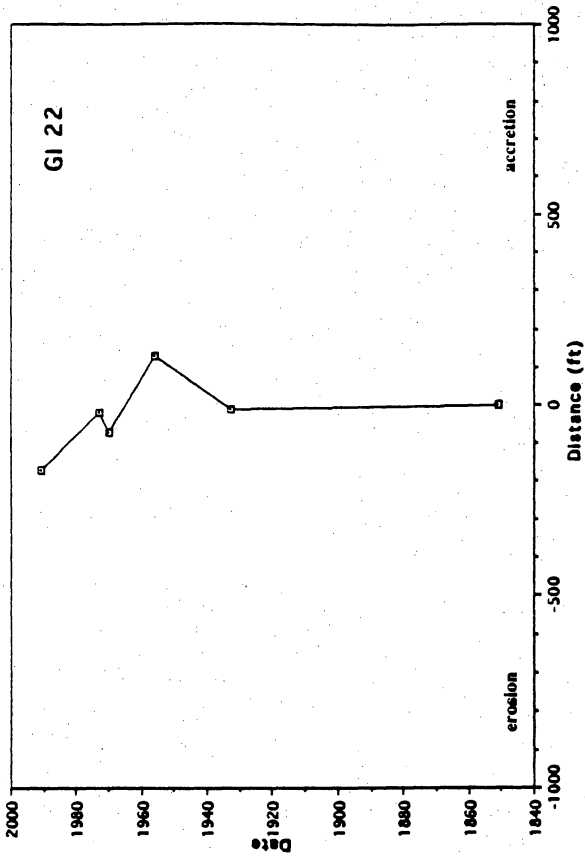
Shoreline Segment: Galveston Island

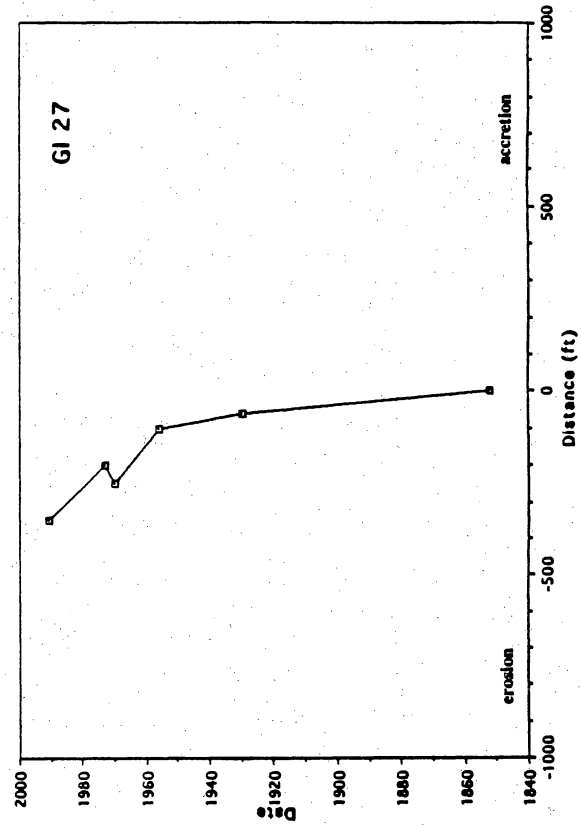
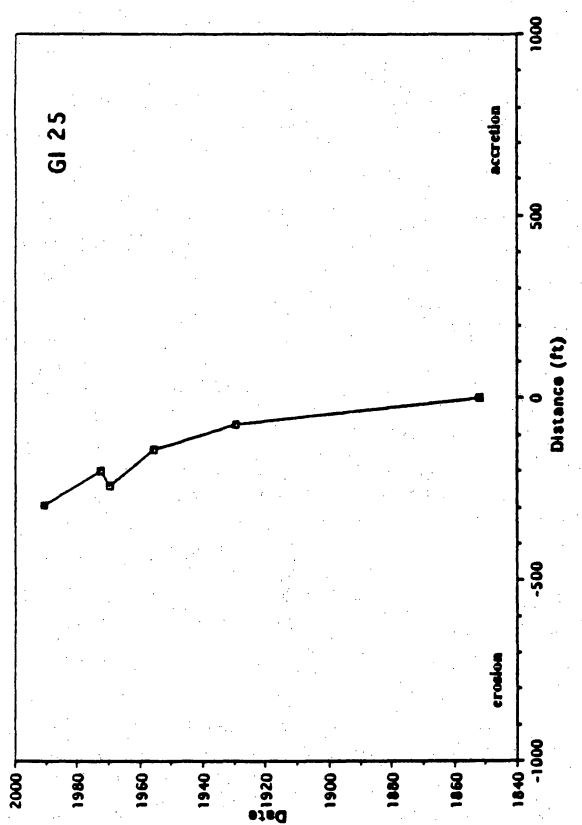
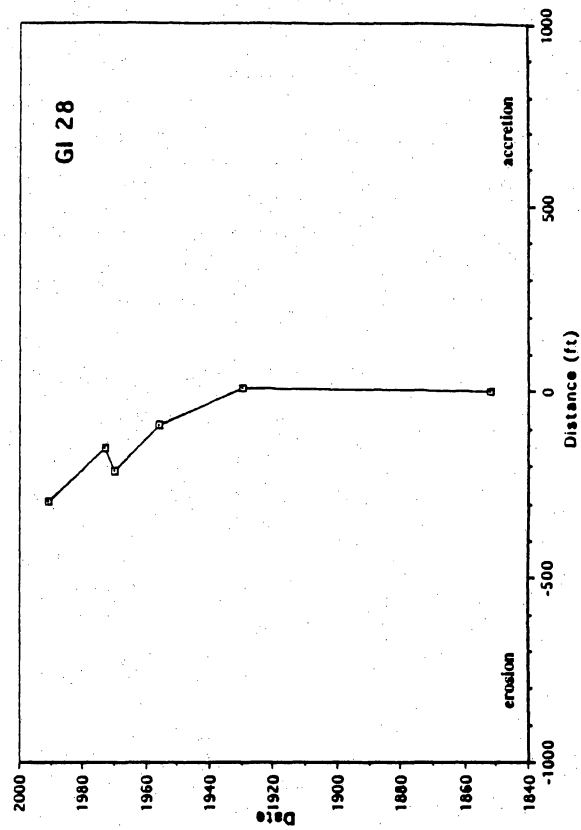
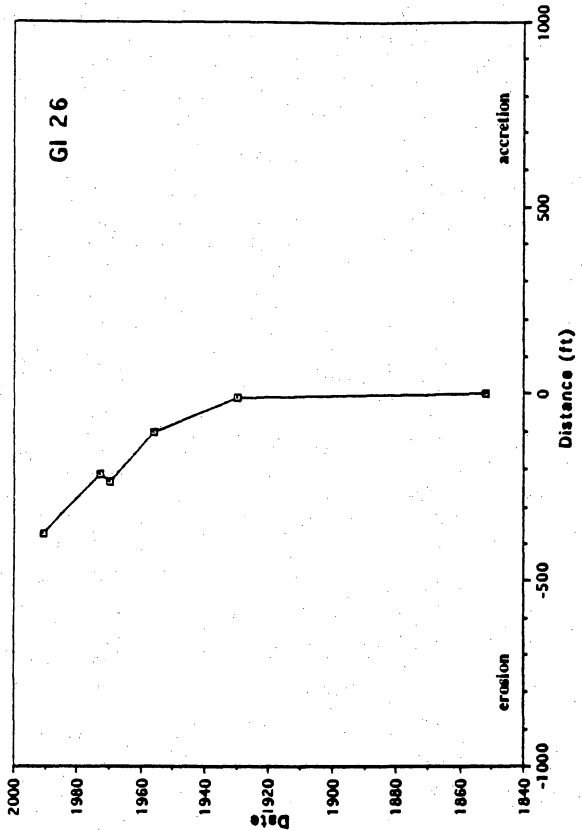
Transect	Period	Average rate (ft/yr)	Class interval
1	1956-1982	+8.2	A
2	1956-1982	+9.8	A
3	1956-1990	-5.6	2
4	1956-1990	-9.5	2
5-12 (seawall)	N/A	N/A	N/A
13	1956-1990	-10.9	3
14	1956-1990	-10.9	3
15	1956-1990	-10.3	3
16	1956-1990	-9.7	2
17	1956-1990	-8.8	2
18	1956-1990	-7.7	2
19	1956-1990	-12.0	3
20	1956-1990	-10.0	3
21	1956-1990	-8.8	2
22	1956-1990	-8.9	2
23	1956-1990	-3.3	1
24	1956-1990	-4.0	1
25	1956-1990	-4.5	1
26	1956-1990	-8.0	2
27	1956-1990	-8.9	2
28	1956-1990	-6.0	2
29	1956-1990	-6.4	2
30	1956-1990	-20.6	3
31	1956-1990	-39.8	3

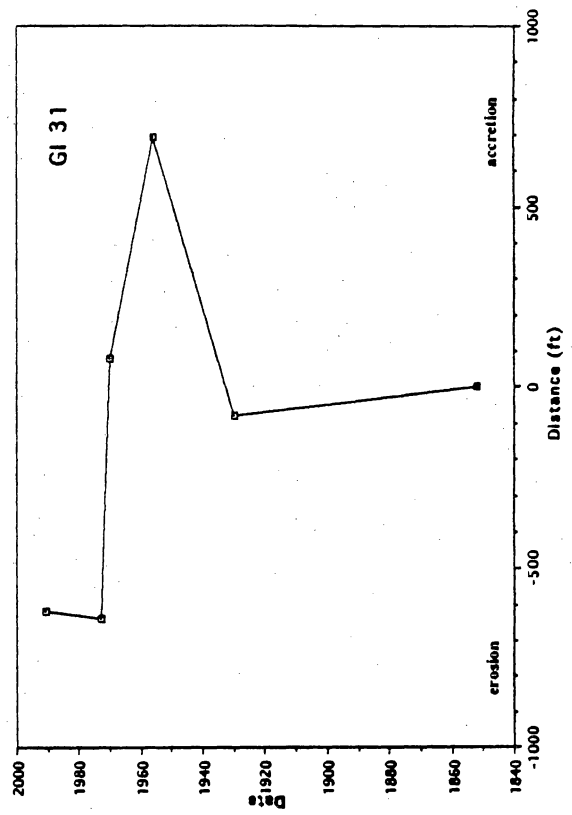
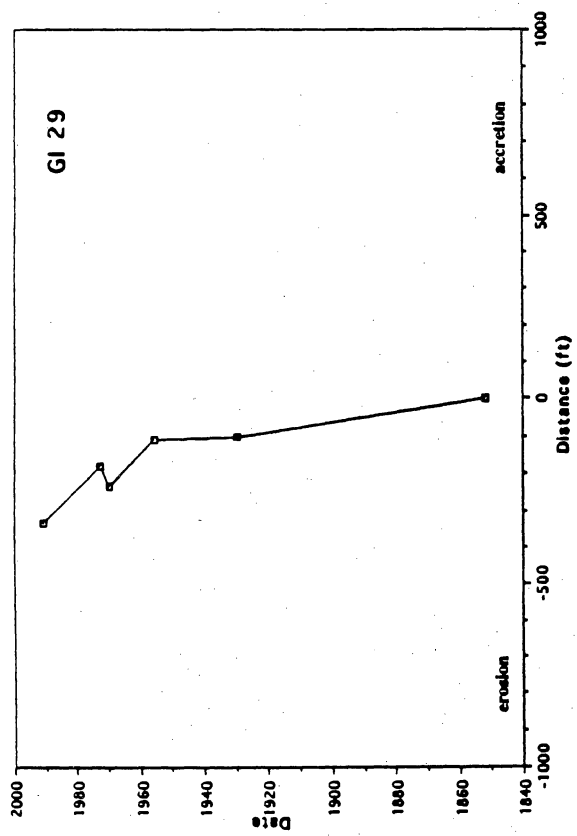
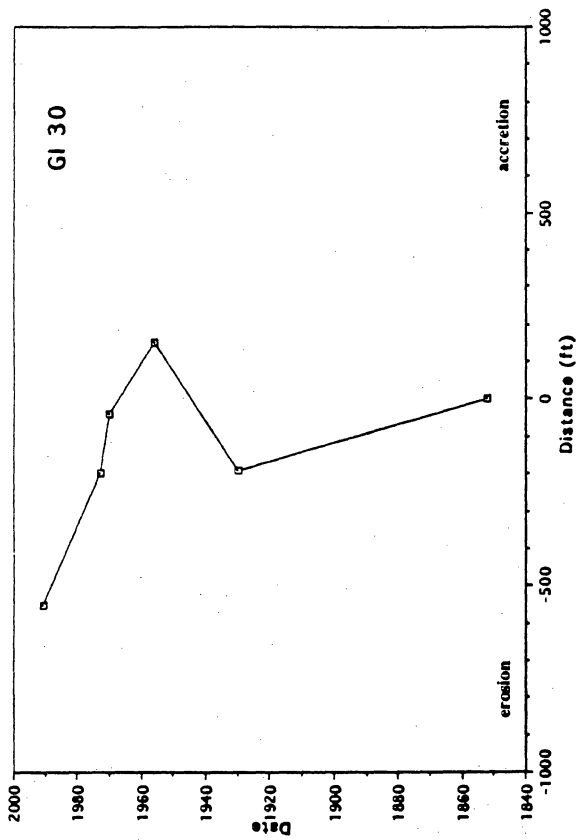








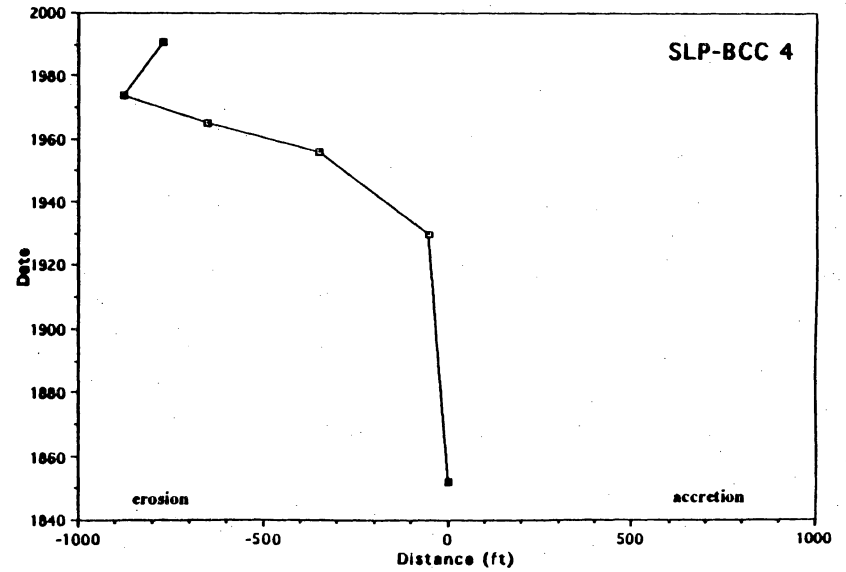
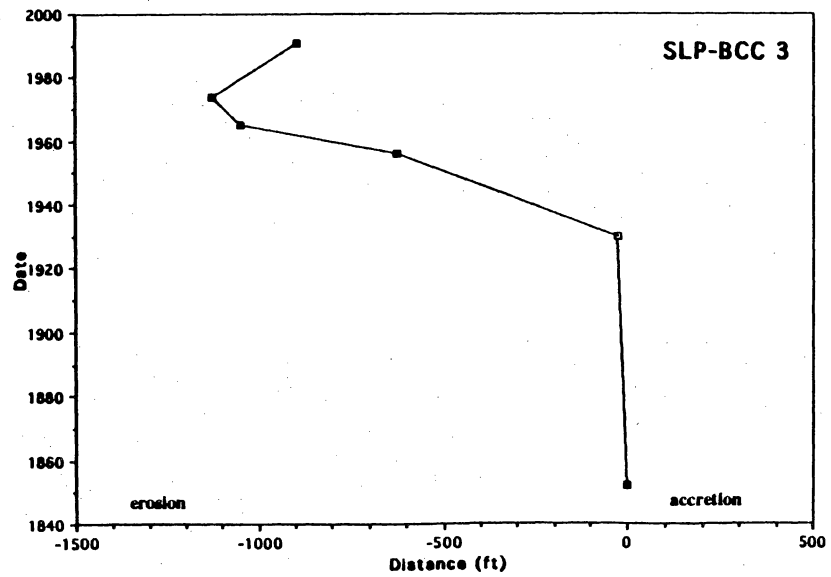
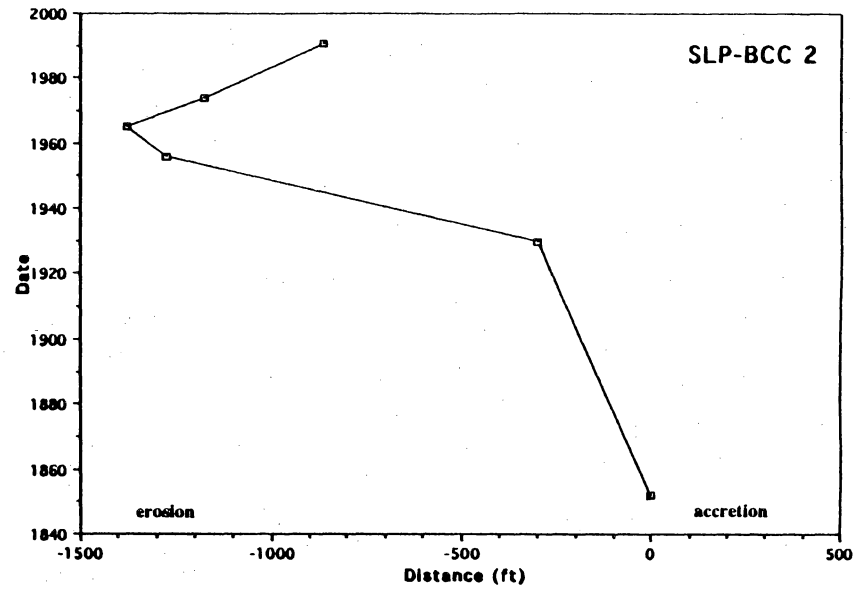
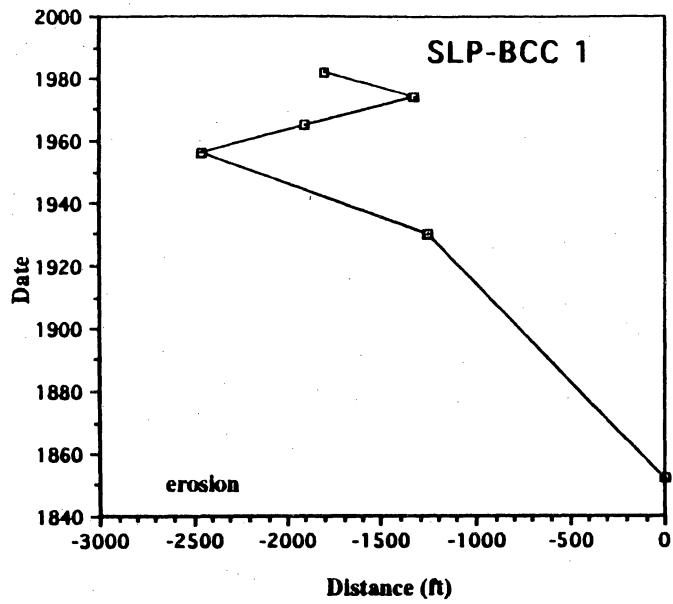


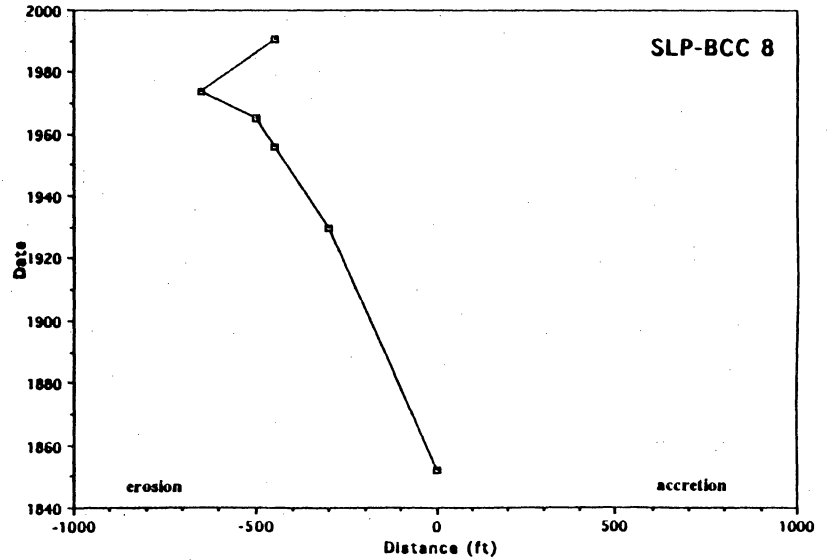
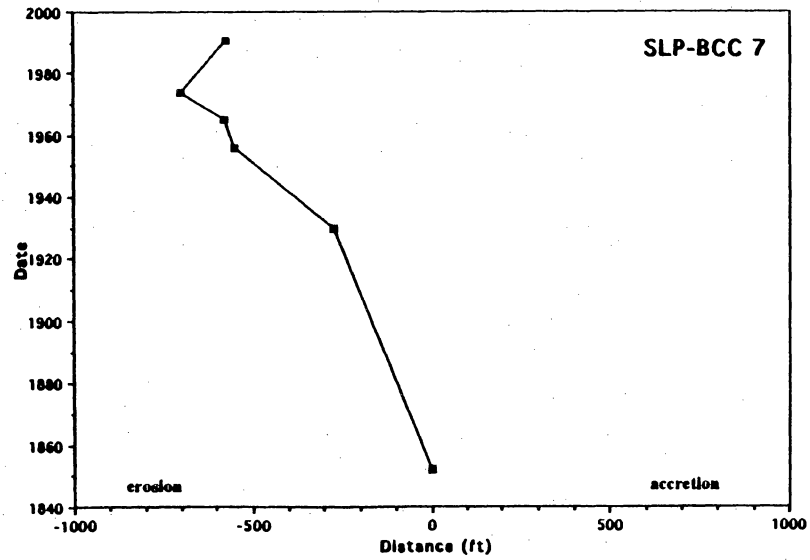
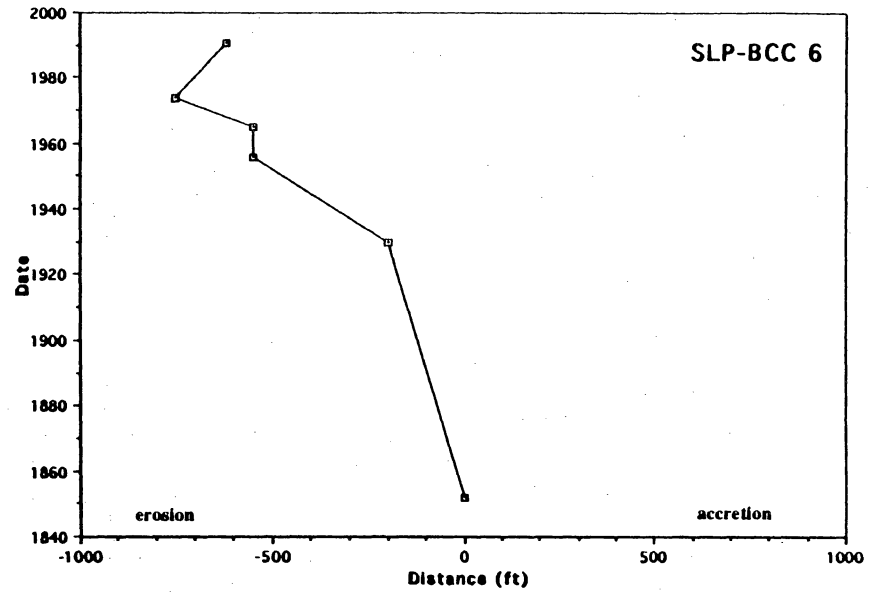
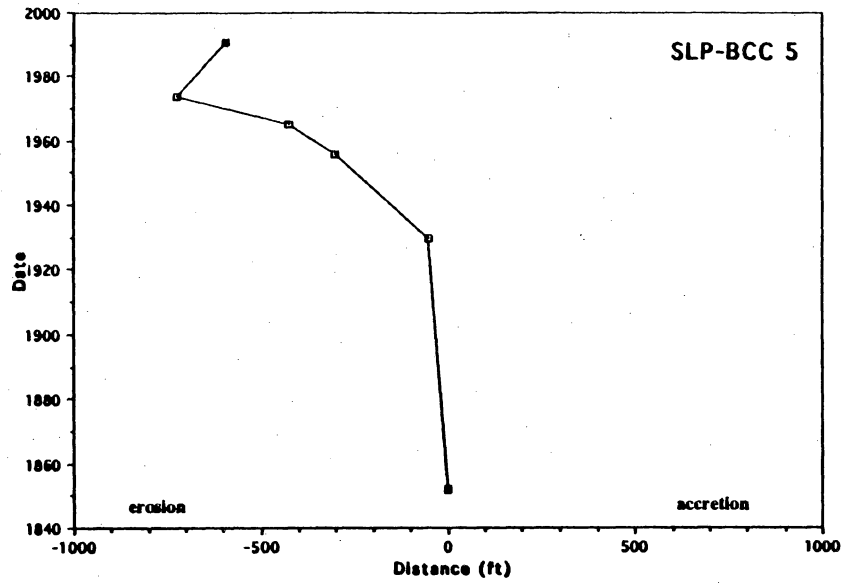


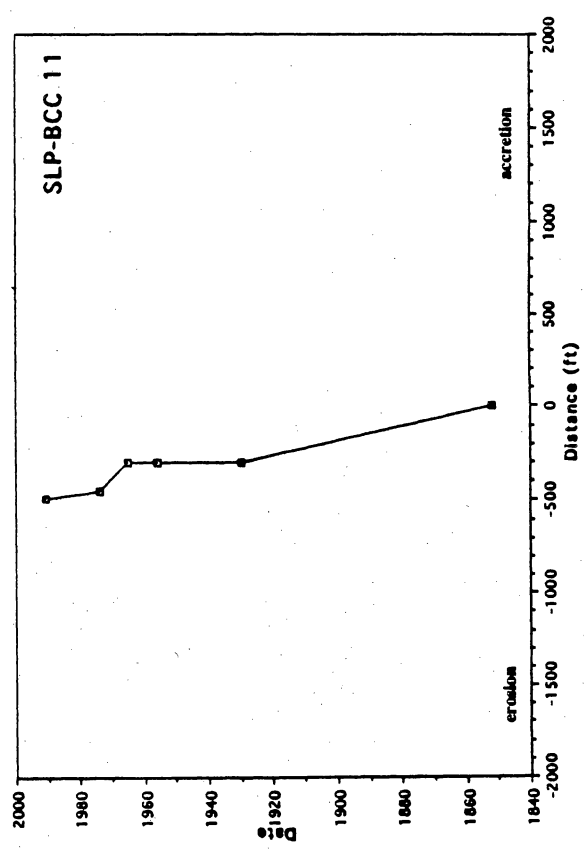
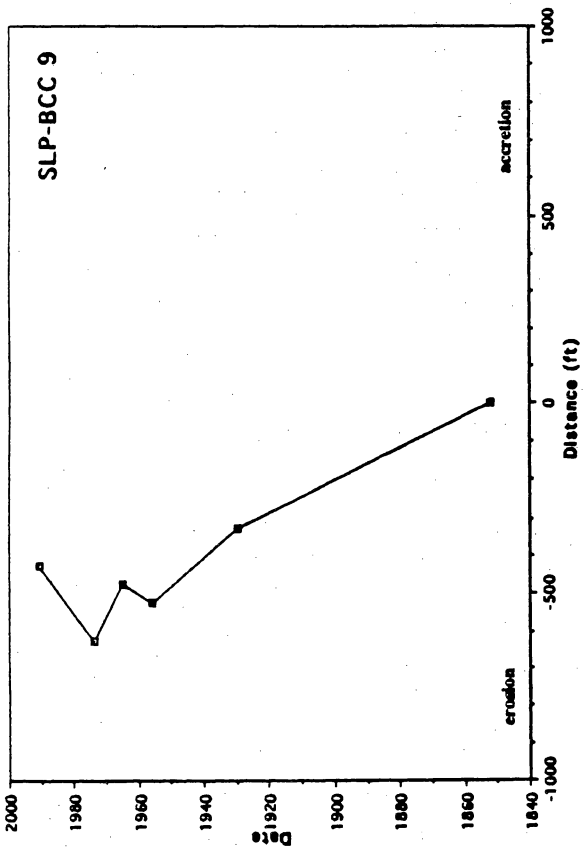
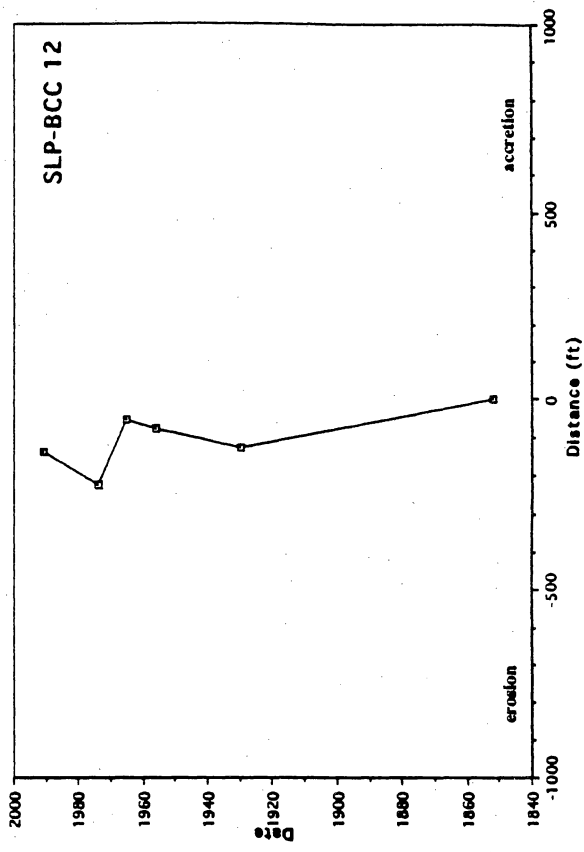
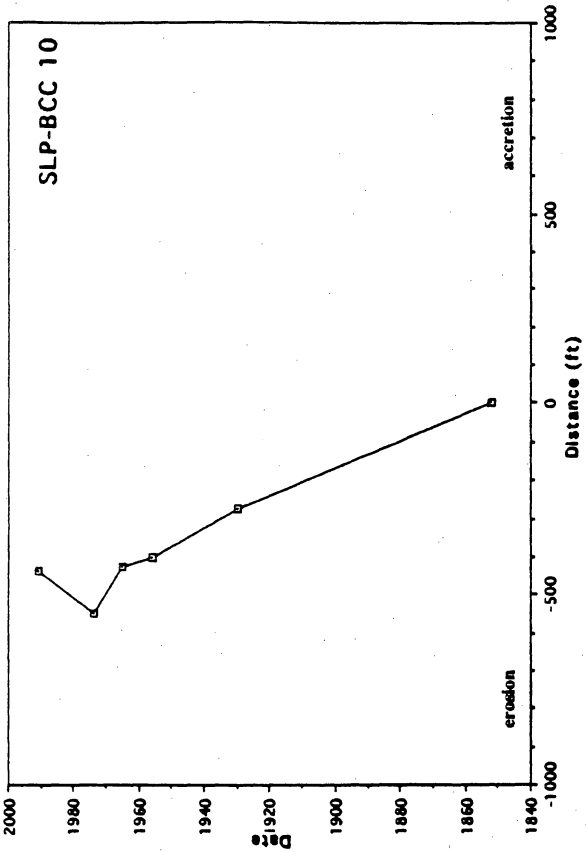


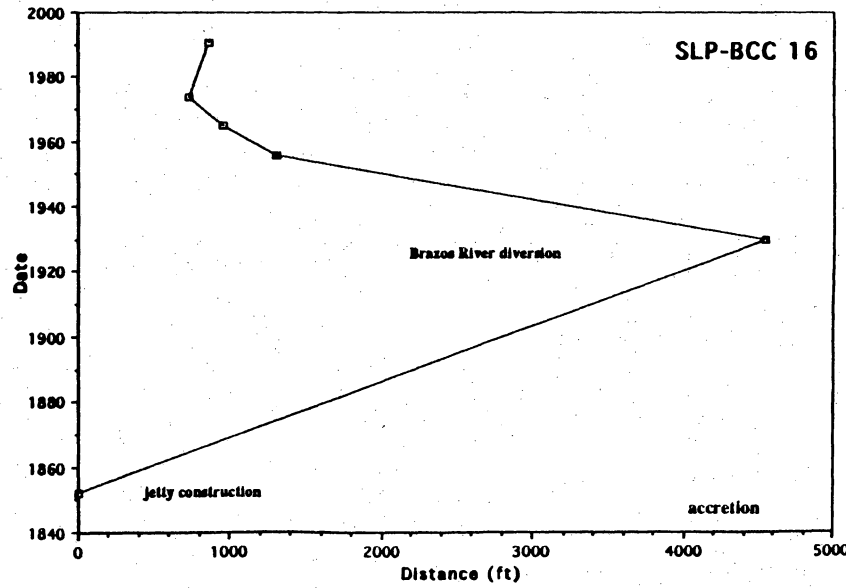
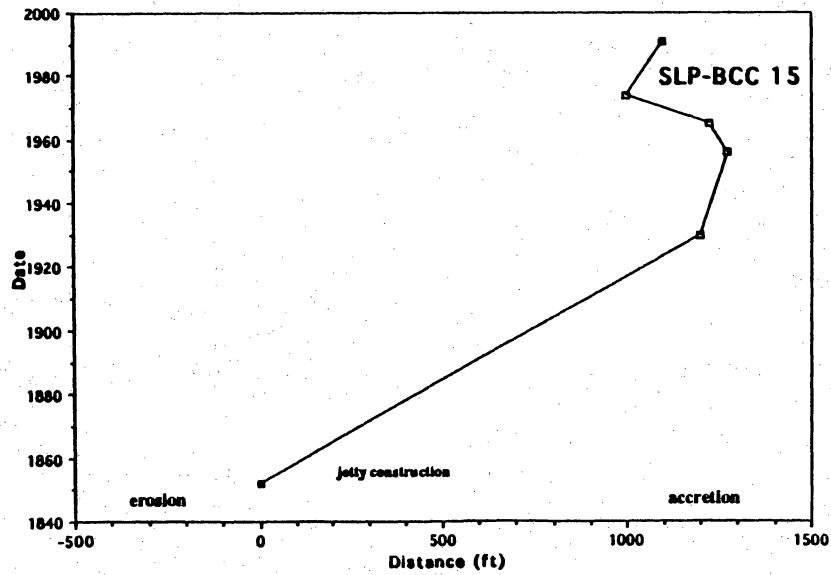
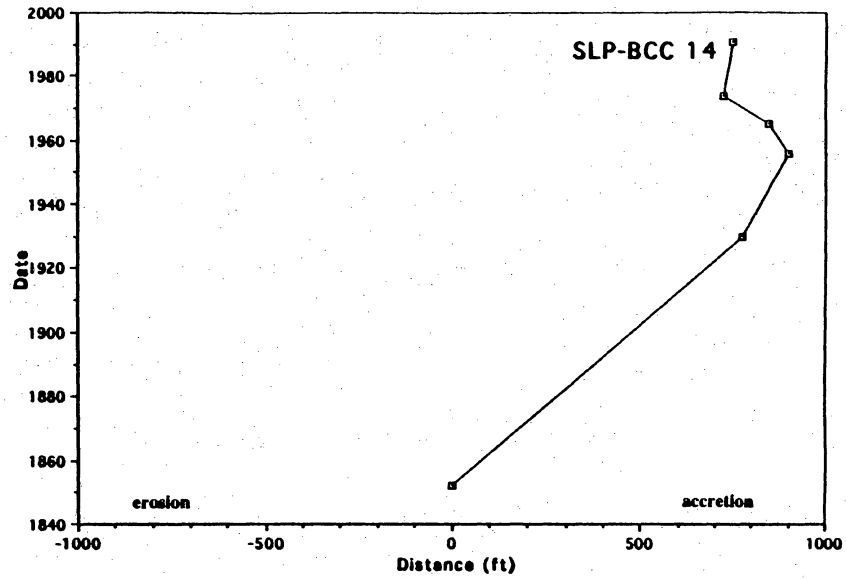
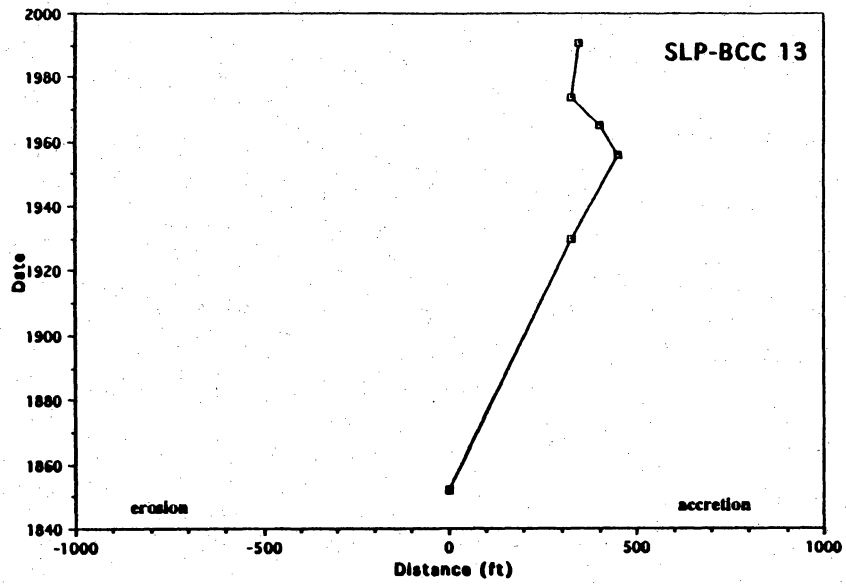
Shoreline Segment: San Luis Pass to Sargent Beach

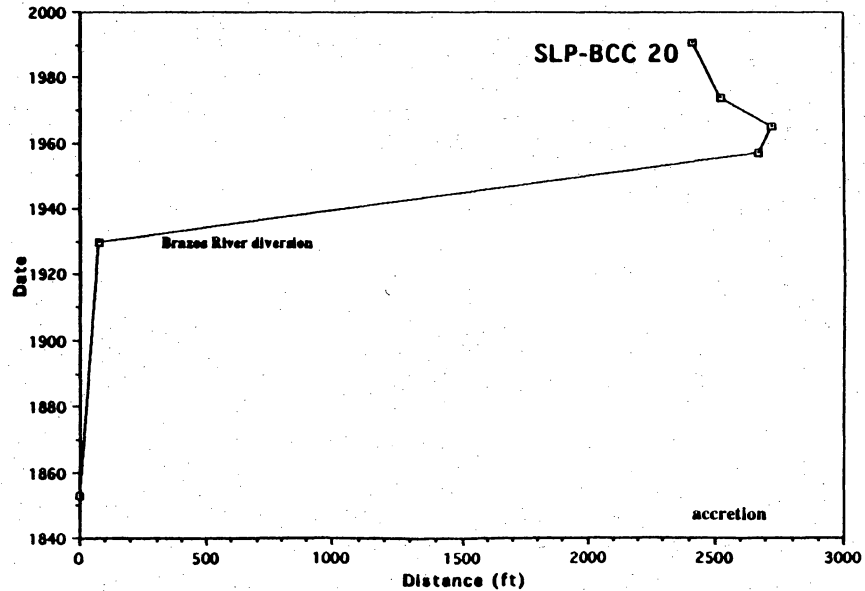
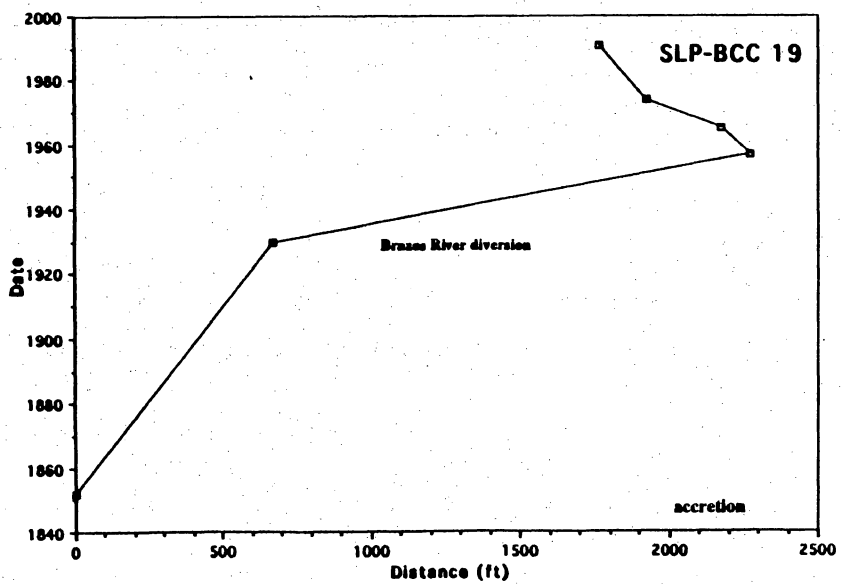
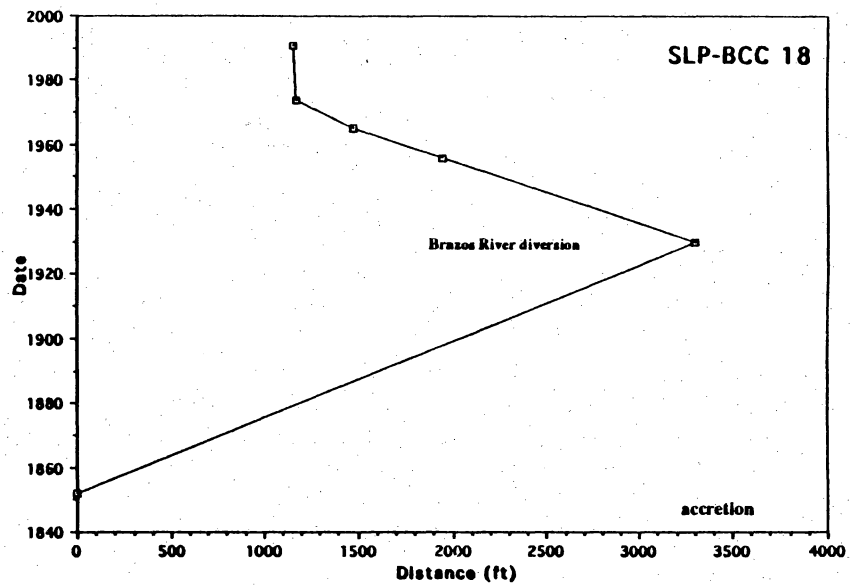
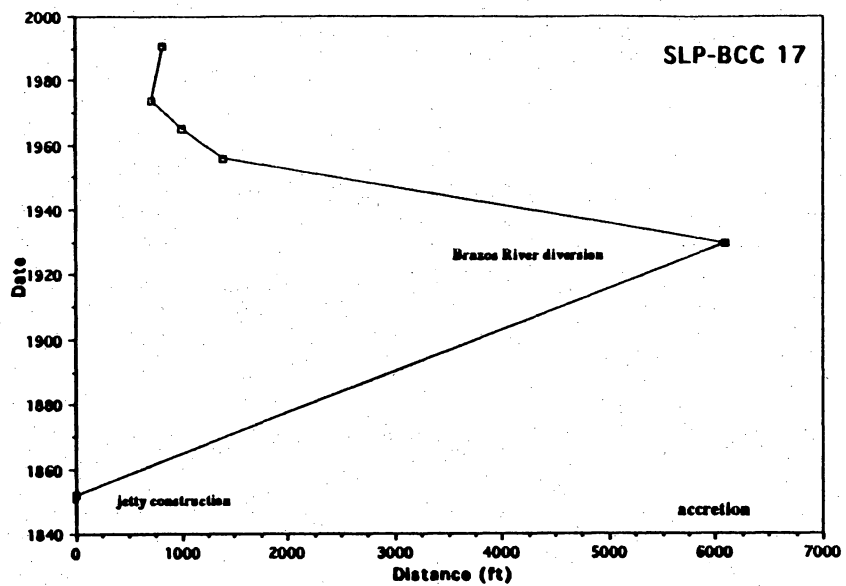
Transect	Period	Average rate (ft/yr)	Class interval
1	1852-1982	-13.9	3
2	1930-1990	-13.2	3
3	1930-1990	-14.5	3
4	1930-1990	-12.0	3
5	1930-1990	-9.6	2
6	1930-1990	-7.0	2
7	1930-1990	-5.0	1
8	1852-1990	-3.3	1
9	1852-1990	-3.1	1
10	1852-1990	-1.4	S
11	1852-1990	-3.5	1
12	1852-1990	-1.0	S
13	1956-1990	-3.1	1
14	1930-1990	-4.4	1
15	1956-1990	-1.7	S
16	1956-1990	-12.8	3
17	1956-1990	-25.1	3
18	1956-1990	-23.2	3
19	1957-1990	-15.5	3
20	1956-1990	-7.9	2
21	1956-1990	-11.5	3
22	1956-1990	-39.0	3
23	1956-1990	-34.7	3
24	1974-1990	-31.5	3
25	1957-1990	+117.1	A
26	1957-1990	+100.1	A
27	1965-1990	+32.6	A
28	1965-1990	+9.7	A
29	1965-1990	-3.5	1
30	1965-1990	-6.6	2
31	1930-1990	-20.5	3
32	1930-1990	-21.9	3
33	1930-1990	-20.4	3
34	1930-1990	-20.1	3
35	1930-1990	-22.4	3
36	1930-1990	-24.6	3
37	1930-1991	-24.1	3
38	1930-1991	-25.5	3
39	1930-1991	-26.0	3
40	1930-1991	-26.3	3
41	1930-1991	-25.6	3
42	1956-1991	-29.1	3

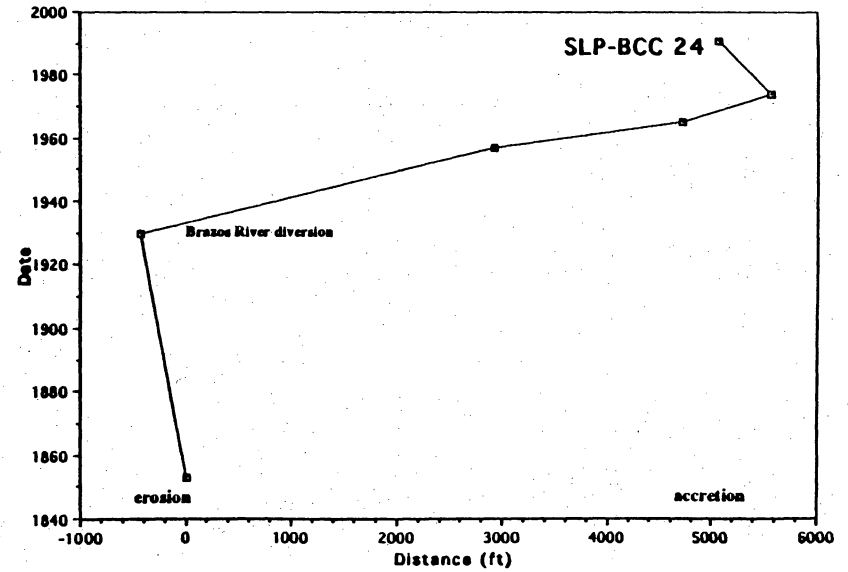
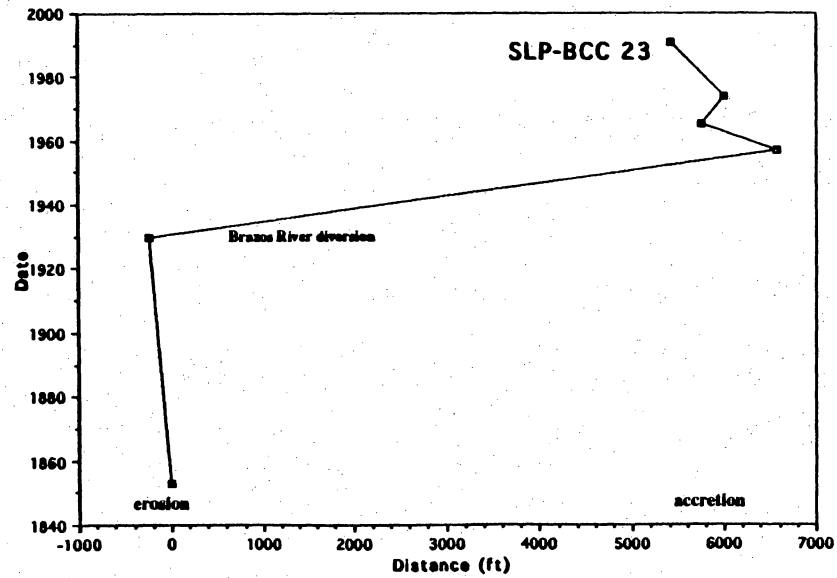
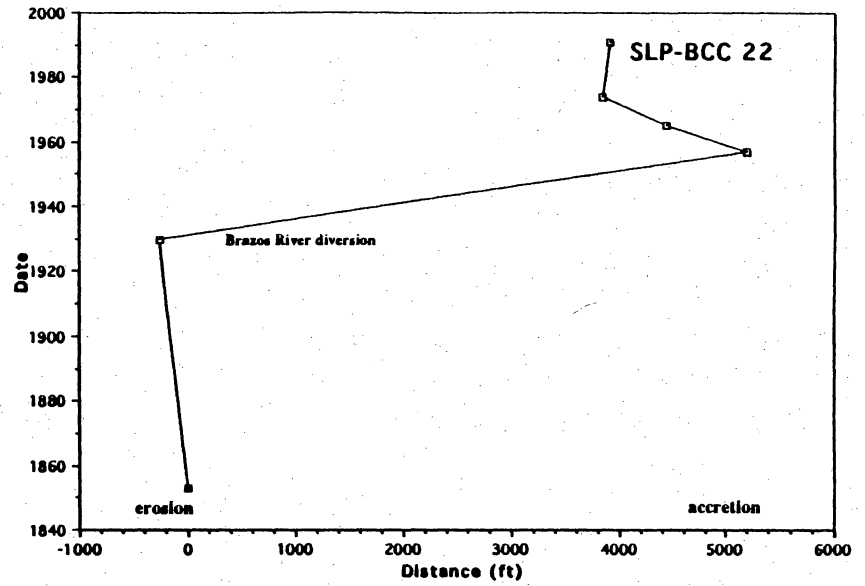
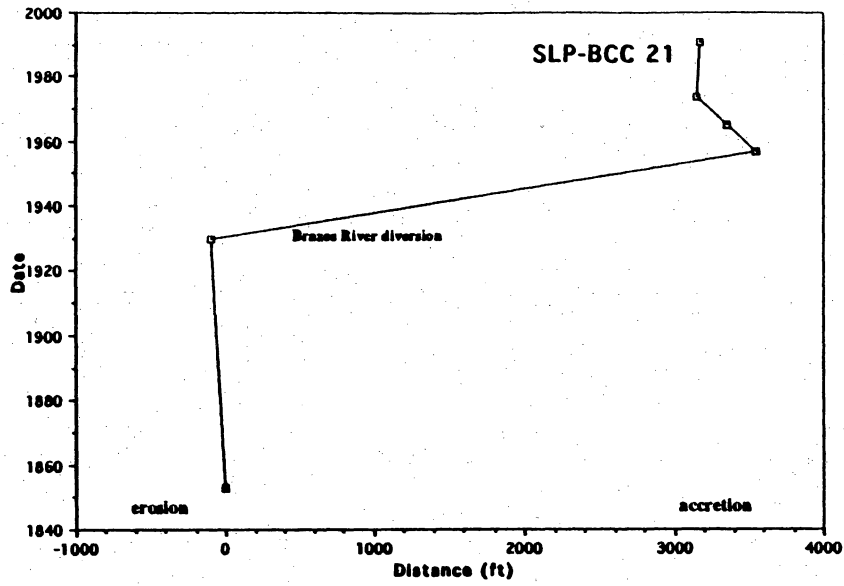


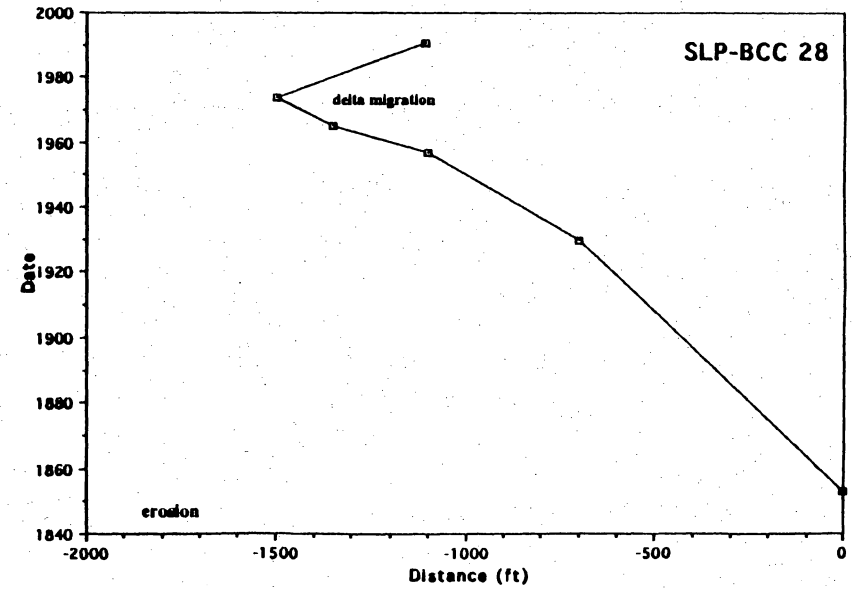
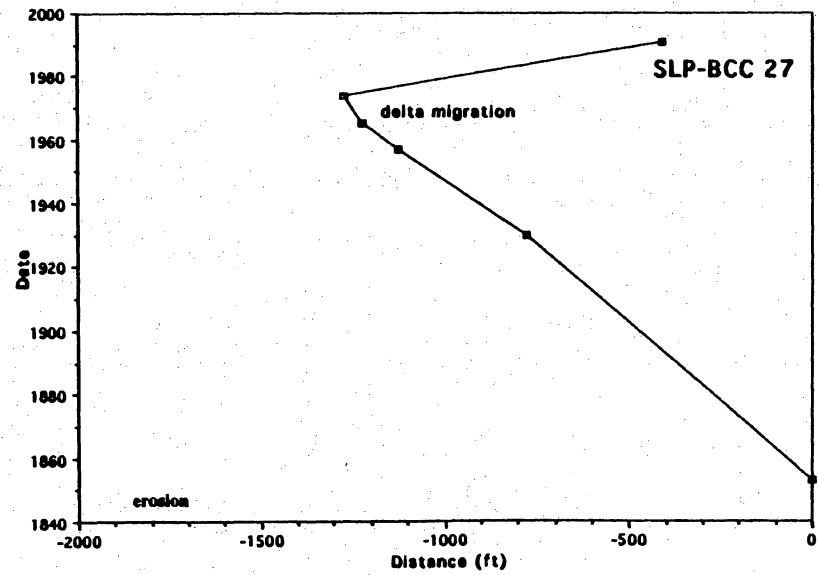
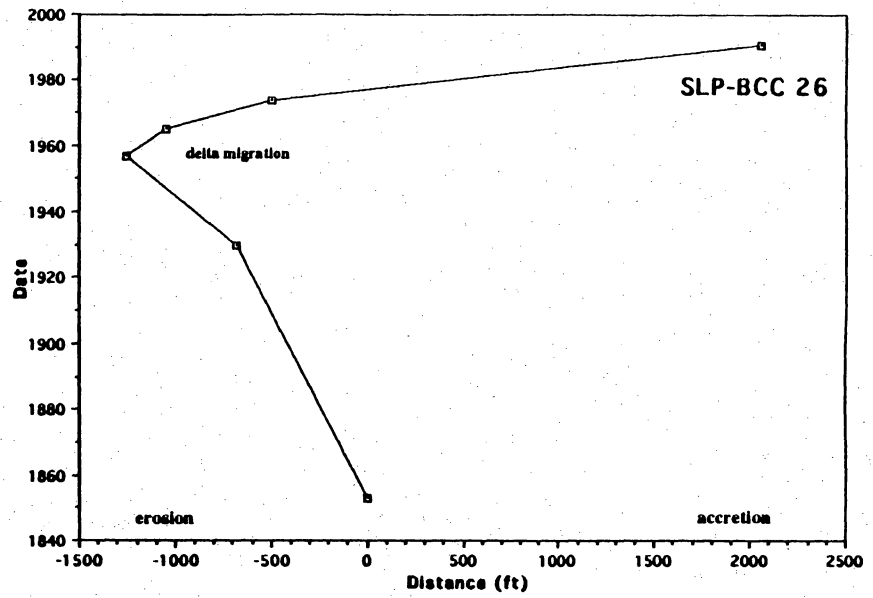
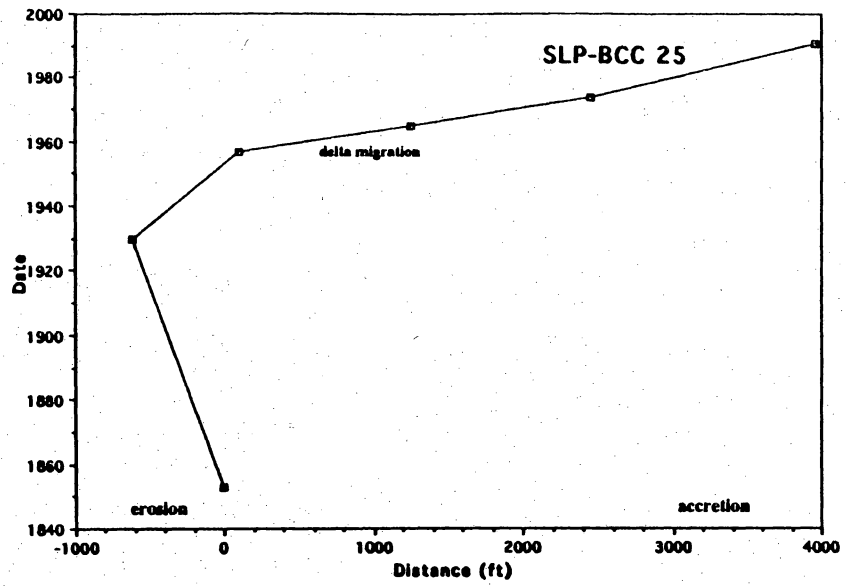




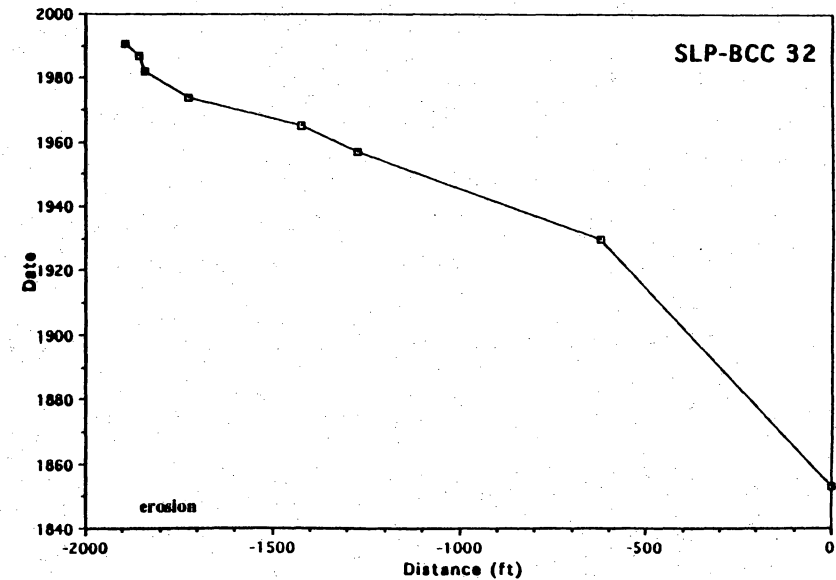
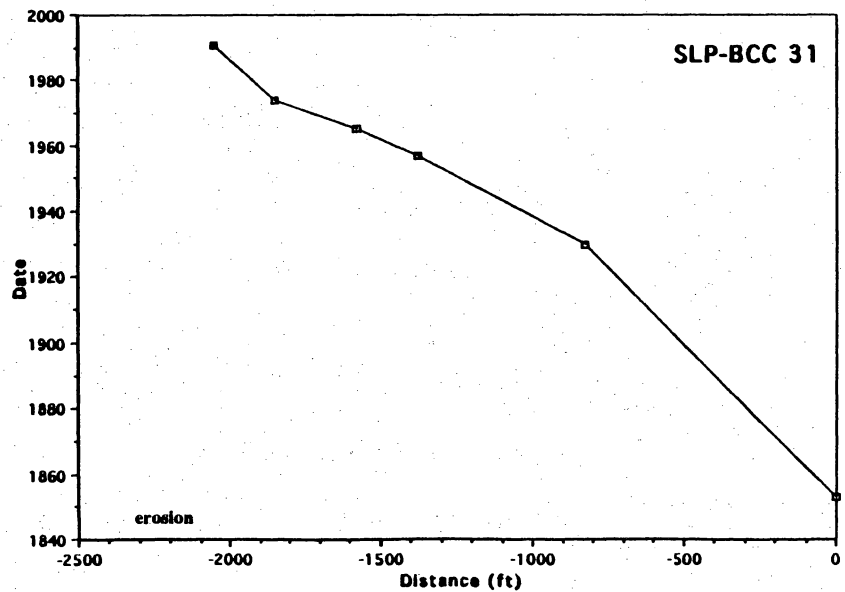
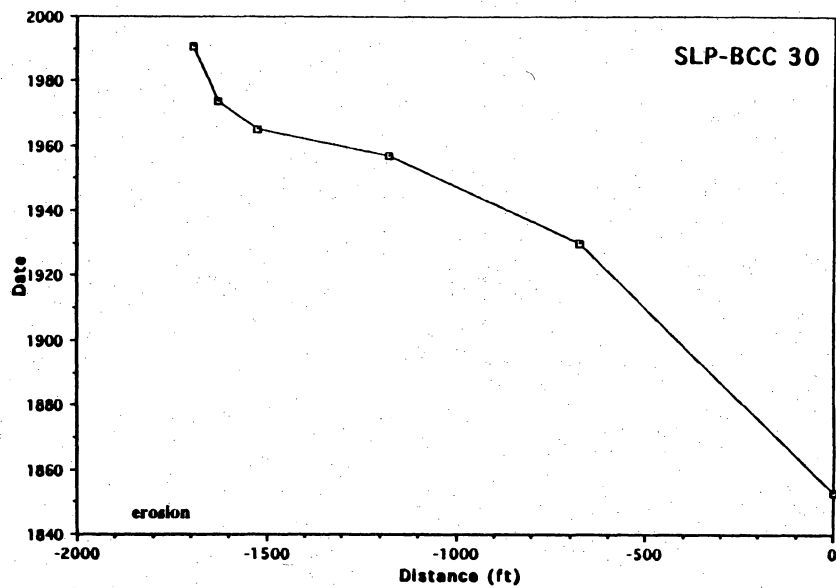
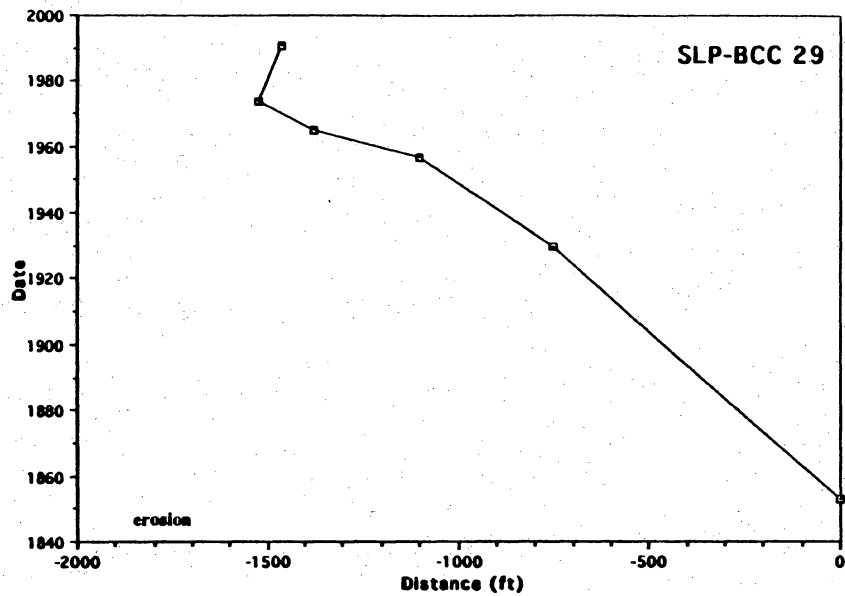


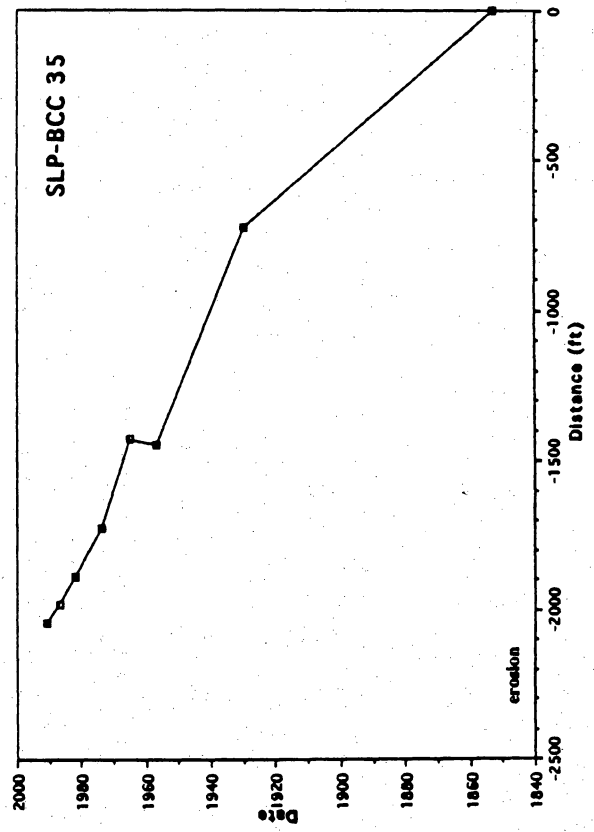
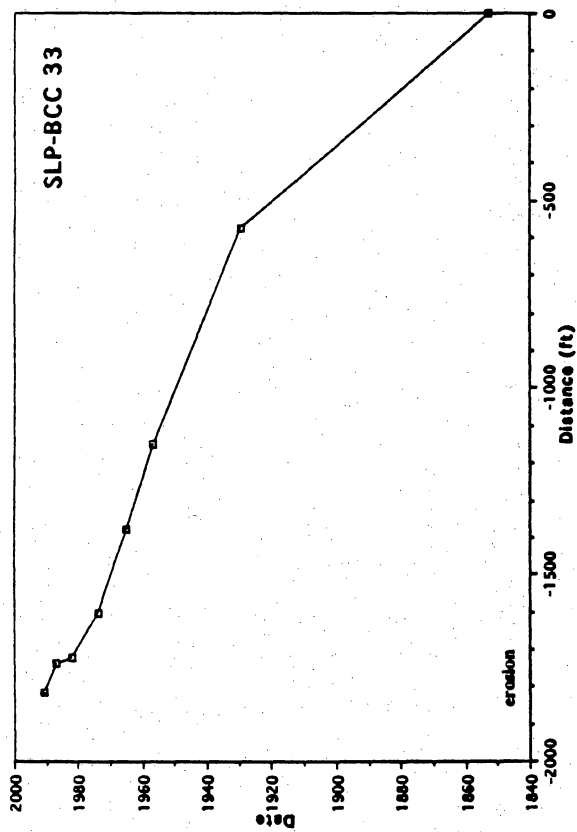
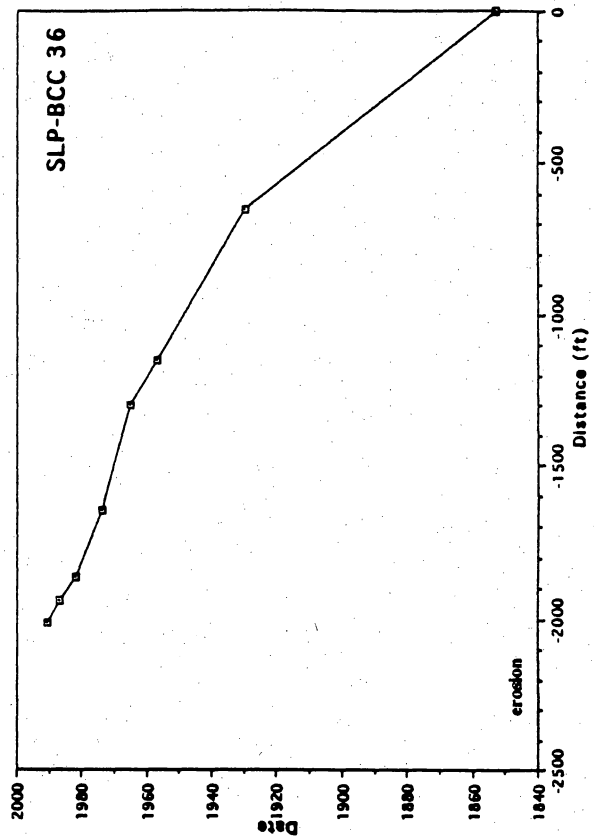
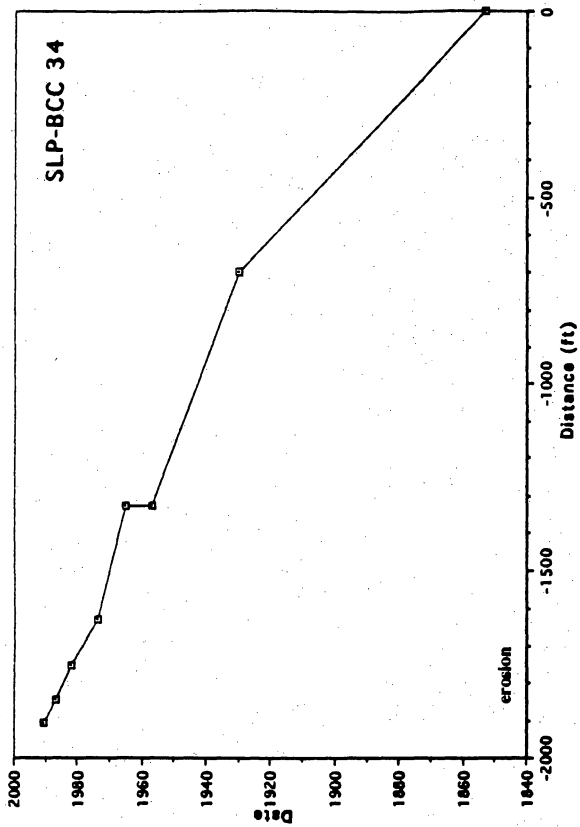


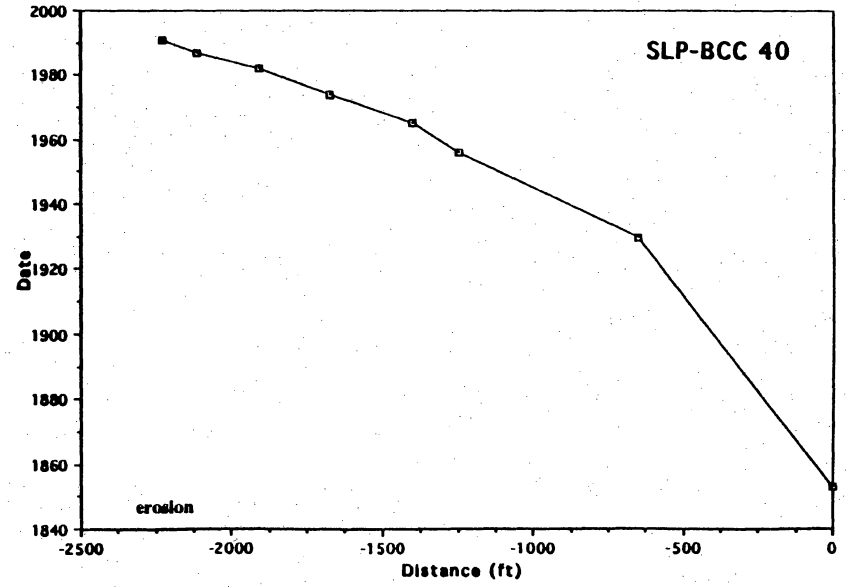
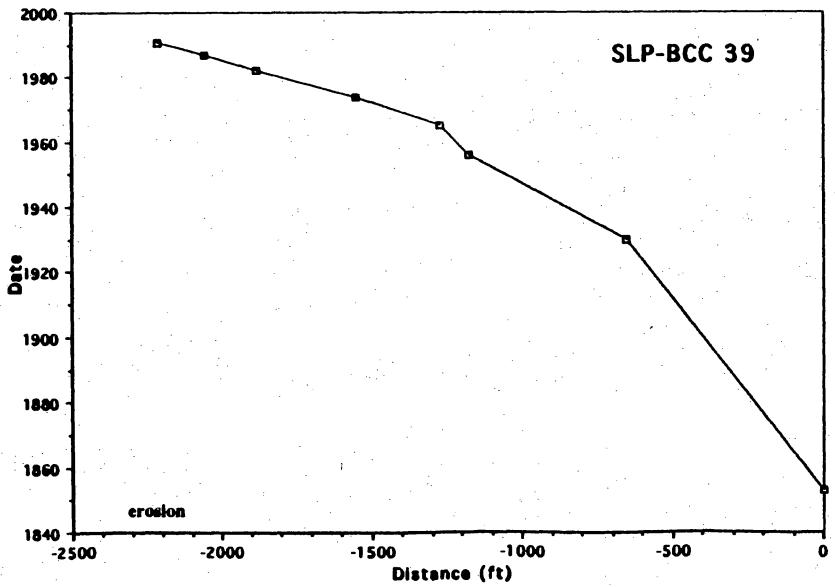
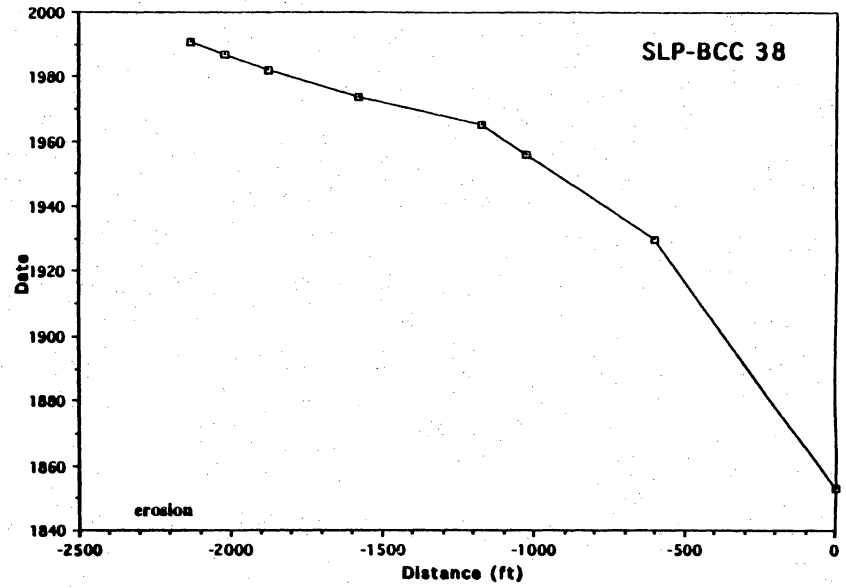
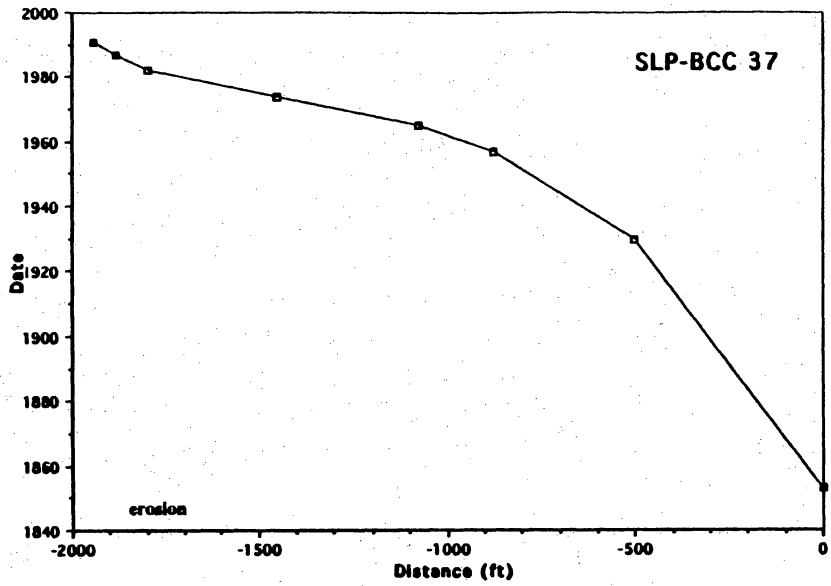


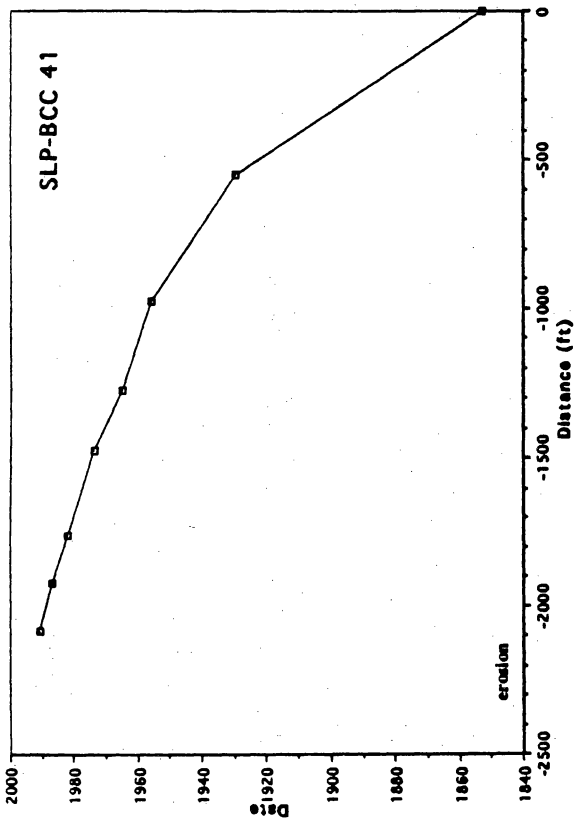
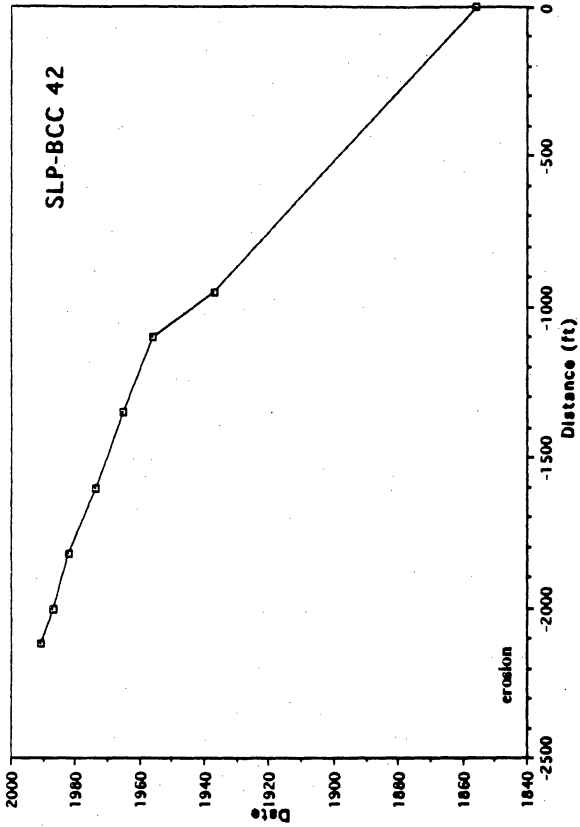








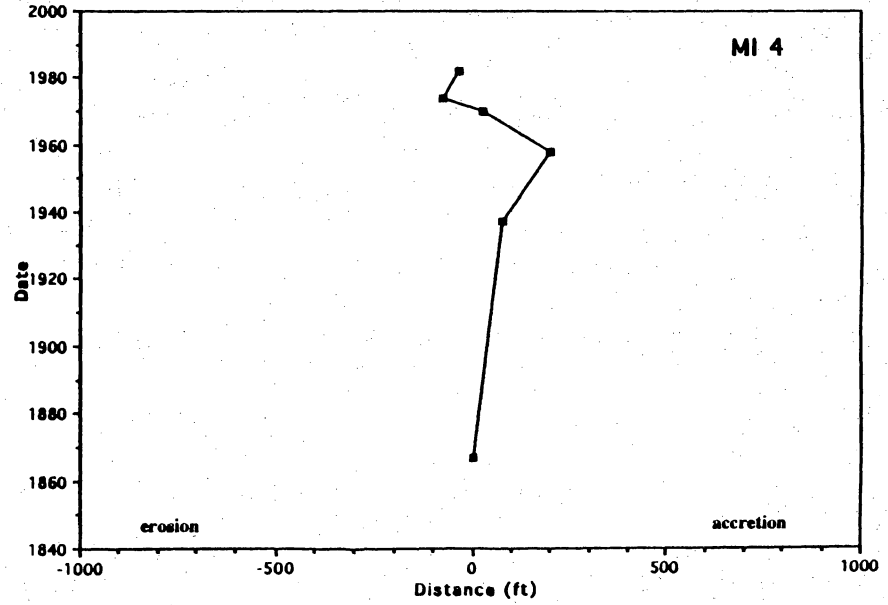
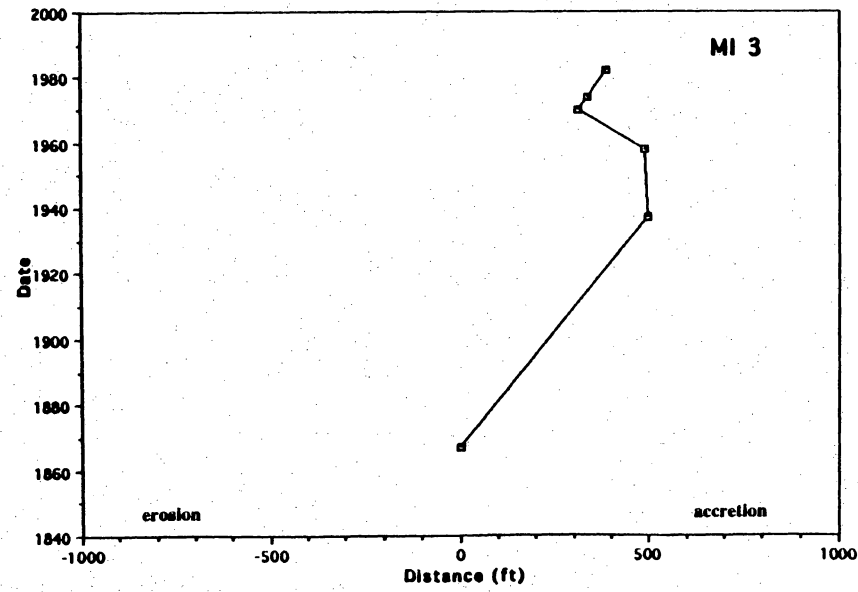
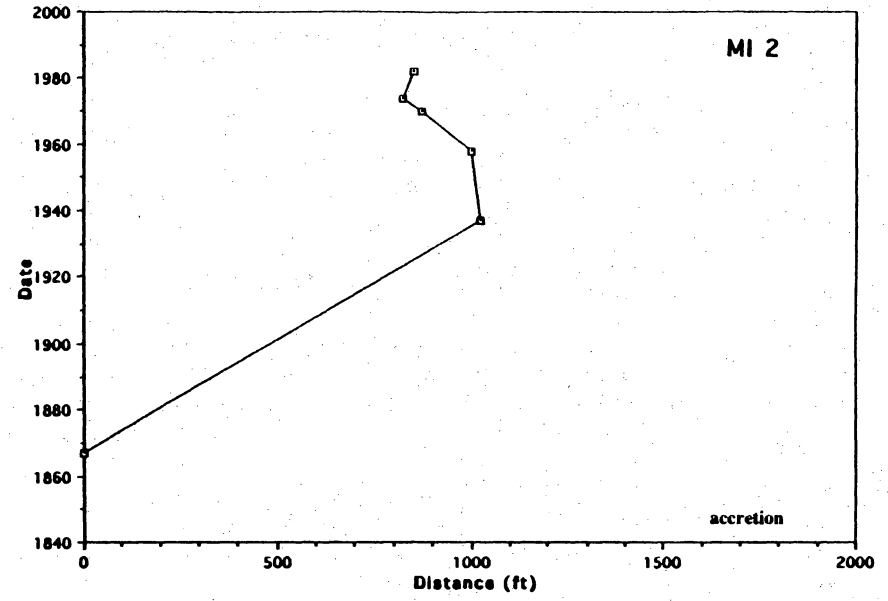
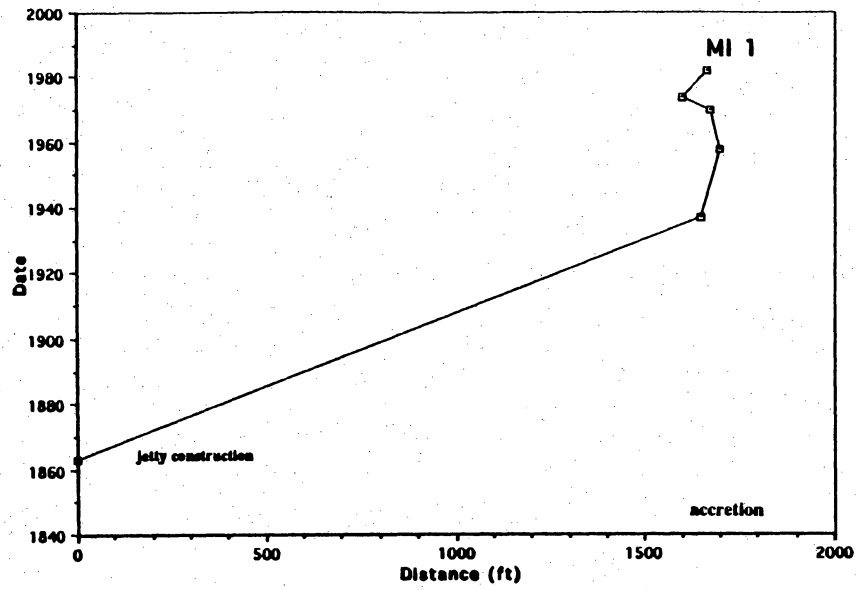


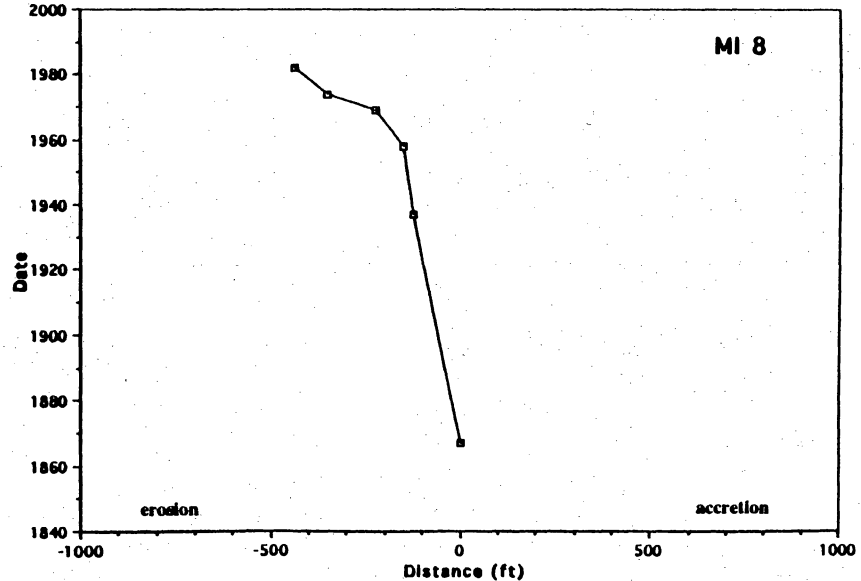
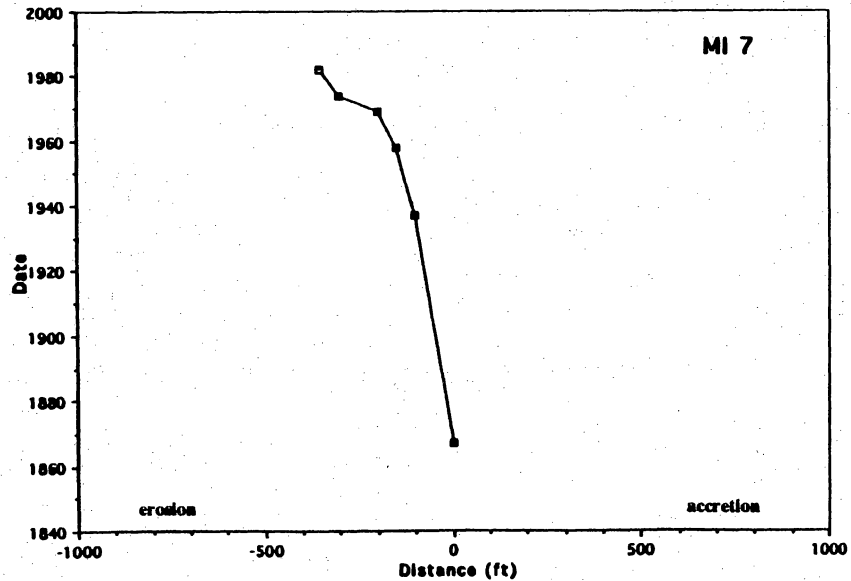
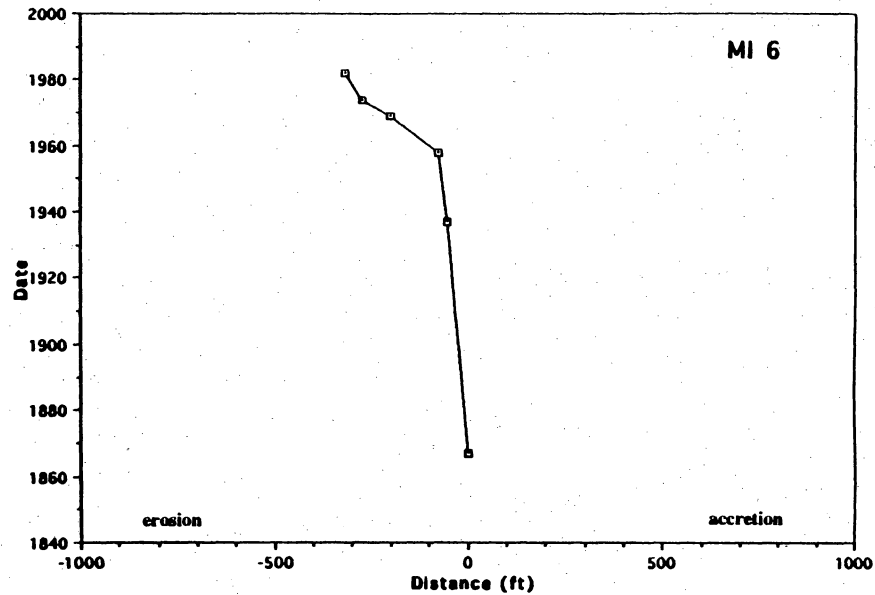
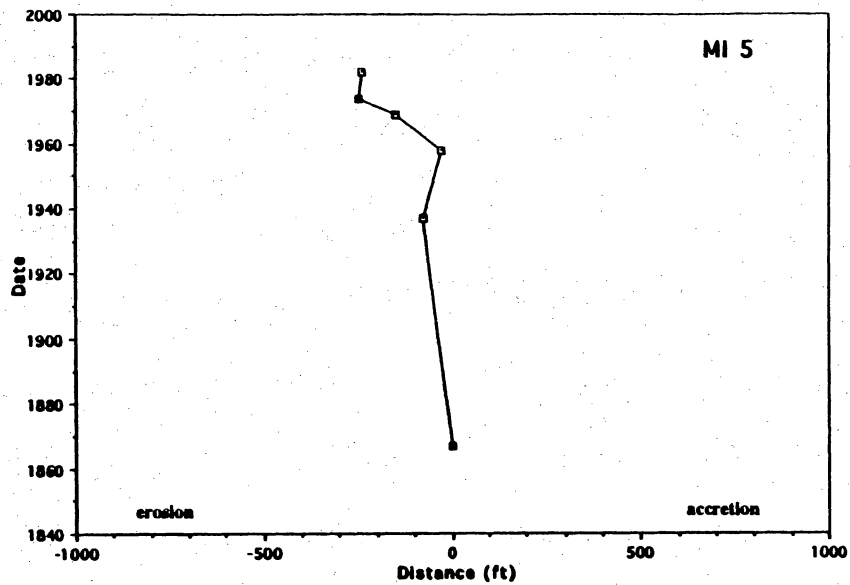


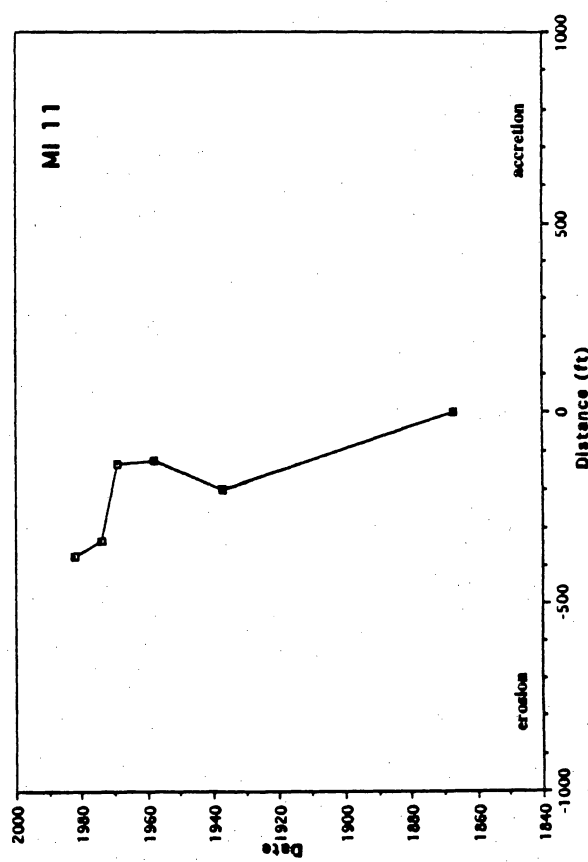
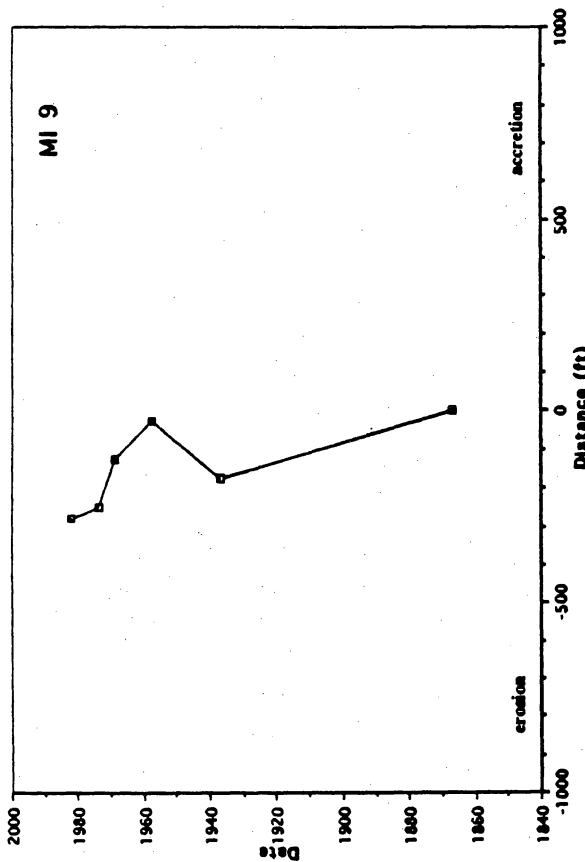
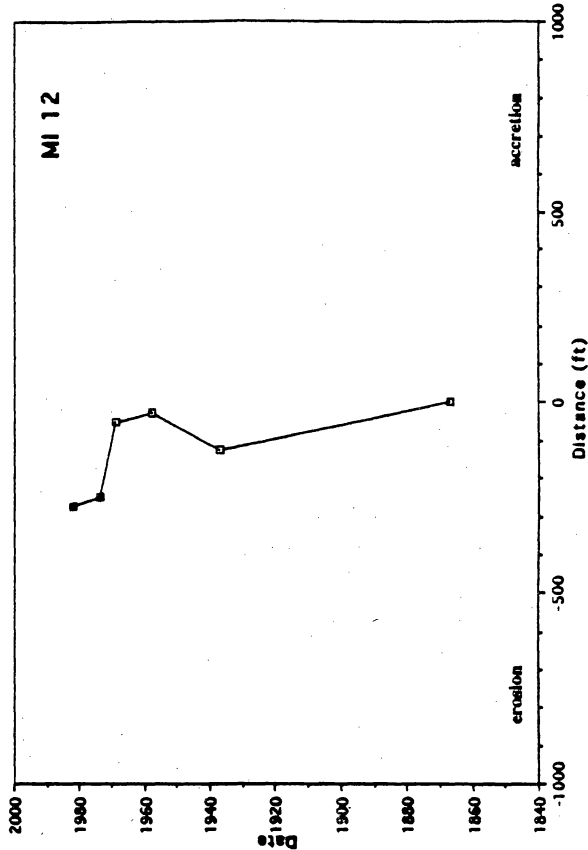
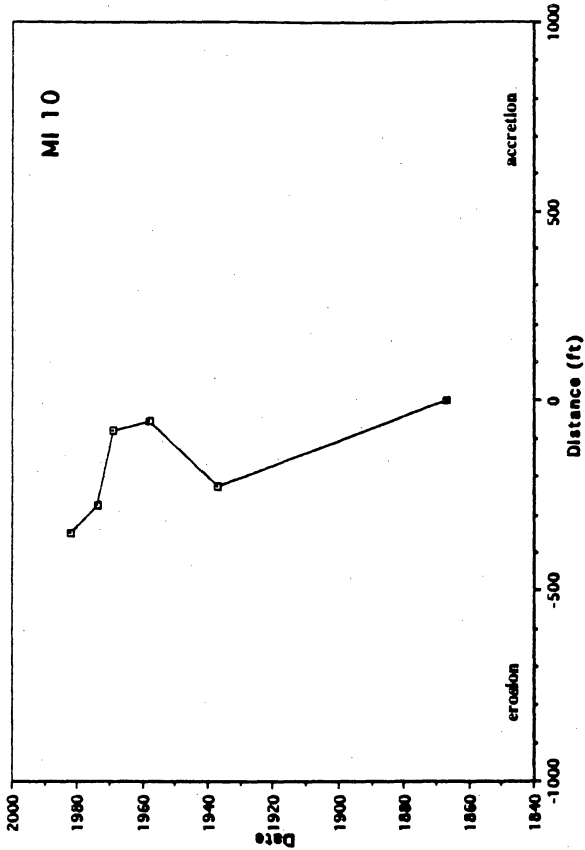
APPENDIX B. Tables and graphs of shoreline movement—Mustang and North Padre Islands. Geographic abbreviations for graphs depicting movement of the Texas Gulf shoreline: MI = Mustang Island, NPI = North Padre Island. Class intervals: A = accretion, S = stability, 1 = -2 to -5 ft/yr, 2 = -5 to -10 ft/yr, 3 = >10 ft/yr.

Shoreline Segment Mustang Island to North Padre  
(Port Aransas to Padre Balli Park)

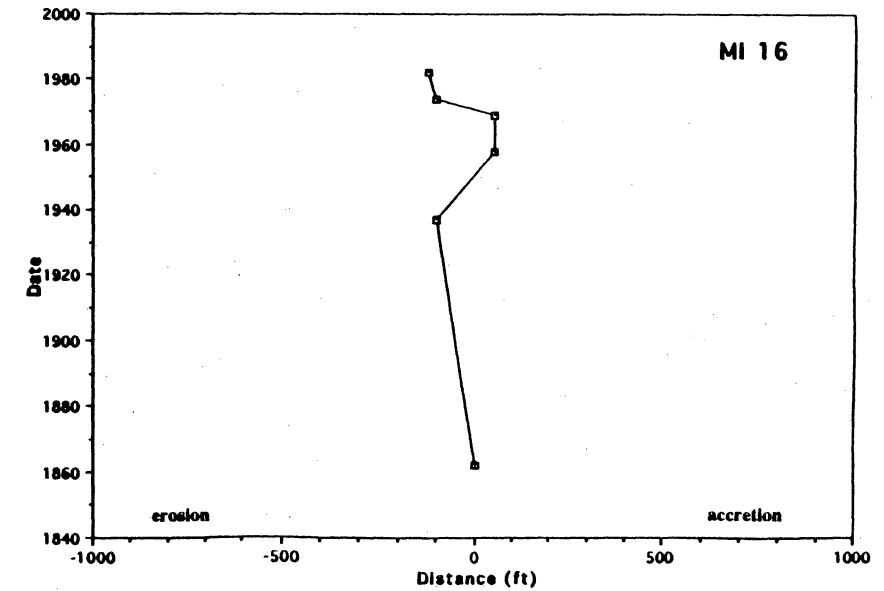
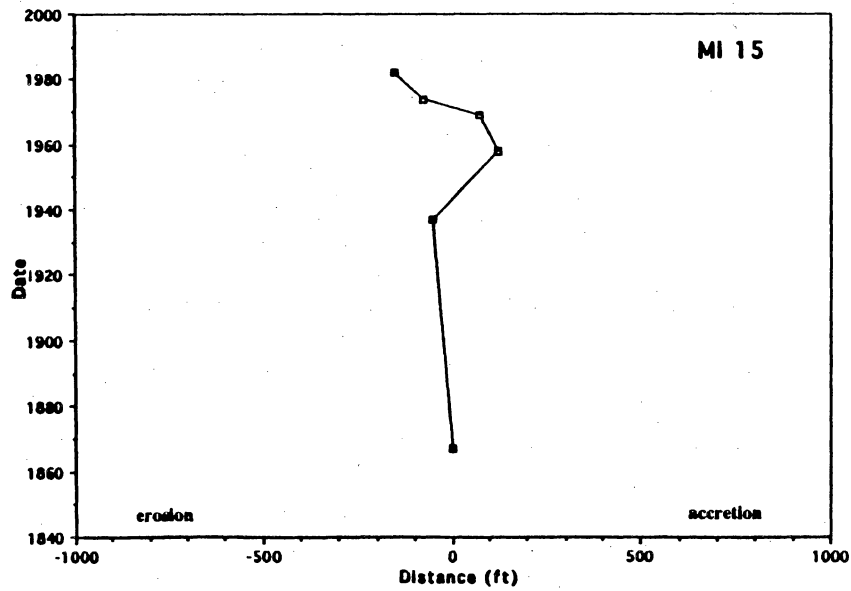
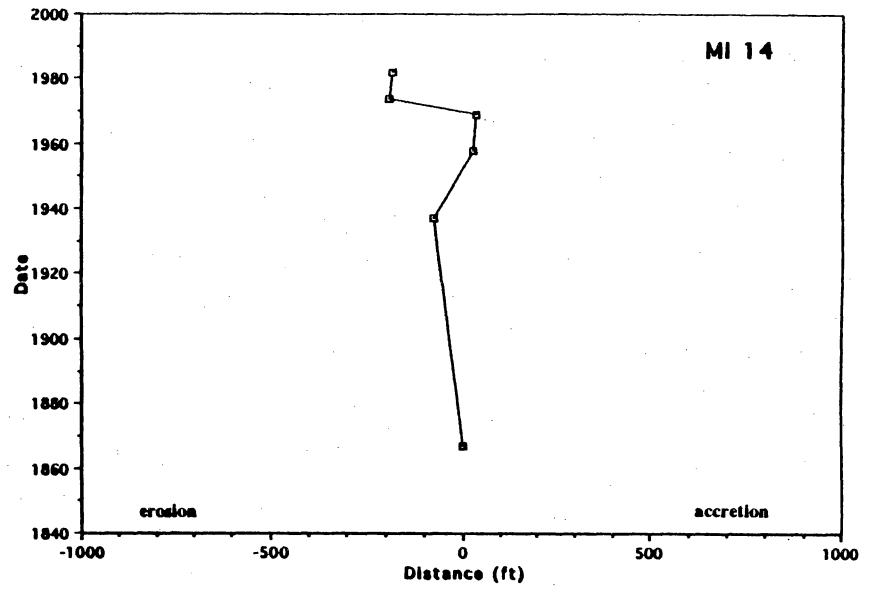
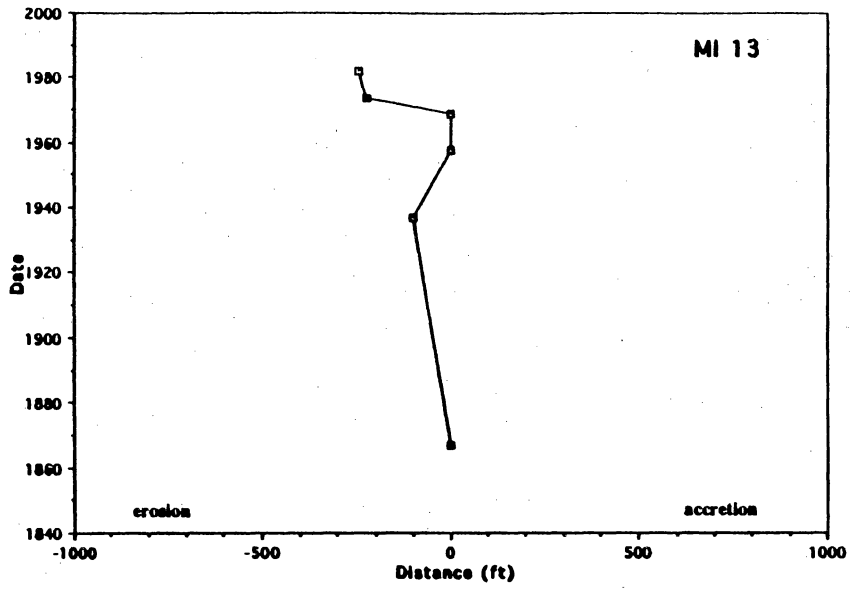
Transect	Period	Average rate (ft/yr)	Class interval
1	1937-1982	+0.4	S
2	1937-1982	-3.8	1
3	1937-1982	-2.5	1
4	1867-1982	-0.3	S
5	1867-1982	-2.1	1
6	1867-1982	-2.8	1
7	1867-1982	-3.1	1
8	1867-1982	-3.8	1
9	1867-1982	-2.4	1
10	1867-1982	-3.0	1
11	1867-1982	-3.3	1
12	1867-1982	-2.4	1
13	1867-1982	-2.1	1
14	1867-1982	-1.6	S
15	1867-1982	-1.3	S
16	1862-1982	-1.0	S
17	1862-1982	-1.5	S
18	1882-1982	-3.9	1
19	1882-1982	-3.2	1
20	1969-1982	-12.8	3
21	1969-1982	-12.7	3
22	1969-1982	-12.1	3

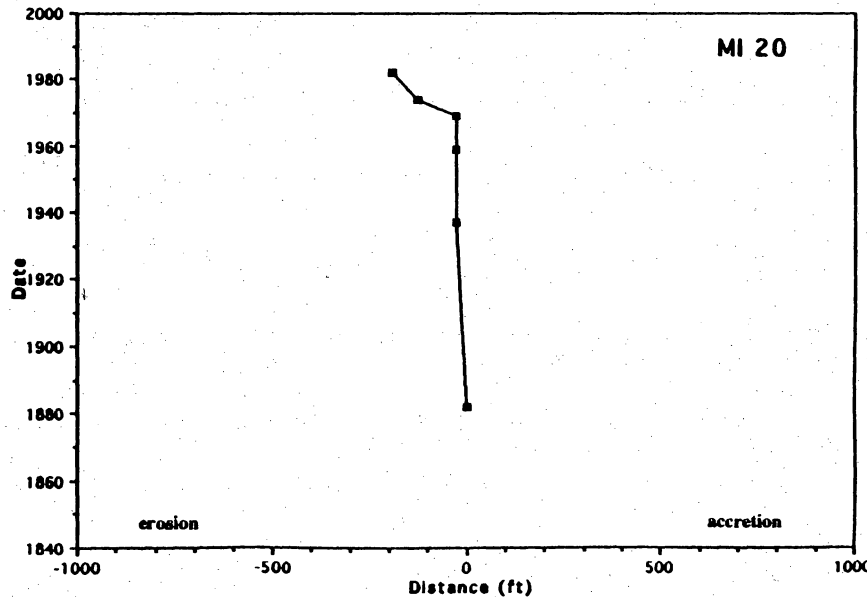
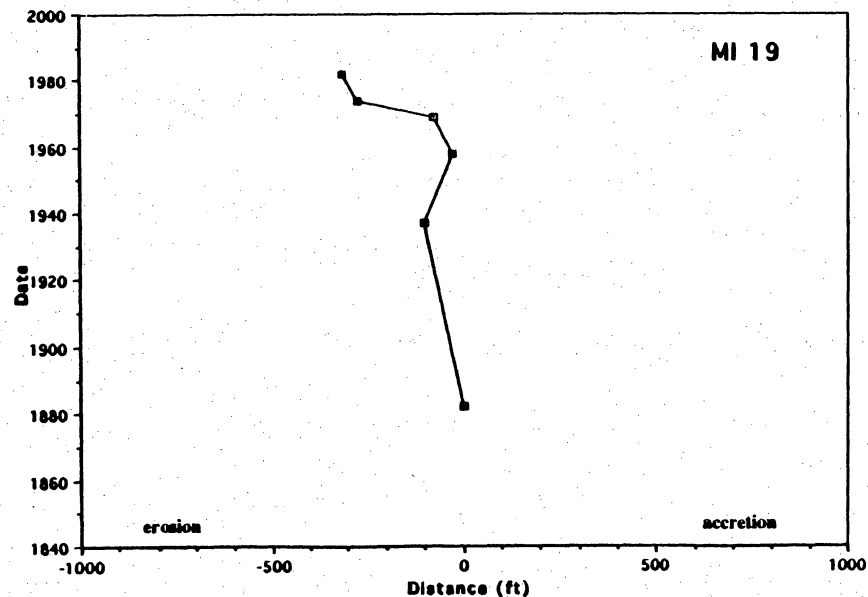
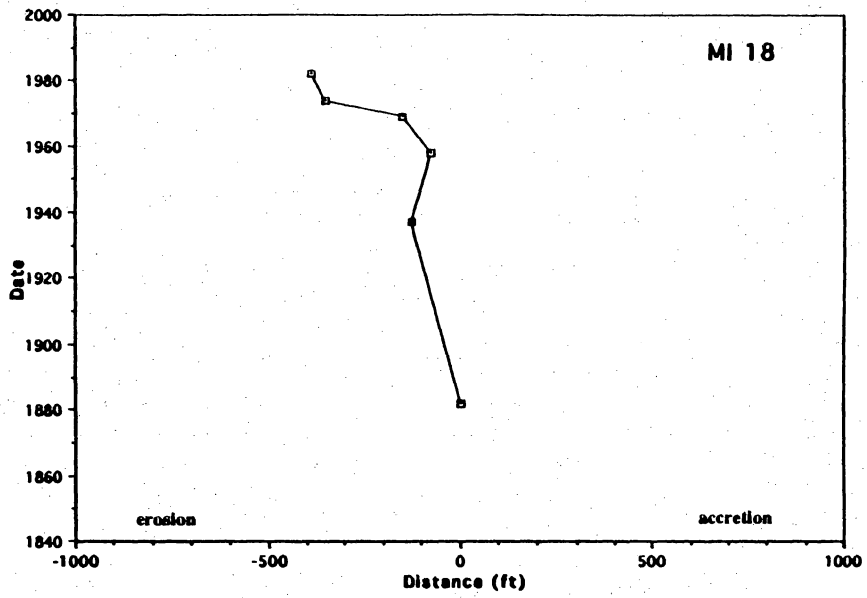
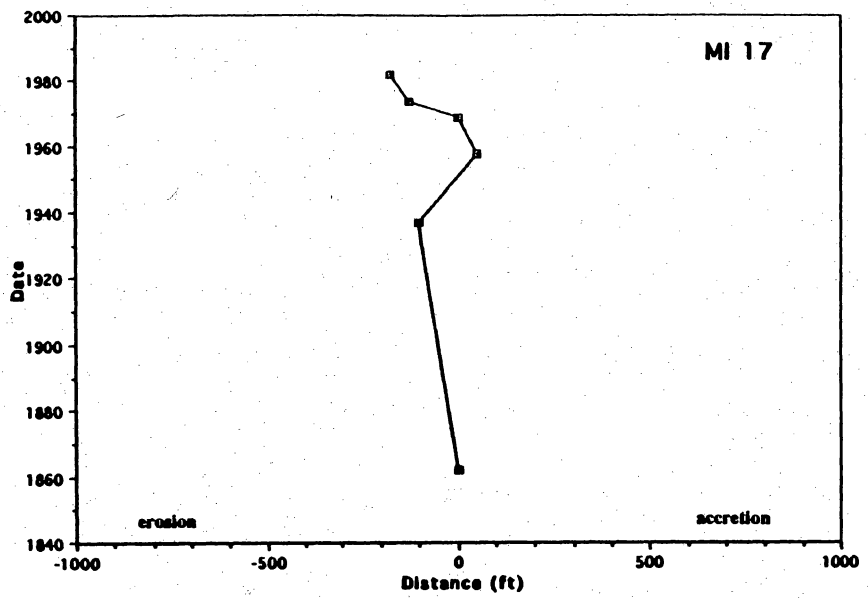


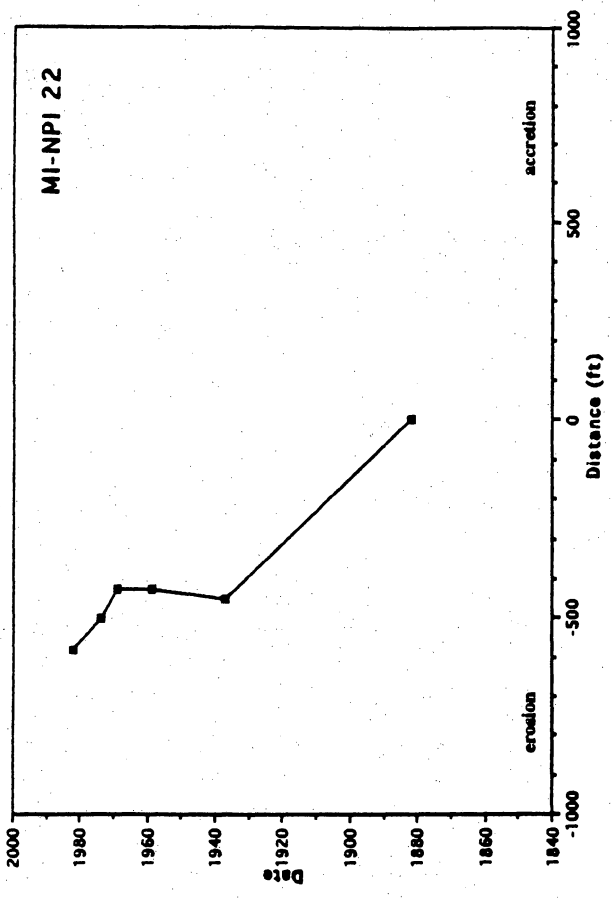
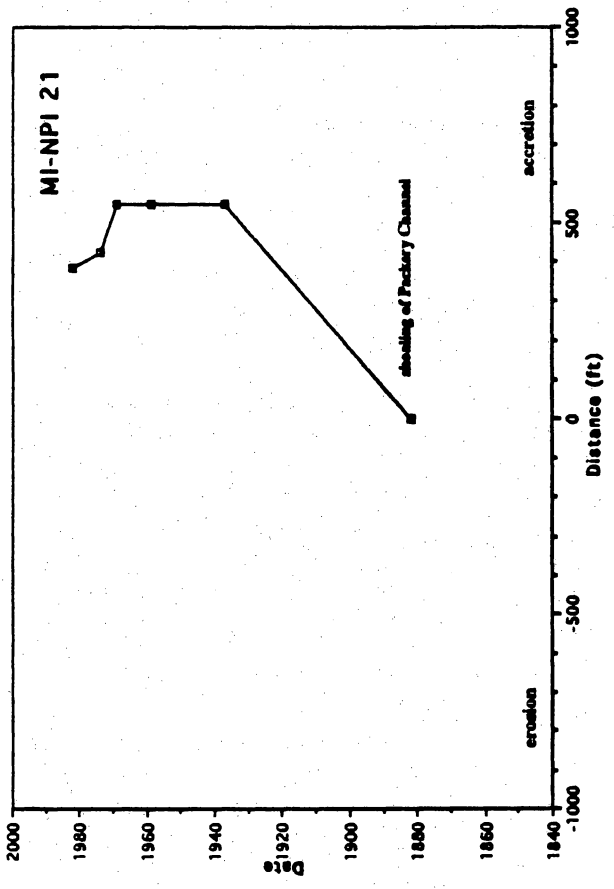










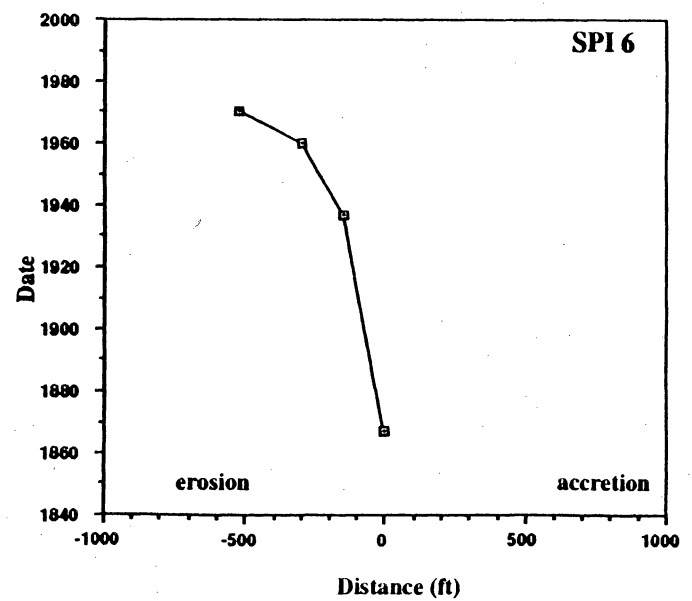
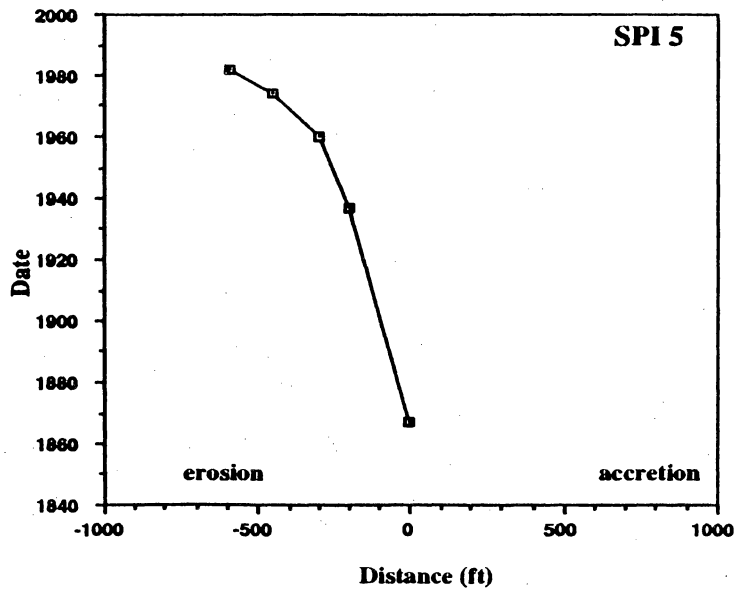
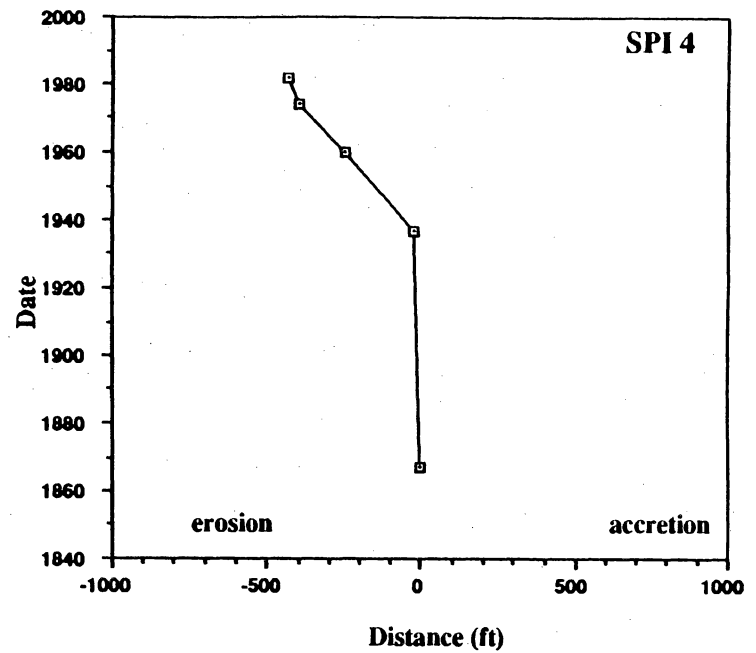
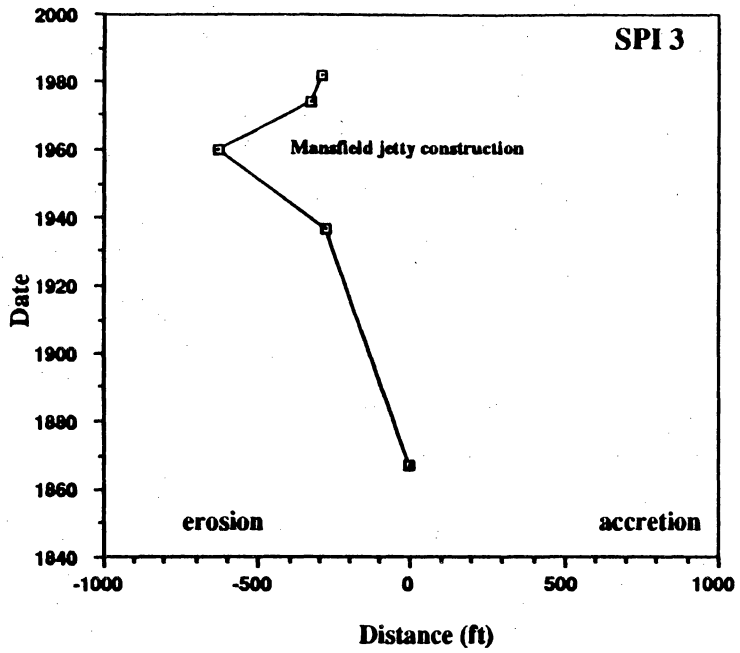


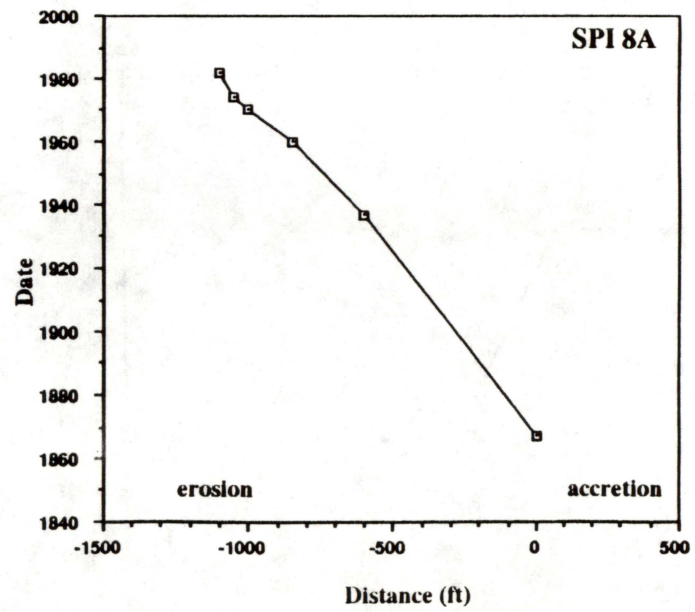
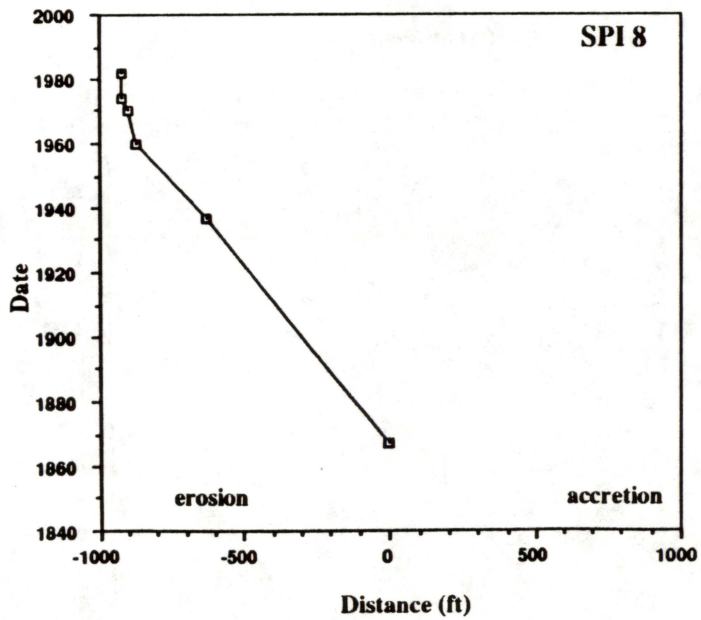
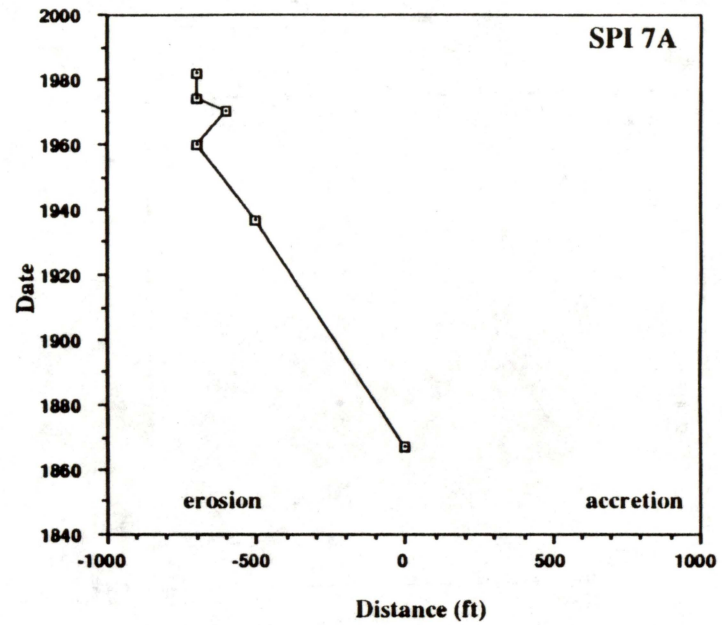
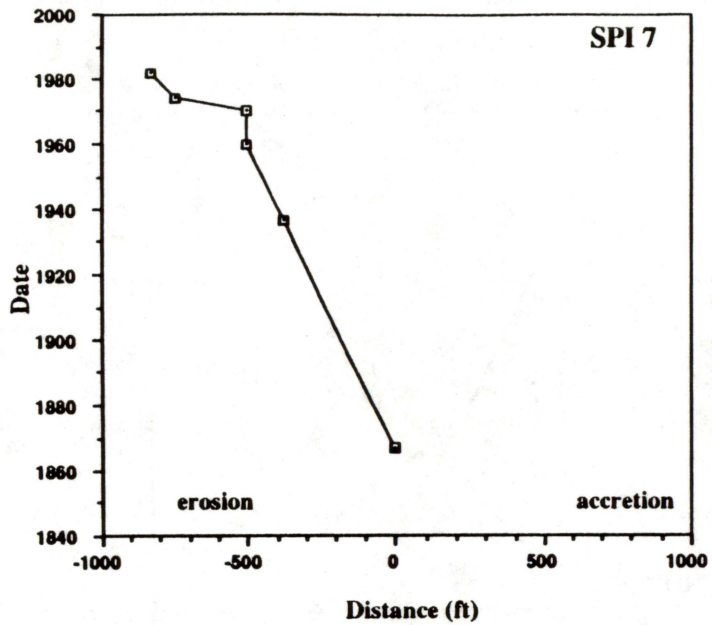
APPENDIX C. Tables and graphs of shoreline movement—South Padre Island. Geographic abbreviation for graphs depicting movement of the Texas Gulf shoreline.

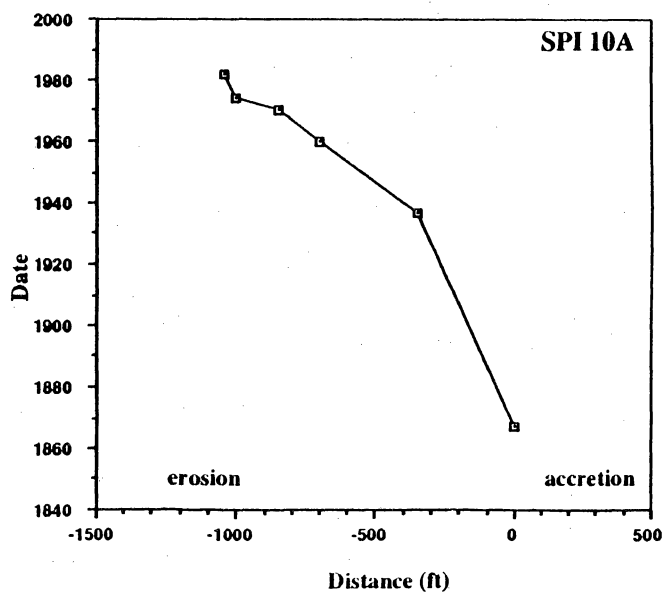
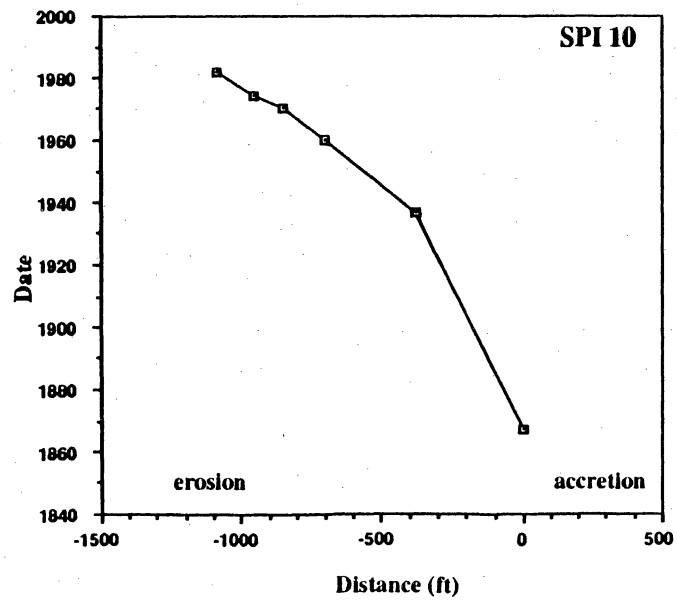
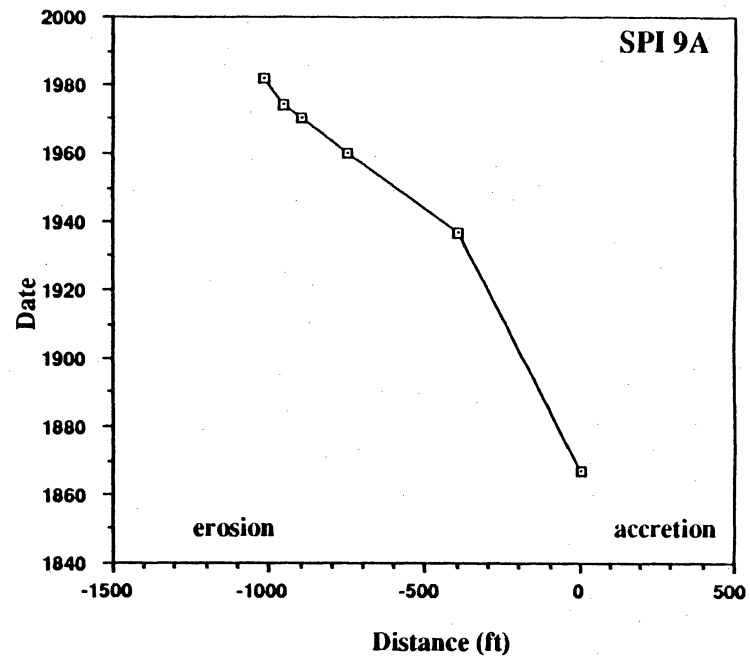
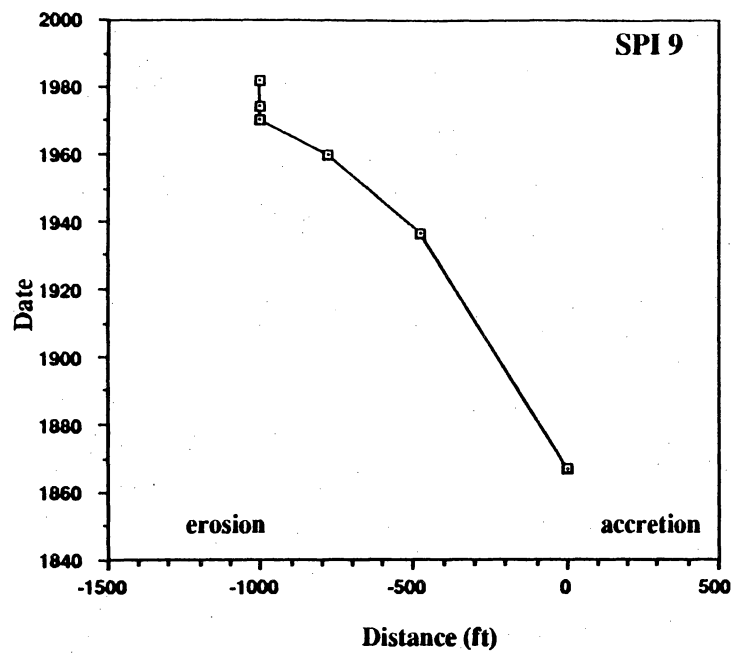
Shoreline Segment South Padre Island (Mansfield Channel to Brazos Santiago Pass)

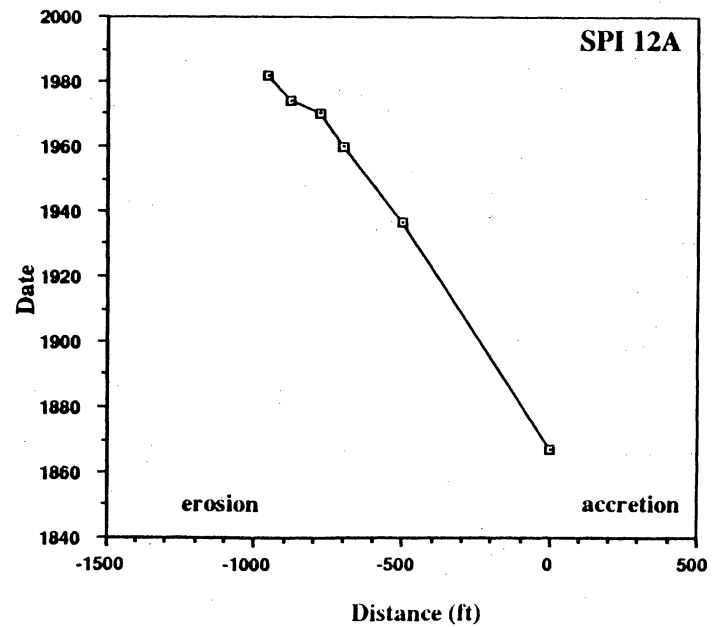
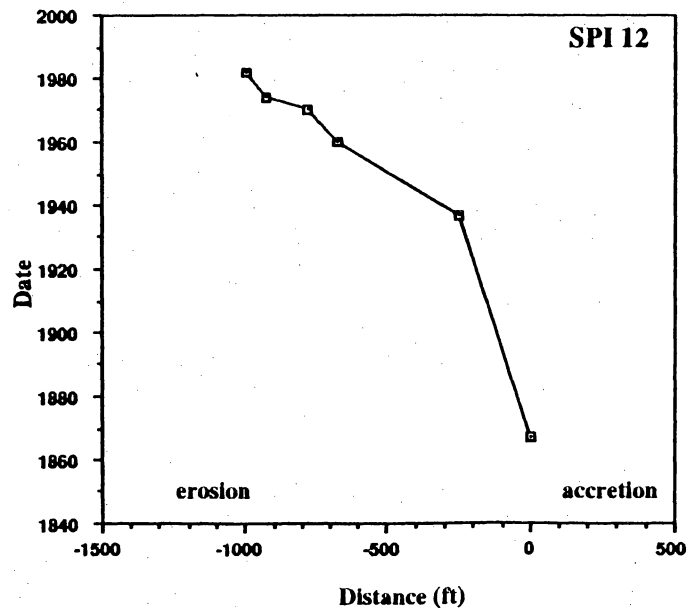
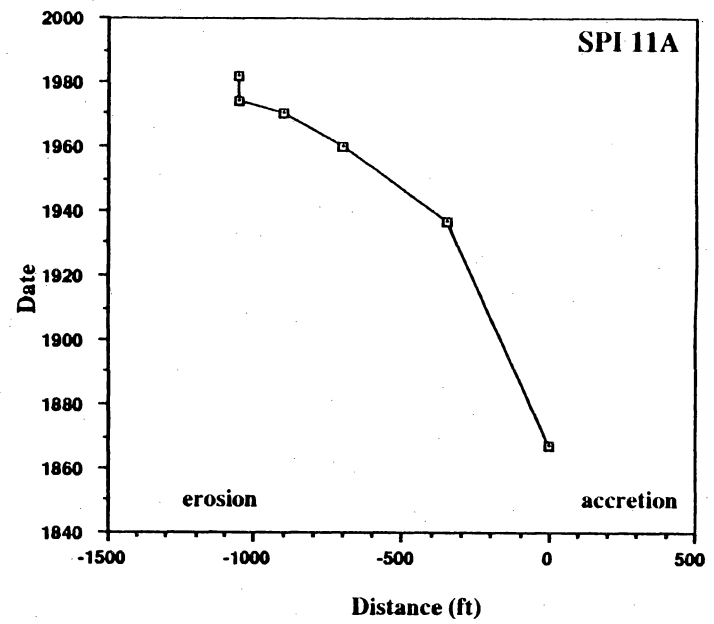
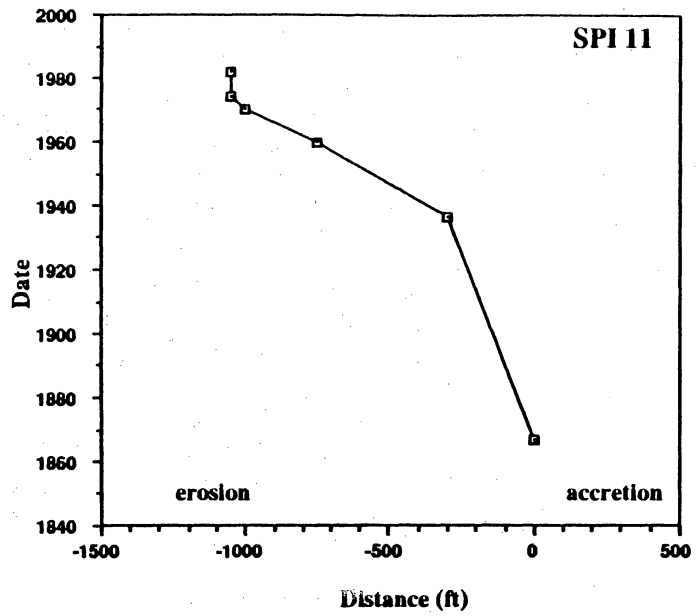
Transect	Period	Average rate (ft/yr)	Class interval
3	1960-1982	+15.1	A
4	1937-1982	-9.0	2
5	1960-1982	-13.5	3
6	1960-1974	-16.1	3
7	1969-1982	-15.1	3
7a	1879-1982	-7.8	2
8	1960-1982	-2.3	1
8a	1960-1982	-10.7	3
9	1937-1982	-6.7	2
9a	1937-1982	-13.5	3
10	1937-1982	-15.8	3
10a	1937-1982	-15.4	3
11	1937-1982	-16.7	3
11a	1937-1982	-15.6	3
12	1937-1982	-16.6	3
12a	1879-1982	-9.3	2
13	1879-1982	-8.9	2
13a	1960-1982	-21.0	3
14	1879-1982	-9.8	2
14a	1879-1982	-8.9	2
15	1879-1982	-6.9	2
15a	1867-1982	-9.8	2
16	1867-1982	-8.4	2
16a	1867-1982	-9.3	2
17	1937-1982	-6.9	2
17a	1937-1991	-6.3	2
18	1937-1991	-7.8	2
18a	1937-1991	-5.2	2
19	1937-1991	-0.4	S
19a	1937-1991	+5.1	A
20	1937-1991	+8.8	A
21	1937-1991	+12.0	A

SPI = South Padre Island. Class Intervals: A = accretion, S = stability, 1 = -2 to -5 ft/yr, 2 = -5 to -10 ft/yr, 3 = >10 ft/yr

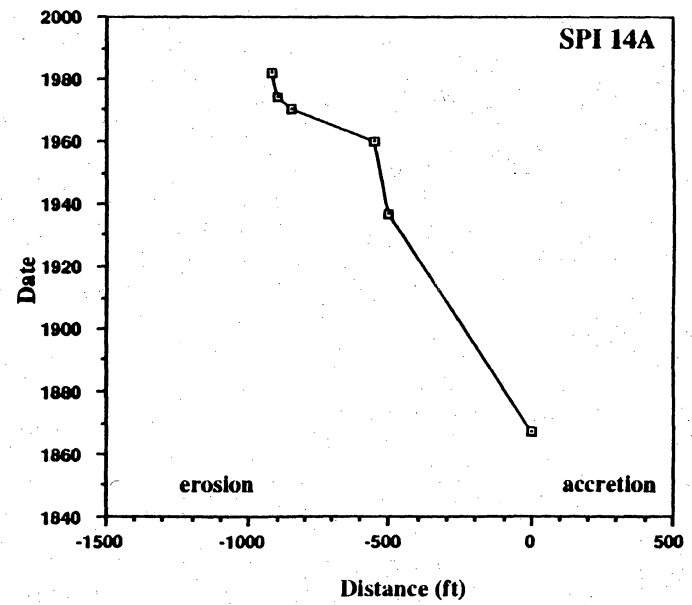
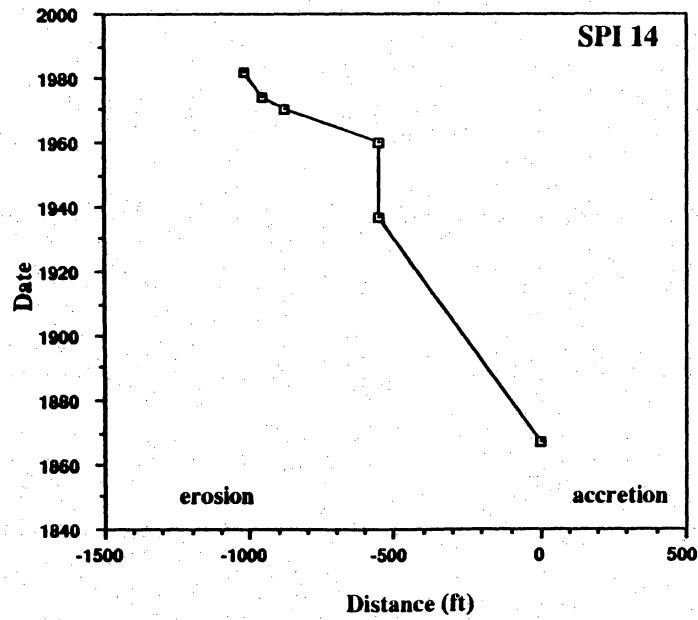
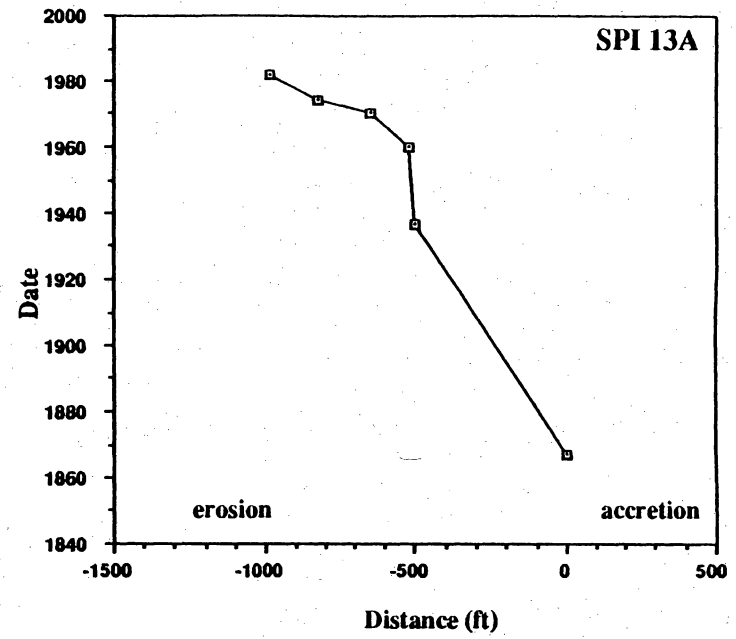
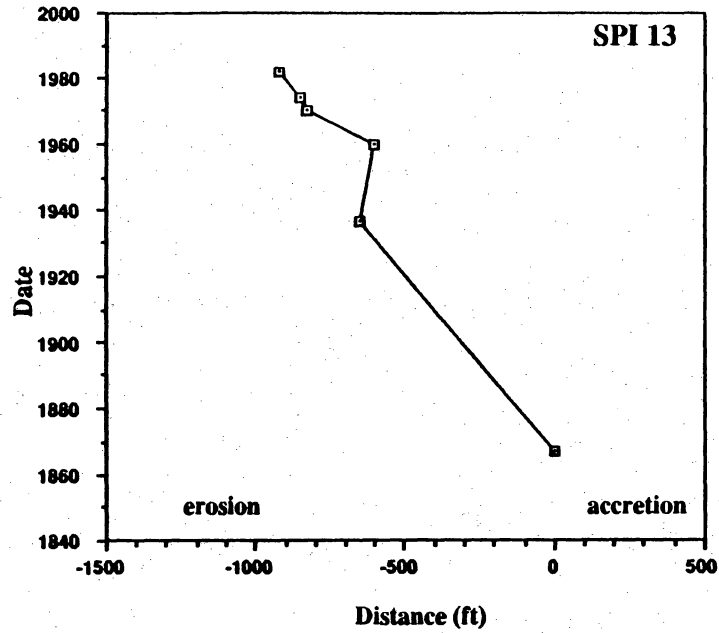


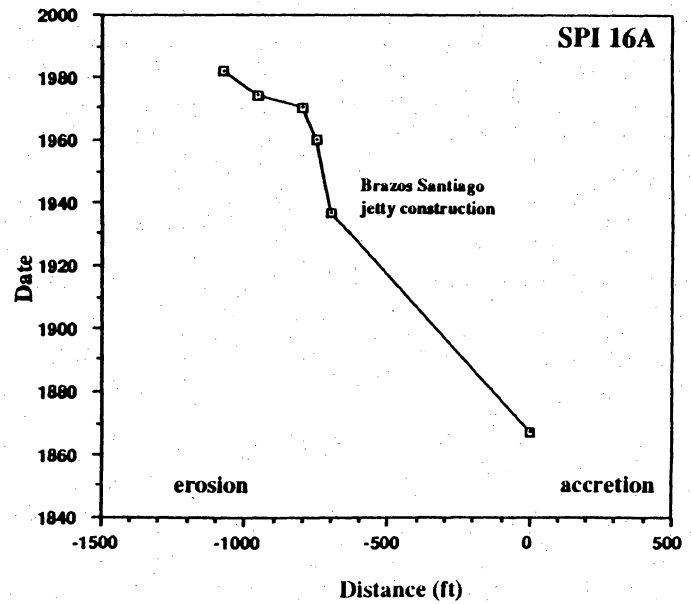
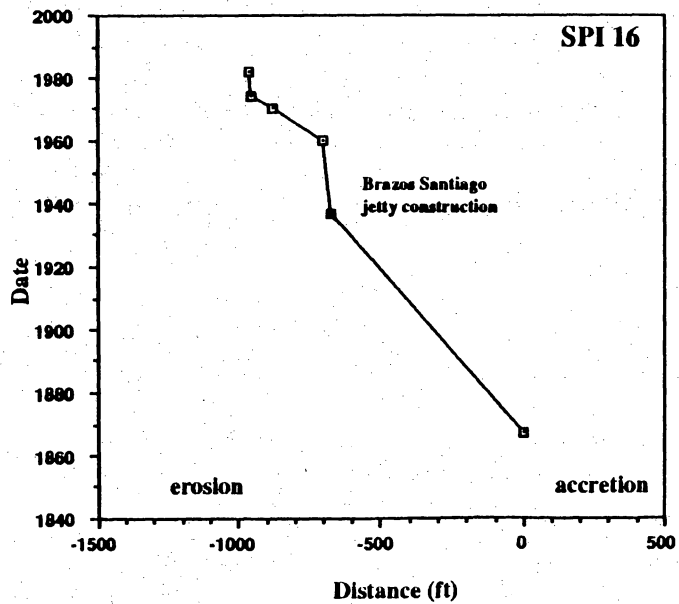
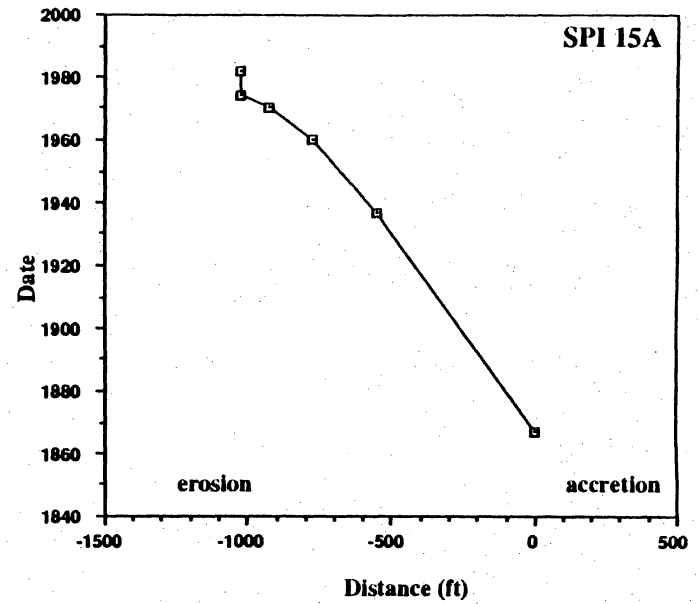
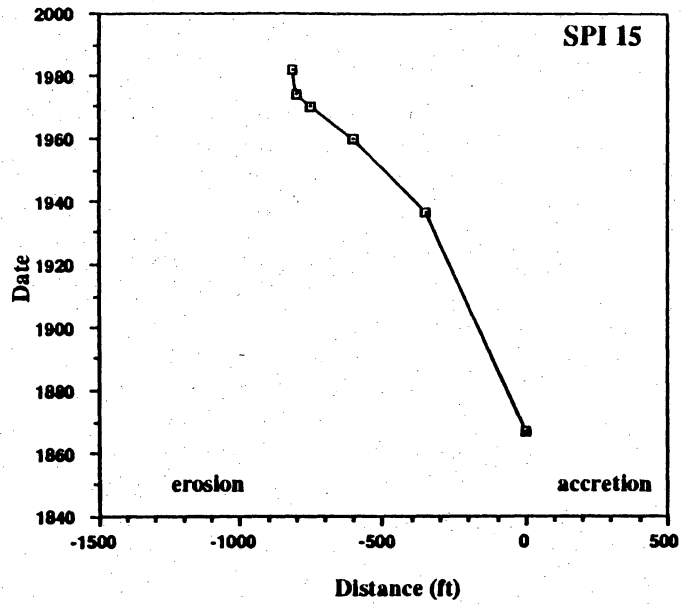


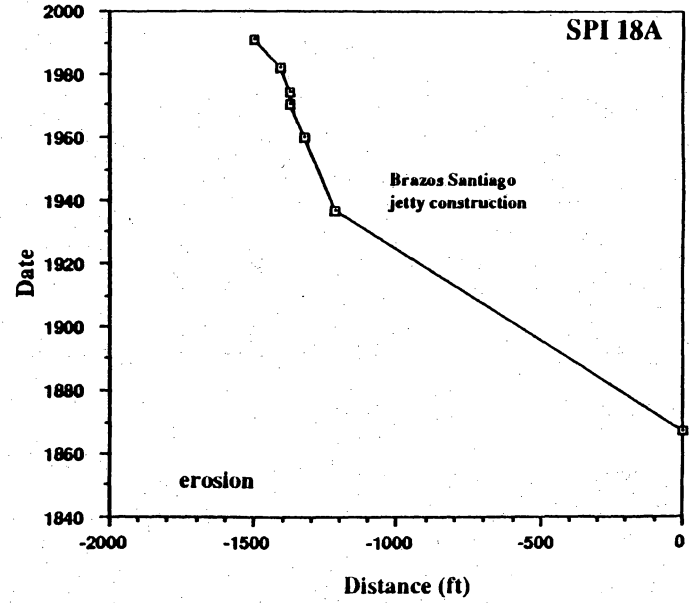
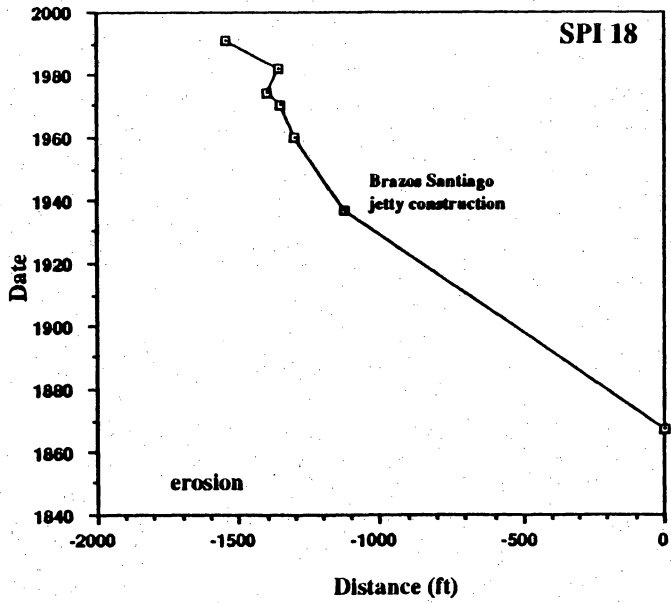
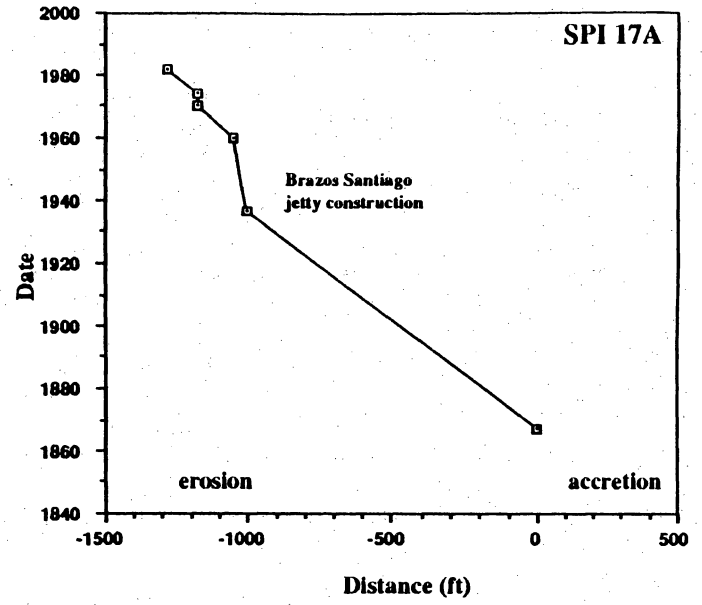
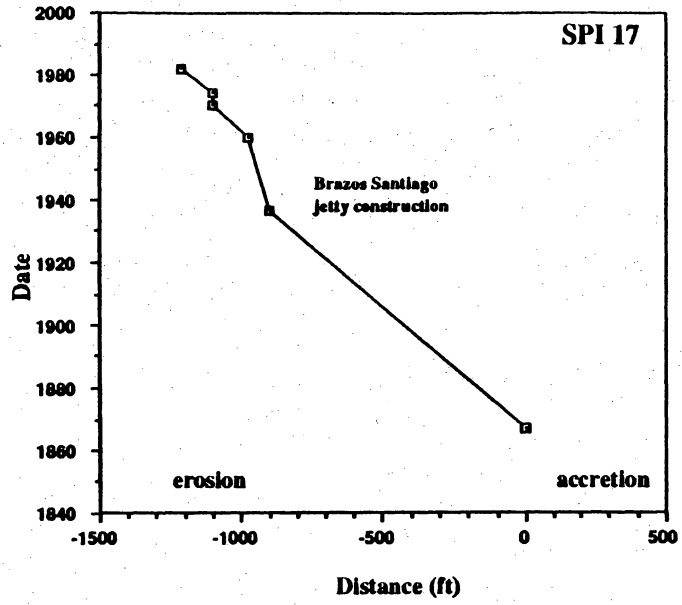


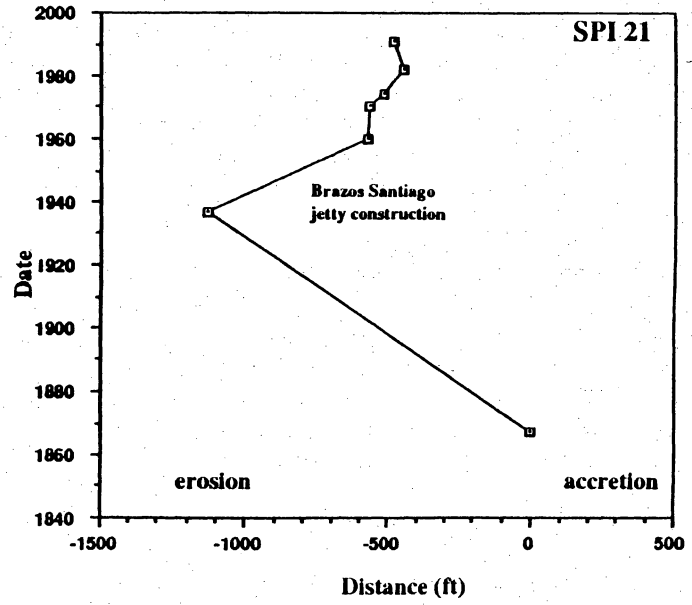
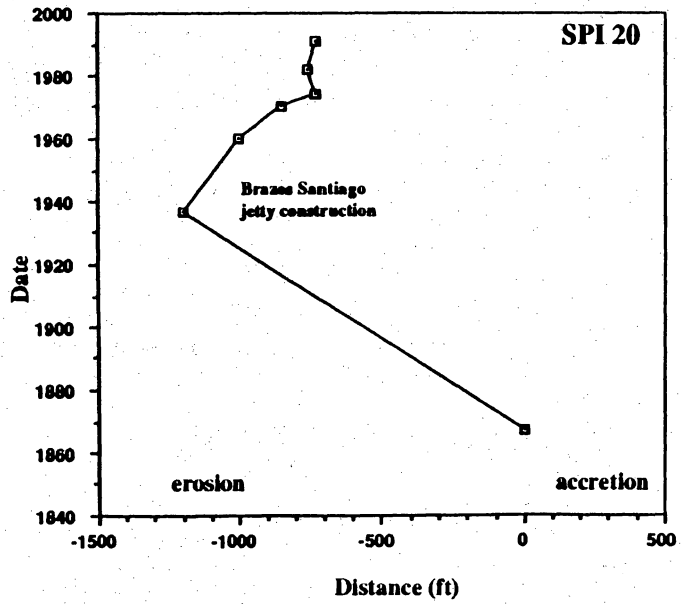
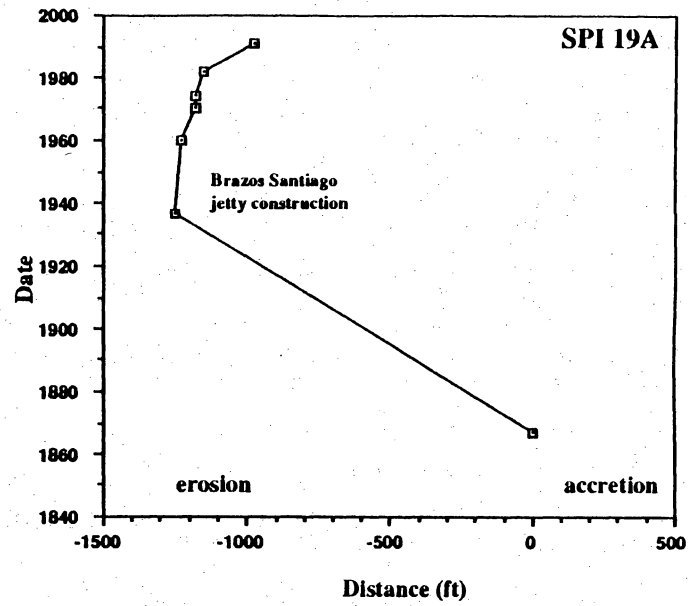
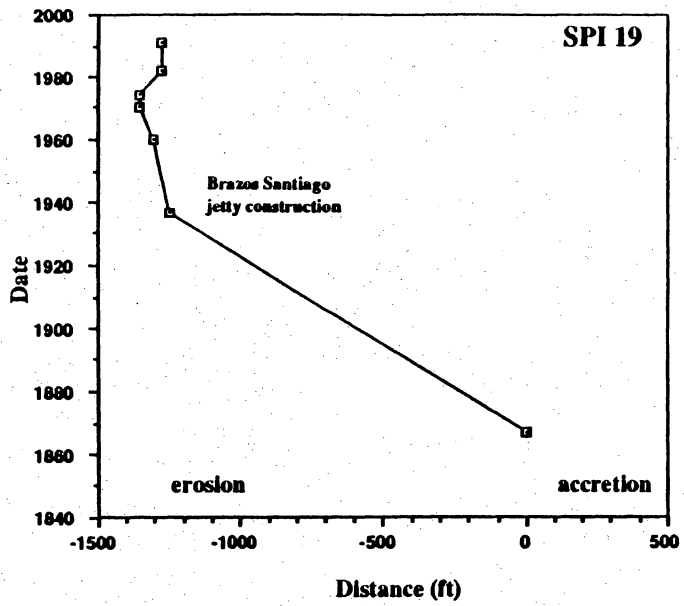












## ADDENDUM 2

### SUBMERGENCE AND EROSION OF WETLANDS, GALVESTON-TRINITY BAY AND SABINE LAKE ESTUARINE SYSTEMS

William A. White  
Bureau of Economic Geology  
The University of Texas at Austin

#### INTRODUCTION

The most extensive losses of coastal wetlands in the United States over the past two decades have occurred along the coast of the Northern Gulf of Mexico. Almost 60 percent of the wetland losses are due to replacement of salt and brackish marshes by open water (Dahl and others, 1991). Extensive losses of this type have been reported in Louisiana (Gagliano and others, 1981) and Texas (White and others, 1985, 1987, 1992; Morton and Paine, 1990), where approximately 58 percent of the Nations salt and brackish marshes are located (Field and others 1991).

In Texas, more than 20,000 ha of vegetated wetlands have been lost in coastal fluvial-deltaic areas (White and Calnan, 1991) and in the Galveston Bay system (White and others, 1992). The most extensive losses are characterized by submergence and displacement of marshes, swamps, and fluvial woodlands by shallow subaqueous flats and open water, indicating that aggradation rates are not keeping pace with rates of relative sea-level rise. Similar relationships between wetland loss and relative sea level rise have been observed in Louisiana. Wetland losses are pronounced along the upper Texas coast where wetlands are most abundant and where subsidence, especially associated with groundwater and petroleum production, is the major component of the relative sea-level rise equation.

#### Physiographic Setting

The modern regional geologic framework of the upper Texas coast (fig. 1) consists of two major estuaries (Sabine Lake and the Galveston-Trinity Bay system) and a complex array of Holocene and Pleistocene depositional systems (Fisher and others, 1972, and 1973). The estuaries formed when valleys entrenched by major rivers during Wisconsin glaciation and sea-level lowstand, were flooded during the post-glacial rise in sea level (Price, 1933 and 1947). Inland parts of the various river valleys have been completely filled, and in the case of the Trinity River, a delta has prograded over estuarine muds at the head of Trinity Bay (McEwen, 1969). Other prominent depositional features along the upper Texas coast include a modern

strandplain-chenier system (Fisher and others, 1973) southwest of Sabine Lake, and an extensive barrier island and peninsula complex that separates the bays and lagoons of Galveston Bay from the Gulf of Mexico (fig. 1).

Salt marshes characterize the mainland and island shores of West Bay and the shores of Bolivar Peninsula in East Bay. Brackish marshes, which are much more extensive than salt marshes, cover broad areas between Sabine Lake and Galveston Bay in the vicinity of the barrier-strandplain-chenier system, along the lower alluvial valleys and deltas of the Trinity and Neches Rivers, and on landward margins of West and Christmas Bays (fig. 1). Fluvial woodlands and swamps (forested wetlands) are most extensive along fresh water reaches of the Sabine, Neches, Trinity, and San Jacinto Rivers (fig. 1).

### Methods of Documenting Wetland Losses

Wetland losses were analyzed primarily from aerial photographs supported by ground truth. Wetlands delineated on aerial photographs were transferred to base maps and spatial and temporal changes determined primarily through digitization and entry of data into a geographic information system (White and others, 1992). In a few areas, mapped wetland changes are based on measurements using a grid system (White and others, 1985 and 1987). Wetland losses along eroding shorelines are based on measurement of differences in shoreline position as mapped on aerial photographs (Paine and Morton, 1986 and 1989).

### AREAL EXTENT AND DISTRIBUTION OF WETLAND LOSSES

Extensive areas of salt, brackish, and locally fresh marshes have been converted to areas of open water and flats as interior wetlands were submerged and bay and Gulf shorelines retreated from erosion. Losses are most pronounced in brackish marshes along the Neches River valley inland from Sabine Lake, and in salt and brackish marshes in the Galveston Bay system.

#### Neches River

The most extensive, contiguous loss of wetlands on the Texas coast has occurred along the lower Neches River (White and others, 1987). The Neches River, which discharges at the head of Sabine Lake, is the site of an extensive marsh-swamp complex that has developed on fluvial and fluvial- deltaic deposits (Fisher and others, 1973). Losses in wetlands in this area have been reported by Wiersema and others (1973), Gosselink and others (1979), and White and others (1987). Between the mid-1950's and 1978, about 3,800 ha of marshes were displaced primarily by open water along an approximately 16-km stretch of the lower Neches River valley (fig. 2).

Additional losses in vegetated wetlands (fresh-water marshes, woodlands, and swamps) occurred upstream from this site where areas of emergent vegetation decreased by about 342 ha between 1938 and 1956, and by approximately 1,305 ha between 1956 and 1987. The rate of loss of vegetated wetlands was 19 ha/yr for the earlier period and 42 ha/yr for the latter period. The major loss in vegetated wetlands between 1938 and 1956 was primarily a result of a large navigation basin dredged in a marsh area adjacent to the Neches River. From 1956 to 1987, marsh losses were primarily due to submergence.

The displacement of marshes by open water and shallow subaqueous flats in the Neches River valley is apparently related to several factors including: (1) relative sea-level rise resulting primarily from subsidence possibly due to oil and gas production, (2) a decline in sediments supplied to this alluvial area as a result of (a) reservoir development in the Neches River basin, (b) artificial levees (dredged spoil, Fisher and others, 1973) along the dredged portion of the river, and (c) changes in hydrology due to artificial channels (Wiersema and others, 1973), (3) active faulting, in which the downthrown side of one identified fault is subsiding at a more rapid rate than the upthrown side (White and others, 1987; fig. 2), and (4) dredged canals, which can cause direct and indirect losses in marshes (Wiersema and others, 1973; Scaife and others, 1983).

Similar changes have occurred in a brackish-water marsh about 50 km east of Sabine Lake on the Chenier Plain (gulfward of Calcasieu Lake, Louisiana). DeLaune and others (1983) reported changes from marsh area to open water are occurring at ever increasing rates apparently because marsh sedimentation rates (averaging 0.8 cm/yr) are not keeping pace with submergence rates (averaging 1.2 cm/yr). The change in marsh area to open water has been increasing by a factor of approximately 2 every 6 years since 1963. DeLaune and others (1983) predict that this marsh area will complete its transformation to open water in less than 40 years if the trends that have characterized the past 25 years continue. Among the human activities that may contribute to the transformation to open water are (1) ship channel construction (promoting salt intrusion and possibly sediment diversion) and (2) oil, gas, and groundwater withdrawals (accelerating subsidence). However, DeLaune and others (1983) concluded that it is difficult to document the human component precisely because of its pervasiveness in this area and because some of the observed trends contradict expected effects.

The factors contributing to marsh loss listed in the preceding discussion of the Neches River valley are complex and difficult to quantify adequately with existing data. But the conversion of marsh to open water indicates marsh aggradation rates are not keeping pace with subsidence rates and relative sea-level rise. Subsidence rates in this area of the Neches River valley are not known, but the rate at Sabine Pass reported by Swanson and Thurlow (1973), for the period 1960 to 1969, is 1.25 cm/yr, a rate equal to that reported by DeLaune and others (1983). In the Neches River valley, the rate of subsidence may be similar or possibly even higher due to withdrawal of

underground fluids (Ratzlaff, 1980) and faulting (White and others, 1987). Over a 22-year period (1956-1978) the marsh has been replaced by open water at an average rate of about 160 ha/yr.

## Galveston Bay System

In the Galveston Bay system 10,710 ha of emergent wetlands was converted to open water and flats from the 1950's to 1989 (White and others, 1992). Major areas impacted include wetlands in the Trinity and San Jacinto River valleys, Virginia Point (an area south of Texas City), and Bolivar Peninsula.

### Trinity River

The Trinity River delta is one of only two Texas bay-head deltas (the other being the Colorado River delta) identified by Shepard (1953) as having undergone significant progradation in recent historic times. Accordingly, analysis of historical shoreline changes indicates local delta shoreline progradation in which marshes have advanced bayward at rates of more than 1.8 m/yr, with a high, locally, of 32 m/yr between 1930 and 1982 (Paine and Morton, 1986). Older inactive parts of the delta retreated at rates of 1.2 m/yr to 3.1m/yr between 1930 and 1974 or 1982. Shorelines at most stations on the active delta lobe prograded (accreted) into the bay during the period 1930 to 1982. However, the shoreline at one monitoring station eroded during this period, while another began eroding after 1956. Shorelines at monitoring stations along the inactive lobe of the delta to the west have retreated at rates of up to 3.3 m/yr (Paine and Morton, 1986).

Losses in the delta are most pronounced in interior regions of the wetlands, where water has encroached into areas previously mapped as marshes (White and others, 1985 and 1992). In fact, losses in vegetated wetlands exceeded 1,742 ha for the period 1953 to 1989 (White and others 1992, fig. 3). About 60 percent of the change can be attributed to submergence. Approximately 40 percent of the change was due to construction of a power plant cooling reservoir (more than 1,010 ha) in the western part of the delta.

Marsh loss in the Trinity River delta and alluvial valley appears to be related to subsidence (fig. 4) and declining river sediment loads (fig. 5). Subsidence rates from 1943 to 1973 approached 7.5 mm/yr (Gabrysch and Bonnet, 1975). Estimated rates of marsh sedimentation (from lead isotope analysis) over the past 50 to 100 years in the Trinity River delta average 5.4 mm/yr, and range as low as 4.2 mm/yr (White and Calnan, 1990). The higher rates of subsidence compared to sedimentation suggest that subsidence has been a major contributing factor to the marsh loss. In addition, marsh sedimentation rates have probably been reduced because of reductions in river sediment load caused by upstream dam construction (Paine and Morton, 1986; White and Calnan, 1990).



The rate at which marshes are being lost in the Trinity River delta, however, appears to have decreased during the more recent period (1974 to 1988, White and Calnan, 1990). This change in rate of marsh loss may be due to the sharp declines in rates of subsidence on the east side of the Harris County subsidence bowl (fig. 4) after 1978 as a result of reductions in groundwater pumpage (Gabrysch and Coplin, 1990). Subsidence rates have declined in some areas by an order of magnitude.

### San Jacinto River

In the lower San Jacinto River valley at the head of Galveston Bay, more than 560 ha of fluvial woodlands, swamps, and fresh- to brackish-water marshes were replaced by open water between 1956 and 1979 (White and others, 1985; fig. 6). Losses were due principally to subsidence caused primarily by ground-water withdrawal (fig. 4, Gabrysch, 1984). Between 1943 and 1978, between 1.2 and 2.1 m of subsidence occurred in this part of the river valley (Gabrysch, 1984). The San Jacinto River lies within an entrenched valley similar to that of the Trinity River and as subsidence occurs, submergence and resulting changes in wetland environments progress inland along the axis of the valley (fig. 6).

The change in wetlands along the San Jacinto River is pronounced because of the proximity of the valley to the center of maximum subsidence. Rates of subsidence, between 1943 and 1978, are as high as 60 mm/yr, which greatly exceeds the rate of wetland aggradation in this area. The volume of sediments reaching the mouth of the San Jacinto River has diminished as a result of reservoir development in the drainage basin. Lake Houston, which is located only a few kilometers ( the San Jacinto River, has an estimated trap efficiency of about 87 percent (USDA, 1959), which suggests that only small quantities of sediment are delivered to the area where wetlands are being submerged. Nevertheless, even without Lake Houston and other reservoirs in the San Jacinto River basin, land-surface subsidence is so pronounced that it is unlikely aggradation rates could keep pace with subsidence rates except farther upstream where the rates decline. It appears that submergence will continue up the axis of the valley in the future, but rates of change should diminish somewhat as bay waters move into areas with slightly higher elevations and lower rates of subsidence.

### Virginia Point

Extensive net losses occurred in the Virginia Point quadrangle located on the inland margin of West Bay south of Texas City (fig. 7). More than 1,450 ha of marshland was replaced by open water and mud flat between the early 1950's and 1989 (White and others, 1992). Losses in the Virginia Point area have previously been reported by Johnston and Ader (1983), and White and

others (1985) (fig. 8). Significant subsidence has been documented in this area (Gabrysch and Coplin, 1990) (figs. 4 and 8). Loss of marshland has been most extensive northwest and west of Jones Bay where salt marshes have been converted to estuarine open water and flats (fig. 7). Additional losses occurred along the margins of Swan Lake (fig. 7). Approximate land-surface subsidence in the Virginia Point quad from 1906 to 1987 ranges from slightly less than 0.6 to 1.8 m (fig. 6). Estimated rates of subsidence, based on data presented by Gabrysch and Coplin (1990) in the area northwest of Jones Bay for the period of 1943 to 1987, exceed 14 mm/yr. This rate apparently was higher than rates of marsh aggradation in this area.

### Bolivar Peninsula

Submergence of marshes on a relict tidal inlet/washover fan complex on the bayward side of Bolivar Peninsula are related to faulting and subsidence (White and others, 1985). Approximately 500 ha of salt-water marsh was replaced primarily by shallow subaqueous flats and open water between 1956 and 1979 (fig. 9). In this area, at least two surface faults intersect marsh substrates. Benchmark releveled profiles along State Highway 87 indicate the faults are active; a marked increase in subsidence occurs on the downthrown side of the faults (fig. 10A). Faulting and subsidence appear to be related to oil and gas production in this area (Kreitler and others, 1988). As vertical displacement occurs along a fault that intersects a marsh, more frequent and eventually permanent inundation of the surface on the downthrown side of the fault can lead to replacement of marsh vegetation by open water if marsh sedimentation rates do not keep pace with submergence rates (fig. 10B). More than 25 faults that cross wetlands along the upper coast (Freeport area to Sabine Pass) have been identified on aerial photographs. Most of the identified faults are in the Galveston Bay area (White and others, 1985).

### Other Marsh areas in the Galveston Bay System

The League City quadrangle, which encompasses Clear Lake on the western margin of Galveston Bay offers another example of the effect of land-surface subsidence and the subsequent intrusion of open water and shallow flats into vegetated wetlands. Approximately 355 ha of vegetated wetlands were replaced by open water and flats between the 1950's and 1980's (White and others, 1992). Losses in emergent wetlands along Armand Bayou, which discharges into Clear Lake, exceeded 91 percent of the resource between the 1950's and 1979 (McFarlane, 1991). The League City quad is representative of the trend occurring along the valleys of bayous and creeks located on the north and west sides of Galveston Bay, an area affected most by subsidence (fig. 4). The trend is one of expansion of open water and flats at the expense of marshes and woodlands, as subsidence promotes the encroachment of estuarine water up the valleys. The

development, locally, of marshes along the valleys in more inland and marginal areas offers only a small measure of compensation for the losses.

## SUBSIDENCE AND WETLAND LOSS

More than 20,000 ha of vegetated coastal wetlands have been replaced by open water and flats on the Texas coast. The majority of the losses have occurred along the upper coast. Major areas affected include fluvial-deltaic wetlands along the Neches, Trinity, and San Jacinto Rivers, and estuarine wetlands as a whole in the Galveston Bay system. Although many activities (for example, reservoir development and dredging) may lead to the conversion of vegetated wetlands to water and flats on a localized scale, there is evidence that the major contributing factor in this change is relative sea-level rise, the major component of which is subsidence.

Rates of "natural" subsidence and eustatic sea level rise, which together may range up to 12 mm/yr in the Galveston area (Swanson and Thurlow, 1973; Gornitz and Lebedeff, 1987; Penland and others, 1988) are dwarfed by human-induced subsidence with rates of up to 120 mm/yr caused by the withdrawal of groundwater, oil, and gas (Winslow and Doyel, 1954; Gabrysch, 1969; Gabrysch and Bonnet, 1975; Pratt and Johnson, 1926; Kreitler, 1977; Verbeek and Clanton, 1981; Kreitler and others, 1988). In the Houston-Galveston area, up to 3 m of man-induced subsidence has occurred between 1906 and 1987 (Gabrysch and Coplin, 1990). The subsidence "bowl" encompasses an area of approximately 943,650 ha where a minimum of 30 cm of subsidence has occurred. Since the late 1970's, however, rates of subsidence in some areas have decreased by an order of magnitude due to the curtailment of ground-water pumpage (Gabrysch and Coplin, 1999).

In areas where subsidence rates exceed sedimentation rates, emergent vegetation is submerged and replaced by open water and flats. Marsh sedimentation rates in fluvial-deltaic wetlands have been affected by declining river sediment loads due to reservoir construction upstream, and by dredged canals, spoil disposal, and artificial levees, which alter hydrologic and sediment dispersal patterns. Locally, loss of wetlands has occurred along active surface faults where more rapid subsidence on the downthrown side leads to the conversion of marshes to open water and shallow subaqueous flats.

## REFERENCES

- Baumann, R. H., Day, J. W., Jr., and Miller, C. A., 1984, Mississippi deltaic wetland survival: sedimentation versus coastal submergence: *Science*, v. 224, no. 4653, p. 1093-1095.
- Boesch, D. F., Day, J. W., Jr., and Turner, R. E., 1984, Deterioration of coastal environments in the Mississippi Deltaic Plain: options for management, *in* Kennedy, V. S., ed., *The estuary as a filter*: New York, Academic Press, p. 447-466.

- Dahl, T. E., Johnson, C. E., and Frayer, W. E., 1991, Wetlands, status and trends in the conterminous United States mid-1970's to mid-1980's: U.S. Department of the Interior, U.S. Fish and Wildlife Service, 23 p.
- DeLaune, R. D., Baumann, R. H., and Gosselink, J. G., 1983, Relationships among vertical accretion, coastal submergence, and erosion in a Louisiana Gulf Coast marsh: *Journal of Sedimentary Petrology*, v. 53, no. 1, p. 147-157.
- Field, D. W., Reyer, A. J., Genovese, P. V., and Shearer, B. D., 1991, Coastal Wetlands of the United States: National Oceanic and Atmospheric Administration in Cooperation with the U.S. Fish and Wildlife Service, A special NOAA 20th anniversary report, 59 p.
- Fisher, W. L., McGowen, J. H., Brown, L. F., Jr., and Groat, C. G., 1972, Environmental Geologic Atlas of the Texas Coastal Zone--Galveston- Houston Area: University of Texas at Austin, Bureau of Economic Geology, 9 maps, 91 p.
- Fisher, W. L., Brown, L. F., Jr., McGowen, J. H., and Groat, C. G., 1973, Environmental Geologic Atlas of the Texas Coastal Zone--Beaumont-Port Arthur Area: University of Texas at Austin, Bureau of Economic Geology, 9 maps, 93 p.
- Gabrysch, R. K., 1969, Land-surface subsidence in the Houston-Galveston region, Texas: United Nations Educational, Scientific and Cultural Organization (UNESCO), Studies and Reports in Hydrology, Land Subsidence Symposium, v. 1, p. 43-54.
- Gabrysch, R. K., 1984, Ground-water withdrawals and land-surface subsidence in the Houston-Galveston region, Texas, 1906-1980: Texas Department of Water Resources Report 287, 64 p.
- Gabrysch, R. K., and Bonnet C. W., 1975, Land-surface subsidence in the Houston-Galveston region, Texas, Texas Water Development Board, Report 188, 19 p.
- Gabrysch, R. K., and Coplin, L. S., 1990, Land-surface subsidence resulting from ground-water withdrawals in the Houston-Galveston region, Texas, through 1987: U.S. Geological Survey Report of Investigations No. 90- 01, 53 p.
- Gagliano, S. M., Meyer-Arendt, K. J., and Wicker, K. M., 1981, Land loss in the Mississippi River deltaic plain: *Gulf Coast Association of Geological Societies Transactions*, v. 31, p. 271-273.
- Gornitz, V., and Lebedeff, S., 1987, Global sea-level changes during the past century: *Society of Economic Paleontologists and Mineralogists, Special Publication no. 41*, p. 3-16.
- Gosselink, J. G., Cordes, C. L., and Parsons, J. W., 1979, An ecological characterization study of the Chenier Plain coastal ecosystem of Louisiana and Texas: U. S. Fish and Wildlife Service, Office of Biological Services, FWS/OBS-78/9 through 78/11, 3 vols.
- Hatton, R. S., DeLaune, R. D., and Patrick, W. H., Jr., 1983, Sedimentation, accretion, and subsidence in marshes of the Barataria Basin, Louisiana: *Limnology and Oceanography*, v. 28, no. 3, p. 494- 502.

- Johnston, J. B., and Ader, R. A., 1983, The use of a GIS for Gulf of Mexico wetland change: in Magoon, O. T., and Converse, H., eds., Coastal Zone '83, Volume I: American Society of Civil Engineers, New York, p. 362-371.
- Kreitler, C. W., 1977, Faulting and land subsidence from ground-water and hydrocarbon production, Houston-Galveston, Texas: The University of Texas at Austin, Bureau of Economic Geology Research Note 8, 22 p.
- Kreitler, C. W., White, W. A., and Akhter, M. S., 1988, Land subsidence associated with hydrocarbon production, Texas Gulf Coast (abs.): American Association of Petroleum Geologists Bulletin, v. 72, no. 2, p. 208.
- McFarlane, R. W., 1991, An environmental inventory of the Christmas Bay Coastal Preserve: Galveston Bay National Estuary Program, GBNEP Publication - 7, 95 p.
- McEwen, M. C., 1969, Sedimentary facies of the modern Trinity delta, in Lankford, R. R., and Rogers J. J. W., Holocene geology of the Galveston Bay area: Houston Geological Society, chapter 3, p. 53-77.
- Morton, R. A., and Paine, J. G., 1990, Coastal land loss in Texas--an overview: Gulf Coast Association of Geological Societies Transactions, v. 40, p. 625-634.
- Paine, J. G., and Morton, R. A., 1989, Shoreline and vegetation-line movement, Texas Gulf Coast, 1974 to 1982: The University of Texas at Austin, Bureau of Economic Geology Geological Circular 89-1, 50 p.
- Paine, J. G., and Morton, R. A., 1986, Historical shoreline changes in Trinity, Galveston, West, and East Bays, Texas Gulf Coast: The University of Texas at Austin, Bureau of Economic Geology Geological Circular 86-3, 58 p.
- Penland, Shea, Ramsey, K. E., McBride, R. A., Mestayer, J. T., and Westphal, K. A., 1988, Relative sea level rise and delta-plain development in the Terrebonne Parish region: Louisiana Geological Survey, Baton Rouge, Coastal Geology Technical Report no. 4, 121 p.
- Pratt, W. E., and Johnson, D. W., 1926, Local subsidence of the Goose Creek oil field: Journal of Geology, v. 34, p. 577-590.
- Price, W. A., 1933, Role of diastrophism in topography of Corpus Christi area, South Texas: American Association of Petroleum Geologists Bulletin, v. 17, no. 8, p. 907-962.
- Price, W. A., 1947, Equilibrium of form and forces in tidal basins of coast of Texas and Louisiana: American Association of Petroleum Geologists Bulletin, v. 31, no. 3, p. 1616-1663.
- Ratzlaff, K. W., 1980, Land-surface subsidence in the Texas coastal region: U. S. Geological Survey Open-File Report 80-969, 19 p.
- Scaife, W. W., Turner, R. E., and Costanza, Robert, 1983, Coastal Louisiana recent land loss and canal impacts: Environmental Management, v. 7, no. 5, p. 433-442.

- Shepard, F. P., 1953, Sedimentation rates in Texas estuaries and lagoons: American Association of Petroleum Geology Bulletin, v. 37, no. 8, p. 1919-1934.
- Swanson, R. L., and Thurlow, C. I., 1973, Recent subsidence rates along the Texas and Louisiana coasts as determined from tide measurements: Journal of Geophysical Research, v. 78, no. 5, p. 2665-2671.
- U.S. Department of Agriculture, 1959, Inventory of the use of sedimentation data in Texas: Soil Conservation Service, Bulletin 5912, 85 p.
- Verbeek, E. R., and Clanton, U. S., 1981, Historically active faults in the Houston metropolitan area. Texas, in Etter, E. M, ed., Houston area environmental geology: surface faulting, ground subsidence, hazard liability: Houston Geological Society, p. 28-68.
- White, W. A., Tremblay, T. A., Wermund, E. G., Jr., and Handley, L. R., 1992, Trends and status of wetland and aquatic habitats in the Galveston Bay system, Texas: The University of Texas at Austin, Bureau of Economic Geology, Draft report prepared for the Galveston Bay National Estuary Program under IAC (92-93)-0660, 203 p.
- White, W. A., and Calnan, T. R., 1991, Submergence of vegetated wetlands in fluvial-deltaic areas, Texas Gulf Coast, in Coastal Depositional Systems, Gulf of Mexico: Society of Economic Paleontologists and Mineralogists, Gulf Coast Section, twelfth annual research conference, program with extended and illustrated abstracts, Houston, Texas, p. 278-279.
- White, W. A., and Calnan, T. R., 1990, Sedimentation and historical changes in fluvial-deltaic wetlands along the Texas Gulf Coast with emphasis on the Colorado and Trinity River deltas: The University of Texas at Austin, Bureau of Economic Geology, final report prepared for the Texas Parks and Wildlife Department, 124 p., 7 Appendices.
- White, W. A., Calnan, T. R., Morton, R. A., Kimble, R. S., Littleton, T. G., McGowen, J. H., Nance, H. S., and Schmedes, K. E., 1985, Submerged lands of Texas, Galveston-Houston area: sediments, geochemistry, benthic macroinvertebrates, and associated wetlands: The University of Texas at Austin, Bureau of Economic Geology, Special Publication, 145 p.
- White, W. A., Calnan, T. R., Morton, R. A., Kimble, R. S., Littleton, T. G., McGowen, J. H., and Nance, H. S., 1987, Submerged lands of Texas, Beaumont-Port Arthur area: sediments, geochemistry, benthic macroinvertebrates, and associated wetlands: The University of Texas at Austin, Bureau Economic Geology Special Publication, 110 p.
- Wiersema, J. M., Mitchell, R. P., and James, S. N., 1973, Sabine Power Station ecological program, v. 1, A. utilization of aquatic habitats in the GSU marsh, B. assessment of GSU thermal discharge on the biota of the Neches River: Austin, Texas, Tracor, Inc., document no. T73-AU- 9507-U(R), submitted to Gulf States Utilities, 215 p.
- Winslow, A. G., and Doyel, W. W., 1954, Land-surface subsidence and its relation to the withdrawal of ground water in the Houston-Galveston region, Texas: Economic Geology, v. 49, no. 4, p. 413-422.

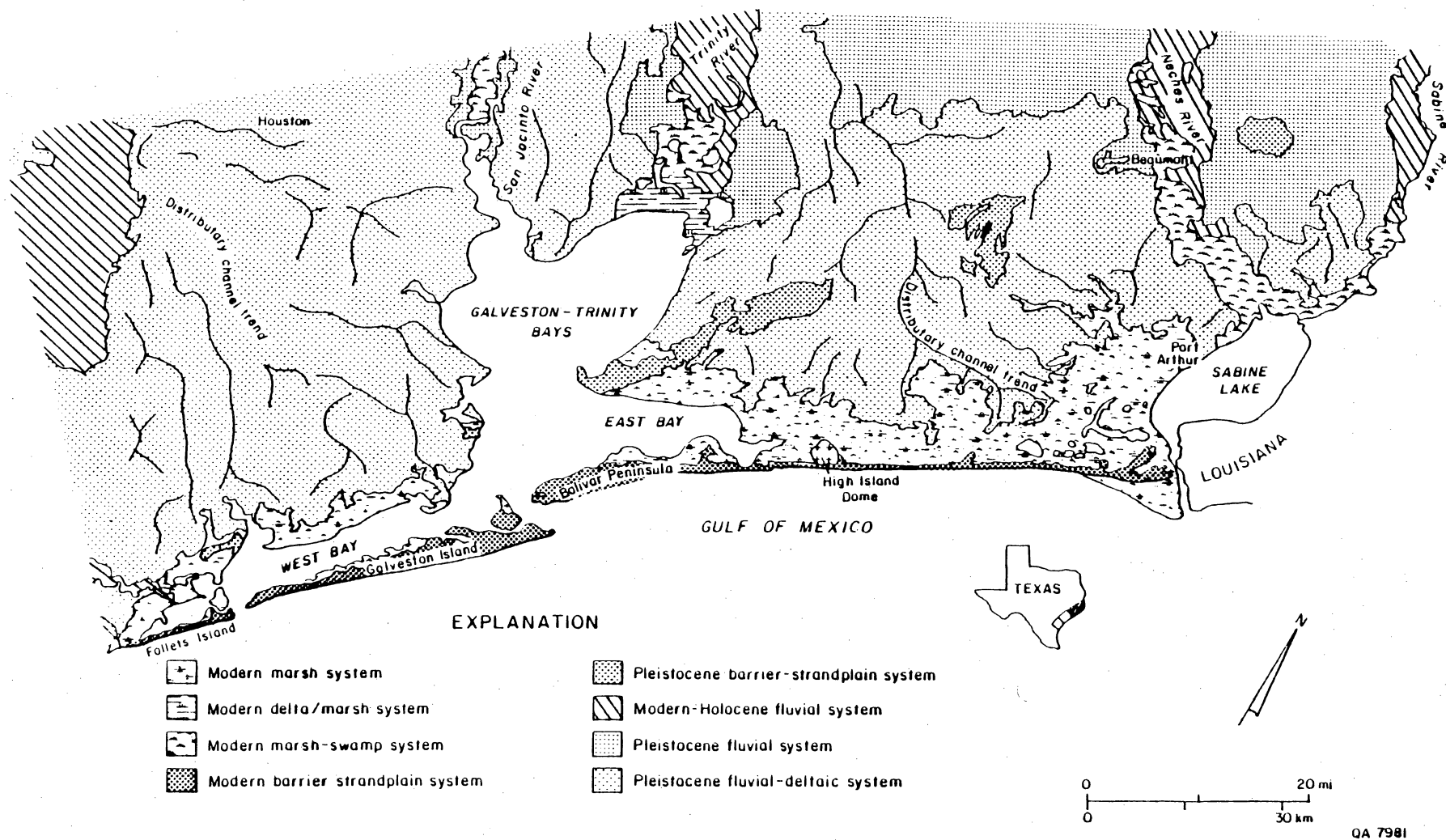
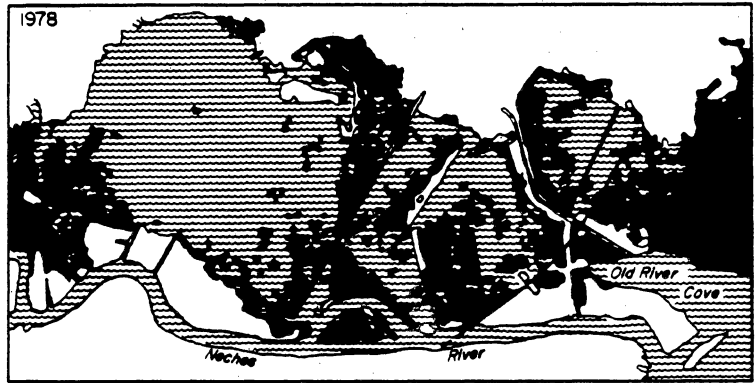
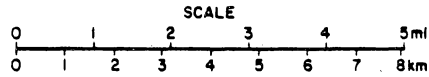
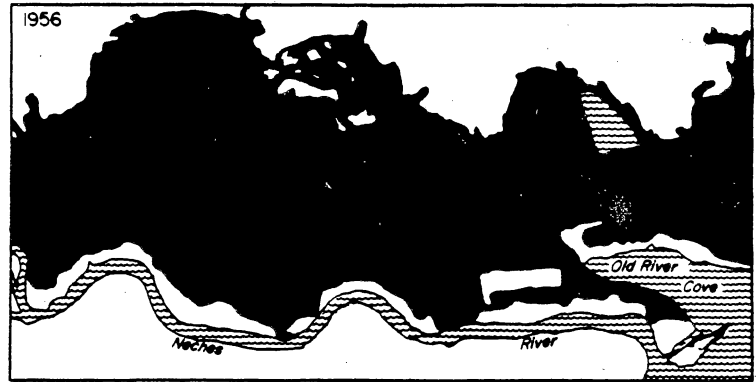


Figure 1. Natural systems defined by environmental mapping of the Upper Texas Coast. These systems are composed of genetically related environments, sedimentary substrates, biologic assemblages, areas of significant physical processes, and man-made features. Modified from Fisher and others (1972 and 1973).



QA 3384

Map Unit	1956		1978		Net Change*	
	Acres	Hectares	Acres	Hectares	Acres	Hectares
Water	2,560	1,037	11,070	4,483	+8,510	+3,446
Marsh	15,740	6,375	6,330	2,564	-9,410	-3,811

\* Loss of additional 900 acres (365 hectares) of marsh primarily due to spoil disposal.

Figure 2. Changes in the distribution of wetlands between 1956 and 1978 in the lower Neches River Valley in the vicinity of and west of Old River Cove. The fault crossing this area has apparently contributed to the changes (D = downthrown side, U = upthrown side). From White and others (1987).



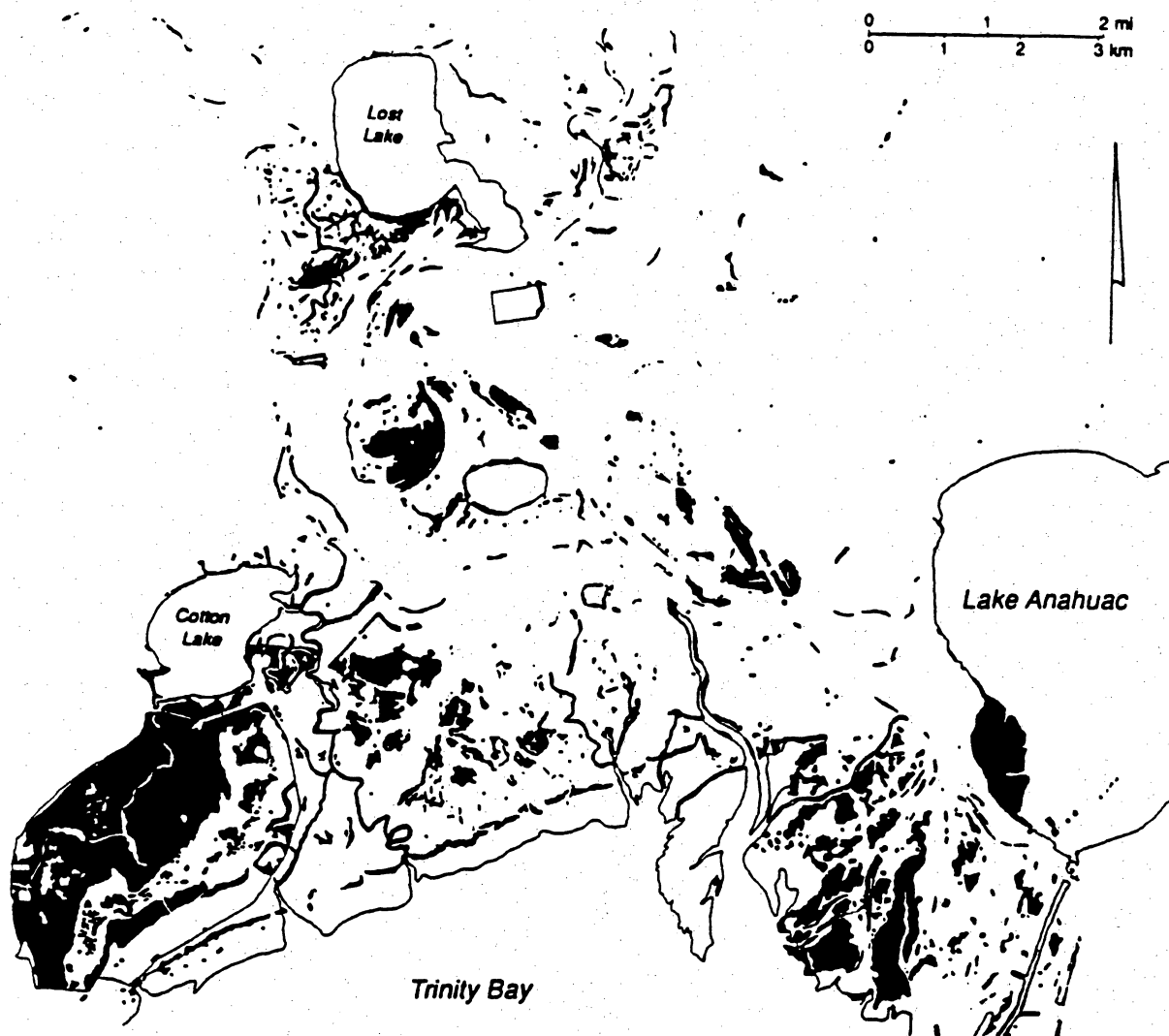


Figure 3. Distribution of marshes (shaded areas) in the Trinity River delta that were displaced by water and flats between the 1950's and 1989. The large loss south of Cotton Lake was caused by a power plant cooling reservoir. From White and others (1992).

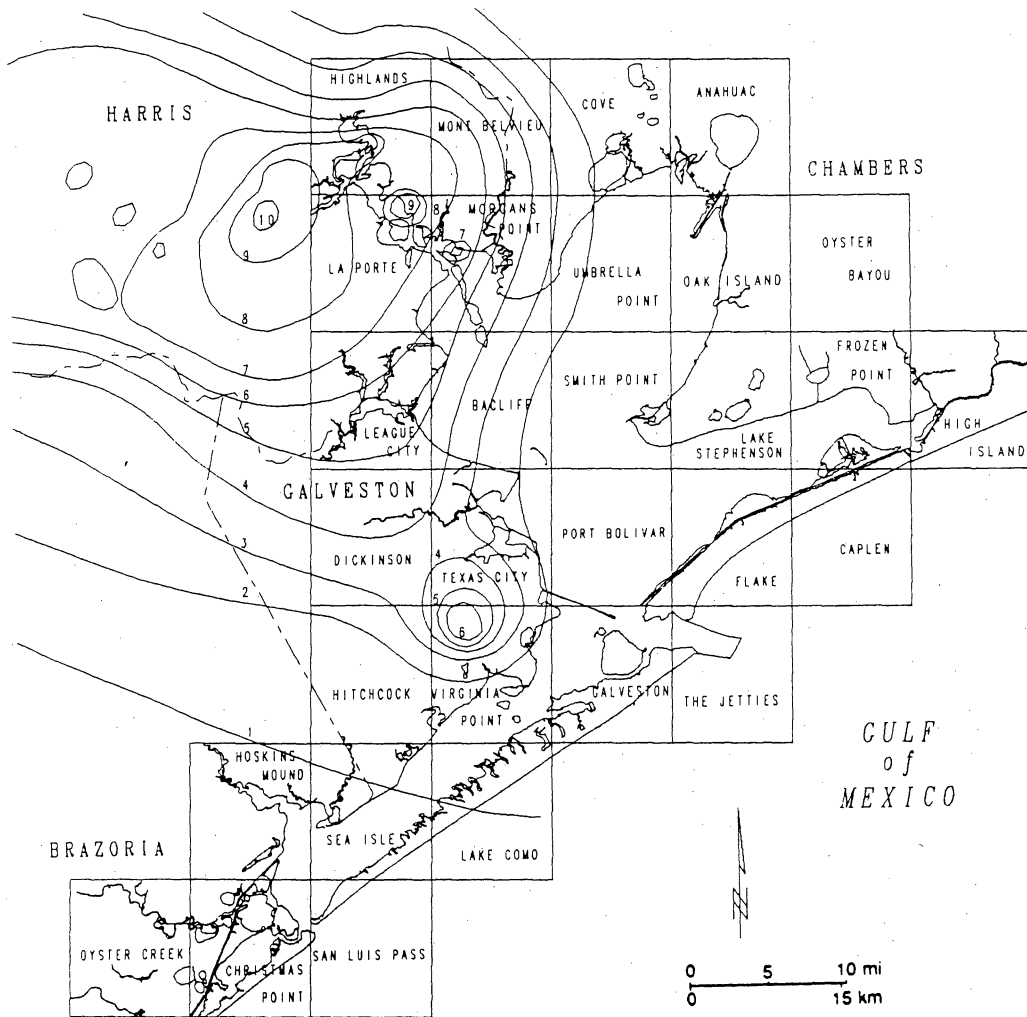


Figure 4. Land-surface subsidence in the Galveston Bay area, 1906 to 1987. Subsidence contours (contour interval = 1 ft) are from Gabrysch and Coplin (1990). From White and others (1992).

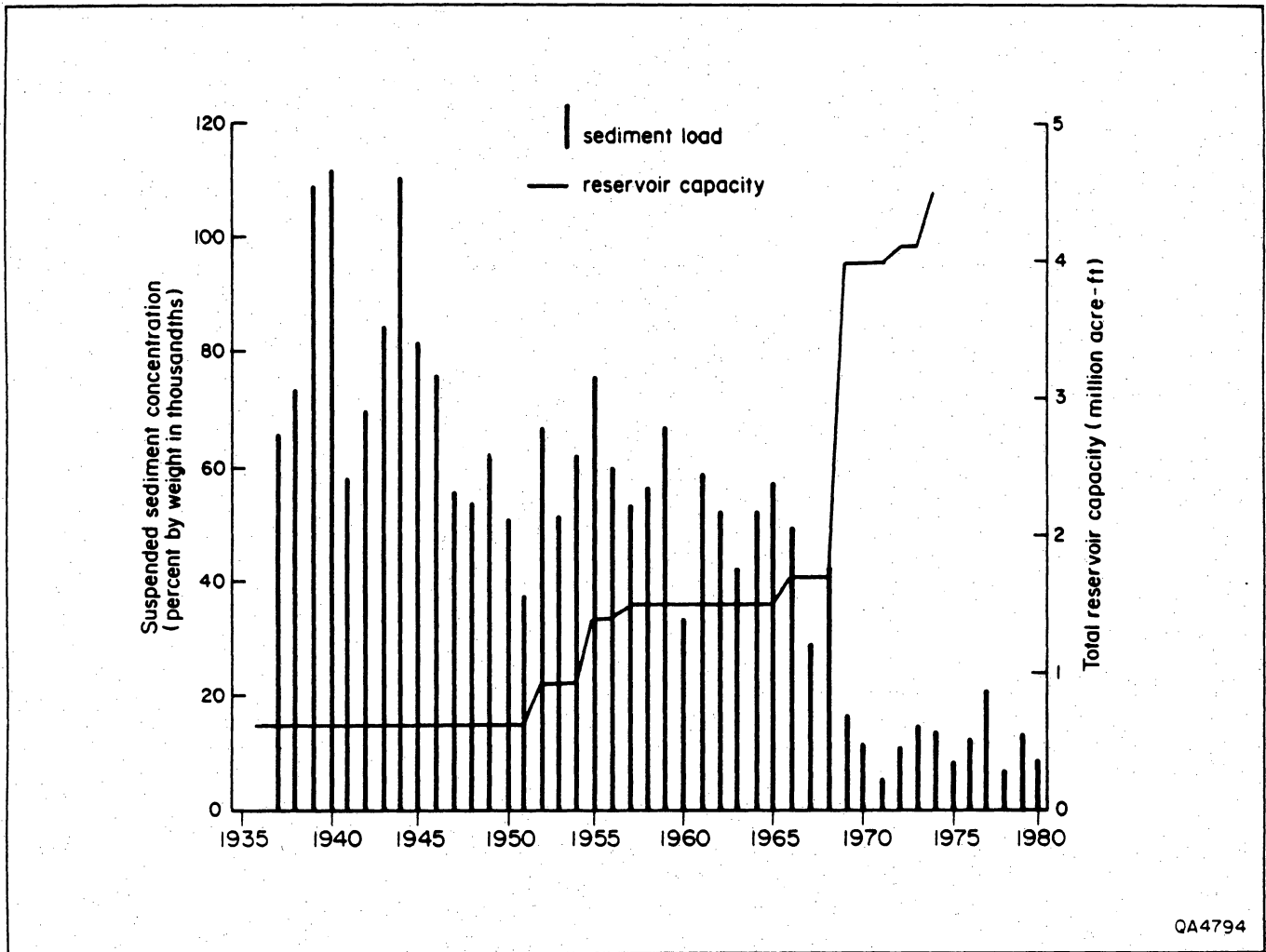
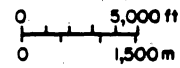
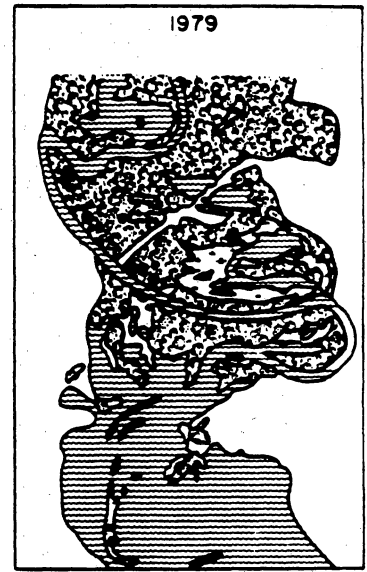
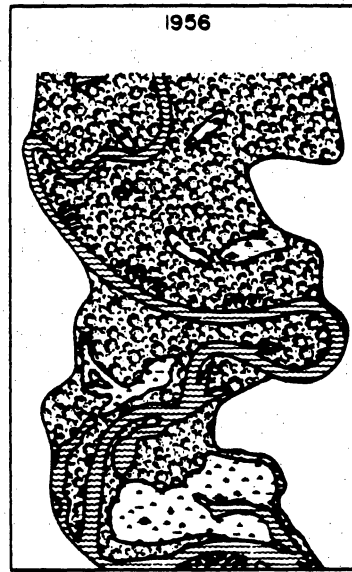
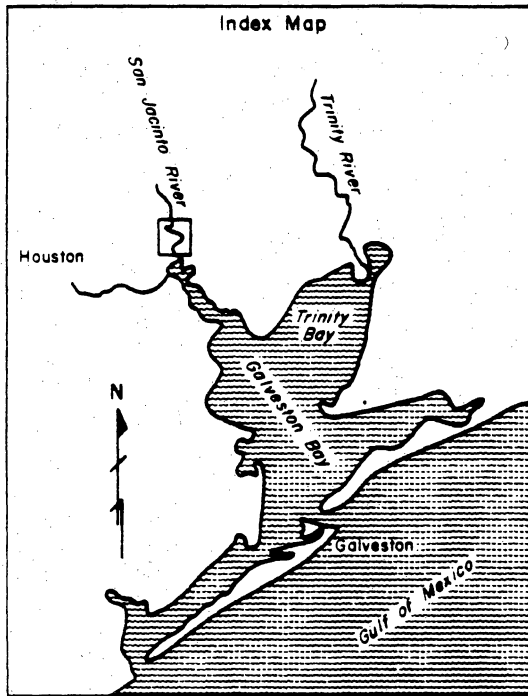


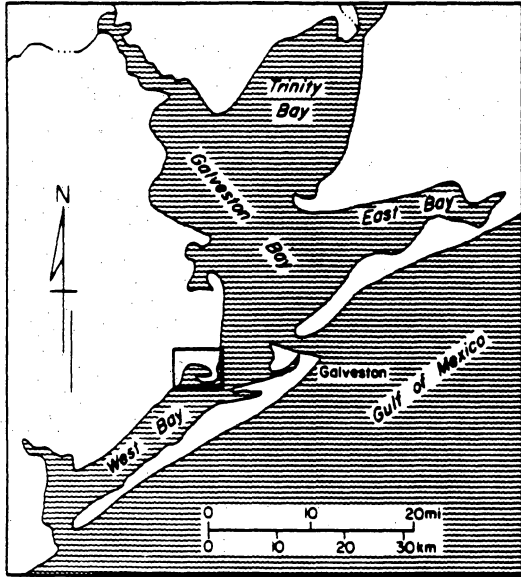
Figure 5. Suspended-sediment load (percent by weight) of the Trinity River at Romayor, and cumulative authorized water storage in reservoirs of the Trinity River basin. From Paine and Morton (1986).






Wetland Map Unit	1956		1979		Net Change	
	Acres	Hectares	Acres	Hectares	Acres	Hectares
Water	875	355	2,295	930	+1,420	+ 575
Fluvial Woodlands & Swamps	3,480	1,410	2,090	845	-1,390	- 565
Fresh to Brackish Marsh	650	265	300	120	-350	-145

QA 937

Figure 6. Changes in the distribution of wetlands between 1956 and 1979 of a subsiding segment of the San Jacinto River near Houston. From White and others (1985).



EXPLANATION

-  Water
-  Marsh
-  Barren land (abandoned tidal creeks)

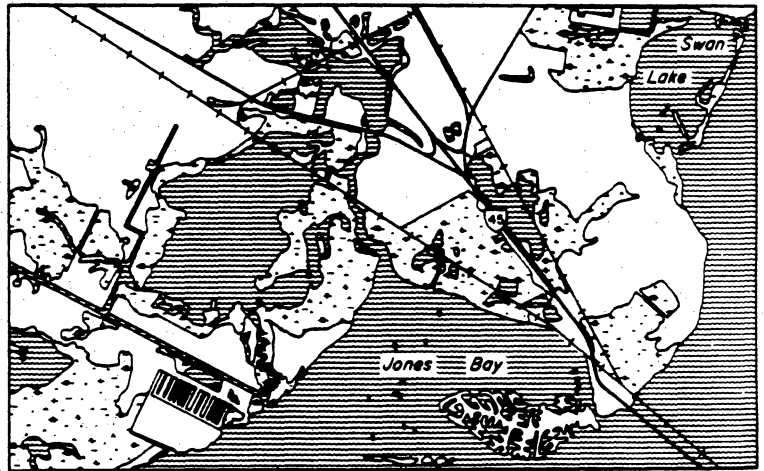
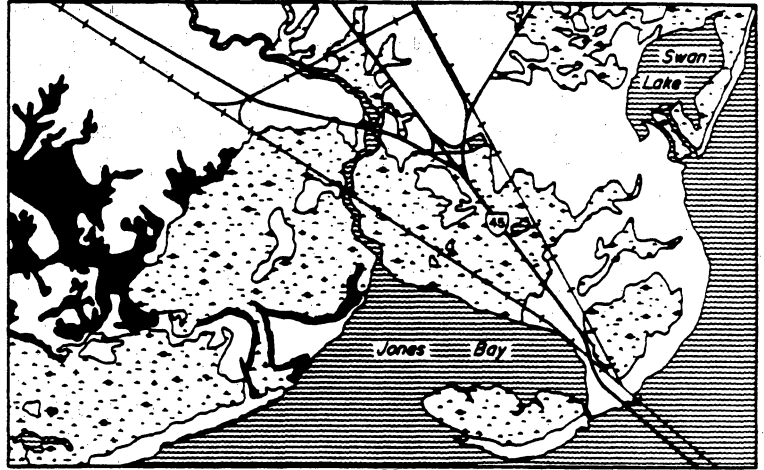
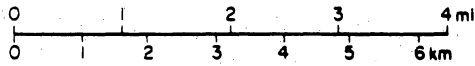


Figure 7. Changes in the distribution of wetlands between 1956 and 1979 near Jones Bay and Swan Lake. Note the increase in open water in 1979. From White and others (1985).

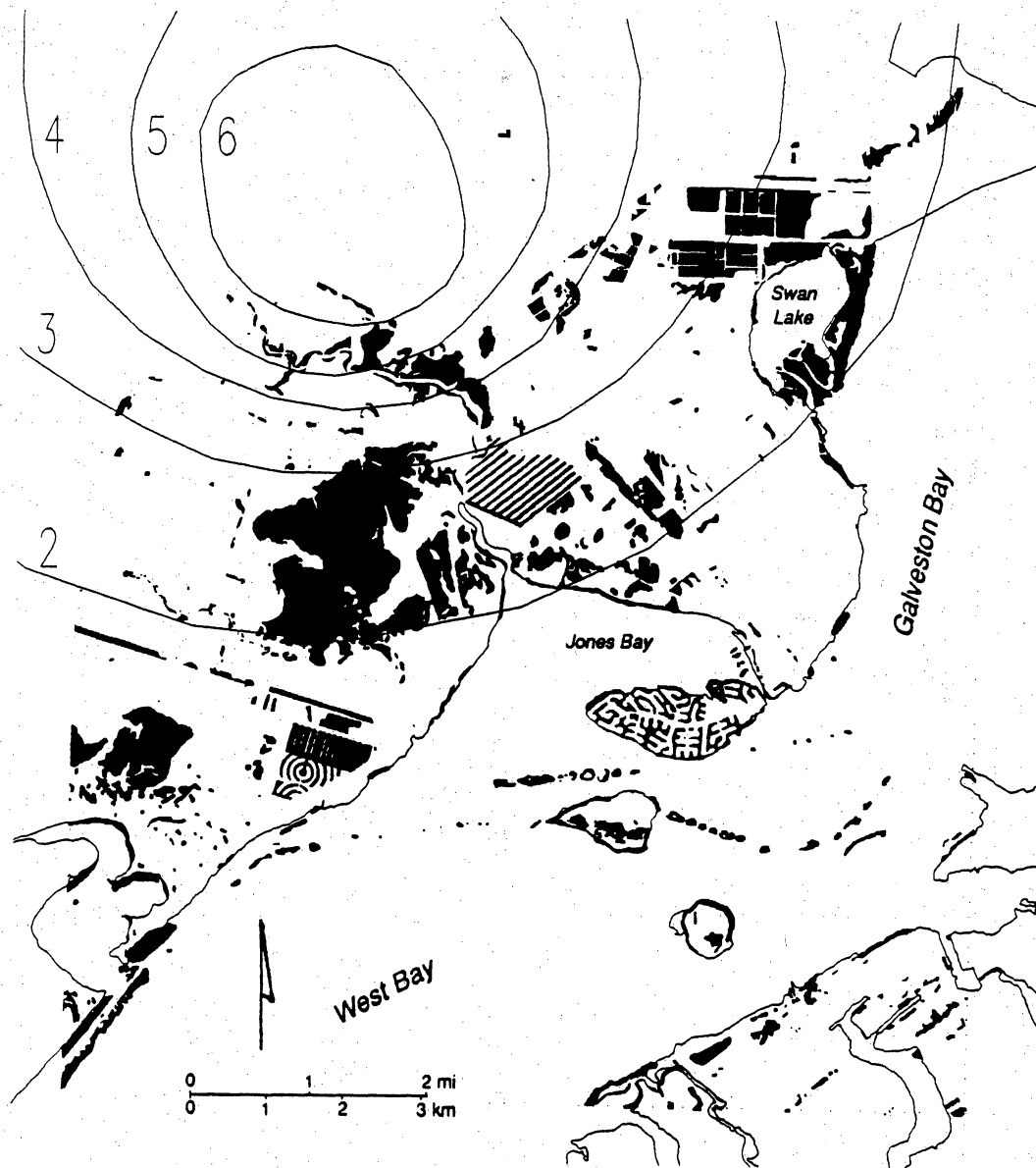
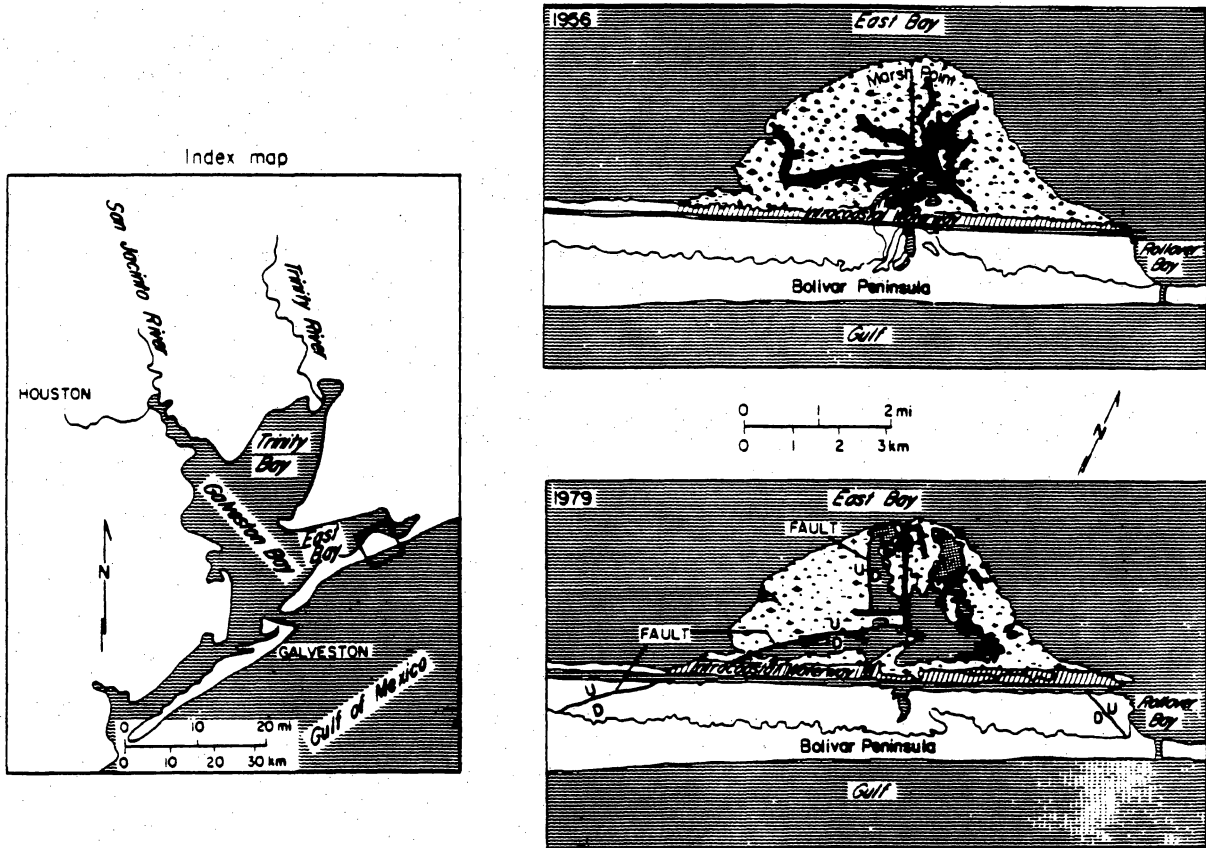


Figure 8. Relationship between subsidence and losses in emergent wetlands (shaded) by conversion to open water and flats in the Virginia Point quadrangle. Contours (in feet) show amount of subsidence that has occurred between 1906 and 1987 (based on maps from Gabrysch and Coplin, 1990). From White and others (1992).



Wetland Map Unit	1956		1979		Net Change	
	Acres	Hectares	Acres	Hectares	Acres	Hectares
Water	140	57	1130	458	+990	+401
Marsh	3480	1409	2560	1037		
Marsh-covered tidal channels	640	259				
<b>TOTAL MARSH</b>	<b>4120</b>	<b>1668</b>	<b>2560</b>	<b>1037</b>	<b>-1560</b>	<b>-631</b>
Barren tidal flats			270	109	+270	+109
Dredged spoil/uplands	520	211	720	292	+200	+81
<b>TOTAL</b>	<b>4780</b>	<b>1936</b>	<b>4680</b>	<b>1896</b>	<b>-100</b>	<b>-40</b>

\* Most of the loss in total area is probably due to erosion of marsh along the margins of East Bay. Historical monitoring indicates that this shoreline is undergoing erosion at rates of up to 3 ft (1 m) per year (Paine and Morton, in preparation).  
 (Areas were calculated using a square-count method; smallest squares used were equivalent to 6.4 acres, or 2.6 hectares).

QA 1774

Figure 9. Changes in distribution of wetlands between 1956 and 1979 near Marsh Point on the bayward side of Bolivar Peninsula. Increases in the areal extent of open water, and decreases in the areal extent of marsh are apparently related to localized subsidence and active faults (D = downthrown side of fault, U = upthrown side). From White and others (1985).

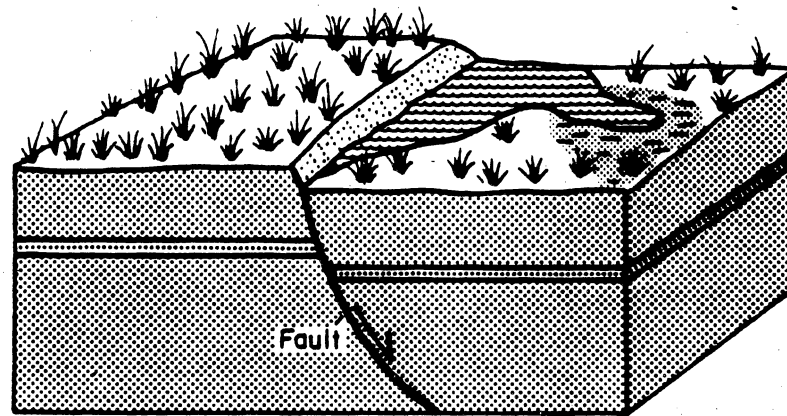
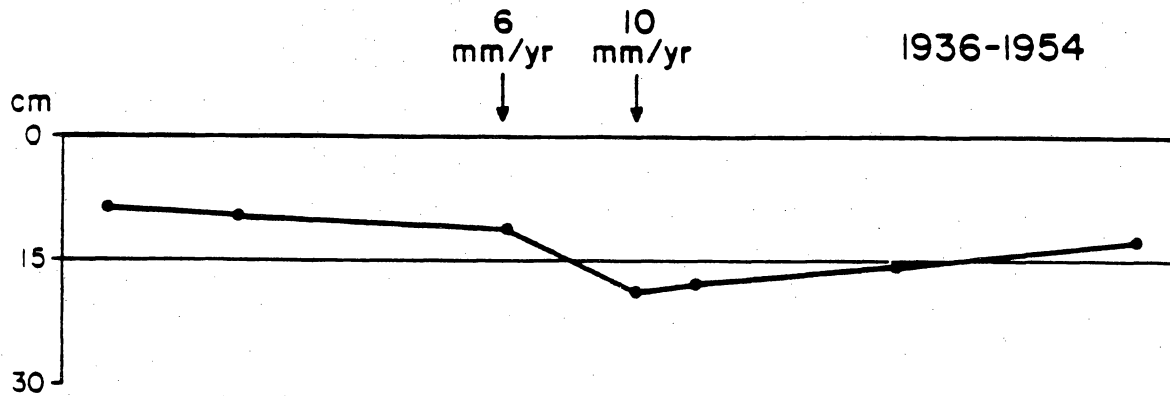


Figure 10. (A). Land-surface subsidence profile based on benchmark-releveling data along Highway 87 on Bolivar Peninsula. The increase in subsidence along the profile indicates that it crosses an active fault, probably an extension of the fault with the NE-SW strike in figure 9. From White and others (1992). (B). Block diagram of changes in wetlands that occur along an active surface fault. There is generally an increase in low marshes, shallow subaqueous flats, and open water on the downthrown side of the fault relative to the upthrown side. From White and others (1992).



## ADDENDUM 3

### GEOLOGIC FRAMEWORK OF INCISED COASTAL PLAIN RIVERS

Robert A. Morton and William A. White  
Bureau of Economic Geology  
The University of Texas at Austin

#### INTRODUCTION

Foundation borings conducted by various agencies including the Texas Department of Transportation, U.S. Army Corps of Engineers, and Fugro-McClelland Marine Geosciences, Inc., provided the data for constructing cross-sections of the San Jacinto, Trinity, Sabine, and Neches River valleys (fig. 1). Knowing depths, widths, orientations, and fill lithologies of each river valley provides a basis for reconstructing the late Quaternary geologic framework of the coastal plain rivers. These reconstructions are necessary to understand the influence of relative sea-level fluctuations and climatic changes on coastal evolution during the past few thousand years. Valley entrenchment by the coastal plain fluvial systems during sea-level lowstand associated with late Wisconsin glaciation provided the setting for the development of the Galveston/Trinity Bay system and Sabine Lake (fig. 1).

Fluvial systems and their associated sedimentary deposits can be influenced by both changes in climate and base level depending on their position within the drainage basin. Essentially three zones can be identified between the headwaters and the river mouth that determine the influence of climatic and base level fluctuations. Along distant upstream segments, climate has the most pronounced influence on channel patterns and composition of fluvial facies. Along midstream segments extending upstream of the highstand shoreline position, both climate and sea level exert an influence on channel patterns and composition of fluvial facies. Along downstream segments, to the basinward limit of fluvial channels, the effects of relative sea level predominate over climatic effects. One of the objectives of this study was to differentiate between climatic and eustatic influences on facies architecture within incised valley fills. The following discussions of river characteristics and valley fill lithologies pertain to river valley locations that are currently near the coast but were far upstream when sea level was much lower and the shoreline was at the edge of the continental shelf.

Thomas (1990) and Anderson et al. (1991) explained the changes in late Quaternary stratigraphy of the Trinity and Sabine entrenched valleys strictly in terms of relative sea level and more specifically in terms of the rate of sea level rise. No consideration was given to climatic changes and their influence on precipitation, sediment yield, fluvial discharge, and sediment load.

Just as sea level fluctuations are recorded in the stratigraphic record, climatic influences should also be recorded in the vertical successions of strata.

## Trinity-San Jacinto Fluvial Systems

### Trinity River System

River Characteristics- The area of the modern Trinity River drainage basin is about 44,012 km<sup>2</sup> (17,190 mi<sup>2</sup>). Annual average discharge of the Trinity at Romayor based on flow records from 1936 to 1959 is approximately 5,000,000 acre/ft (Stout and others, 1961). The modern Trinity River has a width of 120 to 150 m and a bankfull depth of 12 m at U.S. Highway 90 and 7 m at IH 10. Average width of the Quaternary alluvial valley fill is 10.4 km between the head of Trinity Bay and U.S. Highway 90 (fig. 2). Near Lake Anahuac, the maximum width of the valley is approximately 14 km, which is almost equivalent to the widest part of Trinity Bay.

Valley Fill Lithology and Depositional Environments- From the bridge at U.S. Highway 90 (fig. 2), fluvial sands capped by flood basin and swamp muds extend down the valley into fluvial and fluvial-deltaic deposits at IH 10. Borings at IH 10 show a primary unconformity that generally separates underlying firm to stiff clay and sandy clay from overlying sand and soft clay. The unconformity is slightly deeper in the western part of the section indicating past positions of the Trinity River (fig. 3). Clay deposited above basal fluvial sands is thickest in this area. The deepest part of the entrenchment is believed to be in the western half of the section where sands dip to -23 m (fig. 3). The maximum depth of the unconformity, which is estimated to be about -18 m is uncertain because it is masked by nested sands. The estimated -18 m places the unconformity along a lithologic contact between clayey sand and clayey sand with gravel. Below the clayey sand with gravel there is a sharp contact with stiff (but locally soft) clay containing caliche nodules.

Aten (1979) charted 5 channel and delta stages showing positions of the lower Trinity River during the past 3,000 years (fig. 4). Channel stages 1, 2, and 3 correspond with past entrenchment's of the Trinity River as shown in the western part of cross section A-A' (fig. 3). It appears that the deepest entrenchment in the western part of the section (fig. 3) corresponds with stage 1 (fig. 4). Stage 5 is the present Trinity River channel.

In the vicinity of the modern Trinity River, fluvial sands are thicker and are nearer the surface than to the west. The sands are blanketed by a relatively thin layer of floodplain marsh and swamp deposits composed of soft blue and gray clay and sandy clay that extends to the surface. Fluvial sand unconformably overlies hard to stiff blue, brown, tan, and gray clay and sandy clay.

Cores taken along the Wallisville dam structure located downstream from IH 10 show two entrenchments separated by an erosional high (Rehkemper, 1969). Fluvial sands lie above the

unconformity in all cores but one in which gray clay with layers of silt and sand occur. Estuarine clays, deposited during the rising sea level, lie above the sands. The clays are in turn overlain by fluvial-deltaic sands deposited as the modern Trinity River delta prograded into the estuary.

The modern Trinity delta is characterized by marsh-covered delta-front churned sands described by McEwen (1969). Marsh muds are only about 0.6 to 0.8 m (2 to 2.5 ft) thick in the modern delta. Delta-front churned sands are approximately 4.2 to 4.5 m (14 to 15 ft) thick, but locally exceed 6 m (20 ft). The oldest dates of the modern delta determined from radiocarbon analysis range from 750 to 810 yrs BP (McEwen, 1969).

Bayward of the modern delta, gray clayey sands prograded over soft gray clay containing organics and shell. These underlying estuarine and prodelta clays are more than 15 m (50 ft) thick in some areas. Locally the clay contains more sand with depth and becomes sandy clay over the deepest 6 m (20 ft) of section. These sandy clays unconformably overlie very stiff olive to gray clay with caliche nodules.

The modern deltaic sands pinchout bayward into soft gray estuarine clay and shell. Underlying the estuarine clay at depths of -9.7 to -13.6 m is clay containing wood and organics--a section interpreted by Anderson and others (1991) as deltaic. Anderson and others (1991) hypothesized that the bayhead delta sequence is one of several that can be paired with tidal delta/tidal inlet facies that comprise backstepping parasequences disconnected by periods of rapid sea-level rise. The bayhead delta sequence characterized by gray clay with organics and peat at depths of -9.7 to -13.6 m is found in cores farther down paleodip. Down paleodip landward of Bolivar Peninsula, peat and wood fragments were found at a depth of about -22 m (Rehkemper, 1969), a deposit that is considered to be an older upper bay-bayhead delta sequence by Anderson and others (1991).

### San Jacinto River System

River Characteristics- The San Jacinto River has a drainage basin area of approximately 7,142 km<sup>2</sup> (at Huffman Station; Stout and others, 1961), which is about 16 percent of the Trinity River drainage basin area. Based on flow records from 1945 to 1952, the annual average discharge of the San Jacinto River is approximately 1,500,000 acre-ft, or less than one-third of the average annual flow of the Trinity River. However, the San Jacinto River's average annual depth of runoff (Q/A) of 9.2 inches is higher than any major Texas River including that of the Trinity (Winker, 1979). The San Jacinto River's high runoff, relatively steep gradient (0.6 m/km) and narrow valley width (average of 3.2 km), coupled with numerous tributary streams that cross sandy substrates in the drainage basin have produced a mixed-load stream characterized by channel and entrenched valley-fill lithologies dominated by sand (figs. 5 to 8).

Formations cropping out progressively farther inland from the Beaumont Formation in the drainage basin include the Bently Formation composed of clay, silt, sand, and a minor amount of

gravel; the Willis Formation composed of clay, silt, sand, and siliceous gravel; the Fleming Formation composed of clay, silt, and sand (mostly clay); and the Catahoula Formation, composed of mudstone and sand (Bureau of Economic Geology, 1968 and 1982).

Valley Fill Lithology and Depositional Environments- Four cross sections were constructed of the San Jacinto River valley from foundation borings taken at bridges at Lake Houston, U.S. Highway 90, IH 10, and at Baytown (figs. 5 to 8). The San Jacinto River valley fill is characterized by thick sequences of fluvial sand. Increasing amounts of clay in facies downdip at IH 10 (fig. 7) and Baytown Bridge (fig. 8) indicate a change from fluvial to fluvial-deltaic depositional environments. Still, fluvial sands appear to rest directly on the major unconformity. Available core data is either not deep enough or not located in a position to provide evidence that the San Jacinto delta prograded over estuarine muds as extensively as the modern Trinity delta.

In the San Jacinto River valley, muds thicken downstream above fluvial and fluvial-deltaic sands, indicating the influence of rising sea level and estuarine flooding and deposition up the valley. Color changes from gray to brown in fluvial sands suggest that the depth of the entrenched valley is about 29 m (95 ft) in borings taken southeast of Clear Lake. There is some evidence that the San Jacinto and Trinity River valleys merge just south of this area. The entrenched valley depth at the modern Gulf shoreline exceeds 36 m (120 ft) (Rehkemper, 1969; Smyth and others, 1988; and Anderson and others, 1991).

### Sabine and Neches Fluvial Systems

Stratigraphic cross sections of the Sabine and Neches river valleys (figs. 9-11) were located so that the following geological settings were investigated: (1) the downstream position of large meander scars where modern fluvial sediments are inset within terrace deposits of intermediate elevation (Neches R. at Hwy 96, Sabine R. at Hwy 12), (2) the downstream reaches where modern fluvial sediments onlap the older fluvial and coastal plain deposits (Neches R. at Beaumont, Sabine R. at Orange, fig. 11), (3) just upstream of the confluence of the Sabine and Neches Rivers, (Neches R. at Hwy 87, fig. 10), (4) downstream of the confluence of both rivers (Sabine Pass), and (5) along the deep entrenchment upstream of the major confluence with the Trinity/San Jacinto River system. The total channel length examined by the stratigraphic cross sections is about 185 km. Along that channel distance the base of channel incision below the surface elevation increases from 18 m to 36 m at an average rate of 0.4 m/km. Comparison of the cross sections show that there are distinct differences in the valley widths, sediment loads, stream gradients, and onlap relationships between the two river systems.

The coarse to fine sands of the channel-fill facies were deposited as point bars by moderately large meandering rivers. The overbank facies probably was not a major component of the older

alluvial deposits or they were removed by subsequent erosion of superimposed channels as rivers aggraded in response to rising base level. The large oversize meanders formed at a time when sediment supply exceeded the sediment transporting capacity of the rivers. Major fluvial incision occurred when the sediment transporting capacity greatly exceeded sediment supply and initially little sediment was stored along the valley walls. As equilibrium between sediment transporting capacity and sediment supply was reached, lowstand terraces formed and minor amounts of fine-grained overbank facies were deposited. During the lowstand in sea level, base level discharge of the large integrated fluvial systems was relatively uniform (not flashy) because of high precipitation.

The subsurface sediment textures and surficial channel patterns indicate that the river systems underwent significant changes in stream load and in channel flow patterns. Basal lithologies of the fluvial sediments are fine to coarse sand with some gravel whereas the modern stream load is mainly suspended sediment with little bed load in transport. Apparently this change in stream load is due to decreased fluvial discharge, which was climatically induced. The fluctuations in sea level and changes in climate were also accompanied by changes in flow patterns. Initially the fluvial systems were characterized by large, high discharge streams that carried a coarse bed load. These meandering streams exhibited broad lateral migration of point bars that filled the entire width of the meander belt. In contrast, the younger streams were sinuous streams with fixed channels that changed position by meander-bend cutoff and avulsion during floods. The modern mud-rich streams cut into the coarser, but older fluvial deposits upstream of Beaumont (Neches R.) and Orange (Sabine R.). Both the Sabine and Neches Rivers exhibit this fine-grained sinuous but nonmigratory pattern upstream of the onlap with modern floodplain deposits.

The overall composition of the valley fill is also partly related to sediment discharge and the stability of sea level at the time of deposition. Sediments deposited at the base of the incised valley during a rapid rise in sea level are more heterolithic than those deposited during a slow rise. The lateral facies changes and stratigraphic discontinuities are the result of rapid backfilling and aggradation and more frequent channel switching as the channels responded to rising base levels. The fact that no soil horizons are preserved in the lower valley-fill deposits also suggests that aggradation attendant with sea-level rise was rapid. The modern fluvial deposits are characterized by stacked fine-grained floodplain deposits and isolated mud-filled channels (mud plug).

### Neches River System

River Characteristics- Along the lower coastal plain, the entrenched Neches River valley is about 7.2 km wide, but valley width increases to about 10 km downstream (fig. 9). At this site the entire valley is filled with oversize point bar deposits. The maximum valley fill thickness is about 17 m, whereas the average valley fill thickness is about 12 m.

Valley Fill Lithology and Depositional Environments- The valley fill is composed of medium to coarse sand with gravel overlain by soft to stiff gray clay with roots (fig. 10). The modern Neches River is about 6-7 m deep and the thalweg is 3-4 m below the sand-mud contact. The upper clay represents the modern floodplain deposits. The valley fill of the Neches River is inset within older Pleistocene fluvial-deltaic deposits of the Beaumont Fm. (Fisher et al, 1973). The surface of the modern Neches River floodplain is about 8 m below the surface of the coastal plain Beaumont deposits near the type locality at Beaumont.

Near the onlap of modern sediments, the Beaumont surface is about 6-7 m above sea level. The Beaumont Fm. is composed of stiff clay and sandy clay with some sand beds of variable thickness. The sand bodies have highly discontinuous stratigraphic relationships. The uppermost muds of the Beaumont Fm. commonly contain oyster shells, which are reported in borings from both sides of the Neches valley at Beaumont. The intermediate terrace surface, or Deweyville terrace, is about 3 m above sea level. The Deweyville deposits are characterized by red gray and yellow gray sediments. Thick Deweyville deposits of fine to coarse sand are overlain by thin red and gray silty clay of the floodplain facies with soil development. The sand deposits are the source of construction aggregate mined in the numerous pits along Interstate 10 east of Beaumont. The base of channeling beneath the Deweyville terrace rises abruptly in two places where valley widening occurred.

The deep, narrow entrenchment of the Neches River is restricted to the extreme western side of the valley where the river was trapped against the valley wall formed by the Beaumont outcrop. At that site the deepest entrenchment is about -20 m. The former incised valley is backfilled with sand and clay deposited after the isotopic stage 2 lowstand unconformity was eroded. The overlying channel fill is sandy at the base and grades up into organic-rich mud. The vertical change in lithology is evidence that there was an abrupt decrease in bed load transported by the river. As the modern stream meandered, remnants of the intermediate terrace deposits were beveled and removed. The modern valley is narrowest at Beaumont where the Neches River remained during the falling phase of sea level. This location also coincides with an abrupt downstream decrease in valley width.

Near the present shoreline of Sabine Lake (Hwy 87), the modern floodplain of the Neches River is at sea level and about 3 m below the Beaumont surface. The top of the Deweyville terrace is not preserved at this site unless it is beneath a veneer of modern overbank muds on the east side of the valley. The base of the incised valley is about 36 m below sea level, but there are also incisions at -27 m and -17 m below sea level. The basal valley fill is about 8 m thick and composed of heterolithic soft silty clay and fine sand, the intermediate fill is about 10 m thick and composed mainly of fine sand and clayey fine sand with rare soft organic clay that represents overbank muds encased in fluvial sand. The upper fill is approximately 17 m thick and represents an upward

fining succession composed of 5-6 m of sand and 8-12 m of mud that grades up into very soft organic clay at the surface of the modern floodplain. The modern river carries only a fine-grained suspended load. Essentially no bed load reaches the downstream segment near present sea level (fig. 10).

The lower reach of the Neches River forms a river mouth entering an estuary, but there is no distinct delta constructed into the estuary (Sabine Lake). Furthermore, there is no evidence of a distributary pattern at the river mouth where the river deposited its load of suspended sediment. At this location the stream is still confined by the valley where the valley is about 6.5 km wide and the stream encounters a microtidal, low wave energy environment. The final stage of valley fill is represented by aggradation of deltaic-estuarine sediments. The change from fluvial conditions to deltaic conditions occurs at about -8 m. The isolated lenticular sands near the top of the fill are probably evidence of minor delta distributaries formed as the fluvial-deltaic system was simultaneously backstepping (retrograding) and changing load. The general absence of discrete sand bodies and high organic content indicate that the mode of sediment deposition was settling of suspended mud in swamps and marshes after large floods rather than switching of delta lobes or distributary channel bifurcation. There is no evidence of marine influence (shells) in the floodplain muds because flushing action within the confined valley and the large volume of fresh water at the river mouth maintained low salinities that prevented the development of a marine fauna.

The general sea level history reconstructed for the northern Gulf of Mexico indicates abrupt rises followed by periods of sea level stability. The distinct levels of fluvial incision of the Neches valley roughly correspond to the pronounced steps in sea level illustrated by Frazier (1974). The youngest incision level (channel base at -17 m) corresponds to the sea level stillstand at -6 m, which occurred about 6 ka BP. The intermediate incision level (channel base at -27 m) corresponds to a sea level stillstand at -15 m about 8 to 9 ka BP. The deepest incision corresponds with the maximum sea level lowstand about 18 ka BP. According to descriptions of the Neches River in the late 1800s, the modern bankfull river near Sabine Lake and sea level was about 2 m deep before dredging. Therefore the base of the channel thalweg was well above the average depth of contact between the fluvial sand and overlying organic-rich mud (fig. 10).

#### Tributaries to the Neches River (Taylor Bayou)

A stratigraphic cross section across Taylor Bayou shows that the erosional unconformity is in three benches at -4 m, -9 m, and -16 m. The unconformity cuts into tan and gray clay and sandy silty clay, probably of the Beaumont Fm. The unconformity is overlain by organic clay and muck even down to -18 m. No beds of clean sand are present in the fill of the valley margin tributary. This is because the local drainage basin was small, the stream gradient was relatively steep, and the unconformity was a sediment bypass surface. As a result of these conditions, fluvial sediments

were not stored during the downcutting phase of river entrenchment. The relatively steep tributary streams were sources of sediment to the trunk stream and they served as zones of sediment transport rather than sediment storage.

### Sabine River System

River Characteristics- Along the outer coastal plain at Deweyville, the Sabine River valley is filled with remnants of large meander deposits. This is the type locality of the Deweyville Fm., which encompasses the terraces of intermediate elevation between the higher Beaumont Fm. and lower modern floodplain. The Deweyville terrace is about 4.5 m below the Beaumont surface and the modern floodplain is about 1.5 m below the Deweyville.

A variety of ages have been reported for the Deweyville terrace deposits ranging from 10 kyBP to more than 100,000 kyBP (Table 1). Some of the variability in reported ages is the result of dating different fluvial systems, using different materials (shell, wood), sampling different stratigraphic positions within the fluvial system, sampling unrelated older facies beneath the channel, and using criteria other than isotopic dating to determine the age of the deposits (Table 1). Most of the reported ages of the Deweyville deposits are from  $^{14}\text{C}$  dates, an exception is the relative age given by Thomas (1990), who used stratigraphic relationships interpreted from seismic reflections and the assumption that the base of the channel represented a sequence boundary formed as a result of a fall in sea level. Thomas (1990) also speculated that the younger dates consistently reported for the Deweyville on the basis of  $^{14}\text{C}$  (Table 1) were caused by contamination and the introduction of more recent carbon.

Table 1. Ages reported for Deweyville terraces and stratigraphically equivalent deposits.

Reported Age	River System	Material	Method	Reference
17-30 kyBP	Sabine, Tx	NR	$^{14}\text{C}$	Bernard and LeBlanc (1965)
			$^{14}\text{C}$	Gagliano and Thom (1967)
13-25 kyBP	Sabine, Tx		$^{14}\text{C}$	Aronow (1967)
20-25 kyBP	Ouachita, Ark	none	inference (climate)	Saucier (1981)
10-13 kyBP			$^{14}\text{C}$	Aten (1983)
> 100 kyBP	Sabine, Tx	none	inference (seismic)	Thomas (1990)

NR - not reported



Valley Fill Lithology and Depositional Environments- The Deweyville terrace deposits are composed of medium to coarse sand and gravel. The foundation borings are located in sloughs and abandoned channels of the modern river and therefore the lithologic control does not record the uppermost composition of the Deweyville. However, descriptions of soils indicate that the surficial sediments are sandy loams. The base of the channel appears to be about -6 to -9 m below sea level. The swale fill of the modern Sabine River is composed of gray fine to coarse sand (reworked) and black organic rich clay and silty clay. Depth of the modern Sabine River is not precisely known, but it appears to be about 4.5 m deep based on the depth of the abandoned channel fill.

At Orange, near the onlap of modern sediments with the intermediate terrace deposits, the deep entrenchment of the Sabine River is on the western side of the valley. The thick valley fill deposits are composed of medium and coarse grained sand with some gravel (fig. 11). The base of the youngest incised channel is at a depth of -9 to -12 m as recognized on the basis of underlying stiff clay. Maximum depth of the entrenched valley is greater than -24 m. The modern deposits of the Sabine River are organic-rich mud overlying the fluvial sand. The modern channel is 6-7 m deep and the base of the modern thalweg is at the top of the sand deposits. The Sabine River was more of a mixed-load stream during lowstand and rising phases of sea level and a suspended load stream during late rising phases and highstand.

#### Combined Sabine-Neches Rivers

Toward the southern part of Sabine Lake and along the navigation channel toward Sabine Bank, the base of the incised valley is greater than 30 m below sea level. Valley fill deposits are composed of a basal sand succession overlain by peat or organic rich muds and then soft gray clay and sandy clay with increasing shell content toward the top. The contact between upper shelly muds and underlying nonfossiliferous muds may represent the ravinement surface. Near the Sabine Pass jetties, the muds immediately above the basal sands were radiocarbon dated at 8-9 ky BP by Nelson and Bray (1970).

The abrupt change in orientation of the Sabine-Neches valley near the confluence with the Calcasieu River system appears to be structurally controlled. The change in alignment of the valley axis from north-south to southwest coincides with the zone of middle Miocene expansion faults (Morton et al., 1988). Even though there is no obvious surficial expression of these faults observed on high resolution seismic lines, it is possible that the faults created a subtle structural sag that influenced the position of the river while it was excavating the valley.

#### Comparison of Sabine and Neches Rivers

Both ancestral streams were larger than their modern equivalents because discharge was greater when precipitation was higher. Both modern streams are sinuous, but there is no evidence of modern meandering with point bar deposition. Instead, discrete channels are cut into older sand-rich meanderbelt deposits of the Deweyville terrace. Overall the Neches River appears to have carried a finer load, the coarse sand and gravel of the Sabine River system extends basinward of the downstream control. The drainage basin was larger and the discharge was greater for the Sabine River than for the Neches River.

The apparent steep incision of the valley upstream of I-10 is a result of the abrupt fall in sea level from the highstand shoreline position and downcutting through the preceding highstand deposits. The lowered base level at the highstand shoreline caused a local disequilibrium of the stream gradient that was accommodated by erosion and removal of the previous channel deposits by the youngest incised channel (isotopic stage 2 lowstand channel). Some older terrace deposits may be preserved along the valley margins farther downstream but the lack of cross-valley transects prevents making any definitive statements other than in the thalweg the older deposits are either unrecognized because of a lack of soil horizons or they have been completely removed by subsequent erosion.

## REFERENCES

- Anderson, J. B., Siringan, F. P., Smyth, W. C., and Thomas, M. A., 1991, Episodic nature of Holocene sea level rise and the evolution of Galveston Bay: Gulf Coast Section, Society of Economic Paleontologists and Mineralogists Foundation, Twelfth Annual Research Conference program and abstracts, p. 8-14.
- Aronow, S., 1967, Place of the Deweyville Formation in the western Gulf Coast Recent-Pleistocene sequence: abst. meeting Southeastern Section, Geological Society of America, Tallahassee, Florida, p. 15-16.
- Aten, L. E., 1979, Indians of the upper Texas Coast: Ethnohistoric and archeological frameworks: The University of Texas at Austin, Ph.D. dissertation, 560 p.
- Aten, L. E., 1983, Indians of the upper Texas Coast: Academic Press, New York.
- Bernard, H. A., 1950, Quaternary geology of southeast Texas: Unpub. Ph.D. dissertation, Louisiana State University, Baton Rouge, Louisiana, p.
- Bernard, H. A., and LeBlanc, R. J., 1965, Resume of the Quaternary geology of the northwestern Gulf of Mexico province, in, Wright, H. E., and Frey, D. G., eds., The Quaternary of the United States: Princeton University Press, p. 137-185.
- Bureau of Economic Geology, 1968, Geologic atlas of Texas, Beaumont Sheet: The University of Texas at Austin.
- Bureau of Economic Geology, 1982, Geologic atlas of Texas, Houston Sheet: The University of Texas at Austin.
- Fisher, W. L., Brown, L. F., McGowen, J. H., Groat, C. G., 1972, Environmental geologic atlas of the Texas coastal zone, Beaumont-Port Arthur area: The University of Texas at Austin, Bureau of Economic Geology, 91 pp.
- Gagliano, S. M., and Thom, B. G., 1967, Deweyville terrace, Gulf and Atlantic coasts: Louisiana State University, Coastal Studies Bulletin 1, p. 23-41.
- McEwen, M. C., 1969, Sedimentary facies of the modern Trinity delta, in Lankford, R. R., and Rogers, J. J. W., Holocene geology of the Galveston Bay area: Houston Geological Society, Chapter 3, p. 53-77.
- Rehkemper, L. J., 1969, Sedimentology of Holocene estuarine deposits, Galveston Bay, Texas: Rice University, PhD Thesis.
- Saucier, R. T., and Fleetwood, A. R., 1970, Origin and chronologic significance of Late Quaternary terraces, Ouachita River, Arkansas and Louisiana: Geological Society of America Bulletin, v. 81, p. 869-890.
- Saucier, R. T., 1981, Current thinking on riverine processes and geologic history as related to human settlement in the southeast: Geoscience and Man, v. 22, p. 7-18.

- Stout, I. M., Bentz, L. C., and Ingram, H. W., 1961, Silt load of Texas streams, a compilation report, June 1889-September 1959: Texas Board of Water Engineers, Bulletin 6108, 237 p.
- Smyth, W. C., Anderson, J. B., and Thomas, M. A., 1988, seismic facies analysis of entrenched valley-fill: A case study in the Galveston Bay area, Texas: Gulf Coast Association of Geological Societies Transactions, v. 38. p. 385-394.
- Thomas, M. A., 1990, The impact of long-term and short-term sea level changes on the evolution of the Wisconsin-Holocene Trinity/Sabine incised valley system Texas continental shelf: unpub. Ph.D. dissertation, Rice University, Houston Texas, 247 p.
- Winker, C. D., 1979, Late Pleistocene fluvial-deltaic deposition, Texas coastal plain and shelf: The University of Texas at Austin, Master's thesis, 187 p.

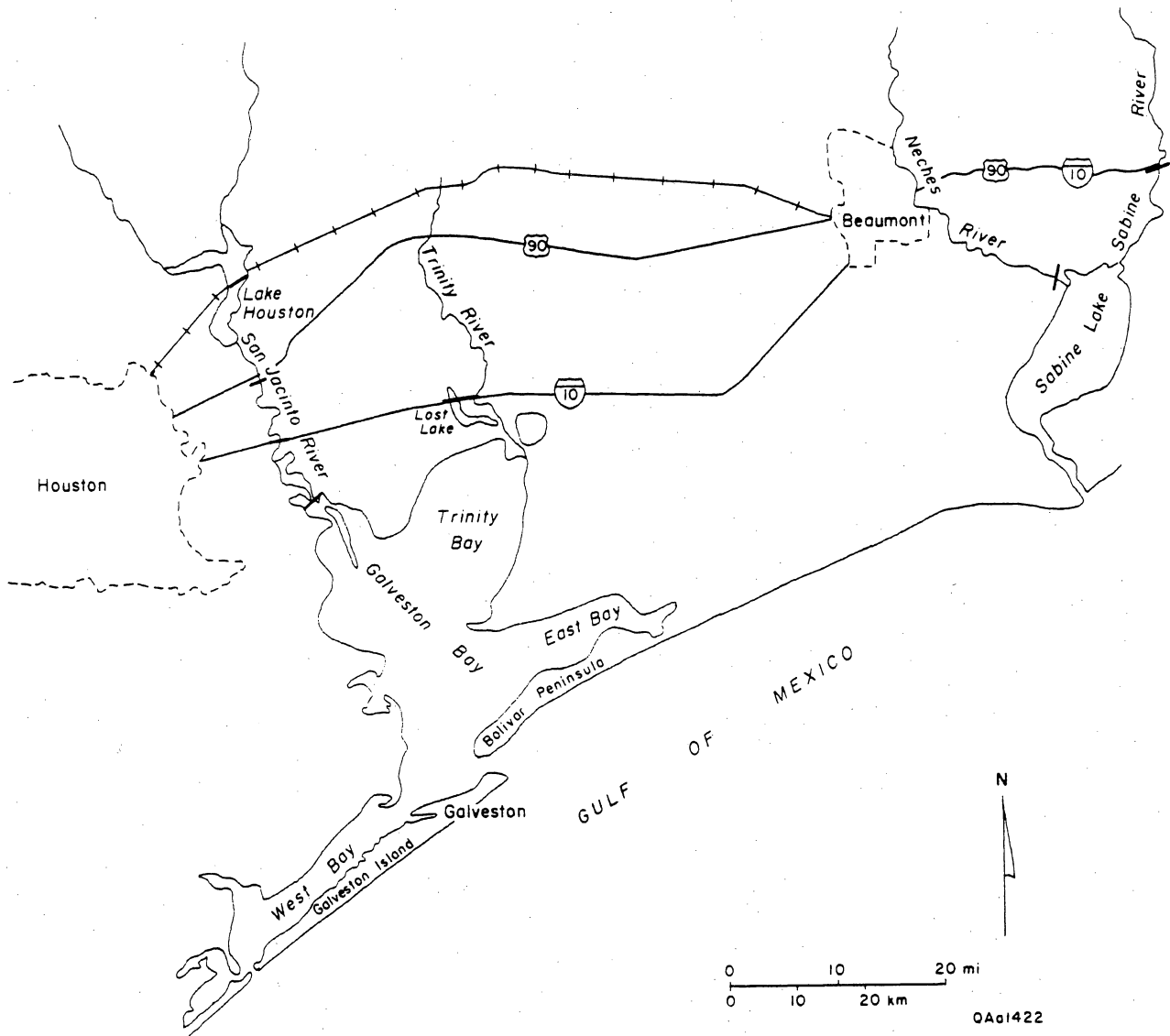


Figure 1. Locations of stratigraphic cross sections for the Trinity, San Jacinto, Neches, and Sabine Rivers.

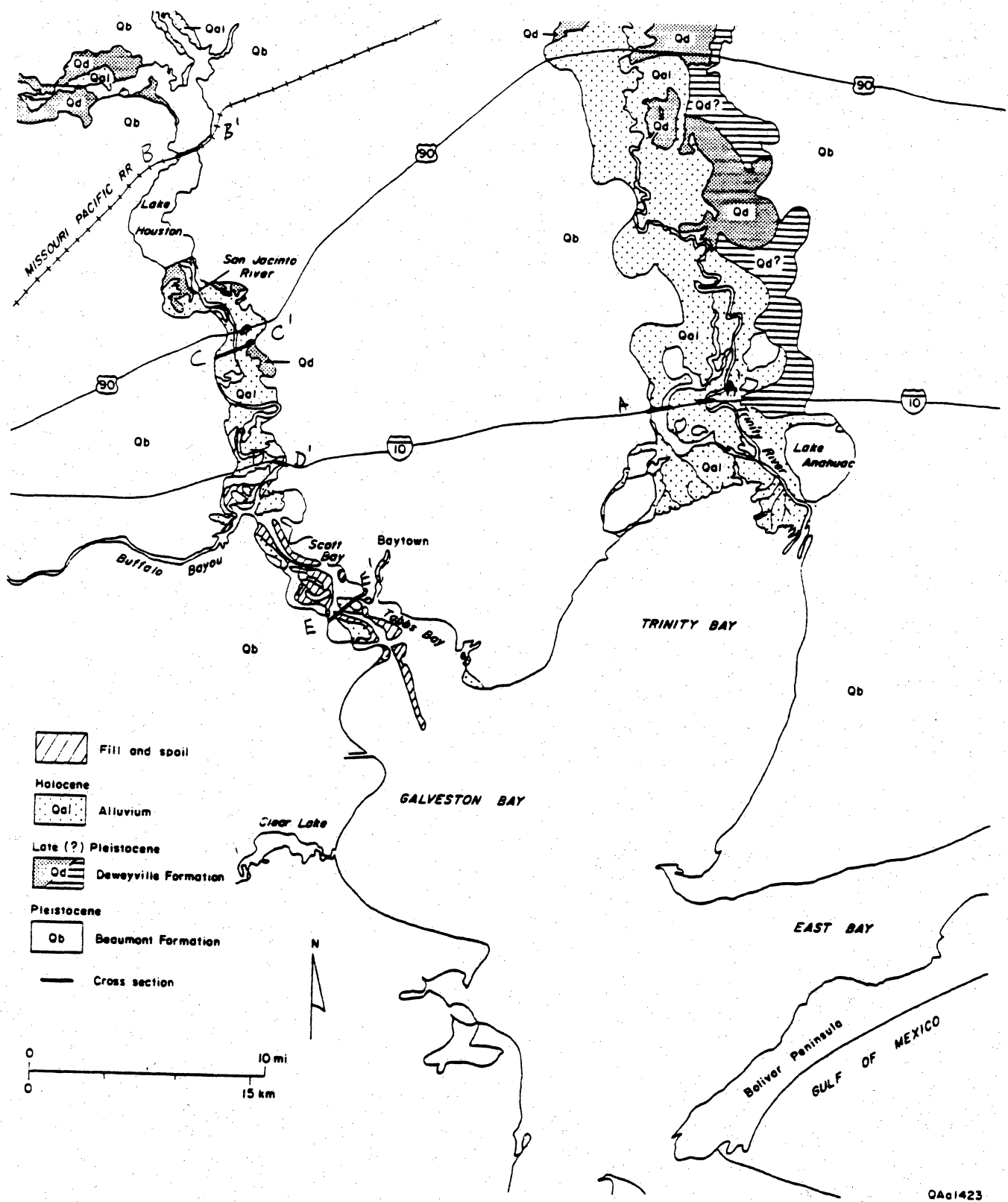


Figure 2. Index map of the Trinity and San Jacinto River valleys showing geologic formations and locations of cross sections.

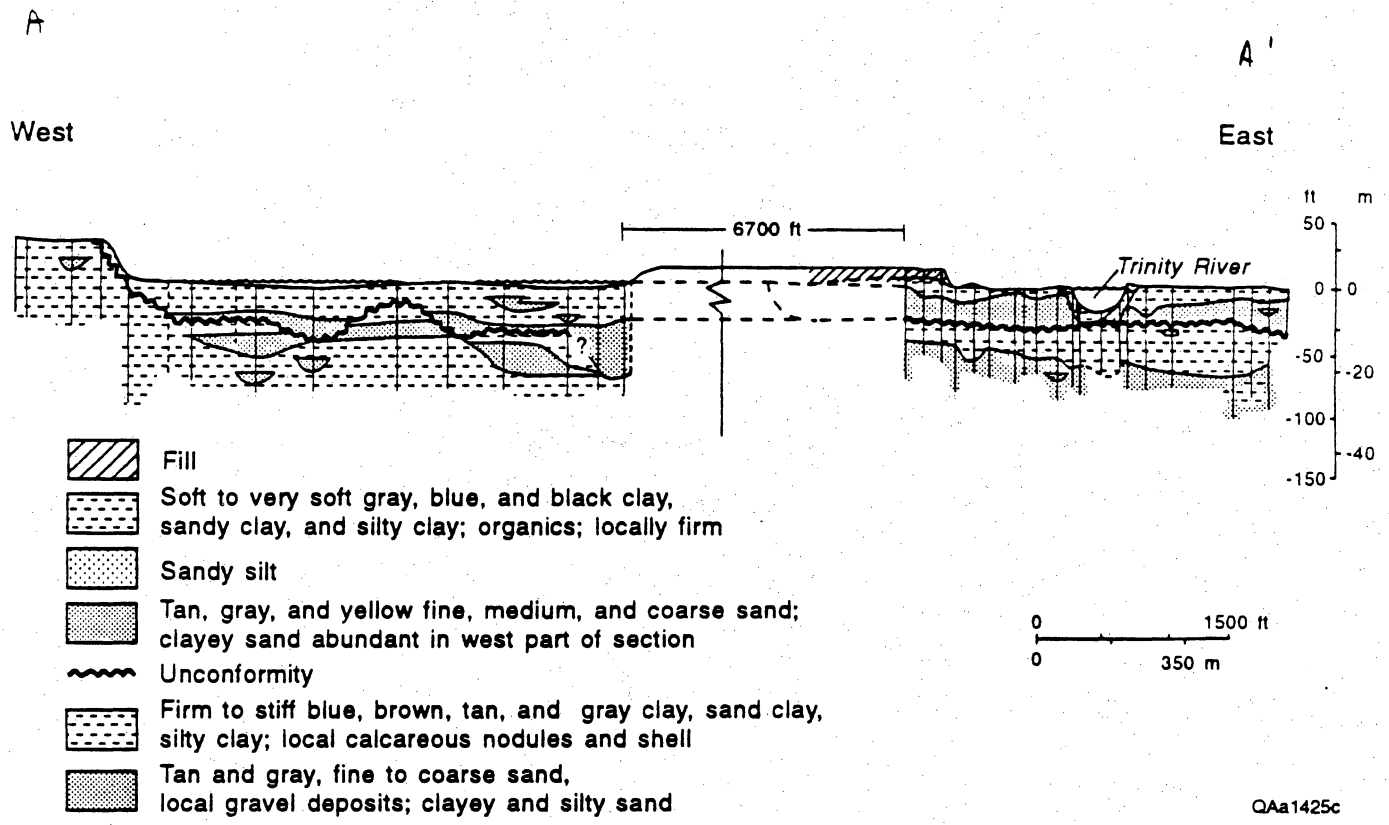


Figure 3. Lithologic cross section A-A', Trinity River valley at IH 10. See figure 1 for location.

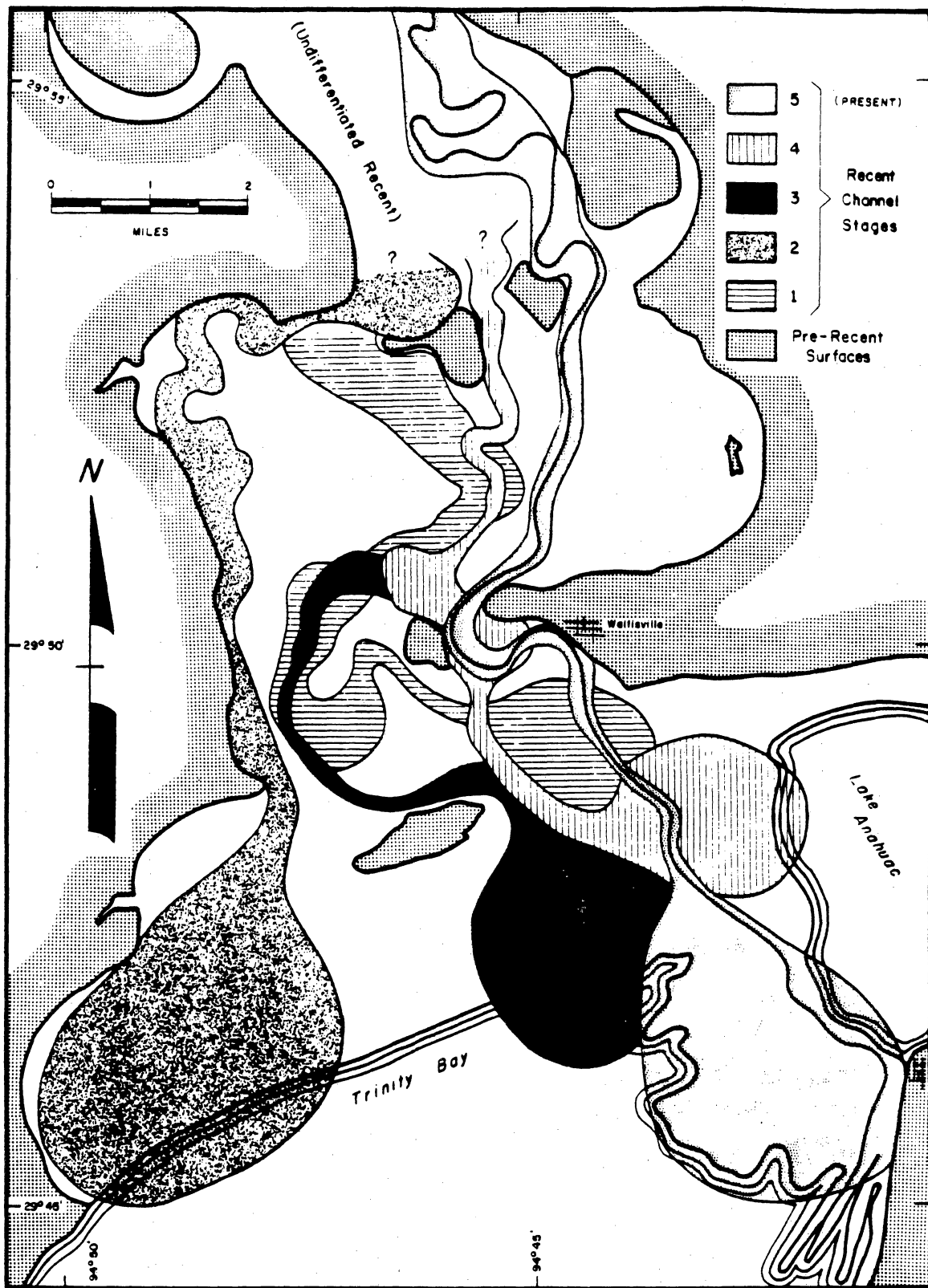


Figure 4. Recent channel stages of the Lower Trinity River. From Aten (1979).





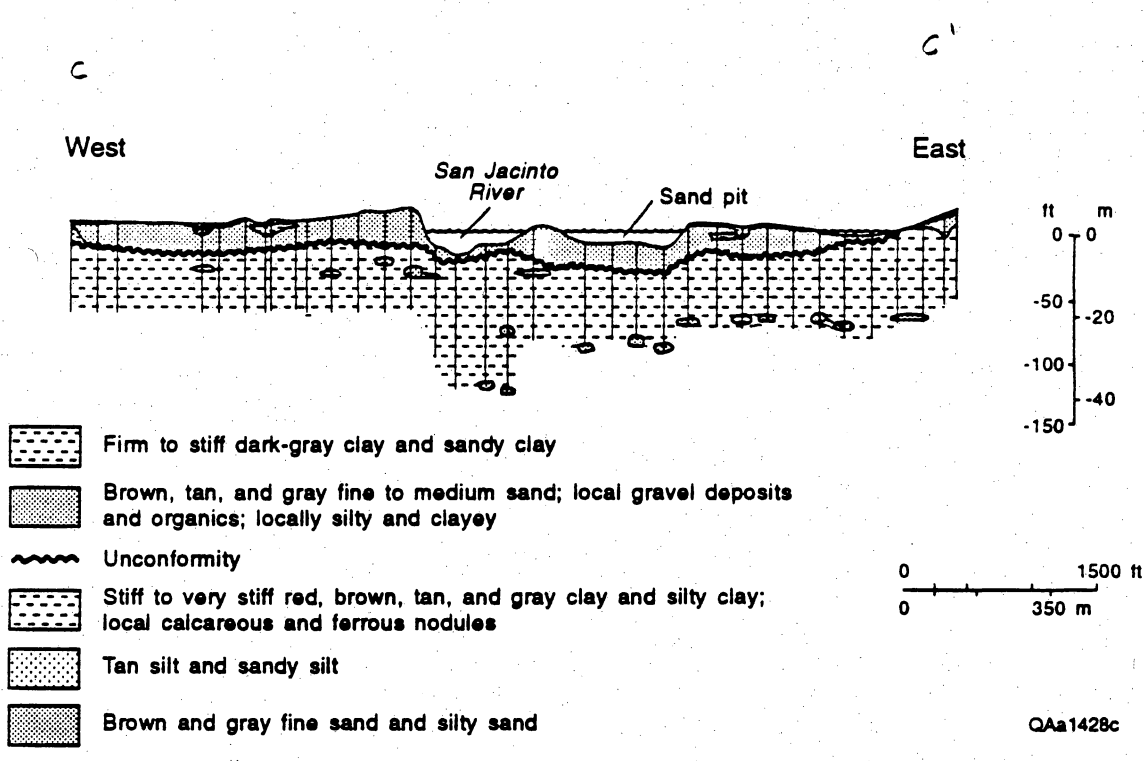
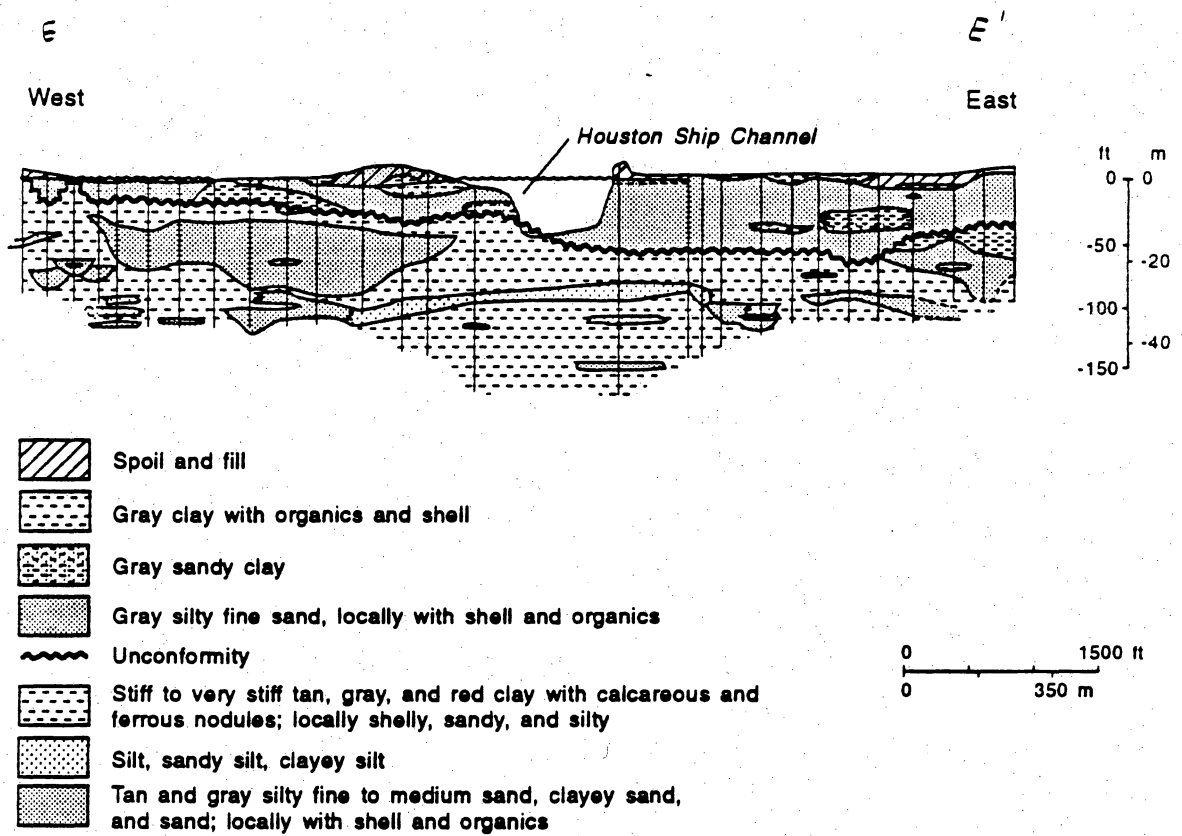


Figure 6. Lithologic cross section C-C', San Jacinto River valley at new U.S. Highway 90. See figure 2 for location.





QAa1427c

Figure 8. Lithologic cross section E-E', San Jacinto River valley at Baytown Bridge. See figure 2 for location.

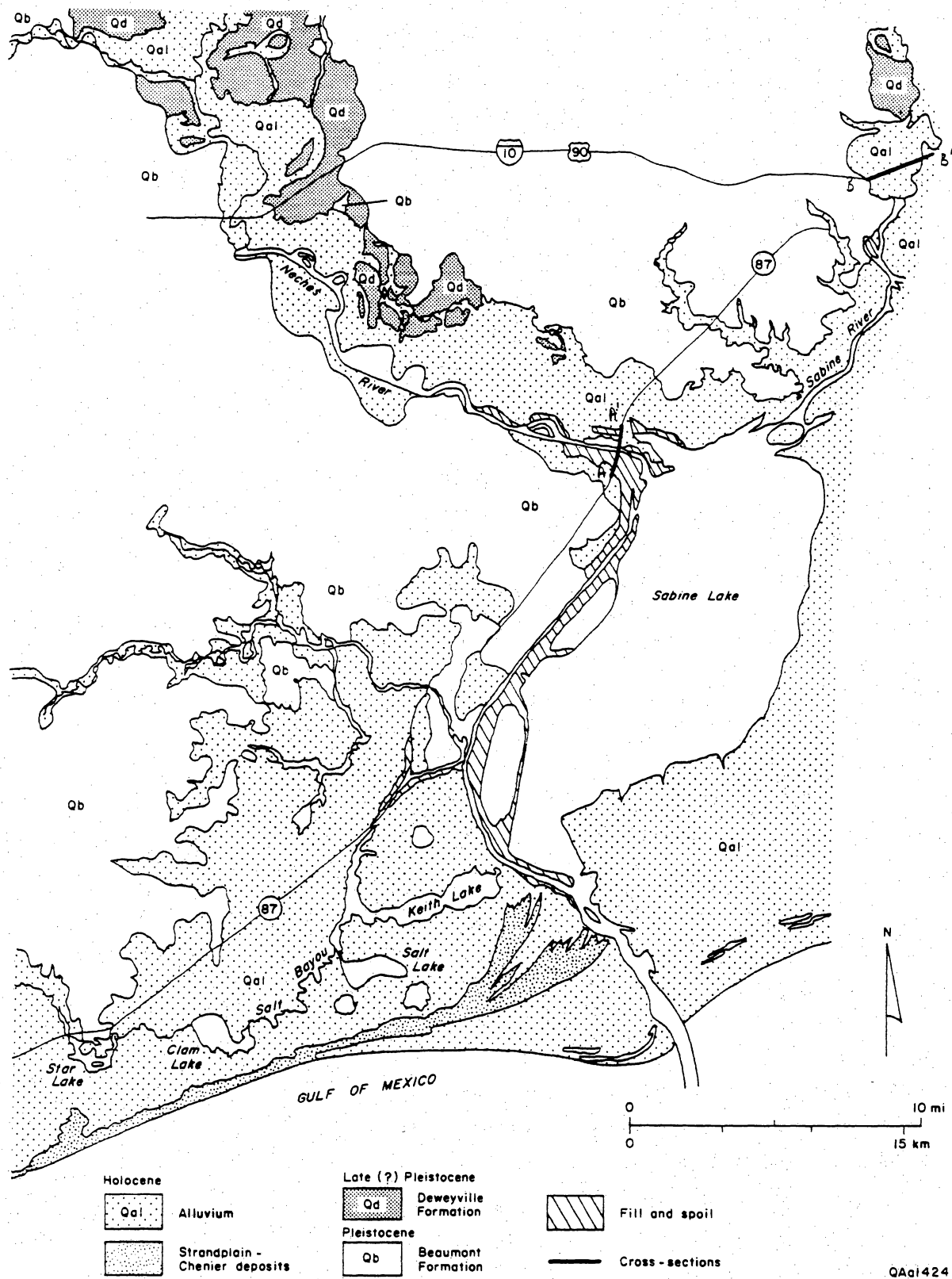


Figure 9. Index map of the Sabine and Neches River valleys showing geologic formations and locations of cross sections.

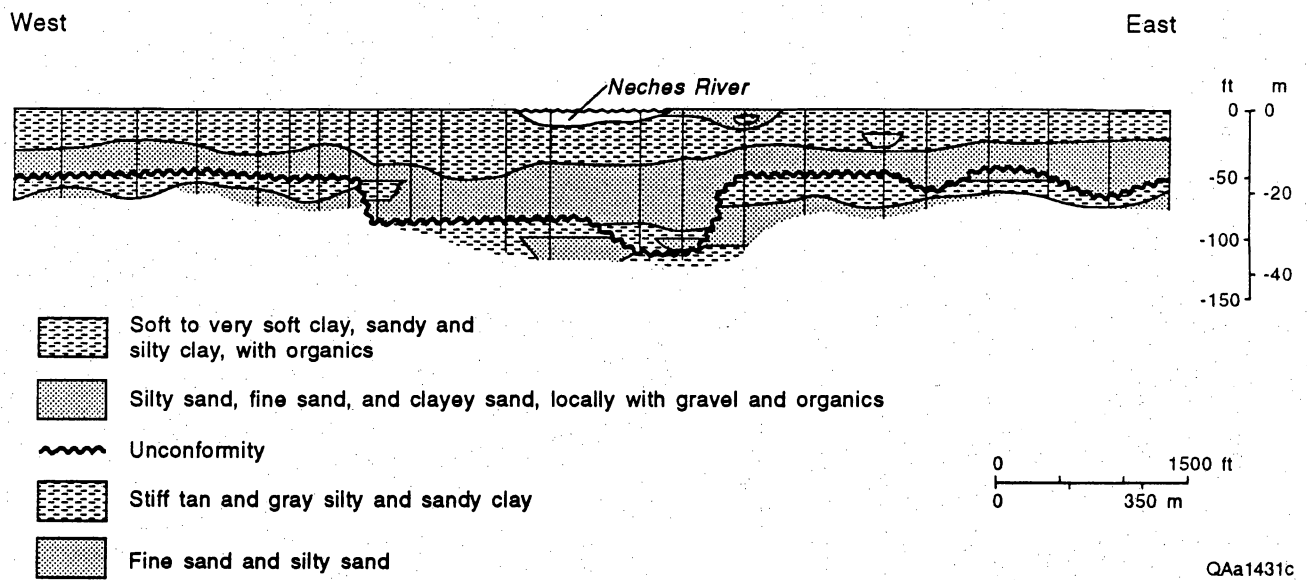


Figure 10. Lithologic cross section of the Neches River valley at State Highway 87. See figure 9 for location.

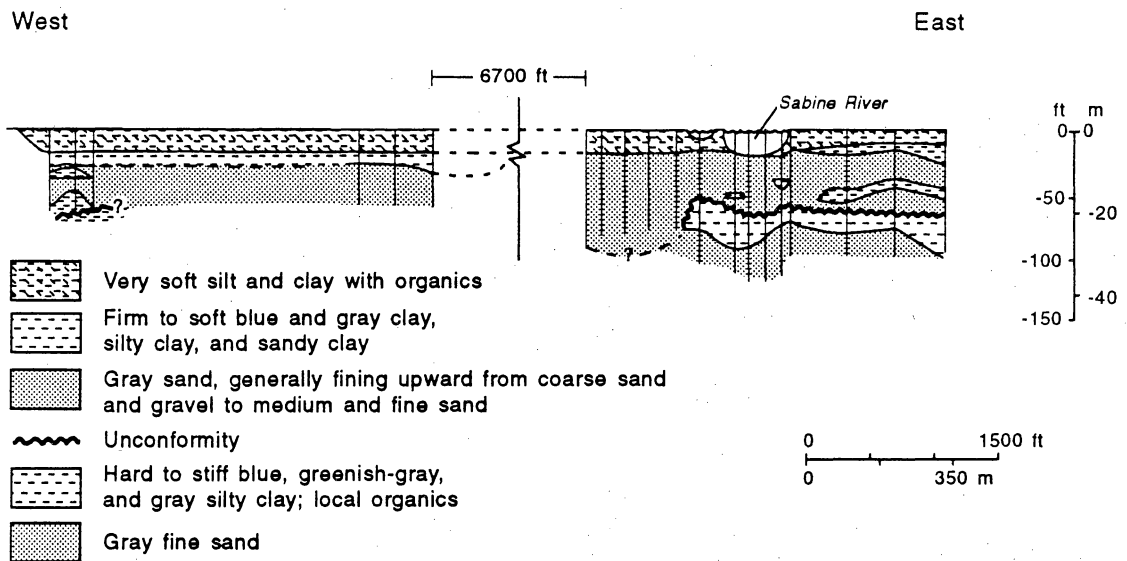


Figure 11. Lithologic cross section of the Sabine River valley at IH 10. See figure 9 for location.

## ADDENDUM 4

### RELEVELING PROFILE ACROSS THE TRINITY RIVER VALLEY

William A. White  
Bureau of Economic Geology  
The University of Texas at Austin

Significant losses in wetlands have occurred in the Trinity River valley as areas of emergent vegetation have been replaced by open water and unvegetated flats (White and Calnan, 1991). The reason for these losses is that rates of subsidence have exceeded rates of sedimentation.

Releveling surveys for bench marks located around Trinity Bay were obtained from the National Ocean Survey, National Oceanic and Atmospheric Administration. The locations of benchmarks were plotted on two USGS 7.5 minute quadrangles (Cove and Anahuac) at the northern tip of Trinity Bay. Rates of subsidence in mm/yr were determined for the period 1973-1978 (Balazs, 1980). A releveling profile between Mount Belvieu and Anahuac (fig. 1) indicates that subsidence rates approach 25 mm/yr near Mount Belvieu but the subsidence rates decrease to less than 10 mm/yr near Anahuac. Subsidence of bench marks along IH 10 in the Trinity River valley ranged from about 6 to 10 mm/yr between 1973 and 1978 (fig. 1). However, comparison of releveling surveys from 1978 and 1987 for the Pasadena area east of Houston show that subsidence has decreased dramatically due to curtailment of groundwater pumpage after 1976 in the eastern part of the region (Gabrysch and Coplin, 1990). Although bench marks in the Trinity River valley were not releveled in 1987, one can assume that subsidence rates in the valley have also decreased significantly.

### REFERENCES

- Balazs, E. I., 1980, The 1978 Houston-Galveston and Texas Gulf Coast vertical control surveys: National Oceanic and Atmospheric Administration Technical Memorandum NOS NGS 27, 60 pp.
- Gabrysch, R. K., and Coplin, L. S., 1990, Land-surface subsidence resulting from ground-water withdrawals in the Houston-Galveston region, Texas, through 1987: U.S. Geological Survey, Report of Investigations No. 09- 01, 53 pp.
- White, W. A., and Calnan, T. C., 1991, Submergence of vegetated wetlands in fluvial-deltaic areas, Texas Gulf Coast: Gulf Coast Section Society of Economic Paleontologists and Mineralogists Foundation, Twelfth Annual Research Conference, Program with abstracts, p. 278-279.



**Subsidence Rates Based on Bench Mark Releveling Surveys,  
1973-1978, Trinity River Delta Area**

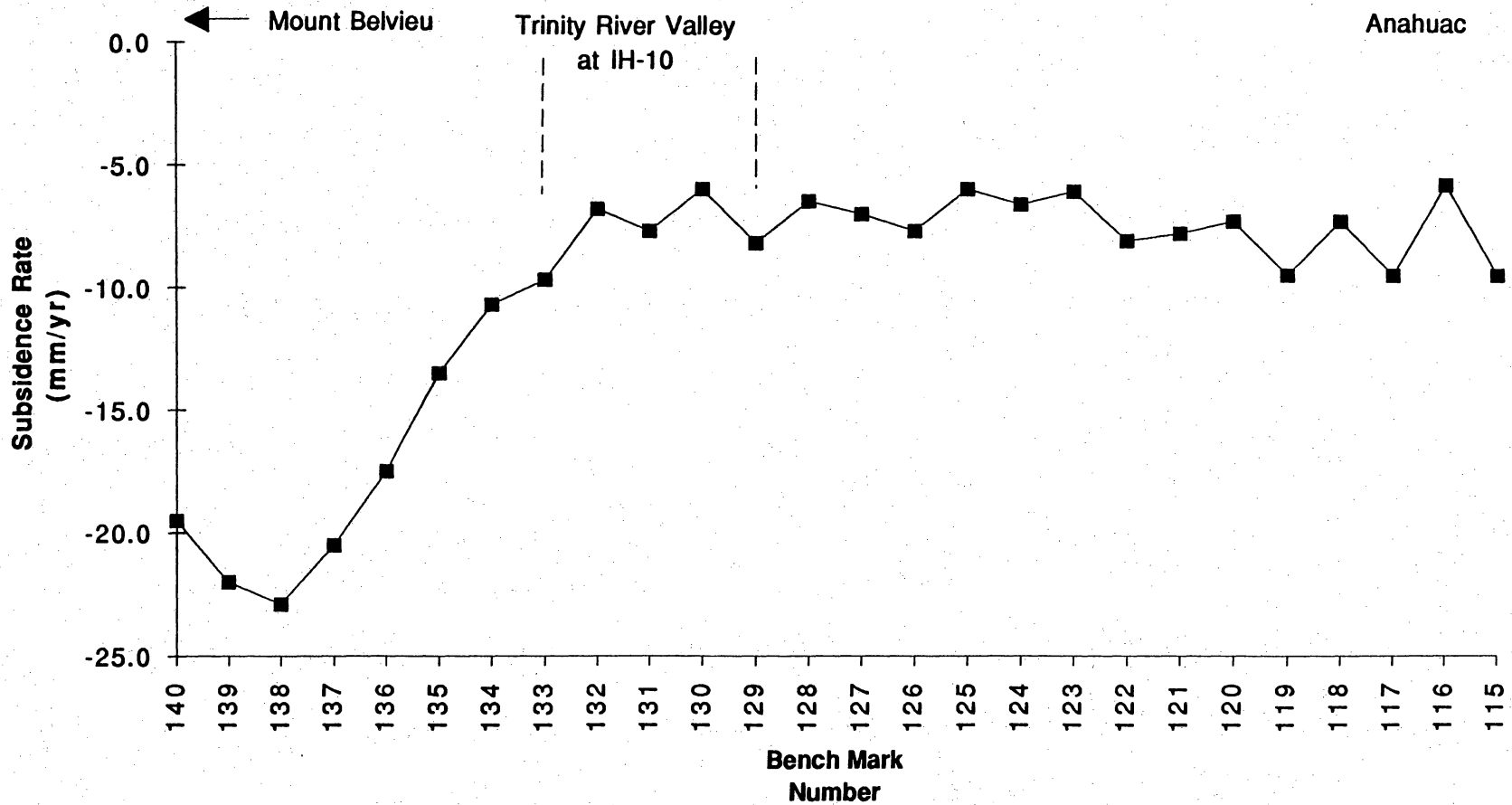


Figure 1. Subsidence rates based on bench mark releveling surveys, 1973-1978, Trinity River delta. Rates from Balazs (1980).

## ADDENDUM 5

### BEACH AND DUNE SEDIMENTATION ON GALVESTON AND FOLLETS ISLAND: HURRICANE ALICIA AND BEYOND

James C. Gibeaut and Robert A. Morton  
Bureau of Economic Geology  
The University of Texas at Austin

#### INTRODUCTION

In December, 1983, the Bureau of Economic Geology (BEG) established six beach profile transects spaced 3 to 6 km apart along the western 29 km of Galveston Island west of the Galveston Seawall (figs. 1 and 2). A seventh transect was established on Follets Island five km west of San Luis Pass. These profiles were established in undeveloped areas to measure the natural recovery of the beach and foredune systems after Hurricane Alicia, which struck the Texas coast near San Luis Pass in August, 1983 (fig. 1). The beach profiles were measured every three months until the fall of 1985 after which they were measured annually. There are now a total of 94 surveys from the seven locations; the latest surveys were conducted in April, 1993.

The seven beach profiles on Galveston and Follets Islands along with other profiles located between Sabine Pass and Galveston are being monitored under the joint U.S. Geological Survey and Bureau of Economic Geology coastal erosion project. This report presents a detailed geomorphic analysis of the beach changes between 1983 and 1993 that supplements and updates the post-Alicia summary of beach changes presented by Morton and Paine (1985).

#### METHODS

The beach profiles were measured using the Emery technique (Emery, 1961). Existing structures such as foundations, telephone poles, and benchmarks as well as datum stakes established by the BEG are used as reference marks landward of the dunes. Profile data are entered in the U.S. Army Corps of Engineer's (COE) Interactive Survey Reduction Program (ISRP). ISRP is used to manage data, to check for errors, and to adjust data to common datums (Birkemeier and Holme, 1992A). The COE computer program called Volume (Birkemeier and Holme, 1992B) reads ISRP files and computes profile volumes and horizontal shoreline positions. For the following analysis of beach changes, profile volumes were computed for an area above mean-sea level and seaward of a point about five meters landward of the foredunes. The landward termination of the profiles is at a position beyond which there was no change in profile volume.

## RESULTS

### Hurricane Alicia Erosion and Deposition

Hurricane Alicia caused extensive beach and dune erosion on Galveston and Follets Islands. Mapping from aerial photographs showed that the vegetation line moved landward an average of 24 m along West Beach of Galveston Island (Morton and Paine, 1985). The storm flattened a 1.5 m high foredune system and deposited 186,000 m<sup>3</sup> of washover sediment on the vegetated barrier flats. Using pre-Alicia profiles taken in 1980 by the U.S. Army Corps of Engineers, Morton and Paine (1985) estimated that another 1,359,000 m<sup>3</sup> of sand eroded from the beach and dunes was transported offshore. This erosion estimate may be slightly high because the 1980 profiles were measured before Hurricane Allen which had a small but measurable impact on Galveston Island.

At each profile, Hurricane Alicia eroded between 60 m<sup>3</sup> and 132 m<sup>3</sup> of sand per meter of beach from an area above mean-sea level and seaward of the erosional scarp. The landward extent of washover deposition from Alicia decreased from San Luis Pass to the east (Morton and Paine, 1985), but the magnitude of beach and dune erosion did not follow a similar alongshore trend. Profile 1 (fig. 3), which is the eastern most profile, lost the least amount of sediment (60 m<sup>3</sup>/m), but profile 2, which is west of profile 1, lost the most (132 m<sup>3</sup>/m). The remaining profiles on Galveston Island each lost about 100 m<sup>3</sup>/m of beach.

### Post-Alicia Profile Responses

The seven profiles along Galveston Island and Follets Island may be placed in four groups based on their response from 1983 to 1993. The centrally located profiles 2, 7 and 3 (fig. 2) are in one group; profiles 4 and 5 near San Luis Pass are in another group; and profiles 1 and 8 at the extreme ends of the monitored segment stand alone. The central group of profiles all showed substantial volume increases as a result of berm widening and beach aggradation for two years after Hurricane Alicia (figs. 4, 5, and 6). By 1985, the berms had fully recovered and the rate of volume increase slowed; all three profiles continued to increase in volume until 1987, but at a slower rate and as a result of foredune accumulation. From 1987 to 1988/89, all three profiles lost volume and experienced shoreline erosion due to berm narrowing. Dune erosion did not contribute to the loss in volume, and profile 7 actually showed substantial dune accretion. Since 1989, the three centrally located profiles either have accreted (profiles 2 and 3) or have remained stable (profile 7). The dunes continued to accrete at all three sites from 1989 to 1993.

Like the centrally located profiles, profile 1 to the northeast underwent a two-year rapid increase in profile volume following Alicia, but between 1985 and 1988, the profile volume did not

change (fig. 3). After 1985, a foredune developed that was similar to those at the other locations, but this accumulation was offset by lowering of the backbeach elevation. The transfer of sand between the beach and dunes may have been partly caused by sand scraping and stockpiling of sand and organic debris to enhance dune formation. Since 1988, profile 1 has steadily lost volume as a result of berm and dune erosion (fig. 3).

The third group of profiles include sites 4 and 5, which are located on the west end of Galveston Island near San Luis Pass (fig. 2). These profiles showed little or no recovery during the two-year period following Alicia, unlike all the other profiles (figs. 7 and 8). Furthermore, dunes did not naturally develop at these sites as they did at the other locations two to five years after Alicia. Between 1985 and 1987/88 these profiles experienced berm and dune erosion, although the dune eroded at profile 5 was artificial. From 1987 to 1990, profile 5 added volume by berm aggradation and artificial alterations, but since 1990, it has remained stable. Since 1988, the profile nearest San Luis Pass (profile 4) has dramatically increased in volume through berm widening and aggradation. In 1991, a new foredune at profile 4 began growing 20 m seaward of the old erosional escarpment.

The beach response at profile 8 on Follets Island has been different than the response at any beach on Galveston Island. Since 1983, this beach has accreted at a rapid rate of 12 m<sup>3</sup>/m per year (fig. 9). From 1983 to 1989, accretion occurred as shoreline advancement, berm widening, and dune formation. Since 1989, the shoreline position has remained stable, but rapid accumulation has continued as a result of berm aggradation and new foredune construction 40 m seaward of the old foredune.

The following discussion summarizes the post-Alicia history of beach changes at each profile. The histories are organized on the basis of the beach response to changes in sediment supply and ocean energy.

#### Tower Base, Profile (1)

December, 1983 to October, 1987- During this period, foredune sand accumulation buried the post-Alicia erosional escarpment and the entire profile aggraded (fig. 3). A distinct berm and convex profile formed causing as much as 30 cm of beach aggradation at the berm crest. Some of the sand covering the post-Alicia escarpment was the result of beach scraping and dumping in front of the foredune, which was observed in October, 1987.

October, 1987 to September, 1989- The foredunes aggraded 30 cm and advanced seaward 3 m partly as a result of natural sand accumulation and partly as a result of continued beach scraping and dumping of sand in front of the foredune. In 1989, the berm was absent and the seaward sloping profile was 30 cm lower and 20 m narrower. The anomalously high elevation at the seaward end of the profile in 1989 was caused by a swash bar migrating onshore as the beach

recovered after Hurricane Chantal. After Chantal, the forebeach elevation was essentially the same as in December 1983. Part of the transfer of sand from the forebeach to the backbeach recorded by the 1989 profile was the result of Hurricane Gilbert, which flooded the beaches of the Texas coast eroding sand from the forebeach and depositing it in the backbeach at the base of the foredunes.

September, 1989 to April, 1993- By 1993, the foredune had lowered 50 cm and the dune ramp had retreated 3 m. The beach was lowered 40 cm and a concave profile developed. In 1993, the forebeach at profile 1 was about 40 cm below the post-Alicia (1983) elevation, which is the lowest forebeach elevation since the monitoring began.

Overall- At profile 1, the beach and foredune recovery processes equilibrated two years after Hurricane Alicia. At that time the beach profile exhibited a prominent berm and the volume of beach sand remained unchanged. After 1988, the beach entered an erosional phase that resulted in a lower and narrower profile and development of a linear to concave shape.

#### Galveston Island State Park, Profile (2)

December, 1983 to October, 1987- A foredune slowly reformed on top of the scarp eroded by Hurricane Alicia (fig. 4). Some of the material in the foredunes was added by dumping sand and organic detritus scraped from the forebeach. Between 1983 and 1986 the backbeach remained stable, but the berm widened and advanced seaward 15 m causing aggradation of 50 cm. In June 1986, the beach profile was convex in shape, the beach had a distinct berm, and the new foredune was 60 cm high. By 1987, this constructed foredune raised the earlier dune 70 cm to a height of 130 cm above the backbeach. At the same time, the vegetation line advanced seaward 4 m, and the shoreline prograded 15 m.

October, 1987 to September, 1989- Between 1988 and 1989, more scraped sand and organic debris was dumped in front of the previously constructed foredune. The elevations of the base of the dune ramp and adjacent backbeach remained stable. In contrast to the stable foredune and backbeach, the berm was almost completely removed and the forebeach was lowered about 50 cm as a result of the combined erosion of Hurricanes Gilbert and Chantal. A post-Chantal recovery swash bar was present on the beachface in 1989 and some sand was artificially pushed landward from the swash bar.

September, 1989 to April, 1993- By 1990, the sand that was dumped in front of the foredune had eroded, but the berm had widened 30 m by advancing seaward. By 1993, however, a new foredune became well established in front of the older dune. This new foredune may have developed from another artificial placement of sand. The new dune development caused seaward dune advancement of 3 m and the raising of the foredune ramp and adjacent backbeach by 50 cm. The crest of the older and larger dune accreted vertically 50 cm. By 1993, the berm present in

1990 had been removed and the profile became linear to concave in shape. Compared to 1989, however, the forebeach was uniformly raised 30 cm, and the shoreline advanced about 20 m.

Overall- The beach recovery processes at profile 2 equilibrated about two years after Alicia and the beach developed a prominent berm. Both the beach and dunes accumulated sand from 1983 to 1987 when accretion leveled off. Significant erosion occurred in 1988 and 1989 at least partly caused by Hurricanes Gilbert and Chantal. Since 1989, the beach has continued to gain volume mainly by artificial and natural additions of sand to the foredunes; whereas the forebeach continues to fluctuate between phases of erosion and accretion. Repetitive profiles for this beach show shapes alternating between convex profiles with berms and linear to concave profiles without berms. In 1993, the beach was slightly concave in shape with no berm.

#### Jamaica Beach, Profile (7)

December, 1983 to October, 1987- In 1983, the profile displayed a scarp eroded by Hurricane Alicia and a convex profile with a runnel occupying the backbeach landward of the berm (fig. 5). After Alicia, no foredunes were present on the beach. By 1987, the berm runnel was filled and the entire profile aggraded as much as 30 to 50 cm. The berm crest also advanced seaward 10 m, but the backbeach width remained about the same. This is because of dune formation and placement of scraped sand on the former backbeach. By 1987, a foredune 75 cm high and about 15 m wide began to develop and bury the Alicia erosional scarp.

October, 1987 to September, 1989- The foredune aggraded another 60 cm; however, the berm crest position retreated 25 m and raised 20 cm while the backbeach elevation remained constant. The beach erosion was greater than dune growth and there was a decrease in overall sediment volume. A recovery swash bar from Chantal was present on the profile in 1989.

September, 1989 to April, 1993- The berm crest advanced 5 m. An incipient foredune 50 cm high and 6 m wide with sparse vegetation began to form 12 m seaward of the primary foredune location. This new eolian deposition caused a slight increase in sediment volume that would have been greater if not for erosion of the forebeach.

Overall- The Jamaica Beach profile accumulated a moderate volume of sand for two years after Hurricane Alicia. Sand accumulation continued at a slower rate from 1985 to 1987 and included foredune development and shoreline advancement. Since 1987, the beach has remained relatively stable with respect to overall sediment volume, but the site of sand accumulation has shifted from the berm to new dunes seaward of the previously established foredunes. The seaward end of the beach had eroded down to an elevation slightly below the elevation of the beach after Hurricane Alicia.

#### Sea Isle, Profile (3)

December, 1983 to October, 1987- The foredune and small, sparsely vegetated dunes in front of the foredune advanced seaward onto the former backbeach burying the Alicia scarp (fig. 6). By 1987 the foredune aggraded 150 cm and increased 20 m in width. The berm also widened and the berm crest advanced seaward 40 m, but the shoreline advanced less than 10 m creating a steep forebeach. As the beach widened, the berm elevation remained unchanged.

October, 1987 to September, 1989- Between 1987 and 1989, the small dunes in front of the large foredune eroded, but the backdune avalanche face migrated landward. On the beach the berm crest retreated landward 30 m, and the berm narrowed from being about 40 m wide to about 20 m. A post-Chantal recovery swash bar was present on the forebeach in 1989.

September, 1989 to April, 1993- The foredune crest aggraded 60 cm and widened seaward 10 m. Small hummocky dunes formed on the seaward face of the foredune. A sparsely vegetated sand ridge was constructed between 1991 and 1993 on the backbeach and in 1993 was separated from the foredunes by a scraped sand road. The backbeach and forebeach uniformly raised 50 cm, and the berm crest advanced seaward 8 m. The berm width narrowed 8 m, however, because of the encroachment of the artificial sand ridge on the backbeach.

Overall- A large volume of sand accumulated rapidly and the berm recovered for two years after Hurricane Alicia. Foredune accretion and seaward berm widening continued until 1987 when the beach volume began to decrease. Erosion in 1988/89 was followed by rapid accumulation of a large volume of sand. Artificial measures have had only a minor effect on accretion since 1989. Throughout the monitoring period, this profile has maintained a convex shape with berms of various sizes. Although this beach and the beach at Galveston Island State Park (profile 2) have experienced similar post-Alicia histories, the beach at Sea Isle is more dynamic than at the State Park.

#### Terramar, Profile (5)

December, 1983 to September, 1985- The initial beach response after Hurricane Alicia was minor retreat (3m) of a 75 cm high scarp (fig. 7). Algal mats formed in a low area on the backbeach just seaward of the scarp while the backbeach and forebeach remained essentially unchanged. During the summer of 1984, an artificial dune ridge 100 cm high and 10 m wide was constructed on the backbeach 25 m from the Alicia scarp. Because this ridge prevented frequent flooding of the backbeach, the erosional scarp, low algal flat, and dune ridge became partly vegetated in 1985. Subsequent eolian deposition seaward of the artificial sand ridge raised the backbeach area 20 cm. The berm crest advanced 10 m seaward, but maintained the same elevation.

September, 1985 to October, 1987- The seaward side of the artificial sand ridge eroded 5 m, and the backbeach in front of the ridge lowered 25 cm returning the beach to its post-Alicia

elevation. The crest of the sand ridge aggraded 40 cm and some sand was deposited on the landward side of the ridge. The forebeach steepened, and the beach width decreased by about 10 m. For this period there was an overall decrease in sediment volume.

October, 1987 to April, 1993- In 1988, Hurricane Gilbert destroyed the artificial sand ridge. The eroded sand was transported to the post-Alicia scarp where it formed a washover deposit that partly filled the low, flat area seaward of the erosional scarp. Another artificial dune ridge composed of red, muddy sand was placed at the same location of the original ridge. By 1990, this ridge had been completely destroyed by winter storms and the area landward of the ridge aggraded where the eroded fill was deposited. The corresponding area adjacent to the profile was artificially stabilized by salt cedar. A small ridge, partly formed by overwash deposits and by human alterations, was present at the former Alicia scarp location. By April, 1993, the area between the former Alicia scarp and artificial ridge locations was completely filled and supported dense vegetation. A small, sparsely vegetated, discontinuous dune formed seaward of a sand fence at the old sand ridge location. In 1993, there was no berm and the profile had a concave shape. Thus during this time, the backbeach area aggraded, but forebeach erosion offset most of the volume gained in the backbeach area.

Overall- At profile 5 there was very little recovery for two years after Hurricane Alicia and most of the observed volumetric additions were caused by construction of an artificial dune ridge. From 1985 to 1987 the beach lost sand. Beach volume increased slightly from 1987 to 1990, but it has remained stable since 1990. A foredune has begun to accumulate only recently with the help of sand fencing. The backbeach accumulation at profile 5 has been influenced by human activities more than any other monitoring site on Galveston Island.

#### San Luis Pass, Profile (4)

December, 1983 to September, 1985- The post-Alicia erosional scarp, which was 40 cm high in 1983, did not change and in 1985 it still marked the edge of continuous vegetation (fig. 8). There was no change in beach shape or significant change in beach volume during this time.

September, 1985 to August, 1988- Sometime between the 1987 and 1988 profiles, the beach elevation was lowered 60 cm and a new scarp 120 cm high formed 6 m landward of the post-Alicia scarp. An off-road vehicle path was created on the vegetated flat 10 m landward of the scarp and a small ridge formed on its seaward edge.

August, 1988 to April, 1993- After 1988, beach volume began to increase rapidly, particularly since the fall of 1991. By 1989, the scarp had retreated another 5 m, but by 1993, vegetated dunes had formed seaward of the scarp and the shoreline had advanced 40 m. The profile exhibited a 50 cm high sparsely vegetated, but continuous incipient foredune that raised the beach 150 cm. A



narrow, 10 m wide berm developed, but most of the beach has a linear sloping profile as in earlier years.

Overall- Unlike the other profiles on Galveston Island, the San Luis Pass profile did not accumulate sand during the two year period after Hurricane Alicia. Instead, the profile remained stable for about 2 years and then began to erode until it reached a minimum volume in 1988. The initial scarp formed by Alicia retreated landward and the beach lost elevation during this erosional period. Since 1988, the volume of beach sand has increased with rapid accretion occurring from the fall of 1991 until April, 1993. A small berm and a foredune began to form during this latest period of sand accumulation.

#### Follets Island, Profile (8)

December, 1983 to September, 1985- During this time, the post-Alicia scarp was completely buried by backbeach aggradation including eolian deposition and the development of a 40 cm high, 5 m wide incipient foredune (fig. 9). The backbeach and berm crest aggraded 40 cm, and the berm crest advanced 30 m.

September, 1985 to September, 1989- The foredune increased to a height of 125 cm above the beach and to a width of 18 m. Eolian deposition raised the backbeach by 25 cm. The berm crest advanced 25 m and increased in height by 25 cm. Eolian deposition in front of the foredune and rapid berm accretion on the seaward end of the profile formed a berm runnel. A post-Chantal recovery swash bar was present on the beach face in 1989.

September, 1989 to April, 1993- From 1989 to 1992, deposition on the backbeach and stabilization by vegetation continued to raise the backbeach by 60 cm. Between the spring of 1992 and the spring of 1993, a new foredune developed 45 m seaward of the previous foredune. The new foredune was 60 cm high and 10 m wide. Between 1989 and 1993, the berm narrowed by about 20 m to a width of 20 m. Berm narrowing was the result of dune formation on the backbeach and a stable shoreline position.

Overall- The Follets Island profile has continuously accumulated sand since Hurricane Alicia in 1983. All of the sand accumulation is natural and the profile has not been altered by human activities. The rate of sand accumulation slowed slightly sometime between 1985 and 1989. Prior to 1989, the accretion was in the form of both dune formation and shoreline advancement. However, since 1989, the shoreline position has stabilized, and accretion has continued as a result of eolian deposition and expansion of the dune system.

## DISCUSSION

### Profile Response to Hurricane Alicia

The amount of sand eroded from the profiles during Hurricane Alicia is related to pre-storm profile shapes (1980 COE surveys) and distance to the eye of the storm where it crossed the coast (fig. 1). Profile 2, which showed the most erosion, had a convex profile and a very well-developed berm that extended 60 m seaward of the foredune. This wide berm, which was anomalous among the profiles in 1980, was available for erosion during Alicia, and hence this profile lost the greatest amount of sand even though it was relatively far from the eye of the storm. Profile 1, which showed the least erosion, had a concave shape with little berm development. The shape, combined with its far distance from the eye of the storm, caused it to lose half as much sand as the other profiles. Profiles 3 and 7 each lost 100 m<sup>3</sup>/m of sand and each had slightly convex profiles. Profile 5 had a configuration very similar to profile 1, but its closeness to the storm's eye caused it to lose much more sand, about 100 m<sup>3</sup>/m. Profile 4 was the closest to the eye, and it had a convex shape, but the berm was only 15 m wide and the dunes were small. As a result of these conditions, profile 4 did not lose any more beach volume than profiles farther from the storm.

#### Hurricane Recovery Stages

Shoreline recovery following Hurricane Alicia occurred in two stages. The first stage involved berm deposition and lasted for two years. During this stage, Galveston Island between the seawall and to a point about 8 km east of San Luis Pass, experienced berm accretion at a rate of 10 to 22 m<sup>3</sup>/m/yr. This berm recovery period may be further divided into two substages. During the first substage, berms and shorelines advanced seaward, and during the second substage, berms aggraded and continued to advance seaward. From the fall of 1983 to the fall of 1984, beaches rapidly advanced seaward and formed berm runnels. During the fall and winter of 1984/85, storms moved sand landward from the berms, filled in the runnels, and aggraded the backbeach. For the next year, the backbeaches continued to aggrade and the shorelines advanced again. The shifting of profile configuration from a berm runnel with low backbeach elevations to a level berm configuration was profound for the recovery of these beaches because foredune reformation could not occur until the berms widened and raised a sufficient amount (Morton and Paine, 1985). The storms of the winter of 1984/85 caused this shift, and thus played an important role in the recovery of Galveston Island.

The second stage of recovery, which involved foredune reformation, lasted two to three years until 1987/88. During this period, backbeach elevations continued to increase through eolian deposition. Vegetation became well-established and foredunes developed at the location of the post-Alicia scarp. Four to five years after Alicia, continuous foredunes were present and rose about 1.5 m above the backbeach at most of the monitoring sites. However, some of this dune

accumulation was aided by placement of sand and organic debris scraped from the beach. During this period, the rate of sand accumulation slowed to about  $6 \text{ m}^3/\text{m}/\text{yr}$  and was largely in the form of eolian deposition. At the end of the four- to five-year recovery period, the beaches between the seawall to about 8 km east of San Luis Pass regained about 30% of the sediment eroded by Hurricane Alicia. Beaches on Galveston Island within about 8 km of San Luis Pass, however, did not undergo post-Alicia recovery stages. In 1987, four years after Alicia, these beaches had  $8 \text{ m}^3/\text{m}$  less sediment than measured during the first post-Alicia survey in December, 1983.

Profile 8 near San Luis Pass on Follets Island showed the same general pattern of recovery as the beaches discussed above on Galveston Island except the Follets Island site has continued to accumulate sand as a result of dune formation, beach aggradation, and beach accretion. This is the only beach that has gained volume for each monitoring period since 1985. Much of this sand that continues to accumulate on Follets Island is the result of sand eroded from Galveston beaches and the ebb tidal delta at San Luis Pass during Alicia. Strong alongshore currents during the storm transported the sand to the southwest and deposited the sand on the shoreface where it has continued to supply the accumulation at profile 8 (Morton and Paine, 1985).

#### Beach Responses Beyond the Two-Year Recovery Period

All the beaches on Galveston Island experienced lows in sediment volume centered around 1988/89. The high incidence of wave energy during Hurricanes Gilbert and Chantal caused the wide-spread erosion, but more study is needed to determine the net losses associated with those storms. After the 1988/89 low in sand volume, Galveston beaches evolved in several ways. The eastern section to within about three miles of the seawall eroded, and by 1993 had  $17 \text{ m}^3/\text{m}$  less sand than after Alicia. This erosional beach response may be at least partly caused by the lack of updrift sediment supply, which in turn, is caused by the Galveston seawall and groin field. Profiles along the beaches to the west alternated between accretion and stability beginning with profile 2, which accreted, profile 7, which remained stable, profile 3, which accreted, profile 5, which remained stable, and profile 4 near San Luis Pass, which showed the greatest amount of accretion.

The pattern of beach accretion along Galveston Island reflects the development of shoreline rhythms since 1989. The wave length of the rhythms is not discernable from the profile data because of the wide profile spacing. These rhythmic features, however, involve variations of as much as  $40 \text{ m}^3/\text{m}$  of sediment.

Profiles 4 and 8 adjacent to San Luis Pass are affected by interaction of the beach with the shoals and tidal channels of the San Luis Pass ebb-tidal delta. The large and continuous accretion of the beaches on Follets Island within a few miles of the Pass may be caused by episodic ebb-channel switching caused by Alicia or the shoreward movement of ebb-tidal delta sand during

Hurricane Alicia. Beaches on the Galveston Island side of San Luis Pass are probably interacting with marginal flood channels. More study of San Luis Pass is required to understand the adjacent beaches.

#### REFERENCES

- Birkemeier, W.A. and Holme, S.J., 1992A, User's Manual to ISRP 2.7, the Interactive Survey Reduction Program: Waterways Experiment Station, U.S. Army Corps of Engineers, Vicksburg, Mississippi, 56 p.
- Birkemeier, W.A. and Holme, S.J., 1992B, User's Manual to Volume 2.1: Waterways Experiment Station, U.S. Army Corps of Engineers, Vicksburg, Mississippi, 30 p.
- Emery, K. O., 1961, A simple method of measuring beach profiles: Limnology and Oceanography, v. 6, p. 90-93.
- Morton, R.A. and Paine, J.G., 1985, Beach and Vegetation-Line Changes at Galveston Island, Texas- Erosion, Deposition, and Recovery from Hurricane Alicia: Geological Circular 85-5, Austin, Texas, Bureau of Economic Geology, The University of Texas at Austin, 39 p.

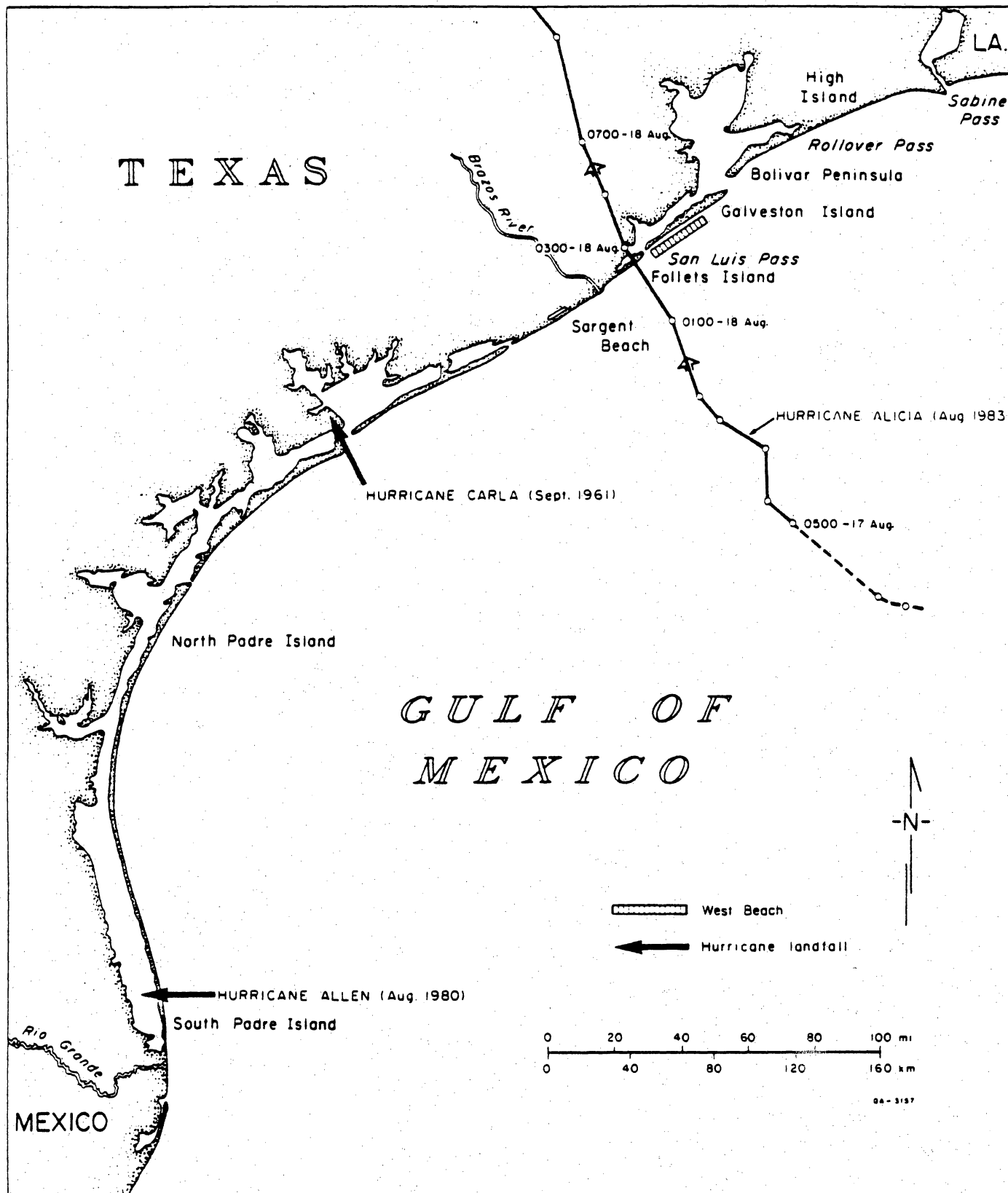


Figure 1 - Location of study area (Galveston and Follets Islands), geographic features, and sites of recent hurricane landfall along the Texas Gulf Coast, from Morton and Paine (1985).

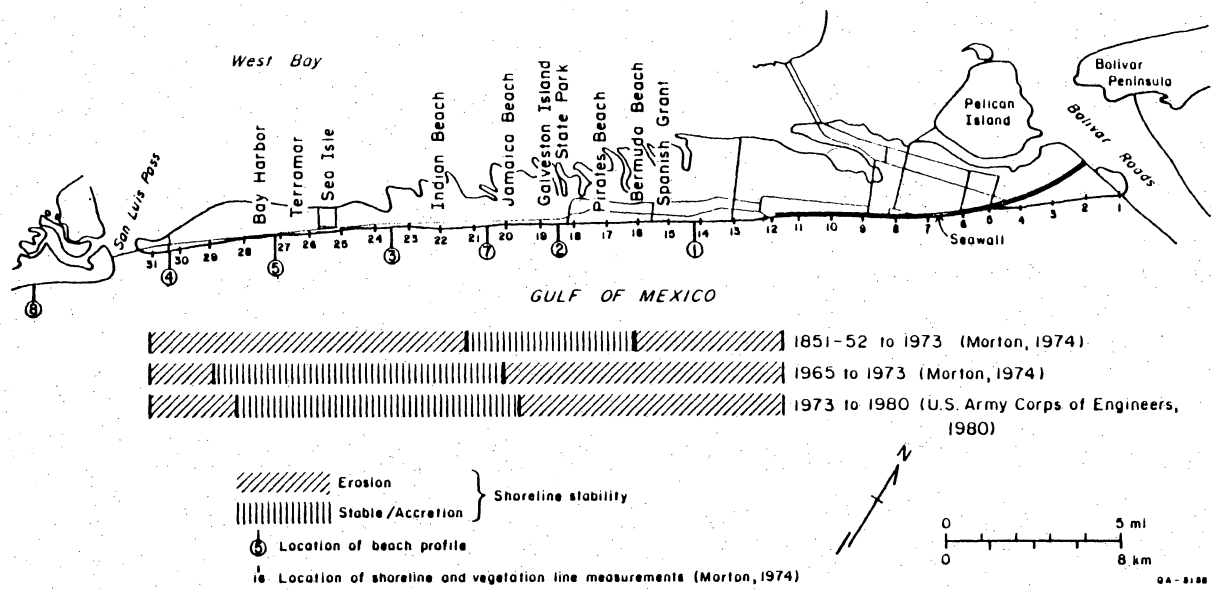


Figure 2 - Beach-profile sites, shoreline measuring stations, subdivisions, and stability of Gulf shoreline, Galveston and Follets Islands. Numbered measuring stations spaced about 1,500 m apart, from Morton and Paine (1985).

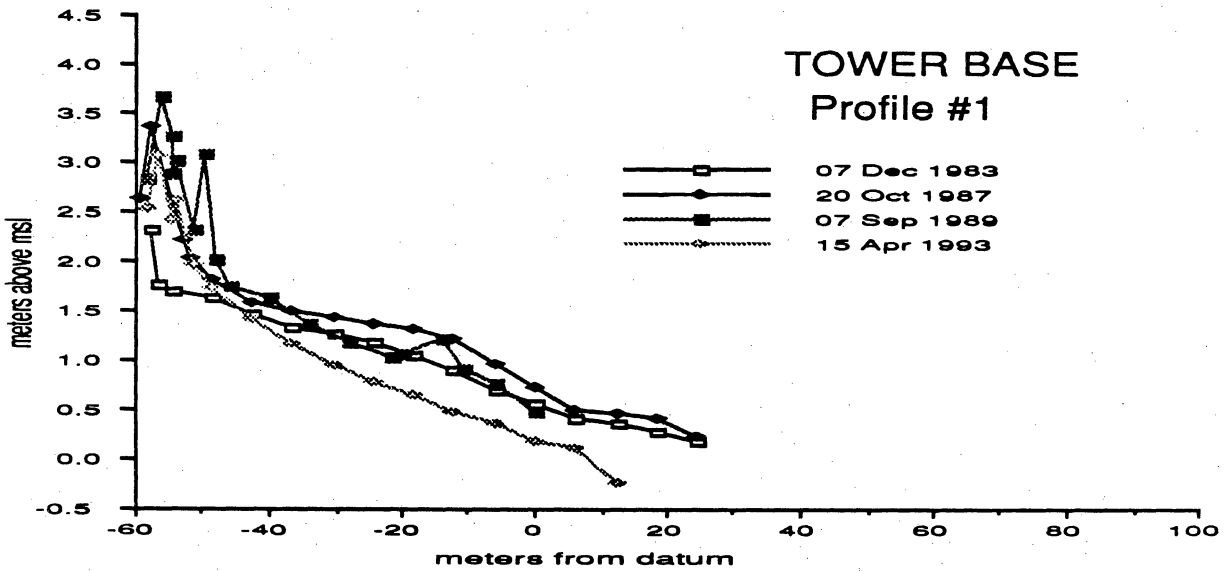
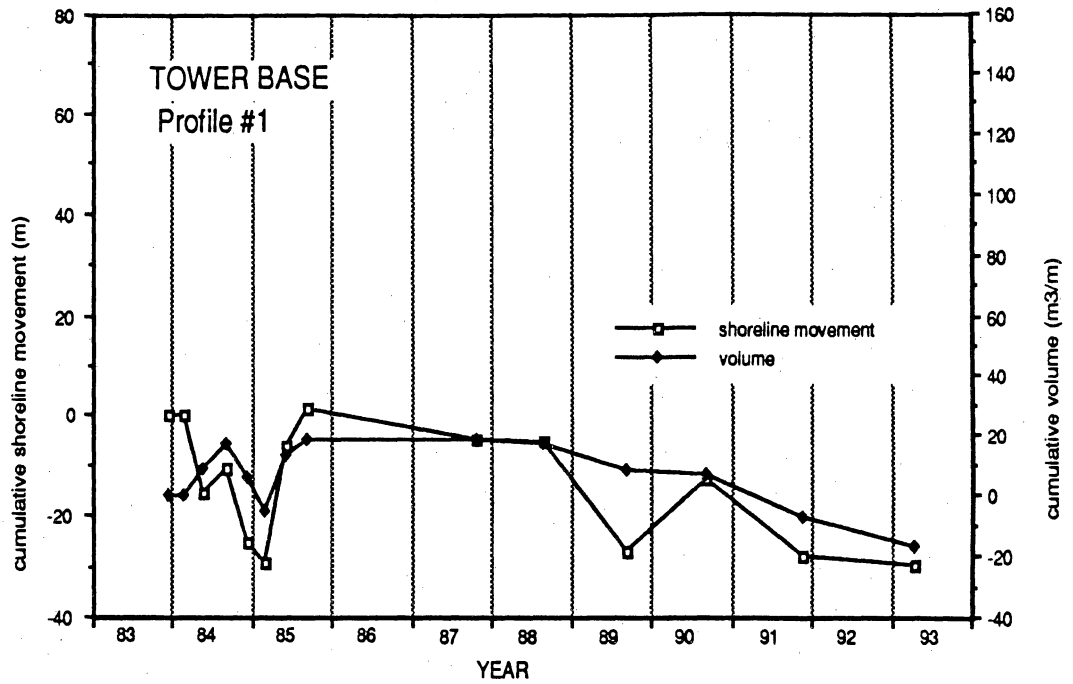


Figure 3 - Shoreline movement, profile volume change, and selected profiles for beach profile 1, location shown in figure 2. Shoreline used is mean-sea level. Volume calculated above mean-sea level and seaward of a point about five meters landward of the foredune.

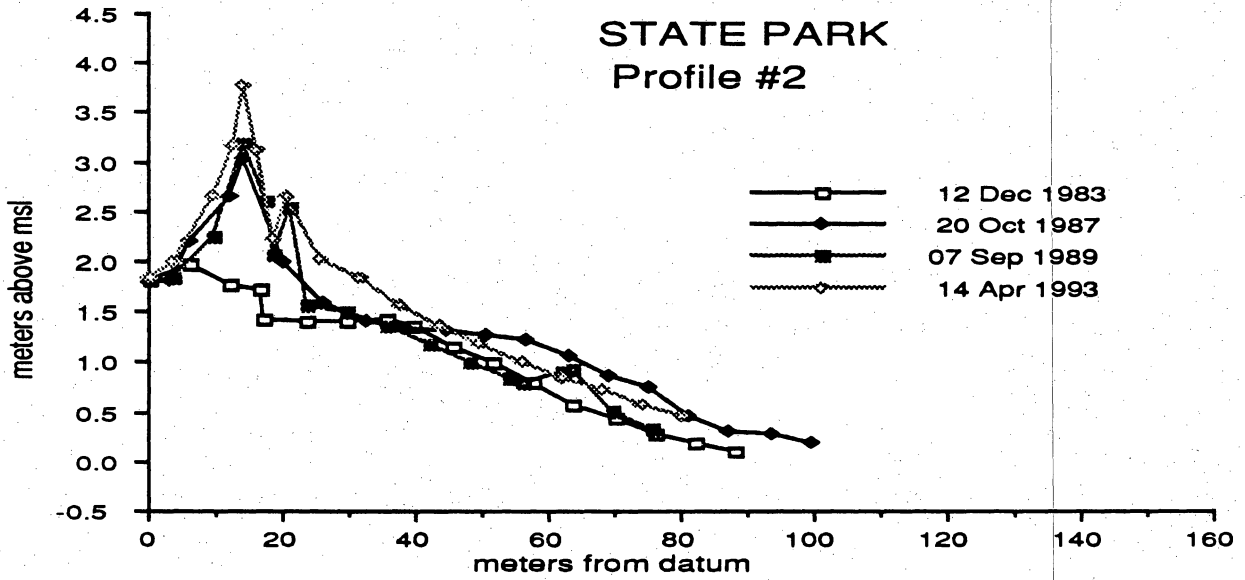
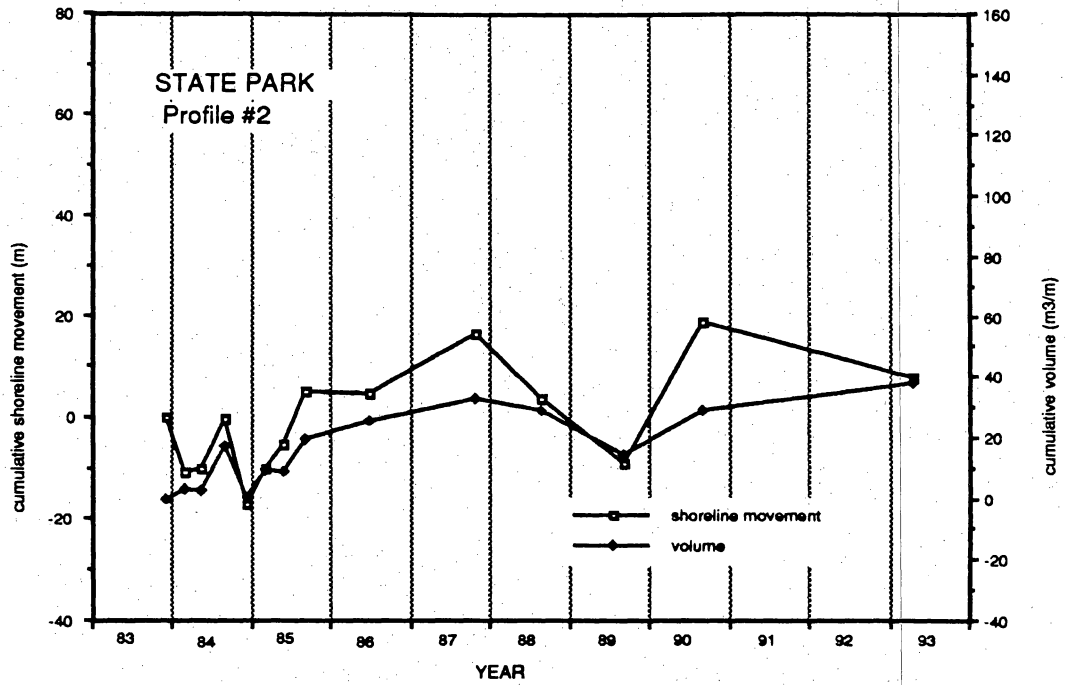


Figure 4 - Shoreline movement, profile volume change, and selected profiles for beach profile 2, location shown in figure 2. Shoreline used is mean-sea level. Volume calculated above mean-sea level and seaward of a point about five meters landward of the foredune.



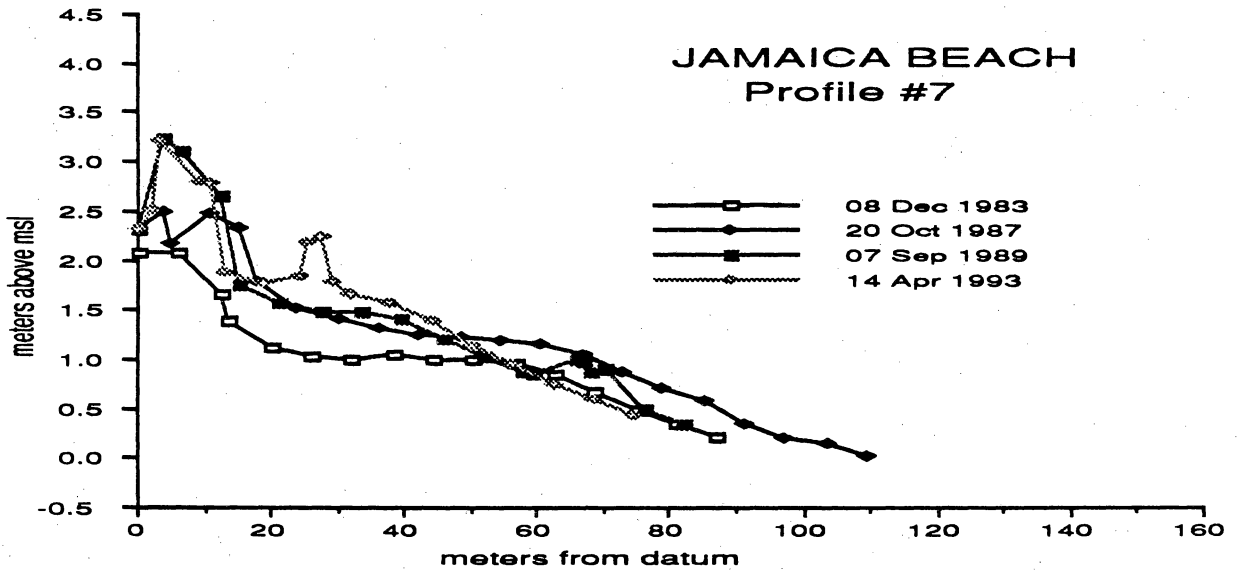
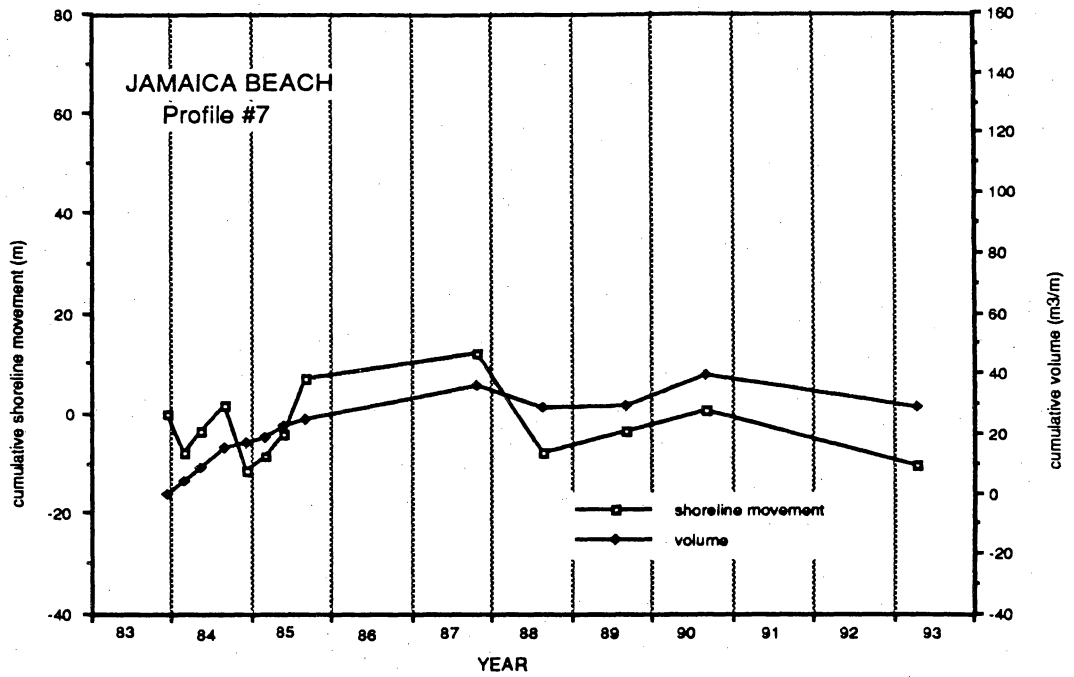


Figure 5 - Shoreline movement, profile volume change, and selected profiles for beach profile 7, location shown in figure 2. Shoreline used is mean-sea level. Volume calculated above mean-sea level and seaward of a point about five meters landward of the foredune.

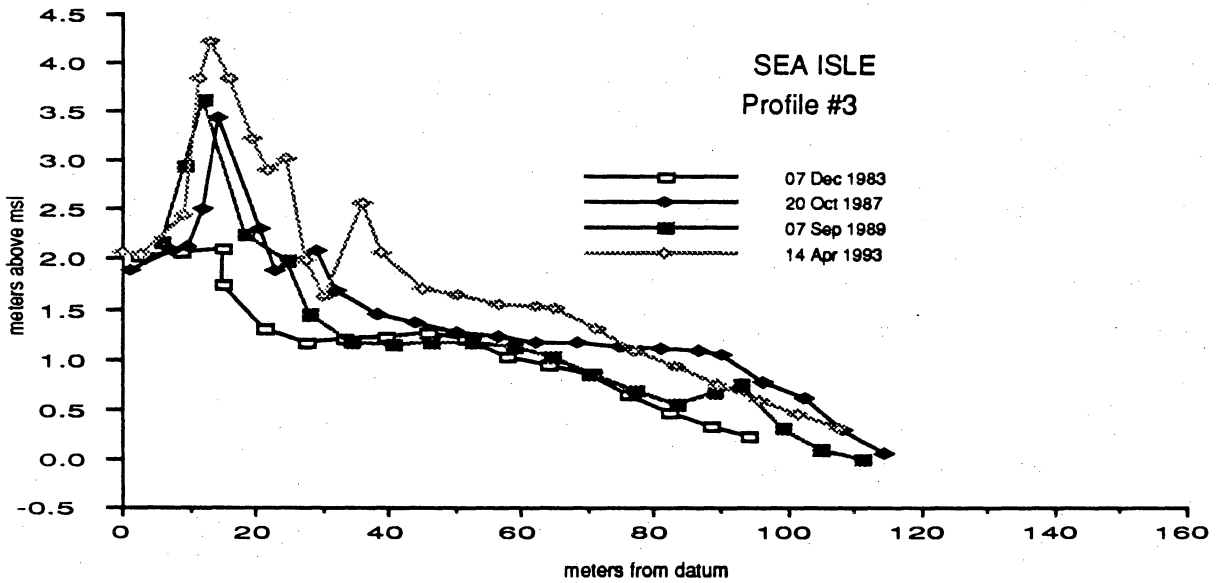
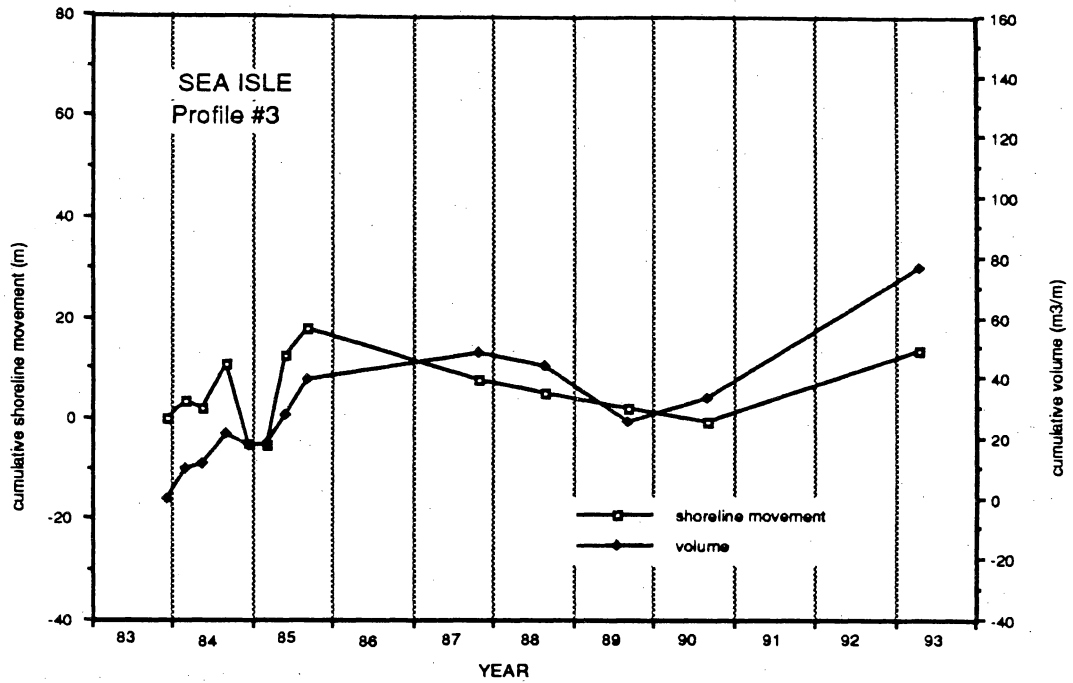


Figure 6 - Shoreline movement, profile volume change, and selected profiles for beach profile 3, location shown in figure 2. Shoreline used is mean-sea level. Volume calculated above mean-sea level and seaward of a point about five meters landward of the foredune.

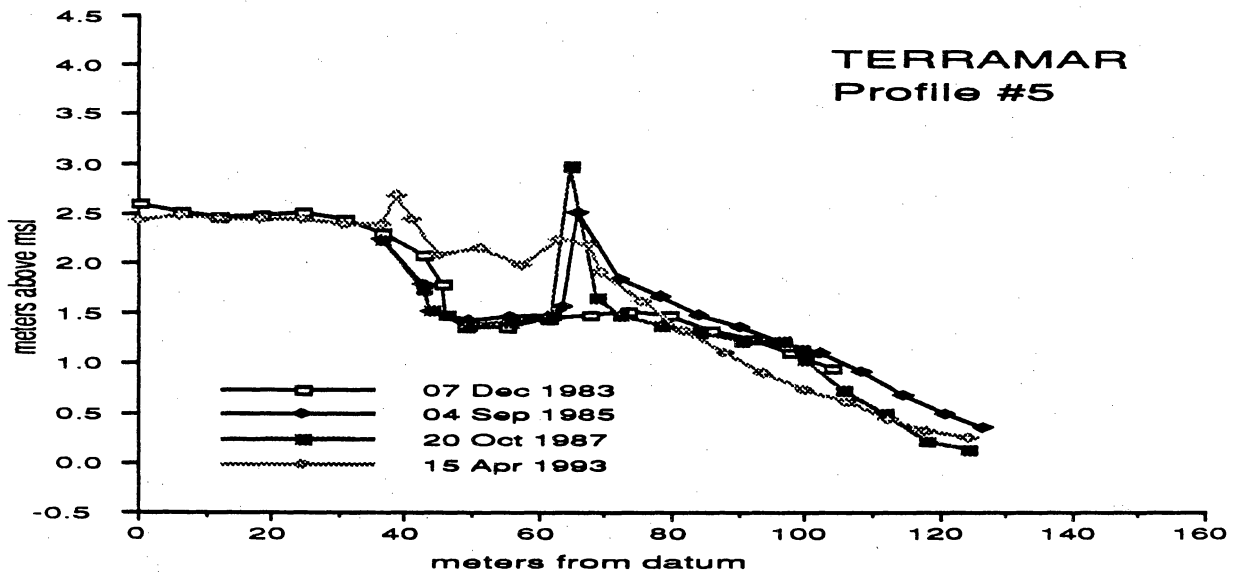
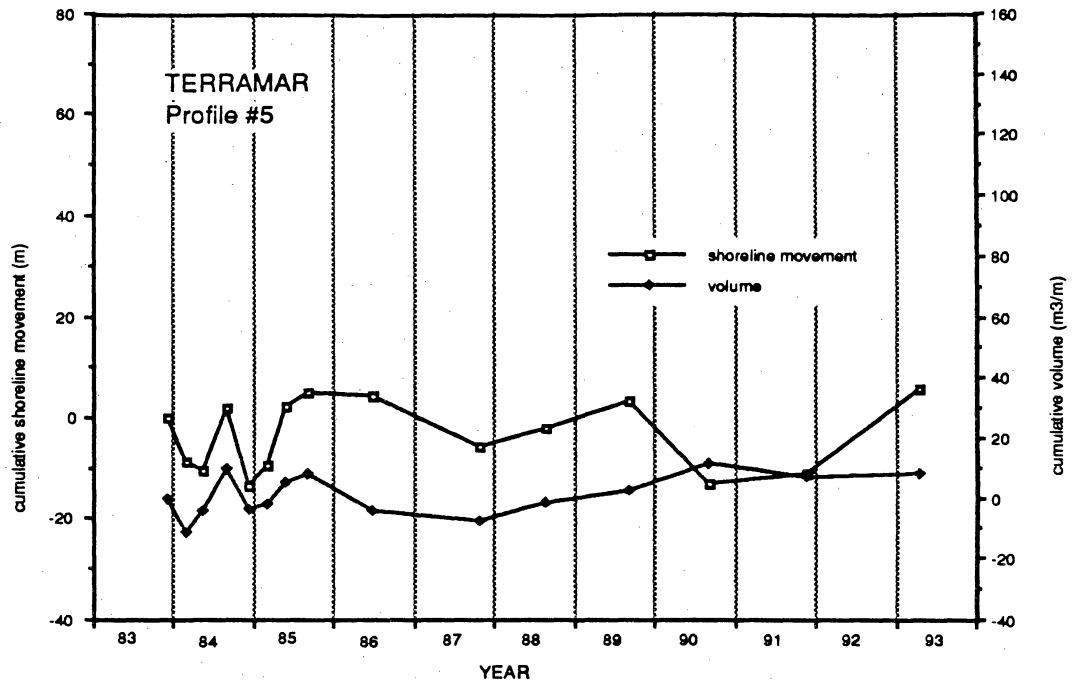


Figure 7 - Shoreline movement, profile volume change, and selected profiles for beach profile 5, location shown in figure 2. Shoreline used is mean-sea level. Volume calculated above mean-sea level and seaward of a point about five meters landward of the foredune.

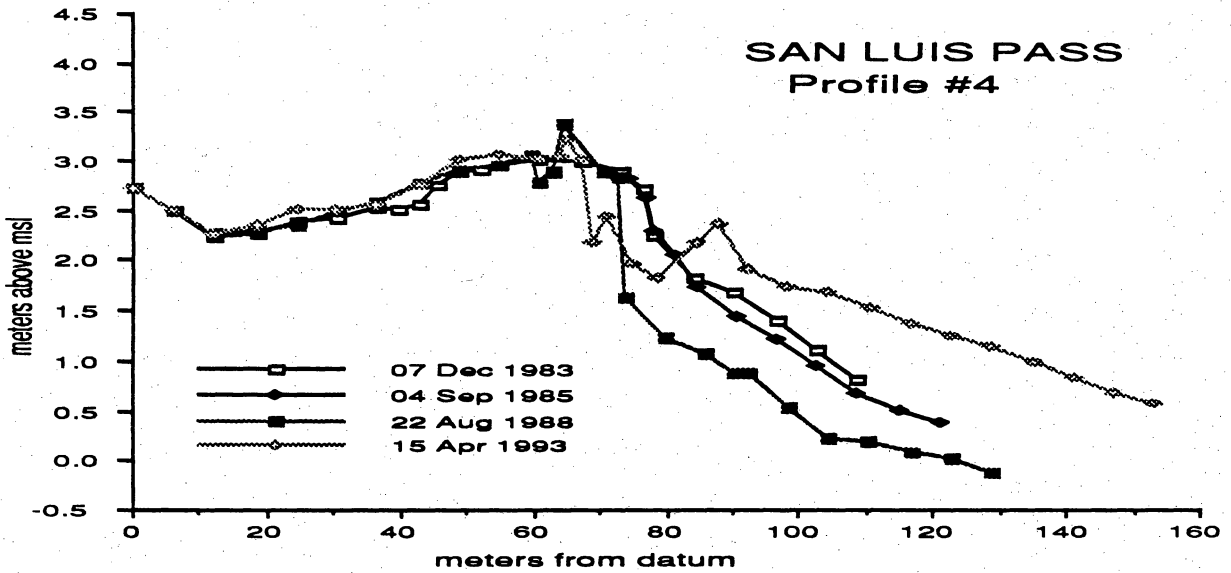
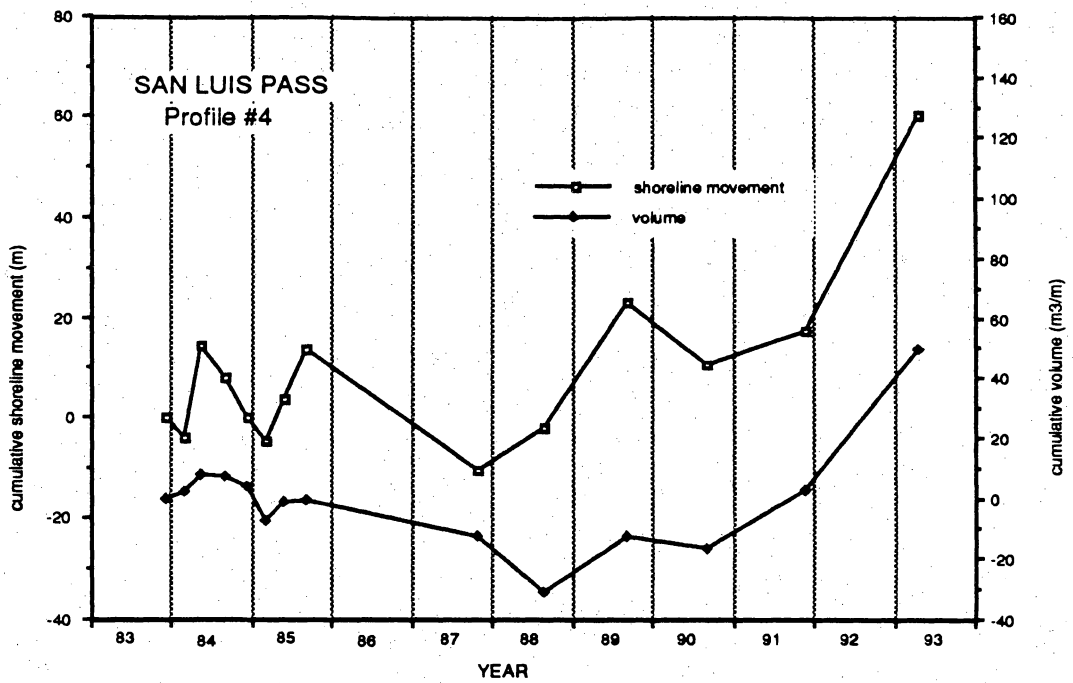


Figure 8 - Shoreline movement, profile volume change, and selected profiles for beach profile 4, location shown in figure 2. Shoreline used is mean-sea level. Volume calculated above mean-sea level and seaward of a point about five meters landward of the foredune.

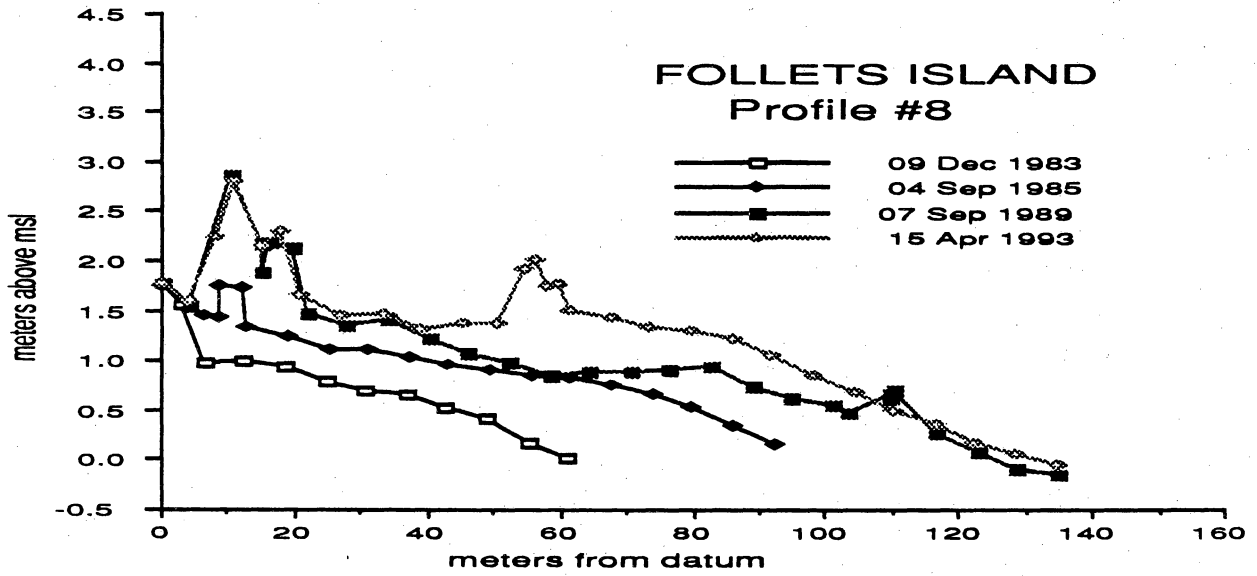
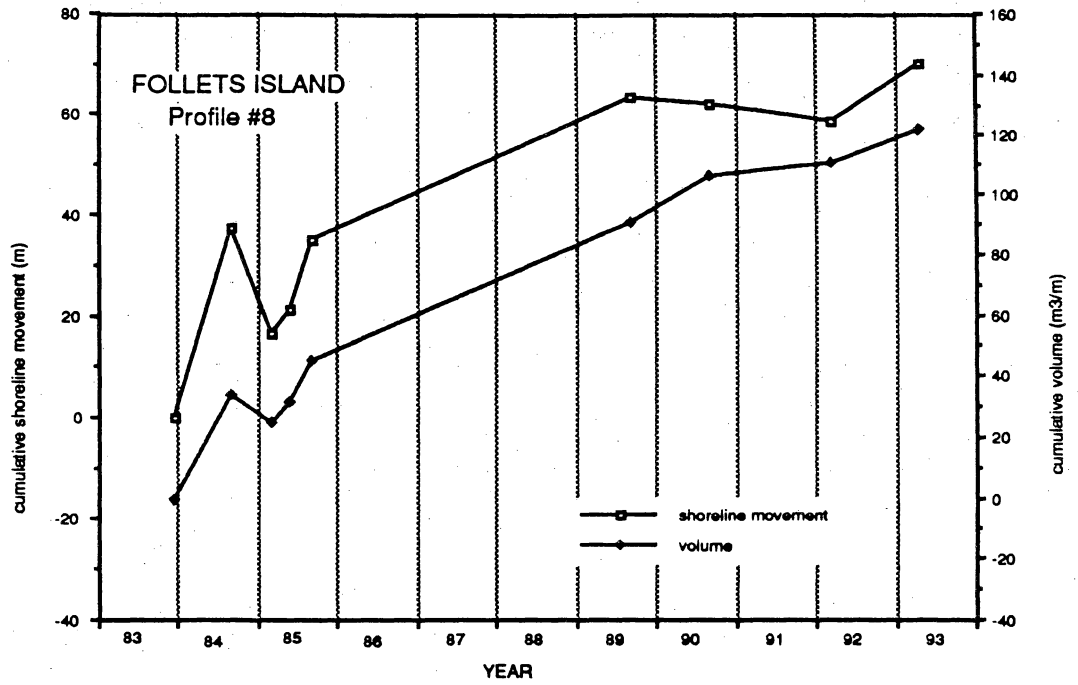


Figure 9 - Shoreline movement, profile volume change, and selected profiles for beach profile 8, location shown in figure 2. Shoreline used is mean-sea level. Volume calculated above mean-sea level and seaward of a point about five meters landward of the foredune.

## ADDENDUM 6

### LARGE-SCALE TRANSFER OF SAND DURING STORMS: IMPLICATIONS FOR MODELING AND PREDICTION OF SHORELINE MOVEMENT

Robert A. Morton, Jeffrey G. Paine, and James C. Gibeaut  
Bureau of Economic Geology  
The University of Texas at Austin

Updrift beach and shoreface erosion are components of the sediment budget equation that are difficult to quantify because much of the dynamic profile is subaqueous and seldom is the depth of closure reached during surveying. Beach and dune erosion is becoming a more important source of sand to stabilize downdrift beaches as the primary sand sources such as rivers, offshore bars, and tidal deltas are depleted or artificially reduced. Large-scale stability of the shore is partly controlled by intense storms that transport large volumes of sand moderate distances in brief periods. During these events, the balance of sand supply to nearby beaches is dramatically altered. Because of the temporary imbalances in sand supply, it is difficult to predict the post-storm location of erosion or deposition or to anticipate the volumes of sediment involved. Consequently, the ability to predict future shoreline positions based on short-term data may be seriously impaired.

In 1983, during Hurricane Alicia, more than 2 million m<sup>3</sup> of sand was stripped from the beaches and dunes along 40 km of western Galveston Island and northeastern Follets Island, Texas. Within 2 years after the storm, about 60% of the sand eroded from Galveston Island could be accounted for in washover deposits and sand returned to the beach in the form of beach aggradation and dune reconstruction. The remaining sand was considered to be either deposited on the inner shelf and lost from the littoral drift system or transported to the southwest by storm currents and deposited on the shoreface. Sedimentological studies of the inner continental shelf conducted immediately after the storm suggested that most of the subaqueous sand was still on the shoreface and not on the inner shelf. Beyond this inference, there were no data regarding the location of the former beach sand and its alongshore distribution.

Comparison of post-storm beach profiles and aerial photographs of Galveston and Follets Island since 1983 show a range of beach responses including continuous erosion, partial recovery and stability, and continuous accretion. The site of continuous accretion (Follets Island) is where the storm-emplaced shoreface sand has been transported onshore for the past nine years. This site is located between 10 and 20 km southwest from the areas

of maximum beach erosion. Before Hurricane Alicia, the beach of Follets Island was stable (short term) to moderately erosional (long term) depending on the length of historical record analyzed. Since Alicia, the beach of Follets Island has accreted more than 60 m and aggraded between 0.75 and 1.4 m.

The rapid large-scale alongshore transfer of sand during the storm and the prolonged systematic onshore transport of sand from the shoreface to the beach are poorly understood. Nevertheless, if numerical models and predictive capabilities are to improve, then shoreline movement at the myriameter spatial scale and decadal temporal scale must be resolved.

## ADDENDUM 7

### BEACH MORPHOLOGY AND VOLUMETRIC CHANGES DETERMINED WITH GPS KINEMATIC SURVEYS

Roberto Gutierrez and Robert A. Morton  
Bureau of Economic Geology  
The University of Texas at Austin

#### INTRODUCTION

The objectives of this task are to 1) accurately measure coastal topography within a precise, global reference frame, 2) use these measurements to describe beach morphology, and 3) use changes in beach morphology over time to characterize the sediment gain or loss in the study area. In order to accomplish these objectives, geodetic surveys using Global Positioning System (GPS) technology were conducted in November, 1991 and April, 1993 of the beach at Galveston Island State Park, Texas (fig. 1). GPS techniques allow a very large number of control points to be rapidly and precisely surveyed over a large area with respect to a standard reference ellipsoid.

GPS kinematic surveys have been able to map in detail the entire state park beach. Comparisons between the 1991 and 1993 surveys reveal differences in beach morphology, and a loss in total sand volume of about  $1 \text{ m}^3$  per meter of beach front.

#### Survey Procedure

During 1991, both fully kinematic surveys of the entire beach area and stop-and-go kinematic surveys of selected shore-normal beach profiles were conducted (Morton et al, 1993). However, in 1993 only fully kinematic surveys of the study area were conducted. In a fully kinematic survey (henceforth referred to as simply a kinematic survey) two GPS receivers record data simultaneously. One GPS receiver remains stationary over a reference point whose geodetic latitude, longitude, and height are precisely known. The second receiver is free to move while recording data. A kinematic GPS survey requires an initialization or indexing period in order to resolve the L1 and L2 carrier phase cycle ambiguities. The carrier phase cycle ambiguity is the integer number of cycles of carrier phase between the broadcasting GPS satellite and the GPS receiver. After the phase ambiguity is established at the beginning of a survey, it remains constant during the remainder of the survey provided the receiver maintains phase lock on the signal and is able to track the subsequent changes in carrier phase.



During indexing the stationary antenna is placed over the reference point while the mobile antenna is placed over an index point. The index point is the starting point of the survey and usually chosen within or near the survey area for convenience. Reference point to index point separation can range from a few meters up to about 10 km. Both antennas remain stationary over their respective marks for several hours until enough data has been collected to resolve the carrier phase ambiguities. If the reference and index points are within a few meters of each other, the antennas can be exchanged between these points to resolve the ambiguities (Remondi, 1985). This antenna swapping is accomplished in a few minutes, and was the method used to initialize each kinematic survey in 1991 and 1993.

After the antenna swap, the mobile receiver, still continuously recording data, is transferred onto a vehicle and its antenna mounted on the vehicle roof. The vehicle then drives over the study area collecting data. At the end of the survey the vehicle returns to the starting point, the mobile antenna is again placed over the index mark, and a second antenna swap is conducted. A position is then computed for the mobile antenna at each measurement time.

### Equipment

The equipment in both the 1991 and 1993 GPS surveys were two geodetic-quality GPS receivers: model 4000SST GPS receivers manufactured by Trimble Navigation. These are battery operated, 16 channel, dual-frequency, C/A-code receivers equipped with geodetic antennas with groundplanes to minimize signal multipathing. During the indexing portion of the GPS surveys both GPS antennas were mounted on standard surveyor's tripods and tribrachs, but during the actual data collection, one antenna was mounted atop a 4x4 vehicle using a commercial roof-rack modified by the BEG staff to support a tribrach. A 2 ft square section of microwave-absorbing foam was placed on the vehicle roof directly beneath the GPS antenna to reduce signal multipathing.

### 1993 GALVESTON ISLAND GPS SURVEY METHODS

GPS surveys were conducted on the 14 and 15 April (calendar days 104 and 105) of 1993 (GPS week 692) on Galveston Island State Park. The reference point used in the 1991 survey was reoccupied in 1993, but a new index point was established. The reference point was a concrete pillar in the state park headquarters' parking lot. The parking lot is landward of the barrier dunes and the reference point is stable relative to the beach itself. The index point was a 20 cm aluminum surveyor's pin driven into the ground 7.47 m NE of the reference point. Two kinematic surveys were conducted on the morning of day 104 and a third kinematic survey was

conducted on the morning of day 105. During all surveys data was collected at a one second sampling rate from all GPS satellites in view above 15° elevation. The number of satellites in view above 15° elevation varied between 5 to 7 and the Relative Dilution of Precision (RDOP) was generally  $\leq 3$  during these sessions. Before and after the surveys, antenna heights were measured above the reference and index points. Also, the mobile antenna was mounted on the 4x4 vehicle and the height from the antenna to ground level was measured (fig. 2).

In 1991 the kinematic surveys involved measuring a set of three shore-parallel beach profiles: along the backbeach, the berm crest, and the forebeach. In the 1993 re-survey we tried two different methods of kinematic beach surveying. A similar set of three shore-parallel beach profiles were measured during the first survey on day 104 (henceforth referred to as survey 104A). However, during the second survey on day 104 (survey 104B) and on day 105, the vehicle was maneuvered down the beach in a zig-zag pattern across the full beach width (fig. 3). This was a test to see if a zig-zag track was more efficient than a series of shore-parallel tracks. Unfortunately, the berm crest track in survey 104A did not coincide with the berm crest track in 1991; it ran unintentionally closer to the forebeach than in 1991 and missed parts of the mid-beach area.

GPS observations during survey 104A extended from 13:15 UTC to 15:25 UTC, with the data collection on the beach lasting an hour and twenty minutes. Observations for survey 104B extended from 15:58 UTC to 17:33 UTC, with the actual beach survey lasting an hour. On day 104, the survey area extended the entire length of the Galveston Island State Park beach; approximately 2 km in length. The survey on day 105 covered the state park beach plus an additional 4.6 km of non-park beach immediately adjacent to the park's southwest boundary. Observations for day 105 spanned from 13:35 UTC to 15:16 UTC, with over an hour of data collection on the beach.

Weather during day 104 was not optimal. Strong seaward winds (about 25-30 mph) saturated the near-surface atmosphere in the beach area with spray causing heavy mist-like conditions. Scattered rain showers also moved through the area during the GPS observation sessions. The strong seaward winds created heavier than normal surf conditions which made surveying on the forebeach difficult. The water level rose significantly during observations, washing out the forebeach survey flags, and eventually caused the early end of survey 104B. On day 105 the wind direction shifted to landward, and beach and weather conditions were significantly improved.

In a kinematic survey it is important to maintain continuous carrier phase lock on all the GPS satellites in view. During survey 104A, continuous phase lock on L1 and L2 was maintained for all satellites. However, during survey 104B and the survey on day 105, difficulty was encountered in maintaining phase lock on L2 for satellites at the lower elevations. Rapid

changes in antenna velocity caused by the zig-zag vehicle motion may have induced the loss of lock since these events occurred most commonly during vehicle turns. The use of full P-code GPS receivers could have reduced the number of L2 cycle slips, but they were not available.

### Data Reduction

GPS survey data was reduced on a desktop computer using the OMNI software developed by the National Geodetic Survey (NGS) (Mader, 1986). Both L1 and L2 carrier phase and C/A pseudorange were observed during the kinematic surveys, but the carrier phase observations rather than the pseudoranges were used to compute the solutions because of the requirement for centimeter level vertical precision. Prior to estimating a solution, data were edited, cycle slips fixed, and the antenna swaps were used to estimate the initial phase ambiguities. Once the ambiguities were estimated to within 2% of full integer values, the L1 carrier phase solutions were estimated for the mobile antenna position at each epoch. L1 phase solutions were estimated because, over a relatively small survey area (<100 km), ionospheric effects are minimal and a single-frequency solution is generally as accurate as an ionospherically-corrected solution.

OMNI produces an independent solution for position of the mobile antenna's phase center with respect to the reference point at each measurement epoch. The reference frame for the OMNI solution is an earth-fixed, cartesian coordinate system with the origin at the earth's center of mass and the Z-direction parallel to earth's mean rotational axis. Preliminary solutions have been estimated for the two surveys conducted on day 104 in 1993. However, the data processing for day 105 survey is currently at an intermediate stage. Also, a solution has been recomputed for the survey conducted on day 319 of 1991. This was done so that beach comparisons between 1991 and 1993 would be based on solutions that were as consistent as possible in terms of data processing.

No GPS satellite maneuvers are indicated for days 104 and 105, however satellites PRN18, PRN26, and PRN29 were in earth eclipse during portions of those days. Comparing the GPS broadcast message with precise ephemerides computed by the Jet Propulsion Laboratory shows large differences between the broadcast and JPL ephemerides for satellites PRN31, PRN18, and PRN29. The largest differences were for satellite PRN29: 84.7m on day 104 and 74.7m on day 105 (Zumberge et al, 1993). An approximate relationship between orbit error and baseline error is

$$\frac{\|db\|}{b} = \frac{\|dr\|}{\rho}$$

where db is the baseline error, dr is the satellite position error, b is the baseline length and  $\rho$  is the range to the satellite (Wells et al, 1987). For a GPS satellite error of 85 m at an altitude of

20000 km and a baseline of 2km, the potential baseline error is about 0.01 m. The height accuracy is worse than the baseline accuracy by a factor of 2 or more, therefore the maximum potential height error is 0.02 m. To minimize orbit error, precise ephemerides for day 104 were obtained from the Scripps Institution for Oceanography and were used during data editing and the solution estimation. The Scripps ephemerides were used because the available JPL ephemerides did not include PRN22, a satellite observed on day 104.

It was discovered during processing that the solution quality for day 104 improved significantly if data from satellites at the lower elevations ( $\leq 25^\circ$ ) were deleted whenever possible. Signal multipathing could have contributed to the noise level for these satellites, however large, time-variable tropospheric effects due to rainstorms and sea spray could also be a factor. The difficulties of high precision GPS surveying in coastal areas is documented, but not fully understood (Dixon et al, 1991). A water vapor radiometer was not used during these surveys, therefore a direct measurement of the wet tropospheric path delays for the GPS signals is not available.

The accuracy of the solutions was assessed by the survey closure. Repeat passes over the same survey points agreed at the centimeter level. Index point solutions were precise at the sub-centimeter level except for the second antenna swap at the end of survey 104A. Because of data editing toward the end of survey 104A, the RDOP rose well above 3 and solution accuracy suffered. This small portion of the solution was not used in the subsequent beach analysis, and the processing problem should be overcome in the final 104A solution.

### Data Analysis

The OMNI solutions were transformed from cartesian coordinates into latitude, longitude, and height with respect to the World Geodetic System 1984 reference ellipsoid (WGS-84). All heights discussed below are heights above the WGS-84 ellipsoid, and not elevations above mean sea level. Geodetic latitude and longitude were converted into Universal Transverse Mercator coordinates so that meters would be the common unit for the data in both the horizontal and vertical planes. This is required for volumetric calculations.

Topographic maps of the beach were generated for day 319 and day 104 by using CPS-1 (Radian Corporation) to interpolate the data onto a uniform grid and then contour the resulting array (figs. 4 and 5). The data from surveys 104A and 104B were combined to construct the topographic map for day 104 (fig. 5). This was done because survey 104A missed large parts of the berm crest area, and survey 104B tended to undersample the backbeach and forebeach.

A set of shore-parallel profiles were constructed from the gridded surfaces for day 319 and day 104 (fig. 6). The profile lines were selected to coincide with the day 319 survey tracks, and

illustrate the variation in height along the backbeach, the berm crest, and the forebeach (fig. 6). In addition, the gridded surface array for day 104 was subtracted from the gridded surface for day 319, and the resulting difference array was contoured by CPS-1 (fig. 7).

## Results

Comparing the maps for day 319 and 104 reveals that the orientation and width of the beach has not changed during the intervening two years. Of the three beach regions (forebeach, berm crest, and backbeach), the backbeach shows the least change from 1991 to 1993. There is no significant height change along the profile, and many small scale features present in 1991 are still recognizable in 1993. The only major change in the backbeach is the deepening of several channels or gullies. Three erosional channels are present in 1991 and by 1993 these channels have all increased in depth by 10 to 20 cm. In 1991 the backbeach showed a gradual increase in height from 2.1 m in the northeast to 2.2 m in the southwest. In 1993 this SW to NE slope is still evident.

The beach berm in 1991 and 1993 are very dissimilar. Day 319 shows a distinct berm crest dividing a steeper forebeach from gentler sloping backbeach. The beach on day 104 has no well defined berm crest and the slope is relatively uniform across the width of the beach. On day 104, the beach height along the berm is consistently 10 to 20cm lower than on day 319. The erosional channels on the backbeach, which are not present on the berm on day 319, have extended themselves out into the berm area by day 104.

The beach berm on day 319 and 104 slopes from SW to NE like the backbeach. In addition to the slope, the berm profile on day 319 varies rhythmically in height 5-8 cm over a spatial wavelength of roughly 360 m. Superimposed on this long wavelength are smaller 2-3 cm height variations that are semi-regularly spaced 10-30 m apart. In contrast, the berm profile on day 104 is more purely sinusoidal than in day 319. It has few of the smaller scale variations present on day 319, but this may be due to sparser sampling in this area during day 104. The berm on day 104 is dominated by a sinusoidal variation with a wavelength of about 40 m and an amplitude of 7 to 10 cm.

The SW-NE slope evident in the backbeach and berm is not present on the forebeach. The forebeach profiles are similar in appearance to the beach berm profiles for their respective days. The forebeach on day 319 has the same rhythmic variation as the berm. The variations are in phase with the berm, but the amplitude is 1-2 cm larger. On day 104, forebeach height variations are also in phase with the berm. Like the berm, they are sinusoidal with a wavelength of about 40m and an amplitude of 5cm. On the topographic map for day 104 (fig. 5), the berm and forebeach height variations resolve themselves in a distinct cusp pattern.

The array created by differencing the gridded surfaces for day 319 and day 104 was numerically integrated by the CPS-1 software to estimate the net change in sand volume. The numerical integration method estimates a positive and negative volume with the net volume simply being their sum. The positive volume was about 2,000 m<sup>3</sup> over 50,700 m<sup>2</sup> of beach while the negative volume was about 4,200m<sup>3</sup> over 58,100 m<sup>2</sup>. The net volume difference between days 319 and 104 is -2,200 m<sup>3</sup>. These values are somewhat biased because the interpolation algorithms used in creating the gridded surface extends data trends out into grid areas where no data exists. However, CPS-1 provides a good first approximation. Obviously the sand loss occurred selectively over the beach, and reflects the absence of a distinct berm crest and the presence of the beach cusps on day 104 (fig. 7).

The accuracy of comparing the GPS surveys was independently checked by comparing shore-normal beach profiles (fig. 8) measured in 1991 and in 1993 at the same time as the GPS surveys. Superimposing the beach profiles, taken at the northeastern end of the State Park, shows that the forebeach and backbeach were slightly elevated in 1993 compared to 1991, whereas the berm crest present in 1991 was planed off. Thus the beach profiles confirm the redistribution of sediment recorded by the GPS surveys and the minor net loss of sediment from the beach profile associated with erosion of the berm crest.

## DISCUSSION

With only two surveys spaced 17 months apart it is difficult to assess the significance of changes in beach morphology and sand volume. Do these changes reflect a permanent sediment loss, a seasonal fluctuation in beach configuration, or merely day to day variations in beach conditions? The small volume involved suggests that the net loss simply reflects temporary erosional conditions due to the weather on day 104. What is significant is that small volume changes can be detected over large areas of beach, and directly related to relatively subtle changes in beach topography.

The 1991 GPS survey on Galveston Island demonstrated the feasibility of kinematic GPS surveying as a tool in coastal research. This 1993 resurvey demonstrates the long-term repeatability of the technology: independent groups operating under different conditions can resurvey a large area with consistent levels of accuracy. The different kinematic strategies (zig-zag vs. shore-parallel tracks) did not work as well as it was hoped; each method tended to under sample some area of the beach. The survey methodology requires further refinement, and new technology needs to be adopted (e.g. full P-code receivers). Never the less, the overall concept of kinematic GPS as a tool to precisely monitor coastal processes has been validated.

## RECOMMENDATIONS FOR FUTURE GPS RESEARCH

Numerical models used to predict future shoreline positions and coastal land loss are limited by a lack of accurate volumetric time-series measurements of nearshore deposition and erosion. The physical monitoring of dynamic coastal and marine environments is also hindered because datum differences are commonly encountered when land-based topographic surveys and sea-based bathymetric surveys are integrated. Also, observed changes between nearshore surveys can be caused by actual sediment flux or they can be an artifact of comparing data collected along profiles having positions different from those previously surveyed. Additional research is needed to develop more accurate methods used to directly measure changes in nearshore environments and to improve platform positioning, which is critical for precise repeat surveys. This can be accomplished by developing real-time kinematic differential GPS techniques, which have the potential to eliminate or to greatly reduce datum differences and reoccupation errors in repeated nearshore surveys. Field studies can also be designed to evaluate (1) the effects of antenna motion and coastal weather on the GPS signal-to-noise ratio and (2) field sampling designs that should increase the density of topographic and bathymetric data while also improving efficiencies of data collection. With slight modifications and improvements, the new methods could become the standard used by scientists and engineers to monitor and accurately quantify changes in nearshore environments. Results of this research could also lead to greatly improved three-dimensional models of coastal sediment flux.

### Description Of Research

Coastal and marine environments are dynamic regions that can change shape rapidly as a result of complex physical forces. Beaches retreat instantaneously and then rebuild after storms, variable waves and currents create and then destroy submerged shoals and bars, tidal inlets migrate and their associated tidal deltas expand or contract depending on sediment supply. To effectively monitor and to model these nearshore changes, accurate measurements of the land surface and sea floor are needed that can be related to the active physical processes. A major weakness of existing deterministic models of coastal response is that the models lack sufficient quantitative data regarding short-term sediment flux in the nearshore zone.

At present, nearshore sediment dynamics are monitored using either land-based or sea-based surveying methods. These independently conducted surveys record topography and bathymetry that are supposedly corrected to the same datum (mean sea level), but invariably datum difficulties are encountered when the two surveys are merged to reveal nearshore sediment movement. Also, it is presently impractical to collect subaerial and subaqueous morphological

data of sufficient density and resolution to satisfy a three-dimensional sediment flux model of long segments of the coast.

The challenge to coastal and marine scientists and engineers is to devise new nearshore monitoring methods that address these needs but at the same time are rapid, reliable, and relatively inexpensive. Furthermore, the new monitoring techniques should maintain or improve existing measurement accuracy. A promising response to this challenge is the adaptation of Global Positioning System (GPS) surveying techniques to monitor coastal and marine environments.

Differential kinematic GPS surveys are designed for rapid, centimeter level positioning on continuously moving platforms (vehicles, planes, and boats) where the platform trajectory and positions of data collected from the platform are of interest. The density of computed positions is determined by the speed of the platform and the sampling rate of the receiver. Results of our previous differential kinematic surveys (Morton et al., 1993) demonstrate that GPS surveys (1) provide the same precision as conventional land surveys, (2) are repeatable at the 1-2 cm level even in the vertical dimension, and (3) provide much denser spatial control than conventional surveys so that the surface being measured is more accurately represented by the field data. This greater spatial resolution means that accurate two-dimensional land and sea-floor surfaces can be generated rapidly by the GPS surveys rather than the conventional one-dimensional beach or bathymetric profiles.

### Research Objectives

The objectives of the proposed GPS research are to eliminate or to greatly reduce the sources of error in repeated nearshore surveys. This can be accomplished by (1) eliminating the need for permanent survey markers, (2) increasing the spatial distribution and density of positioning data without significantly increasing the time or cost of surveying, and (3) minimizing differences in the positions of subsequent survey transects. We can achieve the first two objectives without real-time positioning, but the third objective depends entirely on precise real-time navigation so that course bearings and positions during subsequent surveys are essentially identical to those of the previous surveys. Other important research objectives include evaluating if the signal-to-noise ratios of the GPS data are effected adversely by (1) rapid accelerations and decelerations of the GPS antenna (quick vehicle turns) or (2) atmospheric conditions (wind and humidity) in the turbulent boundary layer at the coast. The GPS approach to data collection will also provide information on shore-parallel (alongshore) sediment transport that is presently undetected by conventional shore-normal transects.



If a GPS monitoring system is used for both subaerial and subaqueous positions, datum problems encountered when merging land-based and sea-based surveys will be eliminated. Furthermore, apparent differences in bathymetry between surveys caused by fluctuations in water level (wave climate and tide stage) can be compensated directly and more accurately using GPS than by extrapolation of water levels from a distant tide gauge.

Results of the proposed GPS research will be applicable to diverse monitoring activities that require accurate reoccupation of positions such as aerial video surveys from helicopters, bathymetric surveys from boats, tracking oil spills, relocating sampling stations for water quality and sediment contamination studies, and coastal damage assessments where pre-storm and post-storm surveys are compared.

#### REFERENCES

- Dixon, T. H., G. Gonzales, S. M. Lichten, and E. Katsigris, 1991, First epoch geodetic measurements with the Global Positioning System across the northern Caribbean Plate boundary zone: *Journal of Geophysical Research*, v.96, p.2397-2415.
- Mader, G. L., 1986, Dynamic positioning using GPS carrier phase measurements: *Manuscripta Geodetica*, v.11, p.272-277.
- Morton, R.A., M. P. Leach, J. G. Paine, and M. A. Cardoza, 1993, Monitoring beach changes using GPS surveying techniques: *Journal of Coastal Research*, v.9, p.702-720.
- Remondi, B. W., 1985, Performing centimeter-level surveying in seconds with GPS carrier phase: initial results: *Journal of the Institute of Navigation*, v.32, p.194-208.
- Wells, D., N. Beck, D. Delikaraoglou, A. Kleusberg, E.J. Krakiwsky, G. Lachapelle, M. Nakiboglu, R.B. Langley, K.P. Schwartz, J.M. Tranquilla, and P. Vanícek, 1987, *Guide to GPS Positioning*: Canadian GPS Associates, Fredericton, N. B.
- Zumberge, J. F., G. Blewitt, M. B. Heflin, D. C. Jefferson, and F. H. Webb, 1993, JPL Analysis Report (week 692): *International GPS Service Electronic Report*, Message no. 262.

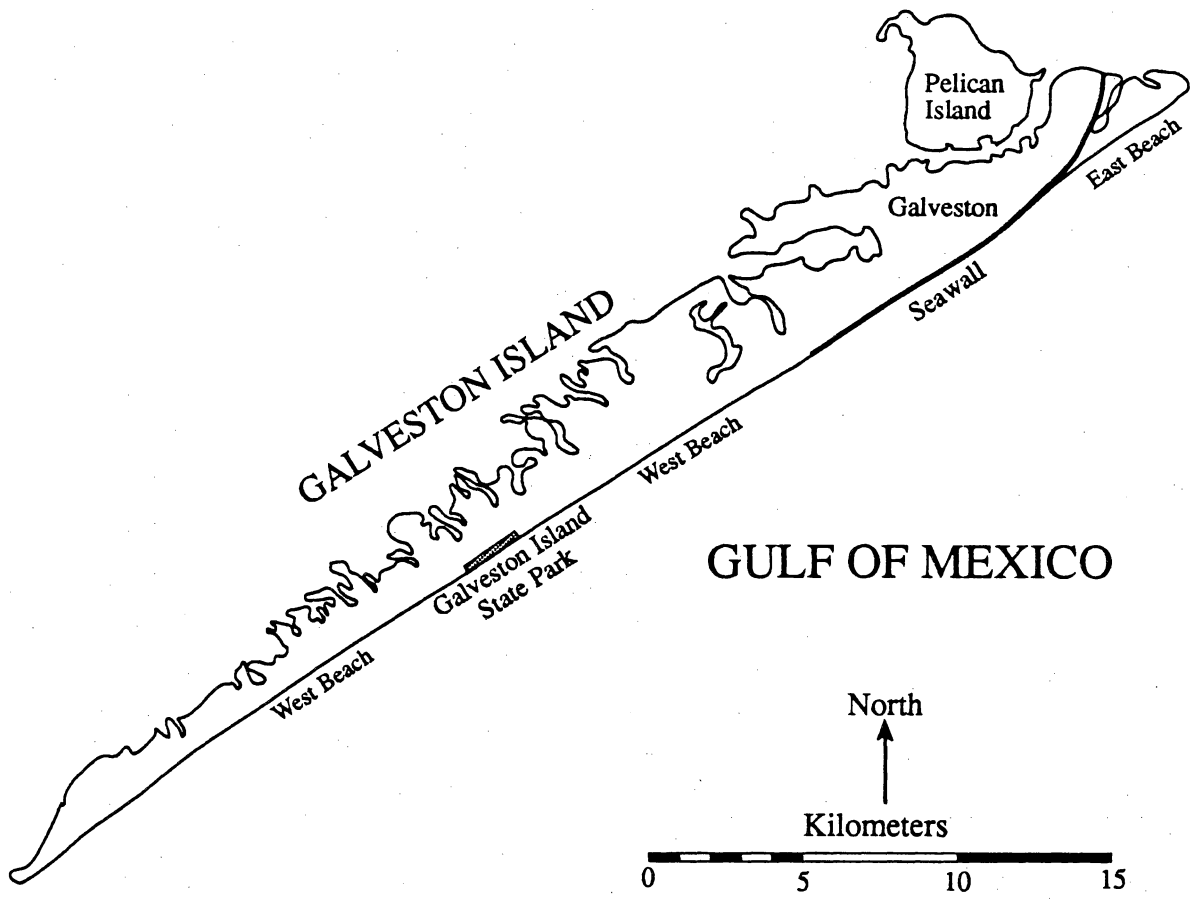


Figure 1. Outline of Galveston Island showing the location of the Galveston Island State Park, site for the 1991 and 1993 GPS surveys. The park beach is the shaded area on the West Beach portion of the island.

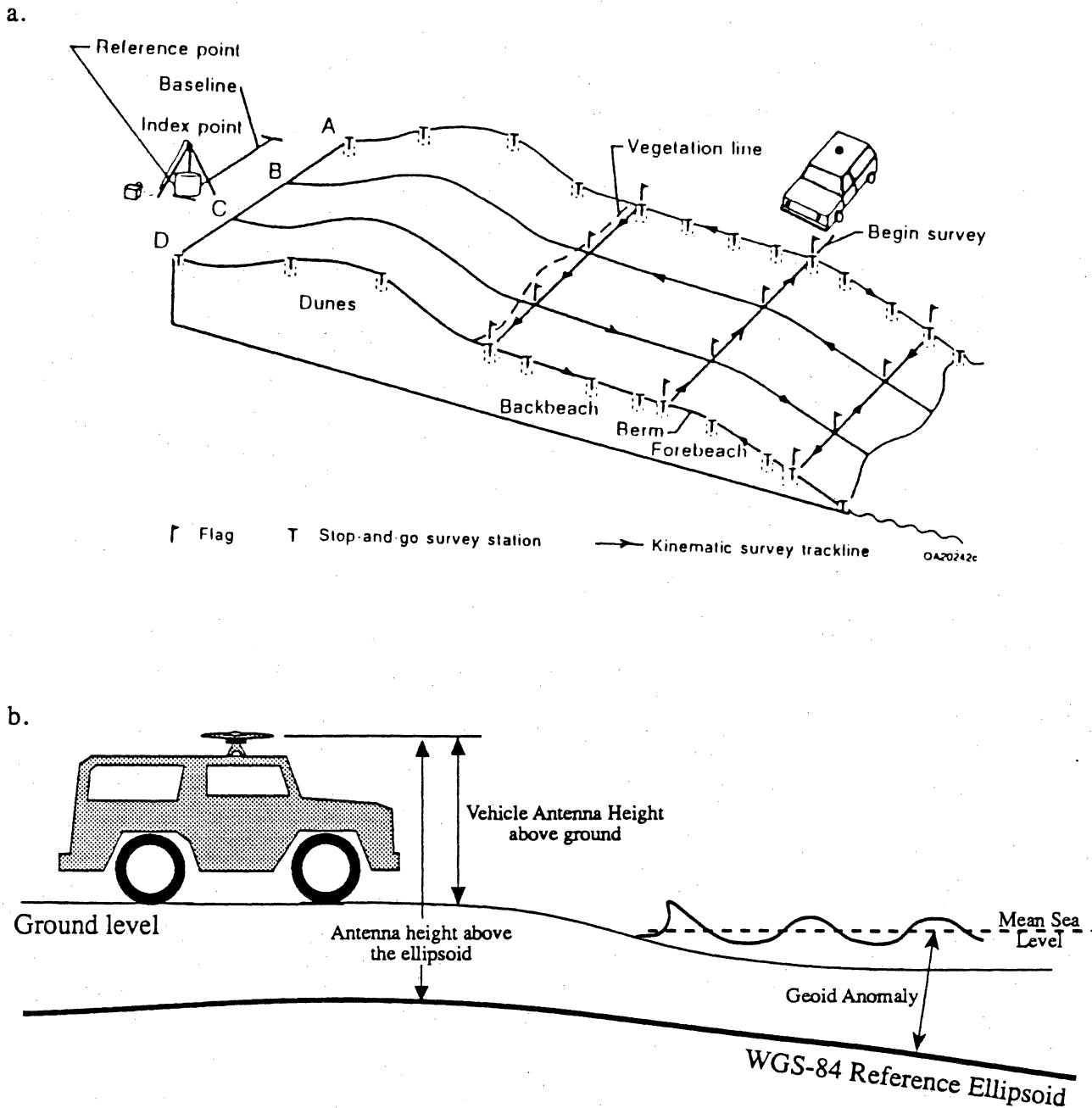


Figure 2.

a. A general layout of the beach, dunes, and the GPS stations is shown. Reference and Index points were adjacent to the beach, just landward of the dunes. Survey flags were used as driving markers during the survey. Drawing not to scale.

b. Cartoon illustrating the measurement model for the kinematic survey. The mobile antenna was mounted on the roof of a 4x4 vehicle. OMNI estimated the position of the antenna above the WGS-84 ellipsoid at each measurement time. Converting antenna height above the ellipsoid into beach height above the ellipsoid meant simply subtracting the vehicle antenna height above ground. Ellipsoid height is not equivalent to height above mean sea level. However, ellipsoid height can be adjusted for the local geoid anomaly to provide an estimated height above mean sea level.

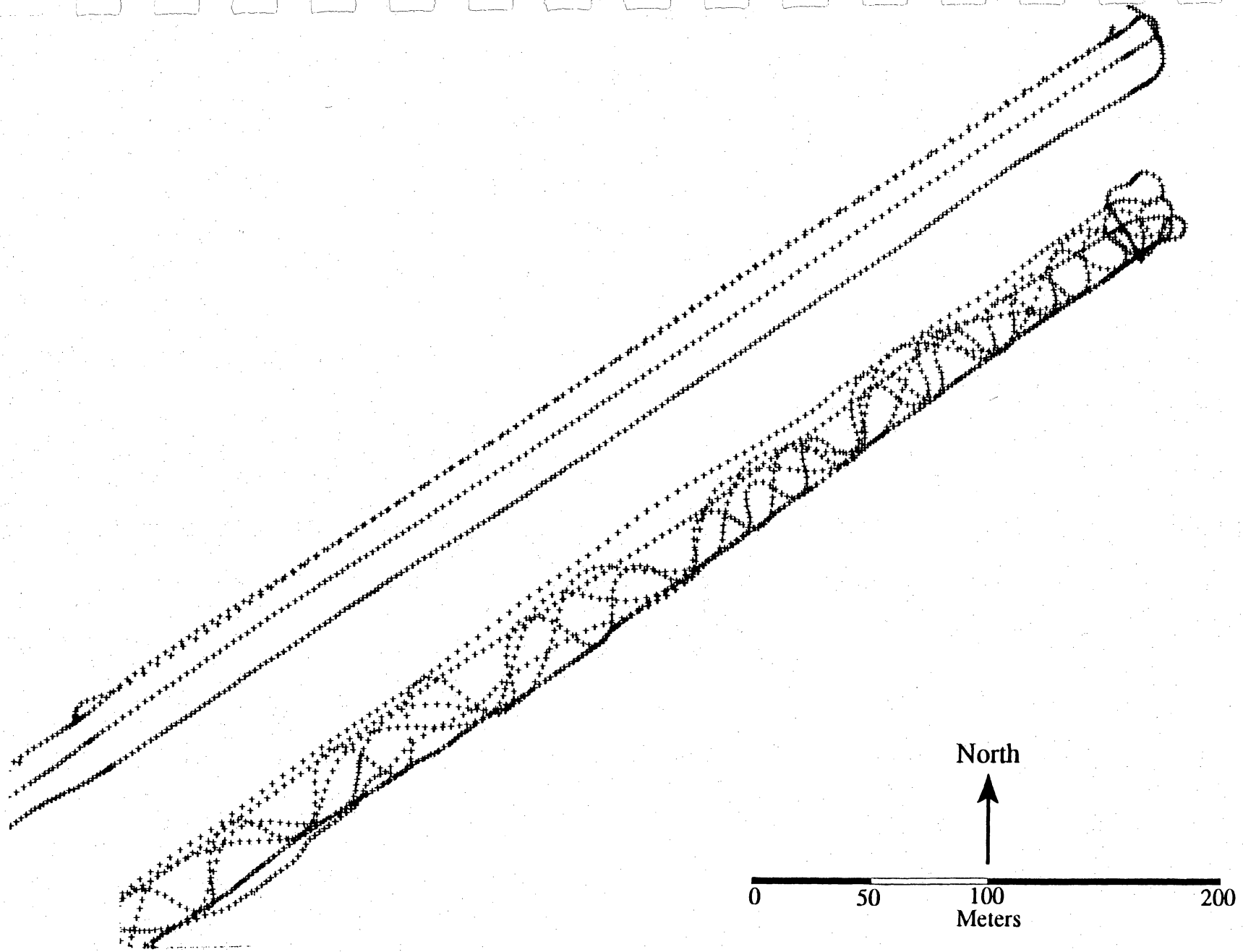


Figure 3. Vehicle ground tracks on day 319, 1991 and day 104, 1993. Symbols (+) show location of individual data points. On day 319 a set of shore-parallel tracks were driven along the backbeach, berm crest, and forebeach. On day 104 both shore-parallel and zig-zag patterns were driven.

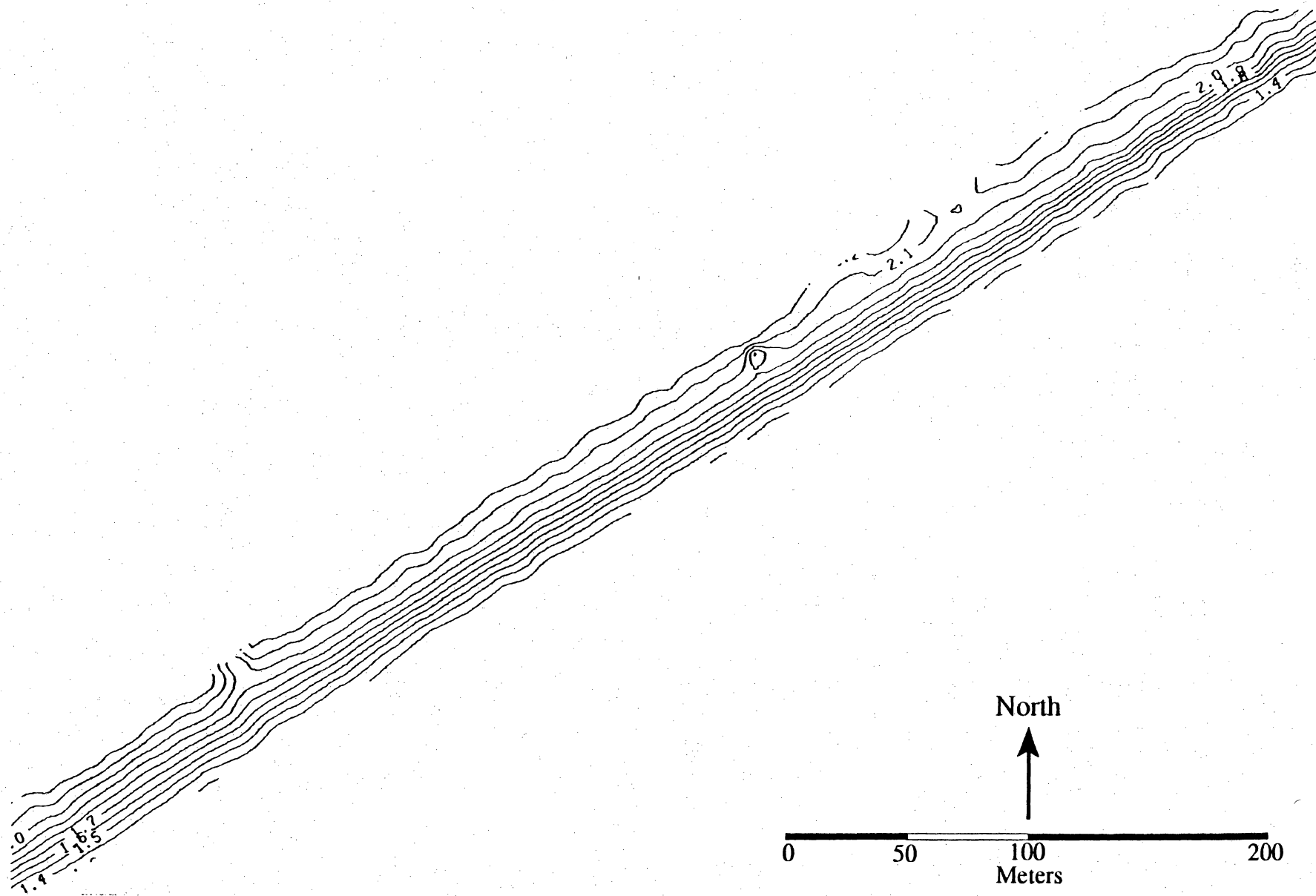


Figure 4. Topographic map of the northeast portion of Galveston Island State Park beach on day 319, 1991. The contour interval is 0.1 m and the horizontal scale is 60m/inch.

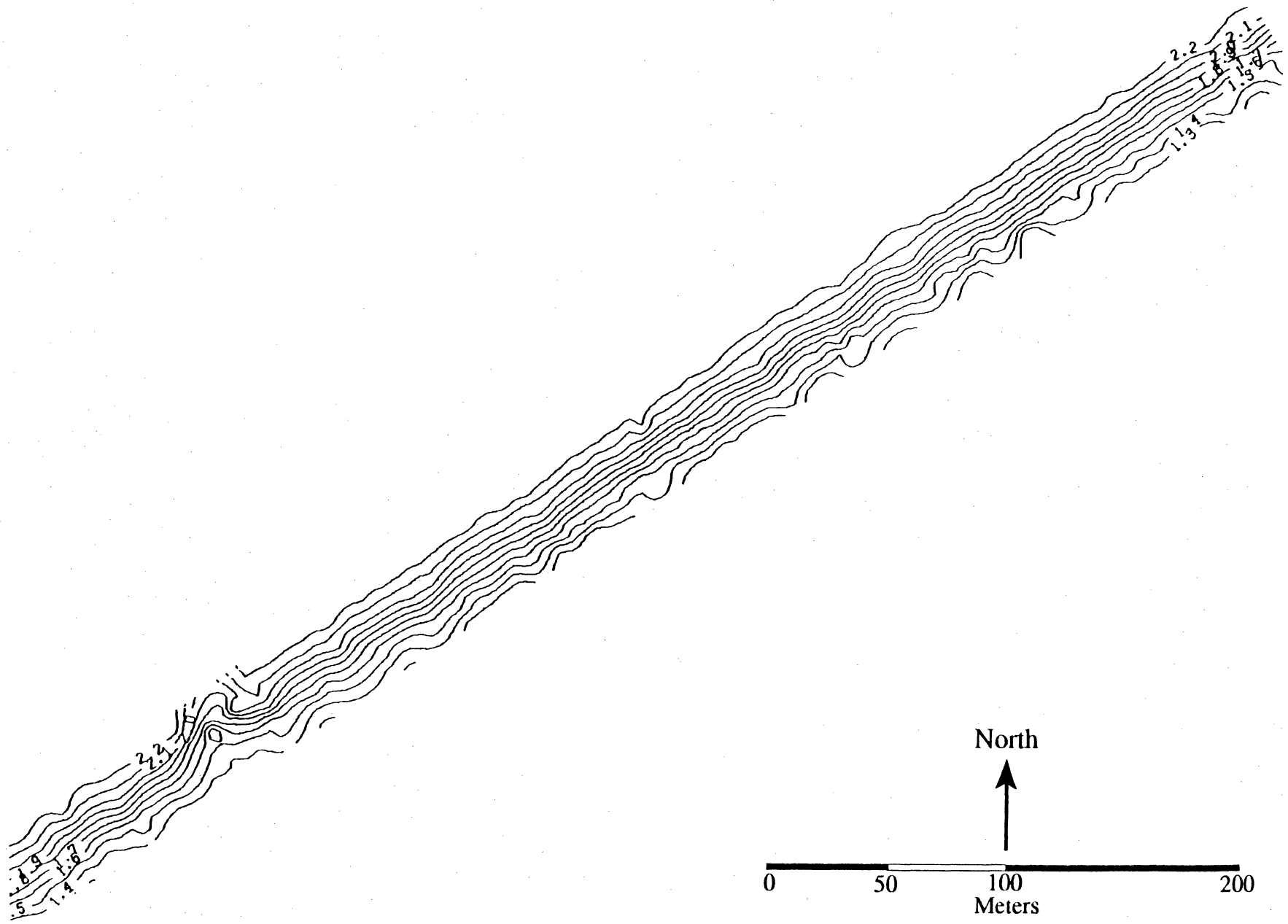


Figure 5. Topographic map of the northeast portion of the state park beach on day 104, 1993. The contour interval is 0.1 m and the horizontal scale is 60m/inch

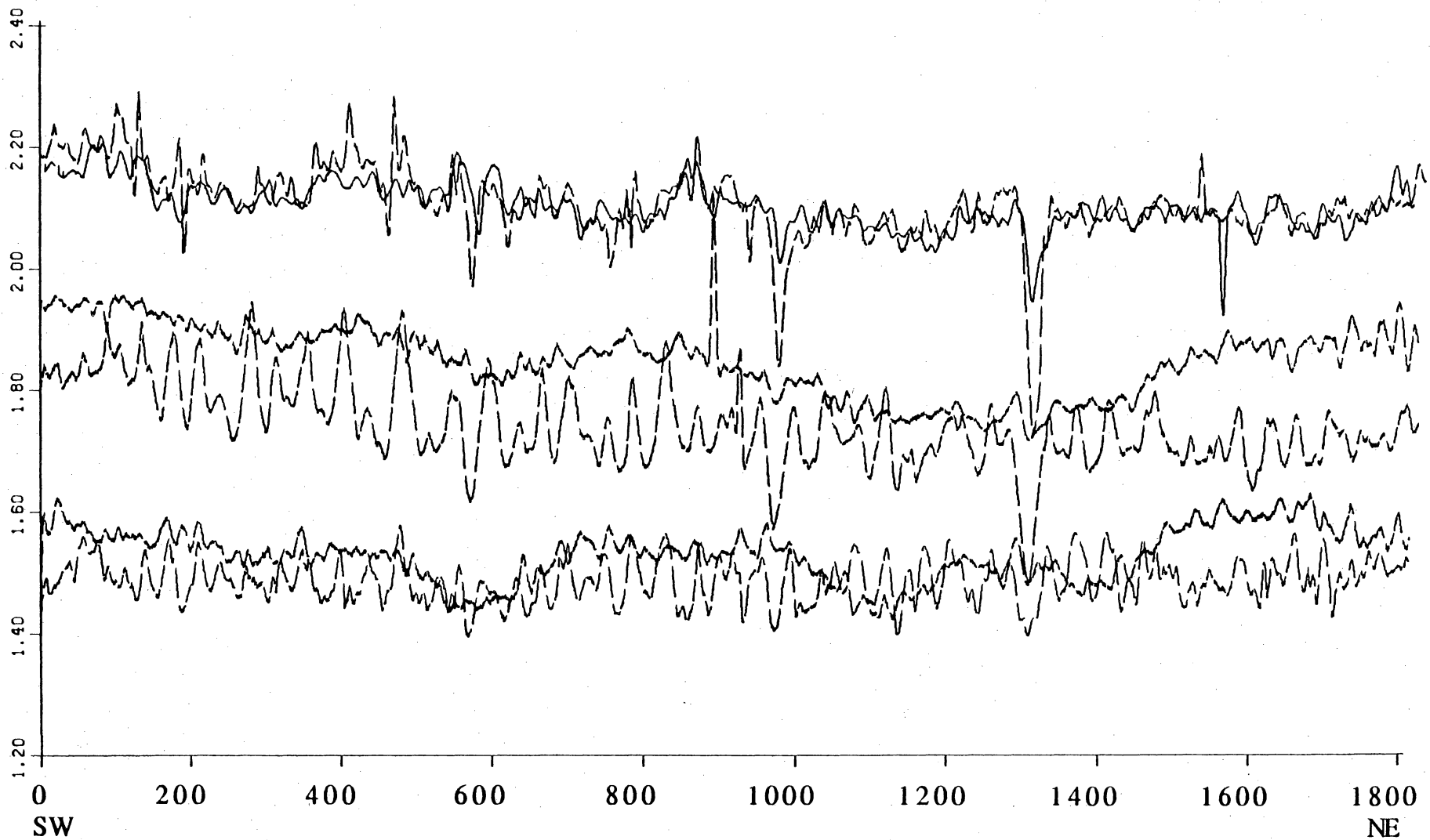


Figure 6. Shore-parallel profiles for the backbeach (top), berm crest (middle), and forebeach (bottom) for day 319 (solid lines) and day 104 (dashed lines). The vertical scale shows height above the WGS-84 ellipsoid in meters, and the horizontal scale shows distance in meters from the southwest to the northeast end of the survey area.

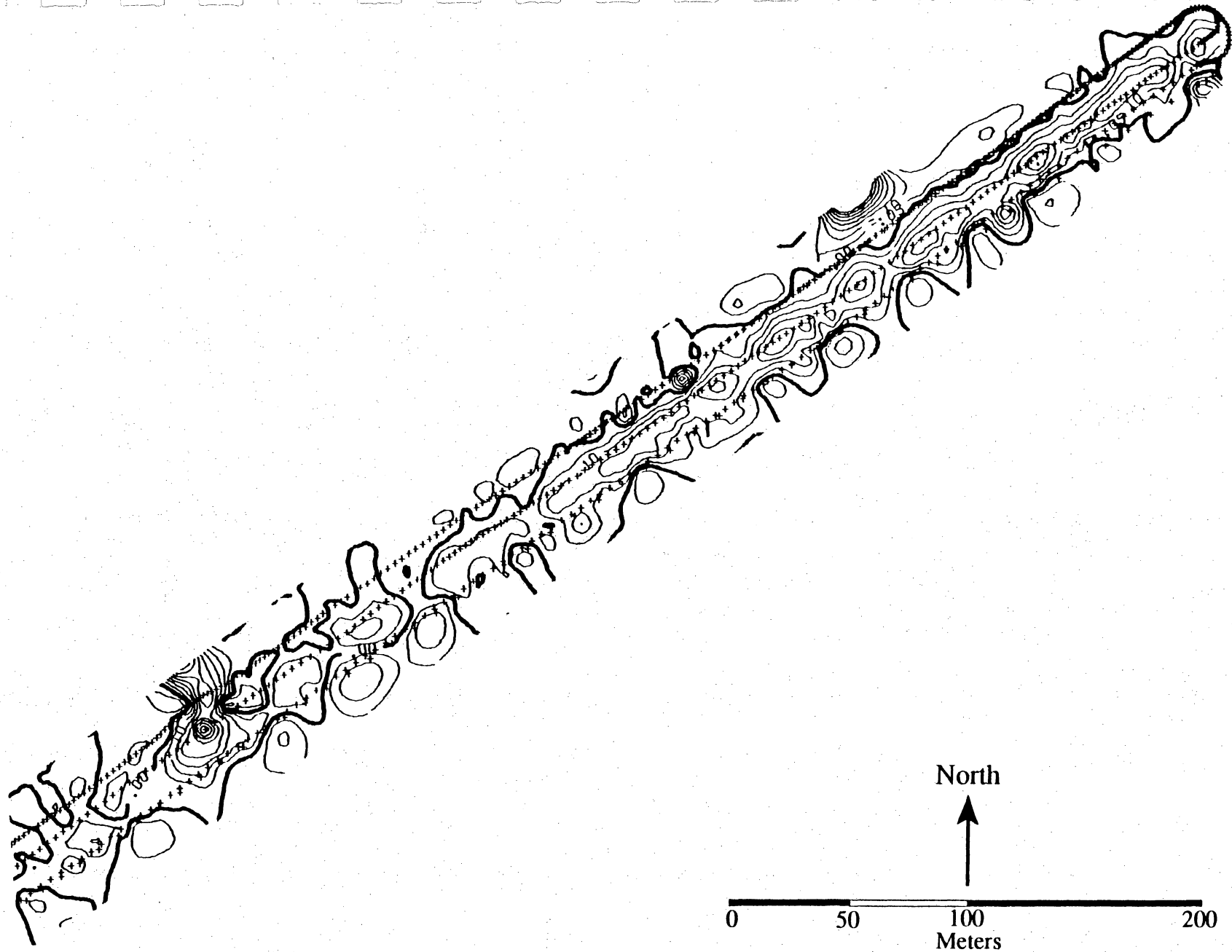


Figure 7. Contour map of the difference array created by subtracting the gridded array for day 104 from the array for day 319. The northeast portion of the state park beach is shown. The contour interval is 0.05 m and the horizontal scale is 60m/inch.



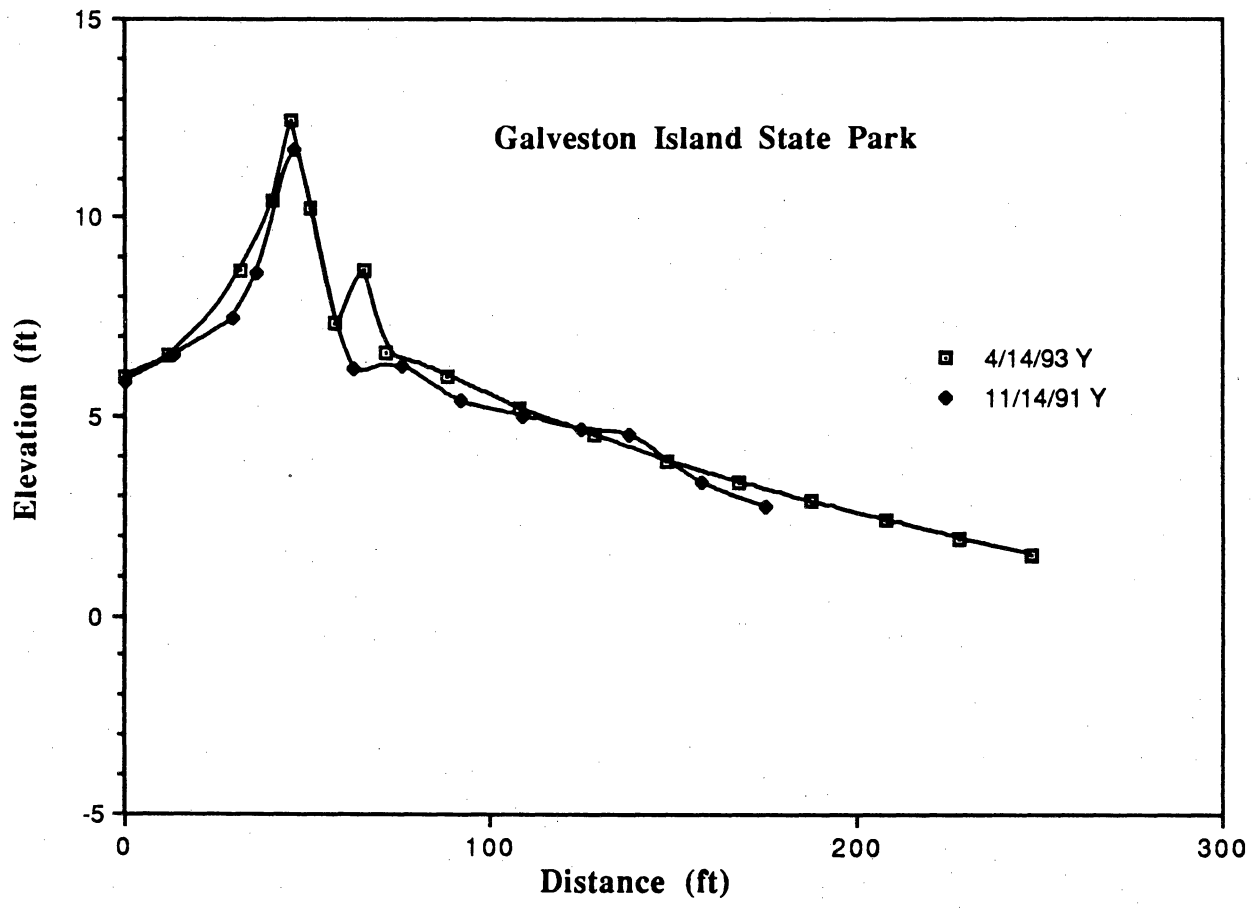


Figure 8. Beach profiles measured at Galveston Island State Park in November 1991 and April 1993 showing minor changes in beach elevation and sand volume.

## ADDENDUM 8

### SHORELINE SHAPE AND PREDICTION PROGRAM (SSAP): A COMPUTER PROGRAM FOR THE STATISTICAL ANALYSIS OF SHORELINE CHANGE AND MORPHOLOGY

James C. Gibeaut and Robert A. Morton  
Bureau of Economic Geology  
The University of Texas at Austin

#### INTRODUCTION

Recently, Dolan et al. (1991) reviewed four statistical methods for calculating shoreline rates-of-change from time series of shoreline positions. These methods include the: (1) end point rate; (2) average of rates (Foster and Savage, 1989); (3) linear regression; and (4) jackknife (Efron, 1982). Later, Fenster et al. (1993) presented a new method that combines polynomial regression, weighted linear regression, and knowledge of site-specific coastal processes. Because of the various methods proposed for calculating shoreline change rates, the long stretches of shoreline for which rates are needed, and the wide-spread use of Geographic Information Systems (GIS) for shoreline mapping, the Bureau of Economic Geology is developing a computer program that will automate the calculation of rates-of-change, compare the different methods, perform morphological analyses, and interact with a GIS.

The development of the computer program is the first step in investigating the merits and detriments of the various statistical methods. Once we obtain the ability to quickly calculate shoreline rates-of-change and project future shoreline positions in a GIS, the overall best method or the need for a new method may be revealed. This document describes the approach the Bureau is taking in this direction.

#### STRUCTURE AND OBJECTIVES OF THE SHORELINE SHAPE AND PREDICTION PROGRAM (SSAP)

SSAP is a modular FORTRAN program that uses subroutines to perform tasks required to compute shoreline rates-of-change and to project shorelines into the future based on those rates-of-change. Shoreline data may be provided as digitized shorelines through a GIS such as ArcInfo or as an ascii file in which data have been reduced to time series of shoreline distances from a baseline at particular locations along the shoreline. Routines are also planned that will perform shoreline morphological analyses on actual and predicted shore. The main program module determines the type of data, reads the data, prompts the user for the desired calculations, and directs the program

flow. Figure 1 illustrates the general structure of the program, and following is an overview of the various subroutines.

#### Shoreline Interpolation Routine (SSAPINT)

This subroutine is invoked to process data delivered to SSAP as a time series of digitized shorelines, such as from a GIS. SSAPINT linearly interpolates shoreline positions at the desired intervals along the trend of a baseline, which may change along the shoreline. Shoreline coordinates are rotated to match the orientation of the trend of the corresponding baseline. In other words, shoreline positions are converted to a new rectilinear coordinate system with the baseline as the ordinate. Baseline coordinates may be passed with the data or determined automatically within the routine. The output of SSAPINT is an array of shoreline coordinates for various times and for equally spaced locations along the trend(s) of the baseline(s).

#### Shoreline Distance Routine (SSAPDIS)

SSAPDIS is a simple routine that computes the distances from the earliest shoreline for each date and for each interpolated location along the baseline. The output is an array that is used as input to the rate-of-change routine (SSAPROC).

#### Shoreline Rate-of-change Routine (SSAPROC)

This routine directs the program to perform rate-of-change calculations using the methods selected by the user. It collects the rate-of-change values and various statistical parameters that are computed by the routines described below and passes these results back to SSAPMAIN for further use.

#### End Point Rate-of-change Routine (SSAPEPT)

This is a simple routine that for each location determines the distance between the earliest and latest shoreline positions and divides by the number of years. The resulting calculation is a single average annual rate-of-change for the entire monitoring period regardless of the history of shoreline movement.

#### Linear Regression Rate-of-Change (SSAP)

For this method, all the available data are used in a linear regression. The slope of the regression line is the shoreline rate-of-change. SSAPREG is actually a program that will compute the coefficients for any desired order of polynomial. When it is called to compute a linear regression rate-of-change, a polynomial order of one is passed to the routine by SSAPROC.

#### Jackknife Routine (SSAPJAC)

This routine uses the Jackknife statistical method as described by Efron (1982) to compute shoreline rates-of-change. A family of linear regression lines are computed by successively eliminating a single and different point. The slopes of these regression lines are then averaged to yield an annual rate-of-change.

#### Average of Rates Routine (SSAPAOR)

Foster and Savage (1989) developed this technique using data from Florida. It involves averaging the end point rates computed for all possible combinations of two points in a time series. Each combination of points must pass a minimum time criterion ( $T_{min}$ ), however, to be included in the average.

$$T_{min} = [\sqrt{(E_1)^2 + (E_2)^2}] / R_1$$

Where  $E_1$  and  $E_2$  are the assumed error ranges for shoreline position measurements 1 and 2, respectively, and  $R_1$  is the end point rate for the longest time span in the time series. The end-point combinations with time spans greater than  $T_{min}$  are considered "long-term" rates and their rates are averaged to yield the rate-of-change value.

#### Fenster Rate-of-Change (SSAPFEN)

This method of rate calculation is relatively complicated compared to the above methods. First an optimum polynomial is fitted to the time series based on the minimum description length criterion (MDL) as follows:

$$MDL_K = MSE_K + [\ln(N) \times K \times \sigma^2] / N$$

where  $MDL_K$  is the minimum description length for a model with  $K$  terms,  $MSE_K$  is the mean squared error of the model,  $K$  is the number of terms in the polynomial,  $N$  is the number of data

points, and  $\sigma^2$  is the noise variance. The model with the smallest MDL<sub>K</sub> is selected for further analysis.

Once the optimum polynomial is determined, points are identified where the slope changes sign. These turning points, or critical points, indicate a change in the direction of shoreline movement at particular times. If there are no changes in the sign of the slope, then a linear regression is used as the rate-of-change. If there is more than one change in the sign of the slope, then the most recent point when the slope changes is selected and all data prior to that time are weighted to zero. A new linear regression is calculated and is called the "zero-weight line." The user has the option of selecting the slope of this line as the best rate-of-change value. This would be the case if specific knowledge of a change in coastal processes suggest that the earlier data should be completely disregarded (weighted to zero).

Often specific knowledge of coastal processes is not available or it is not clear to what extent the earlier data should be considered. The Fenster method allows an objective means of evaluating the data (shoreline positions) that precede a change in the trend of shoreline movement. This is accomplished by incrementally increasing the weights of the earlier data and recalculating the linear regression and MDL<sub>K</sub>. The weights are increased until the MDL<sub>K</sub> is equal to or just less than that of the MDL<sub>K</sub> for the earlier determined optimum polynomial. Thus a nonlinear model is forced to be linear through a weighted linear regression technique.

SSAPFEN graphically displays the raw data, optimum polynomial, the linear regression line with all data treated equally, the zero-weight line, and the weighted linear regression line. The user may select the line that best represents the data and use its slope for the rate-of-change value.

#### Shoreline Projection Routine (SSAPPRO)

The user may select any of the rate-of-change values provided by SSAPROC to project the position of a shoreline in the future. The user may select multiple projections for various periods of time. SSAPPRO determines the coordinates of the projected shoreline in the rotated baseline coordinate system determined in SSAPINT and then re-rotates the coordinates so that they may be passed back to the GIS for plotting. This routine is under development.

#### Shoreline Morphological Analysis Routine (SSAPMOR)

This part of SSAP is still in the conceptual phase of development. SSAPMOR will be a collection of subroutines that will perform various morphological analyses of actual and predicted shorelines. Such analyses may include fractal, fourier, and new hybrid techniques. Actual shorelines will be morphologically characterized, and using these characterizations, the

"naturalness" of the predicted shorelines will be evaluated. Predicted shorelines that have unnatural shapes would suggest unreasonable rate-of-change values were used. This information may be used to go back and modify rate-of-change values for particular locations or to provide a limit on how far in the future one may reasonably project shorelines.

## DISCUSSION

At many sites along the Texas coast the trends of shoreline movement and rates of change have been greatly influenced by human activities. These activities have locally altered the littoral processes and sediment supply, causing either the trends of shoreline movement to abruptly reverse or to rapidly accelerate and decelerate. Therefore it is important to analyze shoreline movement in a historical context that recognizes the altered physical conditions and their impact on future shoreline movement.

The Fenster method (Fenster et al., 1993) improves the statistical analysis of shoreline movement by identifying turning points and providing several analytical options, but all of the options involve linear regression of segments of the curve, including the most recent segment of the curve. Although subdividing the curve into shorter time periods has advantages over previous techniques, the linear analysis does not provide an accurate rate-of-change value if the rate-of-change is accelerating or decelerating. We tested the Fenster method using data from the Texas coast and the results were mixed. Some of the calculated rates-of-change were accurate and others were not. Our preliminary evaluation indicates that another empirical model is needed that will calculate rates-of-change when the shoreline movement is nonlinear.

Improving our ability to predict shoreline movement and future shoreline positions will continue to be a primary objective of our research during the next year of the study.

## REFERENCES

- Dolan, R., Fenster, M.S., and Holme, S.J., 1991, Temporal analysis of shoreline recession and accretion: *Journal of Coastal Research*, v. 7, no. 3, p. 723-744.
- Efron, B., 1982, *The Jackknife, the Bootstrap and Other Resampling Plans*: Philadelphia, Pennsylvania: Society for Industrial and Applied Mathematics, 92p.
- Fenster, M.S., Dolan, R., and Elder, J.F., 1993, a new method for predicting shoreline positions from historical data: *Journal of Coastal Research*, v. 9, no. 1, p. 147-171.
- Foster, E.R. and Savage, R.J., 1989, Methods of historical shoreline analysis: in Magoon, O.T., Converse, H., Miner, D., Tobin, L.T., and Clark, D., (eds.), *Coastal Zone '89*, American Society of Civil Engineers, v. 5, p. 4434-4448.

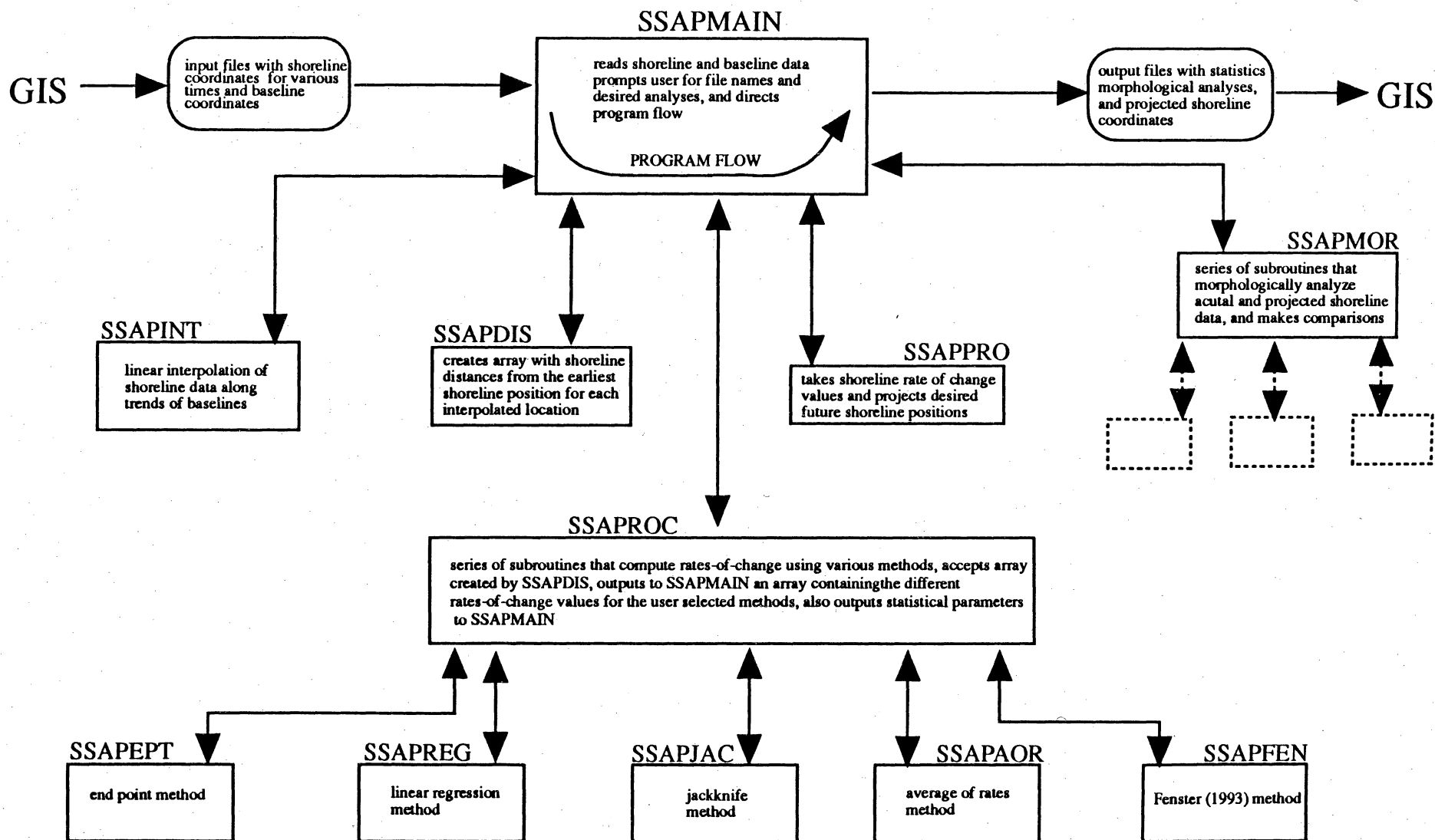


Figure 1 - General structure of the Shoreline Shape and Prediction (SSAP) computer program.